Universitat Autònoma de Barcelona

Asymmetric synthesis of chiral amines using transaminases: a multienzymatic approach by pyruvate decarboxylase coupling

Natàlia Alcover Fortuny

Universitat Autònoma de Barcelona

Escola d'Enginyeria

Departament d'Enginyeria Química, Biològica i Ambiental

Asymmetric synthesis of chiral amines using transaminases: a multienzymatic approach by pyruvate decarboxylase coupling

Memòria per a optar al grau de Doctora per la Universitat Autònoma de Barcelona dins el programa de Doctorat en Biotecnologia sota la direcció de la Dra. Marina Guillén Montalbán i del Dr. Gregorio Álvaro Campos

Natàlia Alcover Fortuny

Bellaterra, 2021

La Dra. Marina Guillén Montalbán, professora del Departament d'Enginyeria Química, Biològica i Ambiental de la Universitat Autònoma de Barcelona, i el Dr. Gregorio Álvaro Campos, professor agregat del Departament d'Enginyeria Química, Biològica i Ambiental de la Universitat Autònoma de Barcelona,

Certifiquem:

> Que la biotecnòloga Natàlia Alcover Fortuny ha dut a terme sota la nostra direcció el treball titulat "Asymmetric synthesis of chiral amines using transaminases: a multienzymatic approach by pyruvate decarboxylase coupling", el qual es presenta en aquesta memòria i constitueix la seva tesi per a optar al Grau de Doctora en Biotecnologia per la Universitat Autònoma de Barcelona.

I per tal que se'n prengui coneixement i constials efectes oportuns, signem la present a Bellaterra, a 8 de febrer de 2021.

Dra. Marina Guillén Montalbán

Dr. Gregorio Álvaro Casas

Abstract

The present thesis is focused on the development and optimization of a biocatalytical approach for the synthesis of chiral amines, which are highly valuable optically active compounds that can be used for the synthesis of numerous targets, especially in pharmaceutical and agrochemical industry. More specifically, 3-amino-1-phenylbutane (3-APB) and 1-phenylethylamine (1-PEA) synthesis is pretended by the cascade reaction of transaminase (TA) and pyruvate decarboxylase (PDC). The mentioned cascade consists in an asymmetric synthesis from their corresponding prochiral ketones and alanine catalyzed by ω-transaminase, which presents an unfavorable equilibrium. To overcome this problem, PDC acts as a by-product removing system by transforming the resulting pyruvate to acetaldehyde and CO_2, which leads to an equilibrium shift.

Aiming to overcome the low PDC commercial availability, which can only be acquired at low amounts and a high cost, a whole production process was developed. *Zymobacter palmae* PDC (*Zp*PDC) gene was cloned and overexpressed in *Escherichia coli.* After that, high amounts of the recombinant enzyme were obtained by the development of a high-cell density culture process in bench-top bioreactor. Regarding TA, four different enzymes were available from *Chromobacterium violaceum* (Cvi-TA), *Vibrio fluvialis* (Vfl-TA) and *Aspergillus terreus* (Ate-TA and Ate-TA_T247S). Both PDC and the different transaminases were characterized to find out the appropriate compromise conditions to construct the enzymatic cascade. Taking into account the found conditions, preliminary screening reactions were carried out, from which Cvi-TA and Vfl-TA were selected for the synthesis of 3-APB; and Vfl-TA for the synthesis of 1-PEA.

After proving the feasibility of TA and PDC cascade reaction, different optimization approaches were applied in order to maximize reaction yields and to improve the low transaminase operational stability. On the one hand, reaction conditions optimization approaches were explored. On the other, reaction medium engineering was applied. After that, enzyme immobilization was carried out. Immobilized derivatives of both Cvi-TA and Vfl-TA were obtained in MANA-agarose and epoxy-agarose supports. In the case of PDC, an innovative simultaneous purification and immobilization process was developed using MANA-agarose. Finally, the obtained immobilized enzymes were applied in reactions and a reaction cycle strategy was developed.

Resum

La present tesi es centra en el desenvolupament i optimització d'una estratègia basada en la biocatàlisi per a la síntesi d'amines quirals, les quals són compostos òpticament actius de gran valor que poden ésser utilitzats per a la síntesi de nombrosos productes, especialment en les indústries farmacèutica i agroquímica. Més concretament, es pretén sintetitzar 3-amino-1-fenilbutà (3-APB) i 1-feniletilamina (1-PEA) a través de la reacció en cascada de la transaminasa (TA) i la piruvat decarboxilasa (PDC). Aquesta cascada es basa en una síntesi asimètrica que parteix de les seves corresponents cetones proquirals i l'alanina, i és catalitzada per ω-transaminases, les quals presenten un equilibri desfavorable. Per tal de solucionar aquest problema, la PDC actua com un sistema d'eliminació de producte secundari, a través de la transformació del piruvat a acetaldehid i CO_2, la qual cosa provoca un desplaçament de l'equilibri.

Amb l'objectiu de superar les limitacions comercials de la PDC, la qual només es pot obtenir en petites quantitats a un cost alt, es va desenvolupar un procés sencer de producció d'aquest enzim. Es va clonar i sobreexpressar el gen de la PDC de *Zymobacter palmae* (*Zp*PDC) en *Escherichia coli*. Posteriorment, es va obtenir l'enzim recombinant en grans quantitats a través del desenvolupament d'un procés de cultiu d'alta densitat cel·lular en bioreactor. Pel que fa a les TAs, es disposava de quatre enzims diferents, procedents de *Chromobacterium violaceum* (Cvi-TA), *Vibrio fluvialis* (Vfl-TA) i *Aspergillus terreus* (Ate-TA and Ate-TA_T247S). Es va caracteritzar tant la PDC com les quatre transaminases per tal de trobar les condicions de compromís adequades per a la construcció de la cascada enzimàtica. Tenint en compte les condicions trobades, es va dur a terme, de forma preliminar, reaccions de cribratge de les quals en van sortir seleccionades la Cvi-TA i la Vfl-TA per a la síntesi de 3-APB; i Vfl-TA per a la síntesi de 1-PEA.

Després de demostrar la viabilitat de la reacció en cascada de la TA i la PDC, es van aplicar diferents estratègies d'optimització per tal de maximitzar els rendiments de reacció i millorar la baixa estabilitat operacional de les transaminases. Per una banda, es van explorar algunes estratègies d'optimització de les condicions de reacció. Per l'altra, es va aplicar enginyeria del medi de reacció. Posteriorment, es va dur a terme d'immobilització dels enzims. Es van obtenir derivats immobilitzats tant de la Cvi-TA com de la Vfl-TA en suports de MANA-agarosa i epoxy-agarosa. En el cas de la PDC, es va desenvolupar un sistema innovador de purificació i immobilització simultània en MANA-agarosa. Finalment, els enzims immobilitzats obtinguts van ser aplicats en reacció i es va desenvolupar una estratègia de reacció en cicles.

Contents

1. Introduction

1.1. Biocatalysis as a powerful tool in organic synthesis

Biocatalysis is the use of enzymes or enzyme containing cells to useful chemical transformations in order to obtain products of industrial interest [1], [2]. Enzymes have been used for more than a century for various applications in food agriculture, polymer synthesis, organic synthesis of fine chemicals and flavors, and especially in the production of pharmaceutical intermediates. However, in the last decades, biocatalysis has matured to a standard technology due to new scientific advances, which is reflected by the biotransformation processes running on a commercial scale [3], [4].

1.1.1. Biocatalysis and Green Chemistry

In the last decades, a growing interest has emerged in industry in the development of processes that follows the Green Chemistry principles as much as possible. Green Chemistry concept appeared during mid-1980s and refers to the design of chemical products and processes in a way in which raw materials are efficiently used, waste is eliminated and use or generation of hazardous substances is avoided [5], [6]. To accomplish with it, a careful planning of the chemical synthesis and molecular design to reduce adverse consequences are fundamental [5].

According to the mentioned point of view, the Twelve Principles of Green Chemistry were formulated as guidelines to follow during process development in order to achieve a high sustainability [5]. These principles described integrated design systems based on waste prevention rather than remediation by the use of less hazardous materials, innocuous solvents and auxiliaries, and preferably renewable raw materials. Also taking into account energetic efficiency and using analytical methodologies in order to prevent waste and pollution generation was recommended. Moreover, new production processes had to be inherently safer, with an atom efficiency, shorter synthesis and with catalytic reagents than stoichiometric. Finally, the twelve principles claimed for resulting products that were safer by design and preferably easily degradable [5]–[7].

Even though the typical chemical syntheses are generally high-yield, their environmental impact is negative and are associated with the production of unwanted by-products that reduce efficiency and complicate downstream [8]. One approach mentioned by the Twelve Principles

for making syntheses more sustainable is to substitute the use of stoichiometric reagents for catalytic alternatives. Especially when complex organic compounds are synthesized, which require several separate reaction steps, the use of stoichiometric reagents is a major cause of waste generation. In contrast, catalytic approaches make processes more atom and step economical, since they are generally shorter and they allow a reduction on energy and raw material consumption [6].

Consequently, biocatalysis supposes a promising alternative of typical chemical processes [9], not only for the inherent features of being a catalytic approach, but also because of other sustainability advantages not always achieved by the use of chemical catalysis. On the one hand, enzymes are non-toxic catalysts acting with a high selectivity, which can lead to efficient reactions with few by-products and, therefore, decrease the waste production [9], [10]. This selectivity can be both chiral (enantioselectivity) and positional (regioselectivity) [10]. As a result, they are suitable both for simple and complex transformations without the need of several steps, which may shorten syntheses [9], [10]. On the other, biotransformations are also associated to the use of aqueous media and mild operation conditions, which result in lowered energy consumption [9].

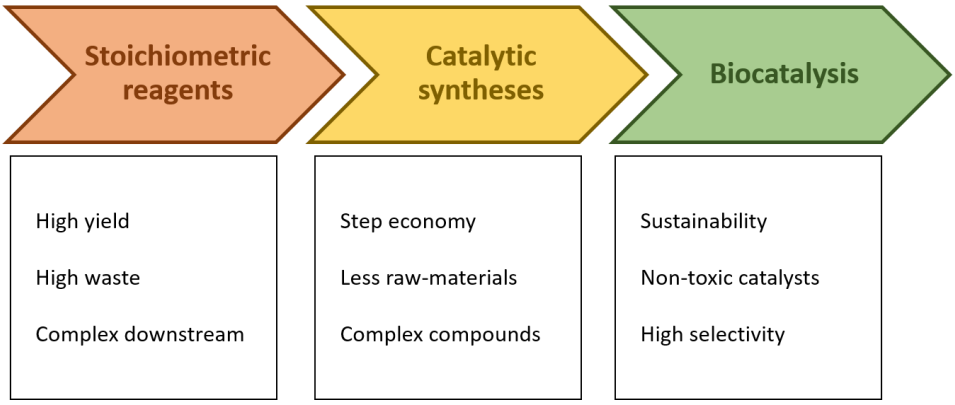

Figure 1.1 Evolution of organic synthesis approaches according to the Green Chemistry principles. By replacing stoichiometric reagents for catalytic syntheses, complex compounds can be produced with less reaction steps and reducing the raw-materials used. When a biocatalytic approach is used, in addition to the aforementioned advantages, products are synthesized with milder conditions, high selectivity and using non-toxic catalysts.

1.1.2. Biocatalysis in industry today

Enzymes have a great potential as catalysts, since they offer more competitive processes than chemical catalysts. A reflect of this is the enzyme-based processes implemented in the production of several valuable products [11], which has grown rapidly in the past decades [12]. Some of the already produced compounds by biocatalytical means are carbohydrates, fat derivatives, steroids, peptides, beta-lactams, aminoacids, sec-alcohols or nucleotides [12].

Even though biocatalysis implementation has been difficult [10], in the last decades, it has been integrated in organic synthesis [6]. However, in many industrial processes, they still represent one of many steps in a complete synthetic scheme. In this line, there is a growing area of research on integrating biocatalysis on the global industrial process [6]. The challenge is the combination of different enzymes to complete cascades of enzymatic reactions [13].

Two of the main areas where the use of biocatalysis has become a proven technology are the production of pharmaceutical intermediates and fine chemicals. This expansion has been triggered in part by an enzyme engineering based on structural information, which has extended the substrate ranges, enabling the synthesis of unusual intermediates [11]. In the especial case of pharmaceutical industry, it is a sector demanding a timeline and costs reduction for developing drugs, at the same time complex molecules must be obtained in preferably greener routes [14]. Moreover, some of the most important compounds in the mentioned industry are optically active. In this sense, one of the key interests of biocatalysis, which will be deeper described in further sections, is the ability of producing enantiomerical pure compounds mainly through high chemoselectivity, regioselectivity, and streoselectivity [11].

1.2. Bioprocess development

The emergence of multiple new biocatalytic approaches for different industrial applications has been triggered by the important biotechnological advances [7]. The development of new interesting bioprocesses requires the multidisciplinary integration of chemistry, molecular biology, enzymology, microbiology and bioprocess engineering [4]. However, even though new enzyme activities are constantly developed in laboratory scale, to achieve a real application, a more rational approach is needed. The starting point is usually a specific product, which may be produced by biocatalytic means. Several biocatalysts must be identified or developed, a process

must be set up and the resulting bioconversion needs to ultimately be economically feasible [10].

According to Kohls 2014 [15], three phases can be distinguished in the development of an industrial process based on biocatalysis. Firstly, the discovery of novel enzyme activities is a powerful tool for finding biocatalytic ways to obtain interesting target products. In this sense, in recent years, protein engineering has allowed the development of novel biocatalytic routes by altering the substrate or reaction specificity of known enzymes. Moreover, the discovery of novel wild-type enzymes is still an important strategy to access new biocatalysts. The second phase would include the advances faced to broadening the catalytic scope. By the rational study of the reaction mechanism, as well as protein structure, substrate scope can be guided, broadening, this way, the enzyme applications. Finally, the new processes need to mature towards industrial scale applications, which requires several strategies based on bioprocess engineering.

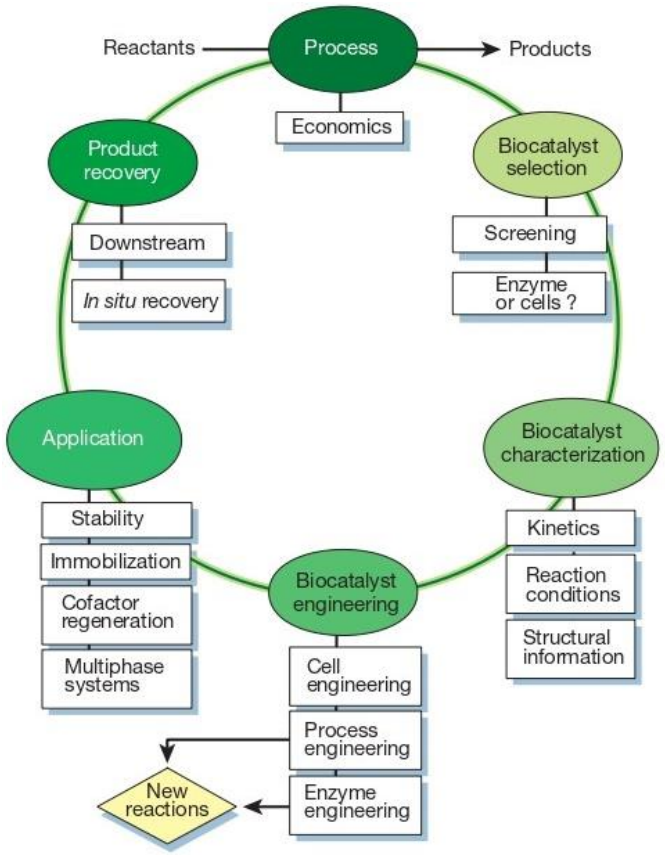

Figure 1.2 Scheme of a biocatalytic process development. After identifying a biocatalytic strategy for obtaining a target product, a rational approach must be followed, which involves, biocatalyst discovery and engineering, as well as a process engineering that leads to an economically feasible industrial procedure. Source: Schmid 2001 [10].

1.2.1. Biocatalyst discovery and engineering

One fundamental part of bioprocess development is the election of biocatalyst. Biotransformations can involve growing cells, resting cells, cell-free enzyme preparations or isolated enzymes, and have been usually divided into two main types. On the one hand, growth-associated whole-cell bioconversions have been typically defined as fermentations, the main goal of which can be both to produce more microbial cells and the production of chemical products. On the other hand, in biocatalytic approaches, cell growth and production phase are separated and substrates are converted by resting whole-cells or isolated enzymes [6], [8]. The main advantage of resting whole-cells is the possibility of using cheap and abundant raw materials and to catalyze multistep reactions taking advantage of biocatalytic routes present into the cells [8]. However, even though with whole-cells separation and purification of enzymes is avoided, the use of isolated enzymes reduce medium contamination by other proteins, which may be fundamental during the production of certain products according to their final application [4]. Moreover, the use of enzymes has other several advantages, such as reduction of by-product generation, downstream simplification and the possibility of using higher biocatalyst concentrations.

Even though many processes can be based on available enzymatic activities, it is also usual to screen for organisms or enzymes that carry out the desired reaction, or to develop completely new enzyme activities by protein design or directed evolution [10]. Nowadays, thanks to high throughput DNA sequencing techniques and advances on DNA recombinant technologies, more enzymes are available and can be more easily produced [2]. The spectacular advances in bioinformatics, gene sequencing and synthesis, ready access to enzyme structures, high throughput screening and genetic manipulation have led to an exponential growth in the number of enzyme catalysts available for potential industrial use [16].

In recent years, a massive increase in enzyme discovery has taken place. The development of new metagenomics tools, which allow the analysis of massive DNA sequence amounts in a short time and low cost, has triggered this evolution in enzyme discovery [3]. This technology has been fundamentally used following two different strategies. On one side, sequence-based metagenomics consists in random and massive sequencing in order to construct metagenomic libraries. On the other side, in function-based metagenomics, metagenome is prepared in a manner that favors gene expression. Then, identification of clones expressing enzymes of interest is performed by different types of screening [3].

Apart from enzyme discovery, biocatalyst engineering approaches have also gained importance in the last decades. Industrial processes often involve transformations of non-natural substrates under different conditions in which wild-type enzymes are not effective, which results in low selectivities, low activities and low space-time yields [6]. Thanks to protein engineering techniques, it is possible to develop tailor made enzymes with predefined features, such as substrate specificity and selectivity, activity, stability or pH profile [3], [7]. There are several powerful approaches for enzyme engineering using a variety of methods. In general, enzymes can be engineered following rational design or random engineering. The first approach is only possible when structure and function information is available and consist in generating mutant libraries and subsequently screening for improved properties [6]. In contrast, random engineering consists in randomly generating mutant libraries, for which detailed information about structure and mechanism is not required [3], [6]. Modern strategies often combine both approaches [3]. This way, it is possible to predefine the necessary parameters of the process and then modify the biocatalyst to achieve them [6].

1.2.2. Bioprocess engineering

As it has already been mentioned, biocalysis integration on the global industrial process is a challenging task. For this mentioned integration, most biocatalytic processes must be improved to have a similar speed of development than a conventional chemistry step [4], [17]. For this reason, after identifying the needed biocatalytic activity and obtaining the appropriate biocatalyst, there are several more variables to be engineered before implementing the bioprocess. Strategies for biocatalysis engineering, with the aim of improving biotransformations or creating new ones, include the engineering of the substrate, the reaction medium, the protein and post-translational modification of the enzyme. Finally, reactor engineering in combination with downstream processing facilitates product recovery and re-use of the biocatalyst [2].

One engineering approach to optimize biotransformations or create new ones, is substrate engineering. Substrate engineering is commonly defined as the use of non-natural substrates, which lead to the discovery of novel enzyme reactions, as well as substrate modification to fit with the biocatalyst [2]. Another extended strategy is medium engineering, which refers to the use of enzymes in non-aqueous medium. Even though they usually function optimally in water, the enzyme use in organic medium can suppose some benefits. For example, it can enhance substrate solubility or it can help to overcome equilibrium limitation. Additional benefits of

non-aqueous biocatalysis are easier product recovery from volatile organic solvents and elimination of microbial contamination [2].

Other challenges of bioprocess engineering are related to the integration of several enzymes in one-pot cascades. In traditional organic syntheses, several steps are required to achieve an interest product, involving several intermediates that must be isolated and purified between steps. In contrast, catalytic processes are generally shorter and allow a reduction of the steps number [14]. Moreover, integrating several catalytic steps into one-pot without the need of isolating intermediates supposes a reduction on reagents and solvents used and, consequently in the amounts of generated waste. For this reason biocatalytic cascades have recently gained a high interest [18]. Using this kind of strategies supposes fewer unit operations, shorter cycle times and higher yields, as well as the already mentioned substrate and solvent expenses reduction and lower waste amounts [2], [6], [18].

Cascade reactions have become the most effective use of biocatalysis. They allow target products synthesis by emulating enzymatic pathways present in living cells. In addition, coupling several reactions can also be used to drive equilibrium towards product without the need of excess reagents. Finally, another well-established biocatalytic strategy is the coupling of several enzymes to introduce cofactor regeneration steps [2], [6]. Combining several reaction steps is easier in biocatalysis than in chemical procedures since enzymes mostly require similar reaction conditions (water, ambient temperature and pressure) [2], [16]. However, it can often be a complex task, because of the different individual operation conditions (such as optimum pH conditions), which can lead to non-optimal behaviors, in addition to possible undesired cross-reactions or inhibitions [14]. In that case, compromise conditions must be found.

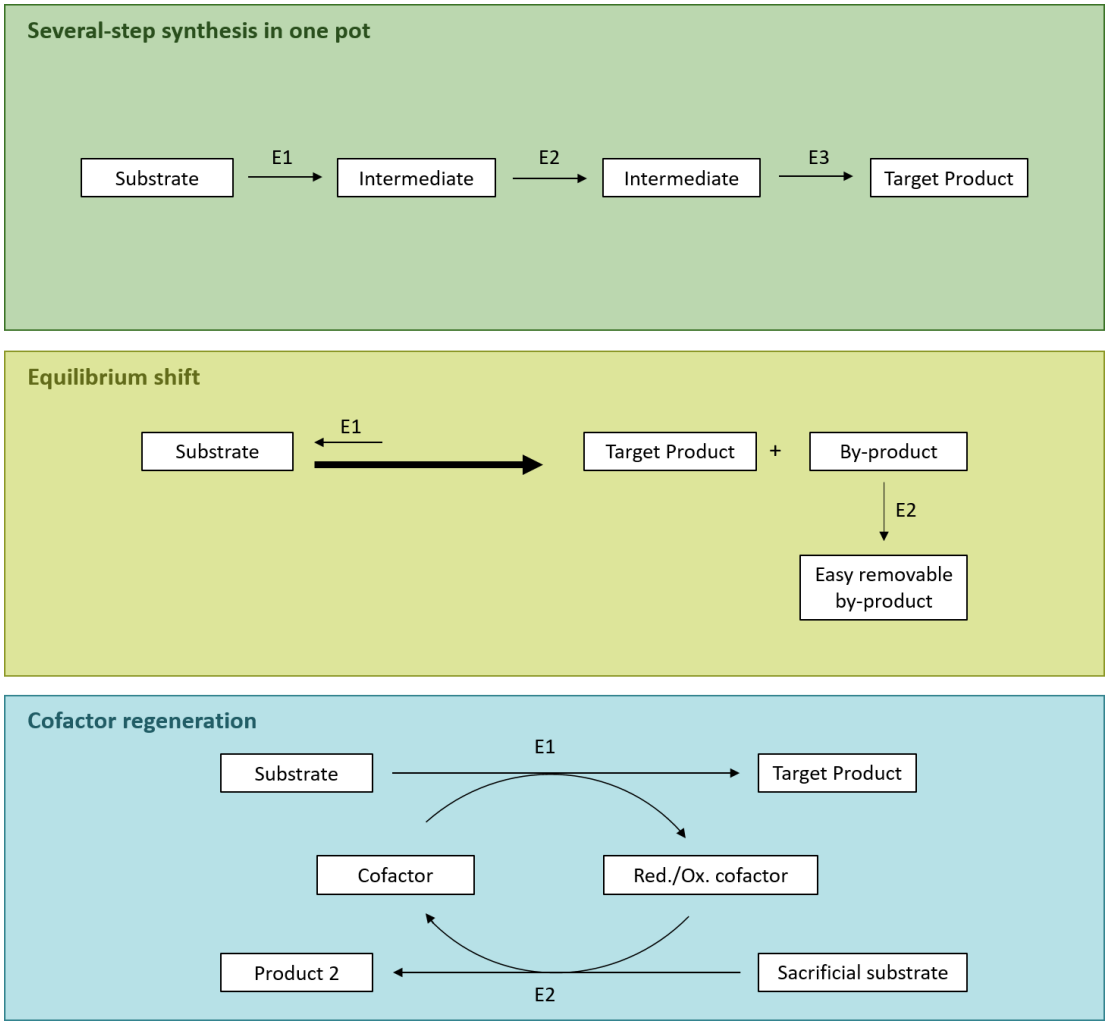

Figure 1.3 Typical uses of enzymatic cascade reactions. In the first case, several reaction steps catalyzed by different enzymes are grouped in one-pot. In the second, an enzyme is coupled to an unfavorable interest reaction to remove a by-product producing, this way, an equilibrium shift. Finally, in the third case, a second enzymatic reaction is coupled to the interest one to regenerate the cofactor.

1.3. Biocatalysis for the synthesis of chiral compounds

One of the main driving forces for the implementation of biotransformations in industry, especially in the pharmaceutical sector, is the need for chirality [9]. Chirality is a molecular asymmetry in which a compound has a non-superimposable mirror image. These mirror images are called enantiomers and have the same chemical and physical properties, such as boiling point, melting point or polarity. The interest for enantiomerically pure active compounds has grown in the last decades after the discovery that the enantiomers of a pharmaceutically active molecules, upon different interaction with bioreceptors, could produce different biological responses [13]. For this reason, stricter regulations were implemented by the administrations at

the end of 20th century. Since 1992, both the Food and Drug Administration (FDA) and the European Committee for Proprietary Medicinal Products (EMA) have stipulated that individually enantiomer physiological action must be characterized [4], [17]. Therefore, racemic forms of many chiral compounds are no longer accepted [19]. Since then, in the development of chiral compounds, it is assumed that enantiomeric excess (ee, %) should be > 99% for pharmaceuticals if no purification is possible. This case is quite rare and ee's > 90% are often acceptable [19].

1.3.1. Target chiral compounds

Optically active intermediates can be used as chemical building blocks, auxiliaries or advanced intermediates [13], [16], [17]. They have a huge interest especially in the pharmaceutical industry since more than the 70% of the active compounds used in this sector are chiral [16]. They also have importance in agrochemicals industry because the targeted synthesis of the respective active enantiomer can improve the economics of the process and lead to less quantities applied reducing, this way, environmental impact [13], [17].

Some of the most important optically active compounds are carboxylic acids, amines, alcohols or epoxides [16], [20]. Among them, chiral amines represent highly valuable target molecules because they are precursors and key intermediates for the synthesis of numerous targets. For instance, about 40% of the optically active drugs are chiral amines, including neurological, cardiovascular, immunological, antihypertensive, antiinfective, and antiemetic drugs [15], [21]–[23]. Some examples of amines with pharmacological activity are (S)-amphetamine, which acts as stimulant and hyperthermic agent, (R)-4-phenylbutan-2-amine, which is a precursor of the anti-hypertensive dilevalol, (R)-p-methoxyamphetamine, a constituent of (R,R)-formoterol, a potent bronchodilator; or 1-phenyl-1-propylamine, which is a precursor of the corticotropin-releasing factor type-1 receptor antagonist, a potent antidepressive agent [23].

Examples of pharmaceuticals based on chiral amines and produced by biocatalytic means can be already commercially found. Probably the most successful case known is the antidiabetic compound sitagliptin, commercialized as a drug for the treatment of type 2 diabetes under the name of Januvia by Merck [11], [20]. The typical synthesis of this compound, involving the use of a rhodium-based catalyst, specialized high-pressure equipment and an accurate downstream process, was replaced for the use of a highly developed transaminase [14], [20]. This mentioned transaminase was engineered by directed enzyme evolution to overcome the substrate size limitation present during the asymmetric amination of the prositagliptin ketone. After additional

process engineering strategies, a 13 % higher overall yield and a 53 % higher productivity compared to the rhodium catalyzed process was achieved [11], [14], [20].

1.3.2. Strategies for chiral synthesis

To accomplish with the aforementioned regulations, development of methods to obtain enantiomerically pure molecules instead of their racemic forms have become crucial [13]. The availability of industrial quantities of many chiral compounds has been typically limited for the complexity of obtaining high optical purities [17]. In the last decades, new perspectives have arisen thanks to the development of new technologies and methods that enabled the production of active compounds in a more economical way and in large-scale [17], [20]. Chemists have been turning their attention to the use of enzymes for the synthesis of chiral chemicals, because of their exquisite selective and reactive properties, which provide an effective synthetic strategy for creating optically pure molecules [20]. Regioselective and stereoselective properties associated with enzymes enable the syntheses of high-size and complexity molecules that would require multiple protection and deprotection steps in typical organic synthesis [4].

According to Blaser 2007 [19], four general approaches for producing enantiopure compounds are used, both implying biocatalysis or chemical methods: separation via classical resolution, chiral pool approach, enantioselective synthesis and enantioselective catalysis. Biocatalysis has been introduced as a powerful tool on enantiomeric resolution and on enantioselective catalysis, since it is used to resolve or create chiral centers [4]. In enantiomeric resolution, the stereoselectivity of enzymes can be used to catalyze the transformation of a specific enantiomer of a racemic mixture. This way, a different product is generated, enabling an easier separation. However, this approach leads to maximum yields of 50 %. For this reason, a high interest is focused on enantioselective biocatalysis. Using this approach, an asymmetric synthesis is carried out transforming, by the use of enzymes, prochiral starting materials to the interest chiral product [19], with the theoretical possibility of obtaining a 100 % yield. Some examples of reactions that can be performed using this biocatalytic strategy are chiral amine synthesis, stereo and regio-specific hydroxylation of complex molecules, and other redox reactions [11].

1.4. Asymmetric chiral amine synthesis with transaminases

As it has already been mentioned, biocatalysis has arisen the last decades as a powerful tool in organic synthesis because of its multiple advantages in comparison with typical chemical syntheses. Moreover, one of the key interests for integrating enzyme-based processes in industry is the possibility of obtaining highly enantiopure products in few steps. For this reason, in the present thesis, a biocatalytical approach is developed and optimized for the synthesis of chiral amines.

Chiral amines are molecules of high industrial interest because of their broad range of applications [24]. They have been widely used as chiral auxiliaries, resolving agents and building blocks for the synthesis of natural and unnatural compounds [13], [24]. They can be broadly found in numerous active pharmaceutical ingredients (APIs), agrochemicals, bioactive natural products and pharmaceutical building blocks, reason why the development of biocatalytic strategies for their synthesis has been identified as a key research priority in the pharmaceutical, agrochemical and chemical industries [25]–[27].

Multiple biocatalytic approaches have been developed for the synthesis of optically pure amines involving the use of several enzymes [25]–[28]. The most commonly used strategy in industry is kinetic resolution, consisting in the enantioselective transformation of a starting racemic amine [17], [29]. However, a more promising strategy is to perform a direct asymmetric synthesis from their corresponding prochiral ketone and a suitable amino donor. This mentioned reaction is catalyzed by ω-transaminases, which are pyridoxal phosphate (PLP)-dependent enzymes, which catalyze the transfer of an amino group from an amino donor to an amino acceptor (in this case a ketone) [13], [28], [30]–[33].

Nevertheless, the described strategy has as a major drawback the unfavorable equilibrium towards amine formation. To overcome this problem, several approaches have been proposed. In the particular case of using alanine as amino donor, pyruvate is generated as a by-product. Pyruvate removal from reaction medium can lead to an equilibrium shift and, in this sense, combining transaminase with other enzymatic routes generating a cascade can be a powerful solution. Among different options described, such as lactate dehydrogenase (LDH) [22], [28], [34]–[36] or alanine dehydrogenase (AlaDH) [28], [34], in the present thesis, pyruvate decarboxylase is used. Pyruvate decarboxylase (PDC) is a thiamine pyrophosphate and Mg^{2+} ion-dependent enzyme that catalyzes the non-oxidative decarboxylation of pyruvate yielding acetaldehyde and carbon dioxide [37]–[42]. This enzyme can be used to directly transform

pyruvate to acetaldehyde and CO_2 [28], [29], [34]–[36] without the need, unlike other options, of any cofactor regeneration system.

1.5. References

[1] U. T. Bornscheuer, G. W. Huisman, R. J. Kazlauskas, S. Lutz, J. C. Moore, and K. Robins, "Engineering the third wave of biocatalysis," *Nature*, vol. 485, no. 7397, pp. 185–194, May 2012.

[2] R. A. Sheldon and P. C. Pereira, "Biocatalysis engineering: the big picture," *Chem. Soc. Rev*, vol. 46, pp. 2678–2691, 2017.

[3] S. Heux, I. Meynial-Salles, M. J. O'donohue, and C. Dumon, "White biotechnology: State of the art strategies for the development of biocatalysts for biorefining," *Biotechnol. Adv.*, vol. 33, pp. 1653–1670, 2015.

[4] D. J. Pollard and J. M. Woodley, "Biocatalysis for pharmaceutical intermediates : the future is now," *Trends Biotechnol.*, vol. 25, no. 2, pp. 66–73, 2006.

[5] P. Anastas and N. Eghbali, "Green chemistry: Principles and practice," *Chem. Soc. Rev.*, vol. 39, no. 1, pp. 301–312, 2010.

[6] R. A. Sheldon and J. M. Woodley, "Role of Biocatalysis in Sustainable Chemistry," *Chem. Rev.*, vol. 118, pp. 801–838, 2018.

[7] R. A. Sheldon, "Fundamentals of green chemistry: efficiency in reaction design," *Chem. Soc. Rev*, vol. 2, no. 10, pp. 1437–1451, 2012.

[8] B. Lin and Y. Tao, "Whole-cell biocatalysts by design," *Microbial Cell Factories*, vol. 16, no. 1. BioMed Central Ltd., pp. 1–12, 13-Jun-2017.

[9] S. Wenda, S. Illner, A. Mell, and U. Kragl, "Industrial biotechnology—the future of green chemistry?," *Green Chem.*, vol. 13, no. 11, p. 3007, Jan. 2011.

[10] A. Schmid, J. S. Dordick, B. Hauer, A. Kiener, M. Wubbolt, and B. Witholt, "Industrial biocatalysis today and tomorrow," *Nature*, vol. 409, no. January, pp. 258–268, 2001.

[11] J.-M. Choi, S.-S. Han, and H.-S. Kim, “Industrial applications of enzyme biocatalysis: Current status and future aspects,” *Biotechnol. Adv.*, vol. 33, no. 7, pp. 1443–1454, Nov. 2015.

[12] A. J. J. Straathof, S. Panke, and A. Schmid, “The production of fine chemicals by biotransformations,” *Curr. Opin. Biotechnol.*, vol. 13, no. 6, pp. 548–556, 2002.

[13] D. Ghislieri and N. J. Turner, “Biocatalytic Approaches to the Synthesis of Enantiomerically Pure Chiral Amines,” *Top. Catal.*, vol. 57, no. 5, pp. 284–300, Mar. 2014.

[14] K. Rosenthal and S. Lütz, “Recent developments and challenges of biocatalytic processes in the pharmaceutical industry,” *Curr. Opin. Green Sustain. Chem.*, vol. 11, pp. 58–64, Jun. 2018.

[15] H. Kohls, F. Steffen-Munsberg, and M. Höhne, “Recent achievements in developing the biocatalytic toolbox for chiral amine synthesis,” *Curr. Opin. Chem. Biol.*, vol. 19, no. 1, pp. 180–192, 2014.

[16] A. Wells and H.-P. Meyer, “Biocatalysis as a Strategic Green Technology for the Chemical Industry,” *ChemCatChem*, vol. 6, pp. 918–920, 2014.

[17] M. Breuer *et al.*, “Industrial Methods for the Production of Optically Active Intermediates,” *Angew. Chemie Int. Ed.*, vol. 43, no. 7, pp. 788–824, Feb. 2004.

[18] M. Filice and J. M. Palomo, “Cascade Reactions Catalyzed by Bionanostructures,” *ACS Catal.*, vol. 4, pp. 1588–1598, 2014.

[19] H. U. Blaser, “Industrial asymmetric catalysis: Approaches and results,” *Rend. Lincei*, vol. 18, no. 4, pp. 281–304, 2007.

[20] G. Zheng and J. Xu, “New opportunities for biocatalysis : driving the synthesis of chiral chemicals,” *Curr. Opin. Biotechnol.*, vol. 22, pp. 784–792, 2011.

[21] F. G. Mutti, C. S. Fuchs, D. Pressnitz, J. H. Sattler, and W. Kroutil, “Stereoselectivity of Four (R)-Selective Transaminases for the Asymmetric Amination of Ketones,” *Adv. Synth. Catal.*, vol. 353, no. 17, pp. 3227–3233, Nov. 2011.

[22] M. Fuchs, J. E. Farnberger, and W. Kroutil, “The Industrial Age of Biocatalytic Transamination,” *European J. Org. Chem.*, vol. 2015, no. 32, pp. 6965–6982, 2015.

[23] D. Koszelewski, I. Lavandera, D. Clay, D. Rozzell, and W. Kroutil, “Asymmetric synthesis of optically pure pharmacologically relevant amines employing ω-transaminases,” *Adv. Synth. Catal.*, vol. 350, no. 17, pp. 2761–2766, 2008.

[24] S. Arrasate, E. Lete, and N. Sotomayor, “Synthesis of enantiomerically enriched amines by chiral ligand mediated addition of organolithium reagents to imines,” *Tetrahedron: Asymmetry*, vol. 12, no. 14, pp. 2077–2082, Aug. 2001.

[25] A. Gomm and E. O’Reilly, “Transaminases for chiral amine synthesis,” *Curr. Opin. Chem. Biol.*, vol. 43, pp. 106–112, Apr. 2018.

[26] A. P. Green, N. J. Turner, and E. O’Reilly, “Chiral Amine Synthesis Using ω-Transaminases: An Amine Donor that Displaces Equilibria and Enables High-Throughput Screening,” *Angew. Chemie Int. Ed.*, vol. 53, no. 40, pp. 10714–10717, Sep. 2014.

[27] S. Schätzle, F. Steffen-Munsberg, A. Thontowi, M. Höhne, K. Robins, and U. T. Bornscheuer, “Enzymatic Asymmetric Synthesis of Enantiomerically Pure Aliphatic, Aromatic and Arylaliphatic Amines with (R)-Selective Amine Transaminases,” *Adv. Synth. Catal.*, vol. 353, no. 13, pp. 2439–2445, Sep. 2011.

[28] S. A. Kelly *et al.*, “Application of ω-Transaminases in the Pharmaceutical Industry,” *Chem. Rev.*, vol. 118, pp. 349–367, 2017.

[29] M. Höhne, S. Kühl, K. Robins, and U. T. Bornscheuer, “Efficient asymmetric synthesis of Chiral amines by combining transaminase and pyruvate decarboxylase,” *ChemBioChem*, vol. 9, no. 3, pp. 363–365, 2008.

[30] F. Guo and P. Berglund, “Transaminase biocatalysis: optimization and application,” *Green Chem.*, vol. 19, no. 2, pp. 333–360, Jan. 2017.

[31] B.-Y. Hwang and B.-G. Kim, “High-throughput screening method for the identification of active and enantioselective ω-transaminases,” *Enzyme Microb. Technol.*, vol. 34, no. 5,

pp. 429–436, Apr. 2004.

[32] M. S. Malik, E.-S. Park, and J.-S. Shin, “Features and technical applications of ω-transaminases,” *Appl. Microbiol. Biotechnol.*, vol. 94, no. 5, pp. 1163–1171, Jun. 2012.

[33] I. Slabu, J. L. Galman, R. C. Lloyd, and N. J. Turner, “Discovery, Engineering, and Synthetic Application of Transaminase Biocatalysts,” *ACS Catal.*, vol. 7, no. 12, pp. 8263–8284, 2017.

[34] S. Mathew and H. Yun, “ω-Transaminases for the Production of Optically Pure Amines and Unnatural Amino Acids,” *ACS Catal.*, vol. 2, pp. 993–1001, 2012.

[35] E. Ricca, B. Brucher, and J. H. Schrittwieser, “Multi-Enzymatic Cascade Reactions: Overview and Perspectives,” *Adv. Synth. Catal.*, vol. 353, no. 13, pp. 2239–2262, Sep. 2011.

[36] D. Koszelewski, K. Tauber, K. Faber, and W. Kroutil, “ω-Transaminases for the synthesis of non-racemic α-chiral primary amines,” *Trends in Biotechnology*, vol. 28, no. 6. pp. 324–332, Jun-2010.

[37] S. E. Lowe’ and J. G. Zeikus’, “Purification and characterization of pyruvate decarboxylase from Sarcina ventriculi,” *J. Gen. Microbiol.*, vol. 138, pp. 803–807, 1992.

[38] S. König, M. Spinka, and S. Kutter, “Allosteric activation of pyruvate decarboxylases. A never-ending story?,” *J. Mol. Catal. B Enzym.*, vol. 61, no. 1–2, pp. 100–110, 2009.

[39] D. Gocke *et al.*, “Comparative characterisation of thiamin diphosphate-dependent decarboxylases,” *J. Mol. Catal. B Enzym.*, vol. 61, pp. 30–35, 2009.

[40] K. Tittmann, A. Balakrishnan, Y. Gao, P. Moorjani, N. S. Nemeria, and F. Jordan, “Bifunctionality of the thiamin diphosphate cofactor: Assignment of tautomeric/ionization states of the 4′-aminopyrimidine ring when various intermediates occupy the active sites during the catalysis of yeast pyruvate decarboxylase,” *J. Am. Chem. Soc.*, vol. 134, no. 8, pp. 3873–3885, 2012.

[41] L. J. Van Zyl, W.-D. Schubert, M. I. Tuffin, and D. A. Cowan, “Structure and functional

characterization of pyruvate decarboxylase from Gluconacetobacter diazotrophicus," *BMC Struct. Biol.*, vol. 14, no. 21, pp. 1–13, 2014.

[42] L. Buddrus, E. S. V. Andrews, D. J. Leak, M. J. Danson, V. L. Arcus, and S. J. Crennell, "Crystal structure of an inferred ancestral bacterial pyruvate decarboxylase," *Acta Crystallogr. Sect. F Struct. Biol. Commun.*, vol. 74, no. 3, pp. 179–186, Mar. 2018.

2. Objectives

Considering the increasing importance of biocatalysis in organic synthesis, the present thesis is focused on the development and optimization of a biocatalytical approach for the synthesis of chiral amines. More specifically, the general objective is to study the feasibility of the enzymatic cascade reaction composed by transaminase (TA) and pyruvate decarboxylase (PDC) for the production of two target chiral amines: 3-amino-1-phenylbutane (3-APB) and 1-phenylethylamine (1-PEA). The mentioned cascade system consists in an asymmetric chiral amine synthesis from their corresponding prochiral ketones catalyzed by the transaminase, which presents an unfavorable equilibrium. To overcome this problem, PDC acts as a by-product removing system by transforming the resulting pyruvate to acetaldehyde and CO_2, which leads to an equilibrium shift.

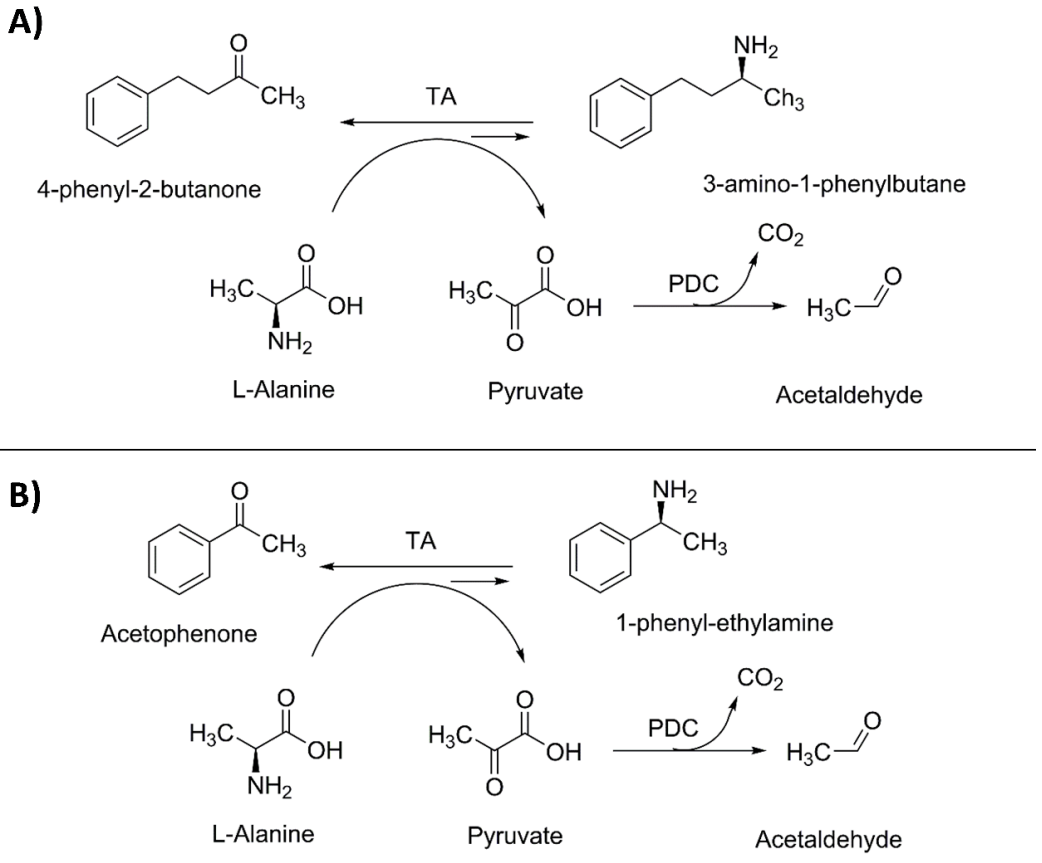

Scheme 2.1 Target enzymatic cascades studied in the present thesis. Transaminase catalyzes the transfer of an amino group from alanine to the prochiral ketones. To shift the unfavorable equilibrium, PDC transforms the resulting pyruvate to acetaldehyde and CO_2. A) Synthesis of 3-amino-1-phenylbutane (3-APB). B) Synthesis of 1-phenylethylamine (1-PEA).

The main objective has been divided in the following specific objectives:

- Considering the low commercial availability of PDC and its high cost, to obtain a recombinant *Escherichia coli* strain able to properly express *Zymobacter palmae* pyruvate decarboxylase. After that, to develop a high-cell density culture process to obtain the enzyme in high amounts.
- To characterize several available transaminases and the obtained PDC to find out the compromise reaction conditions to couple both enzymes in one-pot. Taking into account the mentioned characterizations, to select the most appropriate transaminases for the target reactions.
- After proving the feasibility of the TA and PDC cascade reactions, to optimize the reaction conditions and to maximize reaction yields by reaction medium engineering. Also to develop an amine purification process, needed for the enantiomeric excess analysis to prove the high enantioselectivity of the process.
- To develop effective immobilization processes both for TAs and PDC to obtain immobilized derivatives that can be applied in the reactions.
- After obtaining immobilized derivatives of both enzymes, to apply them in the reactions as a strategy for improving enzyme operational stability. To study the feasibility of reusing the immobilized derivatives in several reaction cycles.

3. Recombinant *Zymobacter palmae* pyruvate decarboxylase production process development

3.1. Introduction

Recombinant proteins can be expressed in several platforms including bacterial systems, yeasts, transgenic plants, mammalian cells and insect cells [1]. The choice of the most appropriate system will depend on several factors such as the final product purpose. Regarding industrial enzymes, approximately 90% of all of them are produced by recombinant microorganisms, especially for high-volume, low-value enzymes [2]. Even though nowadays a high variety of expression hosts are available, one of the most commonly used is still *Escherichia coli* [1]–[4]. This Gram-negative bacteria remains the preferred system for laboratory investigations and initial development in commercial activities and is a benchmark for comparison among the other various expression platforms [4], [5].

One of the main reasons that makes this microorganism attractive as an expression host is the large scientific knowledge about its physiology, genetics and manipulation, which has transformed it to an easy-to-handle system because of the high availability of cloning tools and expression systems [1]–[3], [6]. Moreover, it is able to grow rapidly in inexpensive culture mediums, which enables the obtaining of high cell-densities. This feature, as well as the large recombinant protein expression levels usually shown (up to 50% of the total cellular protein), makes *E. coli* a highly useful platform in the industrial point of view [1], [2], [6]. However, one of the main disadvantages is that protein is not secreted, which may complicate the downstream processes [2], [4], even though it could suppose an advantage when cell-free extracts can be used in the final product application, since the volume to purify is highly reduced. In addition, disulfide bonds may not form as intended, which lead to improper protein refolding resulting in the protein aggregation in inactive inclusion bodies [1], [2]. Finally, *E. coli* is not able to perform post-translational modifications [1], [2], [6], reason why it is not adequate for the expression of certain products.

There are several factors to take into account during the construction of a recombinant system, including the host *E. coli* strain or the vector design [1], [6]. One of the key points when choosing an appropriate vector system is the strength and control of its promoter, which must be strong enough to allow a high expression level of the recombinant protein [6]. Since leaky expression can be detrimental for cell growth, it is important to tightly regulate the basal expression by the

use of inducible promoters [3]. Among the multiple successfully used promoters, one of the most common in research and industry is *lac* and its derivatives [6]. In this system, the Lac operon repressor binds to its operator in the absence of an inducer. To start recombinant protein expression, the adequate inducer must be added to inactivate the mentioned repressor by dissociating it from the operator [3]. The most commonly used inducer is isopropyl-β-D-thiogalactopyranoside (IPTG), with which expression level can be regulated by varying its concentration into the medium [7].

After obtaining the new recombinant strain with an optimal and well-regulated protein expression, scale-up can be performed to produce the desired product in large amounts. Fermentation technology is generally applied, which provides a control of several parameters to obtain high cell densities [6]. High cell density culture (HCDC) techniques for culturing *E. coli* have been developed to improve productivity, and also to provide advantages such as reduced culture volume, enhanced downstream processing, reduced wastewater, lower production costs and reduced investment in equipment. Fed-batch operation is extensively used to obtain high cell density *E. coli* cultures, which consists in the addition of concentrated nutrient to extend cell growth. A common approach includes an initial batch phase, which is based on growing at the maximum specific growth rate that can be sustained with the nutrients initially present. When the nutrients are depleted, various regimes of nutrient feed are imposed until fermentation is completed [8]. Among the different fed-batch techniques, the most extensively used and also applied in the present thesis consists in limiting a nutrient, usually the carbon source, to maintain a constant growth rate value, but sufficiently low to avoid by-products formation, which could negatively affect the culture[9]. The use of exponential feeding has been widely used as an efficient strategy to maintain a desired specific growth rate before the induction of protein expression [6], [10], [11].

In the present chapter, all the research group experience in *E. coli* protein expression and production in HCDC [12] was applied to obtain large amounts of *Zymobacter palmae* pyruvate decarboxylase (PDC). The obtained recombinant ZpPDC was used in the further chapters to accomplish with the thesis objectives of constructing an enzymatic cascade for an efficient chiral amine production. For the first time recombinant PDC production in *E. coli* using a fed-batch strategy in bench-top bioreactor was reported [13]. Nowadays, pyruvate decarboxylase commercial availability is limited and the prices are high, reasons why the development of the mentioned strain was of high interest. The main reason of the low PDC commercial availability is that it is common in plants, yeasts and fungi but rarely found in bacteria [14], which hampers its efficient recombinant production in high amounts. Even though PDC has been identified in

several bacteria, such as *Gluconobacter oxydans* [15], *Sarcina ventriculi* [16], *Acetobacter pasteurianus* [17], *Gluconoacetobacter diazotrophicus* [18] and the one used in this thesis, *Zymobacter palmae* [14], [19], the most well-known prokaryotic PDC is from *Zymomonas mobilis* [20], [21]. In this sense, several studies have focused on the heterologous expression of *Z. mobilis* PDC, together with alcohol dehydrogenase in *E. coli* to confer it the ability of efficiently produce ethanol [22]–[26]. With the same intention, the structural gene for PDC has been cloned and overexpressed in *Hansenula polymorpha* [27]. Finally, PDCs from *Saccharomyces cerevisiae* and *Sarcina ventriculi* have been expressed in *E. coli*, but their production in high amounts have not been reported [28], [29].

3.2. Materials and methods

3.2.1. Reagents, bacterial strains and plasmids

All the reagents were purchased from Sigma Aldrich® (St. Louis, MO, USA) and were of analytical grade if not stated elsewhere.

A pJAM3440 plasmid containing the *Zymobacter palmae* PDC gene was kindly donated by the Microbiology and Cell Science Department of the University of Florida (Gaisnesville, FL, USA). To obtain a protein overproduction, the gene was cloned to a pQE-40 vector and transformed to two *E. coli* strains, M15[pREP4] and SG13009[pREP4]. M15 and SG13009 strains derived from *E. coli* K12 and have the phenotype NaIS, StrS, RifS, Thi–, Lac–, Ara+, Gal+, Mtl–, F–, RecA+, Uvr+, Lon+. Both pQE-40 and the strains were obtained from a QIAexpress type IV vector kit from Qiagen® (Venlo, Netherlands). ZpPDC gene was also cloned to a pET21d vector, which was transformed to an *E. coli* strain BL21[pLysS] from Novagen® (Merck, Darmstadt, Germany).

3.2.2. PDC cloning in *E. coli*

Plasmid pJAM3440 containing the *PDC* gene was isolated from the donated *E. coli* strain using PureYield™ Plasmid Miniprep System from Promega® (Madison, WI, USA) according to the manufacturer's instructions. Then, *PDC* was amplified by PCR using Phusion High-Fidelity DNA Polymerase from Thermo Scientific® (Waltham, MA, USA) and two primers designed with the restriction sequences of *Bam*HI and *Sal*I inserted. Double digestion of *PDC* gene, pQE-40 and pET-21d was performed with the mentioned restriction enzymes, followed by an overnight

ligation at 16ºC. After cleaning up with Wizard® SV Gel and PCR Clean-Up System (Promega®), the new plasmid constructions were transformed to M15[pREP4] and SG13009[pREP4] in the case of pQE-PDC, and to BL21[pLysS] in the case of pET-PDC. In all cases, electrocompetent cells from the mentioned strains were obtained by performing four centrifugation cycles and resuspending them in progressively lower volumes of 10 % glycerol solution. Then, transformations were carried out with a Gene Pulser II electroporator from Bio-Rad® (Hercules, CA, USA) (V= 2500 v; C= 25 μF; R= 200 Ω). Transformed clones were selected using LB-agar plates supplemented with ampicillin 100 $mg \cdot L^{-1}$ and kanamycin 0.05 $g \cdot L^{-1}$ in the case of K-12 derived strains, and with ampicillin 100 $mg \cdot L^{-1}$ and chloramphenicol 0.05 $g \cdot L^{-1}$ in the case of BL21. Transformations were confirmed by colony-PCR using GoTaq® Green Master Mix (Promega®).

3.2.3. Media composition

Luria-Bertrani (LB) medium, containing 10 $g \cdot L^{-1}$ tryptone, 5 $g \cdot L^{-1}$ yeast extract and 10 $g \cdot L^{-1}$ NaCl, was used for pre-inoculum preparations and preliminary production studies in shake-flaks.

A defined medium (DM) with glucose as the main carbon source was used for shake flasks and bioreactor cultivations. For shake flasks inoculums, the media contained 5 $g \cdot L^{-1}$ glucose, 13.2 $g \cdot L^{-1}$ K_2HPO_4, 2.6 $g \cdot L^{-1}$ KH_2PO_4, 2 $g \cdot L^{-1}$ NaCl, 4.1 $g \cdot L^{-1}$ $(NH_4)_2SO_4$, 0.5 $g \cdot L^{-1}$ $MgSO_4 \cdot 7H_2O$, 0.026 $g \cdot L^{-1}$ $FeCl_3$, 0.005 $g \cdot L^{-1}$ $CaCl_2 \cdot 2H_2O$, 0.1 $g \cdot L^{-1}$ thiamine, 0.033 $g \cdot L^{-1}$ citrate, 0.1 $g \cdot L^{-1}$ ampicillin, 0.05 $g \cdot L^{-1}$ kanamycin and 3 $mL \cdot L^{-1}$ of trace elements solution (TES) (TES: 0.04 $g \cdot L^{-1}$ $AlCl_3$, 1.74 $g \cdot L^{-1}$ $ZnSO_4 \cdot 7H_2O$, 0.16 $g \cdot L^{-1}$ $CoCl_2 \cdot 6H2O$, 1.55 $g \cdot L^{-1}$ $CuSO_4 \cdot H_2O$, 0.01 $g \cdot L^{-1}$ H_3BO_3, 1.42 $g \cdot L^{-1}$ $MnCl_2 \cdot 4H_2O$, 0.01 $g \cdot L^{-1}$ $NiCl_2 \cdot 6H_2O$, 0.02 $g \cdot L^{-1}$ Na_2MoO_4). The same composition was used for the batch phase cultivation in bioreactor but increasing glucose concentration to 25 $g \cdot L^{-1}$.

Feeding medium for fed-batch phase contained 425 $g \cdot L^{-1}$ glucose, 11.6 $g \cdot L^{-1}$ $MgSO_4 \cdot 7H_2O$, 0.6 $g \cdot L^{-1}$ $FeCl_3$, 0.35 $g \cdot L^{-1}$ thiamine, 0.09 $g \cdot L^{-1}$ $CaCl_2 \cdot 2H_2O$, 0.1 $g \cdot L^{-1}$ ampicillin, 0.05 $g \cdot L^{-1}$ kanamycin and 76.6 $mL \cdot L^{-1}$ of TES.

Stock solutions of ampicillin and kanamycin were prepared in a concentration of 10 $mg \cdot mL^{-1}$ and 50 $mg \cdot mL^{-1}$ respectively and stored at -20ºC. IPTG stock was prepared at 100 mM and stored at -20ºC.

Vitamins, antibiotics, TES $FeCl_3$, $CaCl_2 \cdot 2H_2O$ and IPTG were sterilized by filtration (0.2 μm). Glucose and saline solutions were separately sterilized by autoclaving at 121ºC for 30 minutes.

3.2.4. Cultivation conditions

3.2.4.1. Pre-inoculum

Out from cryostocks stored at -80ºC, pre-inoculums were prepared in 15 mL LB-medium containing 0.1 $mg \cdot L^{-1}$ ampicillin and 0.05 $mg \cdot L^{-1}$ kanamycin in the case of K-12 derived strains and 0.1 $mg \cdot L^{-1}$ ampicillin and 0.05 $mg \cdot L^{-1}$ chloramphenicol in the case of BL21 strain. The growth was performed in Falcon tubes overnight at 37ºC and 150 rpm.

3.2.4.2. Shake flask cultures in LB and define medium (DM)

Around 5 mL of pre-inoculum were transferred to shake flasks with 100 mL LB or defined medium containing the same antibiotic concentrations for each case previously described in order to obtain an initial optical density OD_{600} of 0.1. Cultures were maintained at 37ºC and 150 rpm until a concentration of 1 OD_{600} was reached. Then, protein production was induced by the addition of 1 mM IPTG.

3.2.4.3. Inoculum preparation for bioreactor cultures

Inoculums were prepared following the same procedure as described for shake flasks cultures in 100 mL defined medium using 10 $g \cdot L^{-1}$ of glucose. The cultures were kept at 37ºC and 150 rpm until the sufficient OD_{600} was reached to inoculate the bioreactor at an OD_{600} of around 0.1 without adding more than 10 % v v^{-1} of inoculum.

3.2.4.4. Batch cultures in bioreactor

Preliminary batch cultures were performed in an Applikon ez-Control (Applikon Biotechnology®, Delft, Netherlands) equipped with a 2 L vessel. For this cultivation, 100 mL of inoculum were transferred to the vessel containing 0.9 L of defined medium. Temperature was kept at 37ºC and pH at 7.00 by the addition of 15 % NH_4OH. Oxygen saturation was maintained at 60 % by supplying air at a flow rate of 1.5 $L \cdot min^{-1}$ and with a cascade agitation from 450 to 1150 rpm. Samples were taken every 1-2 hours to monitor cell growth and glucose consumption. Batch cultures ended when glucose was totally depleted.

3.2.4.5. Fed-batch cultures in bioreactor

Substrate limiting fed-batch cultures were performed in the same Applikon ez-Control (Applikon Biotechnology®, Delft, Netherlands) equipped with a 2 L vessel. A first batch phase was performed by transferring 80 mL of inoculum to 720 mL defined medium, which supposed an initial OD_{600} of around 0.1. Temperature was kept at 37ºC and pH at 7.00 by the addition of 15 % NH_4OH, which at the same time acts as a nitrogen source. Oxygen saturation was maintained at 60 % by supplying air at a flow rate of 1.5 $L \cdot min^{-1}$ and with a cascade agitation from 450 to 1150 rpm. When the cascade was not enough to maintain that pO_2 value, pure oxygen was added with a maximum flow rate of 0.5 $L \cdot min^{-1}$.

Substrate limiting fed-batch phase started when glucose was totally exhausted. An exponential addition of feeding medium took place to maintain a specific growth rate of 0.225 h^{-1} using an automatic microburete of 2.5 mL capacity. Equation 3.1 was applied, where ΔV is the feeding solution to add each time, X_0 biomass concentration, V_0 the liquid volume of the bioreactor, S is de glucose concentration in the feed solution, $Y_{X/S}$ is the biomass/glucose yield and μ the specific growth rate [11]. Furthermore, every 30 OD_{600} increase, 5 mL of a concentrate phosphates solution (500 $g \cdot L^{-1}$ K_2HPO_4 and 100 $g \cdot L^{-1}$ KH_2PO_4) was injected into the bioreactor, since adding higher concentration at the beginning would suppose solubility problems. When OD_{600nm} reached a value of approximately 70, IPTG was injected with a final concentration of 100 μM in order to induce protein production. Fermentation ended when a glucose accumulation was detected. Fed-batch cultures were carried out in duplicate. The calculated error indicates the confidence interval with a confidential level of 90%.

$$\Delta V = \frac{X_0 \cdot V_0}{S \cdot Y_{X/S}} \cdot (\exp(\mu \cdot t) - 1)$$

Equation 3.1

3.2.5. Analytical methods

3.2.5.1. DNA electrophoresis

DNA electrophoresis was performed in 1 % agarose gels prepared in TAE buffer with 0.1 % Syber® safe DNA gel stain (Life Technologies, Carlsbad, USA). After preparing samples with 6X DNA loading dye (Thermo scientific, Waltham, USA), gels were run at 90 V in TAE running buffer for one hour. Pictures were taken with a *Gel Doc EZ Imaging System* (Bio-Rad®) and analyzed with *Image Lab™ 6.0 Software* (Bio-Rad®).

3.2.5.2. Monitoring bacterial growth

Optical density measurements at 600 nm (OD_{600}) were performed to determine cell concentration using a HACH D3900 (Hach®, Loveland, CO, USA) spectrophotometer. Biomass concentration expressed as Dry Cell Weight was calculated considering that 1 OD_{600} is equivalent to 0.3 gDCW · L^{-1} [30]. Analyses were carried out in duplicate.

3.2.5.3. Glucose analysis

Biomass was removed from 1 mL broth sample by centrifugation and filtration (0.45 µm). The obtained supernatant was then used for the glucose analysis using an enzymatic analysis performed on an YSI 20170 system (Yellow Spring System). Analyses were carried out in duplicate.

3.2.5.4. Total protein content

Culture samples were adjusted to an OD_{600} of 4 and centrifuged at 10,000 *g* during 10 minutes at 4°C. The obtained pellet was then re-suspended in lysis buffer (200 mM citrate buffer (pH 6), 1 mM of $MgCl_2$ and 1 mM TPP). Cell suspensions were kept in ice and sonicated using Vibracell® model VC50 (Sonic & Materials, Newton, CT, USA) with four 15 seconds pulses and 2 min intervals in ice between each pulse. The lysate was then centrifuged at 10,000 *g* during 10 minutes and the clear supernatant was used for protein content analysis. Total intracellular protein content present in cell lysates was determined with the Bradford Method using Coomassie Protein Assay Reagent Kit (Thermo Scientific®) and Bovine Serum Albumin (BSA) as standard. The assays were performed in 96-microwell plates and Thermo Scentific® Multiskan FC equipment was used for the absorbance reading. Analyses were carried out in duplicate.

3.2.5.5. SDS-Page electrophoresis

To determine the percentage of enzyme among the rest of intracellular soluble proteins present in the lysates, a NuPAGE electrophoresis system (Invitrogen®, Carlsbad, CA, USA) was used. Lysates were obtained as previously described. A volume of 10 µL sample was mixed with 5 µL

NuPAGE™ LDS Sample Buffer (4X), 2 µL *NuPAGE™ Reducing Agent* (10X) and 3 µL deionized water. After 10 min incubation at 70ºC samples were charged to NuPAGE 12 % Bis-Tris electrophoresis gel and it was run using MES-SDS as running buffer at 200 V during 40 minutes. After that, the gel was fixed with a solution containing 40 % v v^{-1} and 10 % v v^{-1} acetic acid in water and stained with *Bio-Safe™ Coomassie Stain* (BIO-RAD). Pictures were taken with a *Gel Doc EZ Imaging System* (Bio-Rad®) and analyzed with *Image Lab™ 6.0 Software* (Bio-Rad®).

3.2.5.6. PDC enzymatic activity assay

PDC activity present in lysates was determined by coupling the pyruvate decarboxylation with alcohol dehydrogenase (ADH) and following NADH oxidation at 340 nm and 25ºC, whose coefficient of molar extinction (ε) is 6.22 $mM^{-1} \cdot cm^{-1}$, with a SPECORD® 200 PLUS (Analytik jena®, Jena, Germany) spectrophotometer. The reaction mixture contained 33 mM sodium pyruvate, 0.11 mM NADH, 3.5 $U \cdot mL^{-1}$ ADH from *Saccharomyces cerevisiae* (Sigma-Aldrich®), 0.1 mM TPP and 0.1 mM $MgCl_2$ in citrate buffer 200 mM and pH 6. One unit of enzyme activity corresponds to the amount of pyruvate decarboxylase that converts 1 µmole of pyruvate to acetaldehyde per minute.

3.3. Results and discussion

3.3.1. Obtaining a new PDC-producer *E. coli* strain

Regarding the low commercial availability of pyruvate decarboxylase, which can only be acquired in small quantities with high prices, the development of new *E. coli* strains able to overexpress the enzyme was of high interest. For this reason, *Zymobacter palmae pdc* gene was obtained thanks to the kind collaboration of Microbiology and Cell Science Department of the University of Florida. *Zymobacter palmae* is one of the few bacteria in which pyruvate decarboxylase has been found [19]. This microorganism was originally isolated from palm sap and characterized as a gram-negative and facultatively anaerobic bacteria able to produce ethanol as a fermentation product from different sugars [14], [31], [32]. The presence of PDC was afterwards established by Raj 2002 [14], which cloned the *Z. palmae pdc* gene, expressed it to *E. coli* and carried out several enzyme characterizations [14]. The next step, which was the aim of this thesis, was to clone the gene to a suitable strain for its production in high amounts.

Z. palmae pdc gene (2007 pb) was amplified from pJAM3440 plasmid by PCR using two primers in which different restriction sites had been inserted: *Bam*HI in the forward and *Sal*I in the reverse. Confirmation that the amplification had taken place was performed by the DNA electrophoresis shown in Figure 3.1. After that, the mentioned restriction enzymes were used to perform a double digestion of *pdc* gene. At the same time, double digestion was also applied to the two different plasmids considered for the construction of two different producer strains: pQE-40 and pET21d. Electrophoresis images shown in Figure 3.2 proved that restriction was successful since, when the two restriction enzymes were used, a band of around 500 bp appeared, which corresponds to the deleted plasmid sequence. The 3433 bp band of pQE, 5421 bp band of pET and the digested pdc band (2013 bp) were recovered and purified. Afterwards, an overnight ligation at 16ºC was performed.

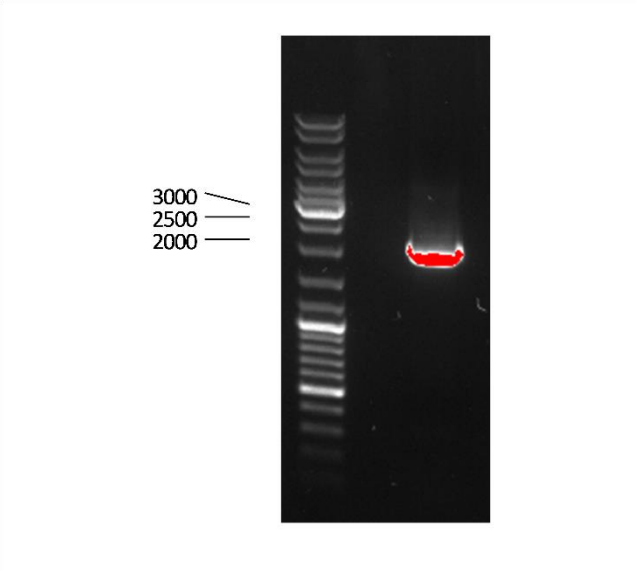

Figure 3.1 Electrophoresis gel image of PDC gene amplification from Escherichia coli DH5α pJAM3440 by PCR. The band observed of around 2000 bp corresponds to the PDC gene.

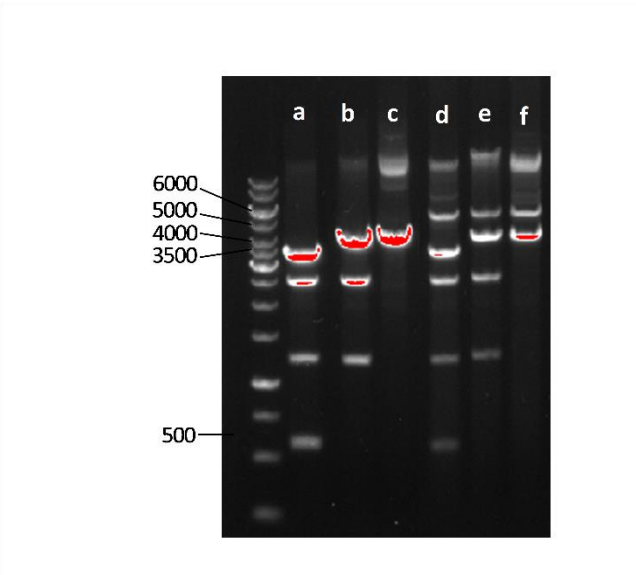

Figure 3.2 Electrophoresis gel image obtained after the plasmid digestion by the restriction enzymes SalI and BamHI. a) pQE-40 double digestion. b) pQE-40 digestion with SalI. c) pQE-40 digestion with BamHI. d) pET 21d double digestion. e) pET 21d digestion with SalI. f) pET 21d digestion with BamHI.

The resulting pQE-PDC plasmid was introduced by electroporation to two different K12-derived *E.coli* strains: M15[pREP4] and SG13009[pREP4]. The other recombinant vector (pET-PDC) was used to transform a BL21[pLysS] strain. In order to select strains that had properly incorporated the desired plasmids, LB-agar plates containing different antibiotics were prepared. The K12-derived transformants were able to grow in LB-agar plates with Ampicillin and Kanamycin, while the BL21[pLysS][pET-PDC] transformants were selected on LB-agar with Ampicillin and Chloramphenicol. In all cases, several clones were recovered and the presence of the plasmid which contained the *pdc* gene was confirmed by colony PCR.

To prove and compare the capability of the three new strains (M15[pREP4][pQE-PDC], SG13009[pREP4][pQE-PDC] and BL21[pLysS][pET-PDC]) to grow and produce PDC, one clone of each one was selected for further studies. Afterwards, preliminary cultures were performed in shake flasks with 100 mL LB medium supplemented with the corresponding antibiotics. Results are exposed and discussed in the following sections.

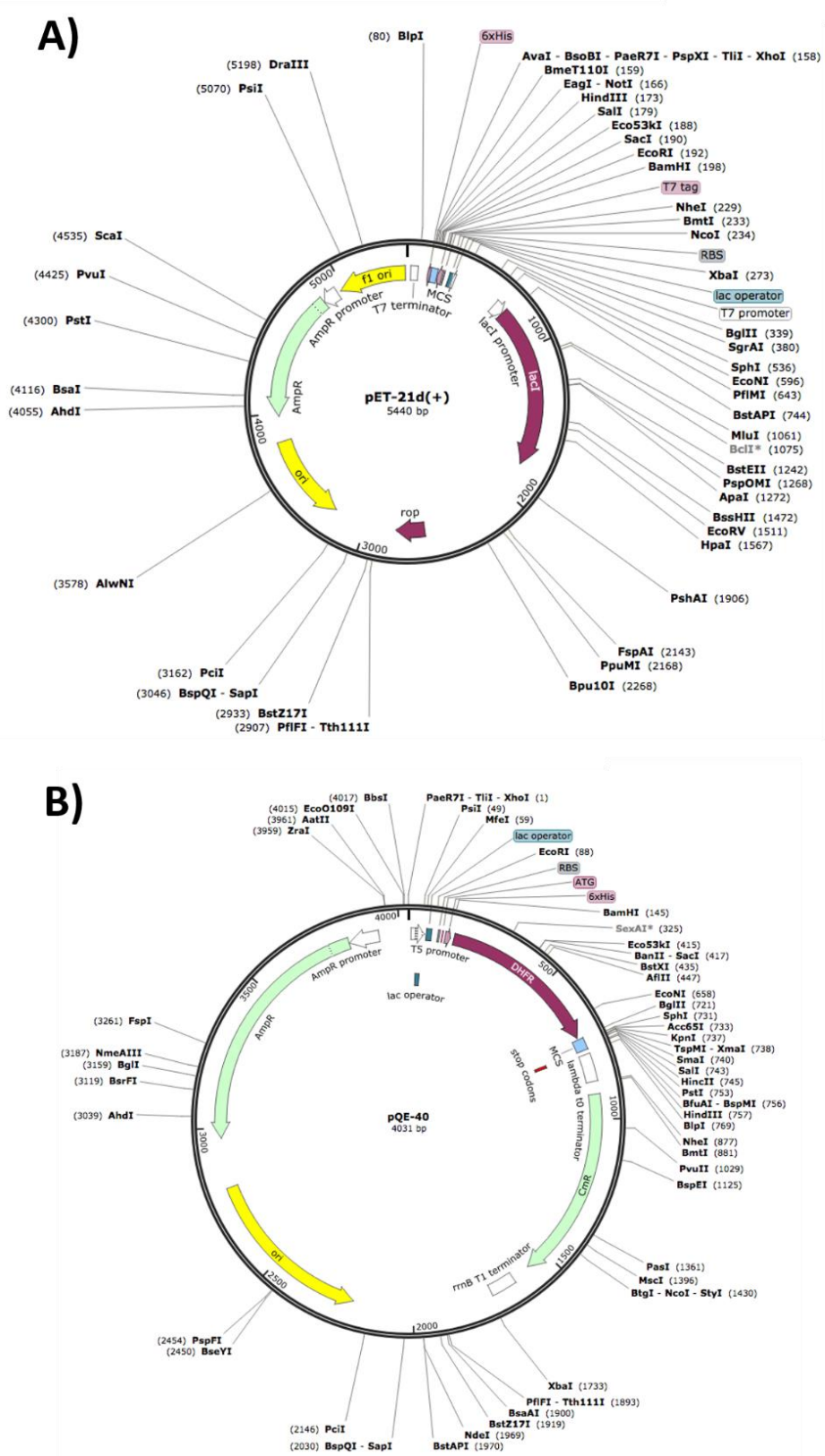

Figure 3.3 Plasmids used for the construction of two different expression vectors. A) pET-21d, which was transformed to a BL21 strain. B) pQE-40, which was used to transform two K12-derived strains: M15[pREP4] and SG13009[pREP4].

3.3.1.1. Strains M15 and SG13009

Commercial pQE vectors (QIAGEN) are characterized for having the T5 promoter and two *lac* operator sequences [33], which ensure the repression of T5 promoter and thus an optimum expression control [34], [35]. The new pQE-PDC plasmid obtained was transformed to the commercial M15[pREP4] and SG13009[pREP4] host strains obtained from the same supplier. These strains contain the low-copy plasmid pREP4, which constitutively expresses the *lac* repression protein [35]. This protein binds to the pQE *lac* operators and can easily be inactivated by the addition of IPTG.[33]. Therefore, the system presents a tight expression control, since basal recombinant protein production can be maintained at low levels and starts when it is induced.

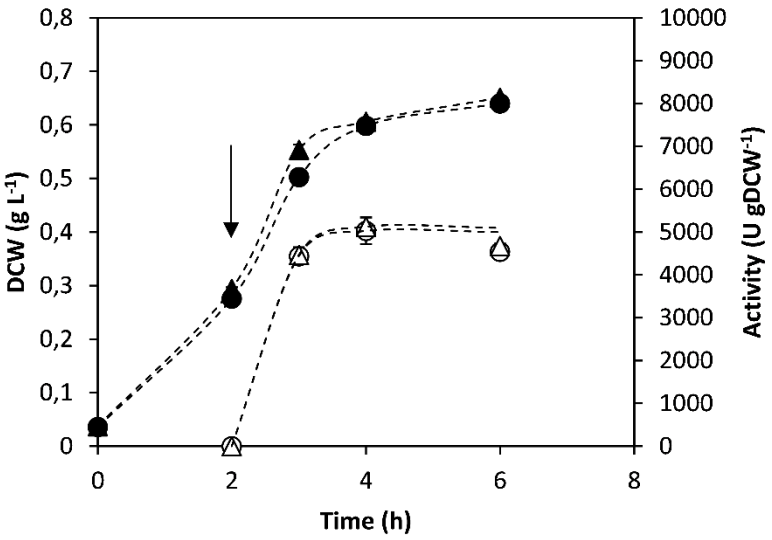

Figure 3.4 Growth and PDC activity profiles obtained during shake-flask cultures in LB-medium of the K12-derived strains in which pQE-PDC plasmid was transformed. (●) Biomass for M15[pREP4][pQE-PDC]. (▲) Biomass for SG13009[pREP4][pQE-PDC]. (○) PDC activity for M15[pREP4][pQE-PDC]. (△) PDC activity for SG13009[pREP4][pQE-PDC]. The arrow indicates the IPTG pulse for induction. Temperature 37ºC; 150 rpm.

Cell-growth profiles and PDC production were studied, as well as the capability of the new recombinant strains to overexpress PDC (Figure 3.4). Both in the case of M15[pREP4][pQE-PDC] and SG13009[pREP4][pQE-PDC], growth took place with a maximum specific growth rate of around 0.9 h^{-1} and a final biomass concentration of about 0.65 $gDCW \cdot L^{-1}$ was achieved. During the exponential growth phase an early pulse of IPTG was applied at 0.3 $gDCW \cdot L^{-1}$ approximately

with a final concentration of 1 mM in order to induce PDC expression. In both cases, 2 hours after induction, a maximum activity of around 5000 U·gDCW^{-1} was achieved and the culture contained a total protein concentration of about 230 mg protein per gDCW^{-1}. Moreover, neither PDC activity nor PDC protein (Figure 3.5) were detected in the samples taken before induction, thus indicating that the PDC promoter was strongly repressed by pREP4 plasmid in both strains. Therefore, both M15[pREP4][pQE-PDC] and SG13009[pREP4][pQE-PDC] were selected as possible candidates to scale-up the PDC production in bioreactor.

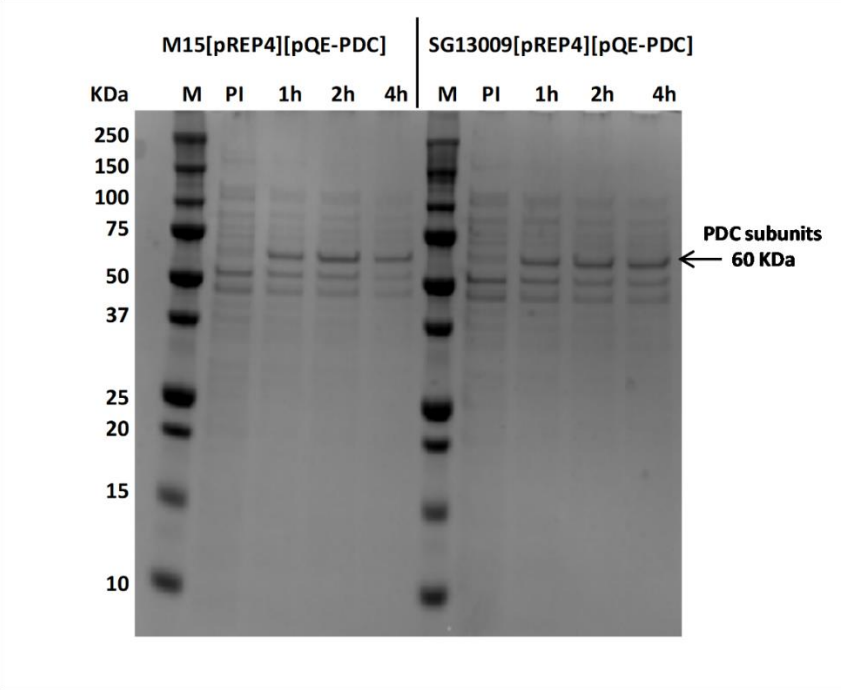

Figure 3.5 SDS-Page electrophoresis of M15[pREP4][pQE-PDC] and SG13009[pREP4][pQE-PDC] samples from shake-flask cultures in LB-medium. M: molecular weight marker. PI: pre-induction sample. 1,2 and 4 h: time after induction with IPTG. PDC subunits correspond to the 60 kDa bands.

3.3.1.2. Strain BL21

Unlike pQE plasmid systems, pET vectors (Novagen) are based on T7 promoter [1], [34], [36]. The pET-PDC construction was transformed to a BL21 strain, in which T7 RNA polymerase is present under the control of the IPTG-inducible *lacUV5* promoter [34]. The strain also included the pLysS vector, which expresses T7 lysozyme to tighten the regulation by suppressing the basal expression of T7 RNA polymerase before induction [34], [37], [38].

Cell-growth of BL21[pLysS][pET-PDC] in LB-medium (Figure 3.6 A) took place with a maximum specific growth rate of 0.66 h^{-1} and a final biomass concentration of 0.88 gDCW·L^{-1} was achieved. However, after induction with 1 mM IPTG at a biomass concentration of about 0.3 gDCW·L^{-1}, no PDC activity was detected. The expected protein bands at a molecular mass of 60 KDa, corresponding to the PDC subunits, did not appear in electrophoresis gel images neither before induction nor after it (Figure 3.6 A). Therefore, the obtained strain was not able to express the *pdc* gene, reason for why it was discarded for further scale-up experiments.

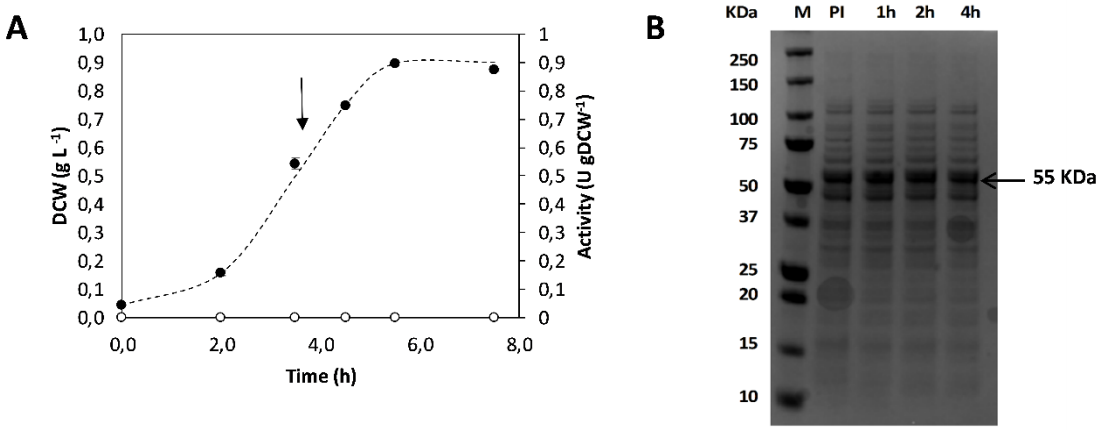

Figure 3.6 A) Growth and PDC activity profiles obtained during shake-flask cultures in LB-medium of BL21[plysS][pET-PDC] (Temperature 37°C; 150 rpm) (●) Biomass concentration. (○) PDC activity. The arrow indicates the IPTG pulse for induction. B) SDS-Page electrophoresis of BL21[pLysS][pET-PDC] samples from shake-flask cultures in LB-medium. M: molecular weight marker. PI: pre-induction sample. 1,2 and 4 h: time after induction with IPTG. PDC subunits corresponding to 60 kDa bands were not detected.

3.3.2. Production process development

After the preliminary LB-medium shake-flask cultures, two strains were selected as possible candidates for PDC production in higher scales: M15[pREP4][pQE-PDC] and SG13009[pREP4][pQE-PDC]. With the aim of developing a high cell-density culture for PDC production in high amounts, further experiments were performed with the mentioned strains.

3.3.2.1. Shake-flasks cultures in defined medium

An essential step before developing a large scale high cell-density cultures is to optimize the process at small scale. In this sense, medium composition is a key factor for optimum cell growth and for the enhancement of recombinant protein expression [1]. Since the main objective was to develop a substrate-limiting fed-batch strategy, the selected strains had to be adapted to defined medium. It is desirable to use this kind of medium during fermentations because it has a well-known composition which can be controlled during the culture [8]. In contrast, using mediums with complex and poorly defined ingredients could lead to non-desired performance variations that could affect product yield and quality [6], [39].

Shake-flask defined medium cultures were performed with the two strains which showed a recombinant expression of PDC: M15[pREP4][pQE-PDC] and SG13009[pREP4][pQE-PDC]. Under these conditions both *E. coli* strains showed longer initial lag phases, which led to lower specific growth rates than in previous shake-flask cultures with LB (**¡Error! No se encuentra el origen de la referencia.**). Even though similar specific growth rates and final biomass concentrations were obtained in all defined medium cultures, PDC specific activity was 1.7-fold higher with SG13009[pREP4][pQE-PDC] compared to M15[pREP4][pQE-PDC]. Moreover, PDC activity per gram of dry-cell weight was 2.4-fold higher in the case of SG13009[pREP4][pQE-PDC]. According to these results, SG13009[pREP4][pQE-PDC] was selected for further scale-up experiments.

Table 3.1 Maximum specific growth rates (h^{-1}), specific PDC activities per total protein content (U mg^{-1}) and final biomass concentrations (gDCW L^{-1}) obtained in shake flask cultures of M15[pREP4][pQE-PDC] and SG13009[pREP4][pQE-PDC] grown with defined medium.

Strain	Maximum specific growth rate (h^{-1})	Specific activity ($U \cdot mg^{-1}$)	Final biomass concentration ($gDCW \cdot L^{-1}$)	Activity per biomass ($U \cdot gDCW^{-1}$)
M15[pREP4][pQE-PDC]	0.43	3.19	0.456	1083.36
SG13009[pREP4][pQE-PDC]	0.41	5.23	0.408	2606.93

3.3.2.2. PDC production in bioreactor cultures using a substrate-limiting fed-batch strategy

Finally, high cell-density cultures of the new PDC-producing strain were obtained by developing a limiting fed-batch strategy in bench-top scale bioreactor. As it has been mentioned, this strategy starts with an initial batch phase [8], [40], which in this case was performed as described in the previous section. As it is well-known, glucose consumption by *E. coli* leads to acetate excretion as a major by-product, which has inhibitory effects on cell growth and protein expression [42]. For this reason, when glucose present into the initial medium is depleted, it is feed in a controlled manner so that it does not exceed certain concentrations which would enhance acid generation [40], [43]. Several feeding strategies have been described to modulate growth rate and achieve high biomass concentrations and maximize protein expression [44]. In this case, an exponential feeding was applied to maintain a constant specific growth rate [9] which was previously established for the cultivation of similar strains in the same research group [45].

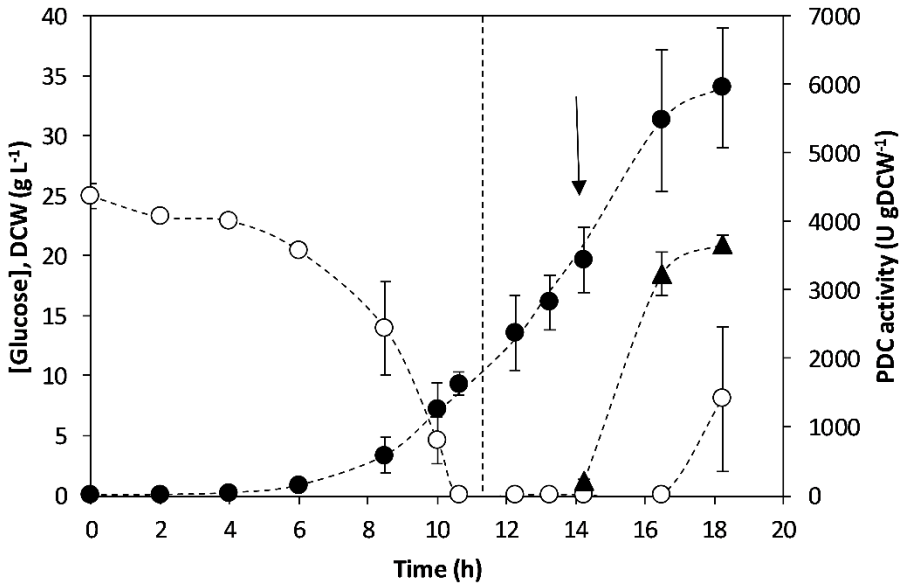

Figure 3.7 PDC production in fed-batch culture in a 2L-bioreactor using the strain SG13009[pREP4][pQE-PDC]. (●) Biomass concentration. (○) Glucose concentration. (▲) PDC activity. The start of the fed-batch phase is represented with the vertical dotted line. The arrow indicates the IPTG pulse for induction.

Figure 3.7 shows glucose, DCW, and specific PDC activity profile along the time. This time, batch phase took place with a maximum specific growth rate of 0.51 h^{-1}. Moreover, due to a longer lag

phase that delayed the total glucose depletion, batch phase lasted 11 hours. Final biomass concentration reached was 9.32 gDCW·L^{-1} and the yield was 0.37 gDCW·g glucose^{-1}, which agrees with previous experiments. Substrate limiting fed-batch phase was then started to maintain a constant growth rate of 0.22 h^{-1}. Once biomass reached 20 g L^{-1} (3.5 hours of fed-batch phase) the induction was performed adding a pulse of IPTG, reaching a concentration in the bioreactor of 100 µM. The culture was stopped after 4 hours post-induction since the glucose started to accumulate in the media, probably due to cellular metabolic stress [31], [41]–[43]. The maximum biomass concentration and PDC specific activity were 34 gDCW·L^{-1} and 3677 U·gDCW^{-1}, respectively. Enzyme volumetric productivity was also calculated achieving 6942 U·L^{-1}·h^{-1}. Protein analysis revealed a total protein concentration of 432 mg·gDCW^{-1} with a 30 % of PDC (128 mg PDC·gDCW^{-1}) which means a quality of 29 U mg·PDC^{-1}. Similar values have been obtained previously by the research group applying the substrate limiting fed-batch strategy with IPTG pulse induction. The production of rhamnulose-1-phosphate aldolase (RhuA) expressed *in E. coli* M15ΔGlyA [pREP4] following the aforementioned strategy led to 160 mgRhuA gDCW^{-1} and 25.5 gDCW L^{-1} [46].

3.4. Conclusions

Two new PDC-producing *E. coli* strains able to overexpress high protein levels (up to 30%) with an effective repression system were obtained by cloning the *Z. palmae* PDC gene: M15[pREP4][pQE-PDC] and SG13009[pREP4][pQE-PDC]. After a preliminary selection, a production process was developed by scaling up SG13009[pREP4][pQE-PDC] in a bench-top bioreactor applying a substrate-limited fed-batch. This strategy led to a volumetric productivity of 6942 U L^{-1} h^{-1} and a final PDC specific activity of 3677 U $gDCW^{-1}$.

3.5. References

[1] N. K. Tripathi, “Production and Purification of Recombinant Proteins from *Escherichia coli*,” *ChemBioEng Rev.*, vol. 3, no. 3, pp. 116–133, Jun. 2016.

[2] R. da G. Ferreira, A. R. Azzoni, and S. Freitas, “Techno-economic analysis of the industrial production of a low-cost enzyme using E. coli: the case of recombinant β-glucosidase,” *Biotechnol. Biofuels*, vol. 11, no. 1, pp. 81–94, Dec. 2018.

[3] W. Schumann and L. C. S. Ferreira, “Production of recombinant proteins in Escherichia

coli," *Genet. Mol. Biol.*, vol. 27, no. 3, pp. 442–453, 2004.

[4] R. Chen, "Bacterial expression systems for recombinant protein production: E. coli and beyond," *Biotechnol. Adv.*, vol. 30, pp. 1102–1107, 2011.

[5] P. T. Wingfield, "Overview of the Purification of Recombinant Proteins," *Curr Protoc Protein Sci*, vol. 80, pp. 1–50, 2016.

[6] C.-J. Huang, H. Lin, and X. Yang, "Industrial production of recombinant therapeutics in Escherichia coli and its recent advancements," *J. Ind. Microbiol. Biotechnol.*, vol. 39, no. 3, pp. 383–399, Mar. 2012.

[7] J. Pinsach, C. de Mas, and J. López-Santín, "Induction strategies in fed-batch cultures for recombinant protein production in Escherichia coli: Application to rhamnulose 1-phosphate aldolase," *Biochem. Eng. J.*, vol. 41, no. 2, pp. 181–187, Sep. 2008.

[8] S. Y. Lee, "High cell-density culture of Escherichia coli," *Ibtech*, vol. 14, pp. 98–105, 1996.

[9] M. A. Eiteman and E. Altman, "Overcoming acetate in Escherichia coli recombinant protein fermentations," *Trends Biotechnol.*, vol. 24, no. 11, pp. 530–536, 2006.

[10] B. H. Yee L, "Recombinant Protein Expression in High Cell Density Fed-Batch Cultures of Escherichia Coli," *BIOTECHNOLOGY*, vol. 10, pp. 1550–1556, 1992.

[11] O. Durany, C. de Mas, and J. López-Santín, "Fed-batch production of recombinant fuculose-1-phosphate aldolase in E. coli," *Process Biochem.*, vol. 40, no. 2, pp. 707–716, Feb. 2005.

[12] J. Ruiz *et al.*, "Alternative production process strategies in E. coli improving protein quality and downstream yields," *Process Biochem.*, vol. 44, no. 9, pp. 1039–1045, Sep. 2009.

[13] N. Alcover, A. Carceller, G. Álvaro, and M. Guillén, "Zymobacter palmae pyruvate decarboxylase production process development: Cloning in Escherichia coli, fed-batch culture and purification," *Eng. Life Sci.*, vol. 19, no. 7, pp. 502–512, 2019.

[14] K. C. Raj, L. A. Talarico, L. O. Ingram, and J. A. Maupin-furlow, "Cloning and Characterization of the Zymobacter palmae Pyruvate Decarboxylase Gene (pdc) and Comparison to Bacterial Homologues," *Appl. Environ. Microbiol.*, vol. 68, no. 6, pp. 2869–2876, 2002.

[15] L. J. Van Zyl, M. P. Taylor, K. Eley, M. Tuffin, and D. a. Cowan, "Engineering pyruvate

decarboxylase-mediated ethanol production in the thermophilic host Geobacillus thermoglucosidasius," *Appl. Microbiol. Biotechnol.*, vol. 98, no. 3, pp. 1247–1259, 2014.

[16] S. E. Lowe and J. G. Zeikus, "Purification and characterization of pyruvate decarboxylase from Sarcina ventriculi," *J. Gen. Microbiol.*, vol. 138, no. May, pp. 803–807, 1992.

[17] K. Chandra Raj, L. Ingram, and J. Maupin-Furlow, "Pyruvate decarboxylase: a key enzyme for the oxidative metabolism of lactic acid by Acetobacter pasteurianus," *Arch. Microbiol.*, vol. 176, no. 6, pp. 443–451, Dec. 2001.

[18] L. J. Van Zyl, W.-D. Schubert, M. I. Tuffin, and D. A. Cowan, "Structure and functional characterization of pyruvate decarboxylase from Gluconacetobacter diazotrophicus," *BMC Struct. Biol.*, vol. 14, no. 21, pp. 1–13, 2014.

[19] L. Buddrus, E. S. V Andrews, D. J. Leak, M. J. Danson, V. L. Arcus, and S. J. Crennell, "Crystal structure of pyruvate decarboxylase from Zymobacter palmae," *Acta Crystallogr. Sect. F Struct. Biol. Commun.*, vol. 72, pp. 700–706, 2016.

[20] D. Dobritzsch, S. KÃ\Pnig, G. Schneider, and G. Lu, "High resolution crystal structure of pyruvate decarboxylase from Zymomonas mobilis," *J. Biol. Chem.*, vol. 273, no. 32, pp. 20196–20204, 1998.

[21] J. M. Candy and R. G. Duggleby, "Structure and properties of pyruvate decarboxylase and site-directed mutagenesis of the Zymomonas mobilis enzyme," *Biochim. Biophys. Acta - Protein Struct. Mol. Enzymol.*, vol. 1385, pp. 323–338, 1998.

[22] H. Bräu, Barbara; Sahm, "Cloning and expression of the structural gene for pyruvate decarboxylase of Zymomonas mobilis in Escherichia coli," *Arch. Microbiol.*, vol. 144, pp. 296–301, 1986.

[23] K. Ohta, D. S. Beall, J. P. Mejia, K. T. Shanmugam, and L. O. Ingram, "Genetic improvement of Escherichia coli for ethanol production: chromosomal integration of Zymomonas mobilis genes encoding pyruvate decarboxylase and alcohol dehydrogenase II.," *Appl. Environ. Microbiol.*, vol. 57, no. 4, pp. 893–900, Apr. 1991.

[24] L. O. Ingram *et al.*, "Enteric Bacterial Catalysts for Fuel Ethanol Production," *Biotechnol. Prog.*, vol. 15, no. 5, pp. 855–866, Oct. 1999.

[25] A. J. Lewicka *et al.*, "Fusion of Pyruvate Decarboxylase and Alcohol Dehydrogenase Increases Ethanol Production in Escherichia coli," *ACS Synth. Biol.*, vol. 3, pp. 976–978, 2014.

[26] M. Yang *et al.*, “Pyruvate decarboxylase and alcohol dehydrogenase overexpression in Escherichia coli resulted in high ethanol production and rewired metabolic enzyme networks,” *World J. Microbiol. Biotechnol.*, vol. 30, no. 11, pp. 2871–2883, Nov. 2014.

[27] O. P. Ishchuk *et al.*, “Overexpression of pyruvate decarboxylase in the yeast *Hansenula polymorpha* results in increased ethanol yield in high-temperature fermentation of xylose,” *FEMS Yeast Res.*, vol. 8, no. 7, pp. 1164–1174, Nov. 2008.

[28] J. M. Candy, R. G. Duggleby, and J. S. Mattick, “Expression of active yeast pyruvate decarboxylase in Escherichia coli,” *J. Gen. Microbiol.*, vol. 137, no. 12, pp. 2811–2815, 1991.

[29] L. A. Talarico, L. O. Ingram, and J. A. Maupin-Furlow, “Production of the gram-positive Sarcina ventriculi pyruvate decarboxylase in Escherichia coli,” *Microbiology*, vol. 147, no. 9, pp. 2425–2435, 2001.

[30] L. Vidal, J. Pinsach, G. Striedner, G. Oria Caminal, and P. Ferrer, “Development of an antibiotic-free plasmid selection system based on glycine auxotrophy for recombinant protein overproduction in Escherichia coli,” *J. Biotechnol.*, vol. 134, pp. 127–136, 2008.

[31] T. Okamoto, H. Taguchi, K. Nakamura, H. Ikenaga, H. Kuraishi, and K. Yamasato, “Zymobacter palmae gen. nov., sp. nov., a new ethanol-fermenting peritrichous bacterium isolated from palm sap,” *Arch. Microbiol.*, vol. 160, no. 5, pp. 333–337, 1993.

[32] T. Okamoto, H. Taguchi, K. Nakamura, and H. Ikenaga, “Production of ethanol from maltose by Zymobacter palmae fermentation,” *Biosci. Biotechnol. Biochem.*, vol. 58, no. 7, pp. 1328–1329, 1994.

[33] Qiagen, *The QIA expressionist Handbook, 5th Ed.*, no. June. 1991.

[34] G. L. Rosano and E. A. Ceccarelli, “Recombinant protein expression in Escherichia coli: advances and challenges,” *Front. Microbiol.*, vol. 5, no. 172, pp. 1–17, Apr. 2014.

[35] G. Jee Gopal and A. Kumar, “Strategies for the Production of Recombinant Protein in Escherichia coli,” *Protein J*, vol. 32, pp. 419–425, 2013.

[36] B. Intl, “Process Development Forum - Optimization of Protein Expression in Escherichia Coli,” vol. 21, pp. 42–45, 2015.

[37] C. P. Papaneophytou and G. Kontopidis, “Statistical approaches to maximize recombinant protein expression in Escherichia coli: A general review,” *Protein Expr. Purif.*, vol. 94, pp.

22–32, 2013.

[38] Novagen, “Competent Cells: What a difference a strain makes !”

[39] J. Zhang and R. Greasham, “Chemically defined media for commercial fermentations,” *Appl. Microbiol. Biotechnol.*, vol. 51, no. 4, pp. 407–421, Apr. 1999.

[40] D. Riesenberg and R. Guthke, “High-cell-density cultivation of microorganisms,” *Appl. Microbiol. Biotechnol.*, vol. 51, no. 4, pp. 422–430, Apr. 1999.

[41] M. Pasini, “Robust microbial construction and efficient processes for recombinant enzymes production in Escherichia coli,” Universitat Autònoma de Barcelona, 2015.

[42] Z. Kang, Y. Geng, Y. zhen Xia, J. Kang, and Q. Qi, “Engineering Escherichia coli for an efficient aerobic fermentation platform,” *J. Biotechnol.*, vol. 144, no. 1, pp. 58–63, Oct. 2009.

[43] T. W. Overton, “Recombinant protein production in bacterial hosts,” *Drug Discov. Today*, vol. 19, no. 5, pp. 590–601, May 2014.

[44] W.-D. Riesenberg, D. ; Schulz, V. ; Knorre, W.A. ; Pohl, H.-D ; Korz, D. ; Sanders, E.A. ; Ross, A. ; Deckwer, “High cell density cultivation of Escherichia coli at controlled specific growth rate,” *J. Biotechnol.*, vol. 20, no. 1, pp. 17–27, 1991.

[45] J. Ruiz, G. González, C. de Mas, and J. López-Santín, “A semiempirical model to control the production of a recombinant aldolase in high cell density cultures of Escherichia coli,” *Biochem. Eng. J.*, vol. 55, no. 2, pp. 82–91, Jul. 2011.

[46] J. Ruiz, A. Fernández-Castané, C. de Mas, G. González, and J. López-Santín, “From laboratory to pilot plant E. coli fed-batch cultures: optimizing the cellular environment for protein maximization,” *J. Ind. Microbiol. Biotechnol.*, vol. 40, no. 3–4, pp. 335–343, Apr. 2013.

[47] T. Schweder, H. Lin, B. Jürgen *et al.*, “Role of the general stress response during strong overexpression of a heterologous gene in Escherichia coli,” *Appl. Microbiol. Biotechnol.*, vol. 58, no. 3, pp. 330–337, Mar. 2002.

[48] M. Mühlmann, E. Forsten, S. Noack, and J. Büchs, “Optimizing recombinant protein expression via automated induction profiling in microtiter plates at different temperatures,” *Microb. Cell Fact.*, vol. 16, no. 1, pp. 220–232, Dec. 2017.

4. Transaminase and PDC initial characterizations and screening

4.1. Introduction

In the present thesis, as it has already been exposed, two different kinds of enzymes were used to generate an one-pot cascade reaction for the synthesis of chiral amines: transaminases and pyruvate decarboxylase. Transaminases (TA) or aminotransferases (EC 2.6.1.x) are pyridoxal phosphate (PLP)-dependent enzymes, which catalyze the transfer of an amino group from an amino donor to an amino acceptor (usually a ketone or aldehyde) [1]–[6]. In nature, they play a central role in nitrogen metabolism of several organisms ranging from bacteria to mammals, since they are responsible of the transfer of amino groups from α-amino acids to α-keto acids [2], [5], [7]. From an industrial point of view, they have been extensively studied because of their ability to perform a direct asymmetric amination of prochiral ketone substrates, producing optically pure amino acids and chiral amines [8], [9].

PLP-dependent enzymes are a large class of enzymes which use the vitamin B6-based pyridoxal-5'-phosphate as a cofactor and are able to catalyze a wide range of reactions including transamination, racemization, decarboxylation, substitution and elimination [10]. They are involved in several pathways, such as aminoacids or aminosugars biosynthesis [4]. This enzyme superfamily is divided into 7 major groups depending on its fold-type [4], [11], [12]. From these groups, transaminases are only found in fold-type I, which are S selective, and fold-type IV, which are R selective [8], [11], [13]. According to the relative position of the amino group to be transferred with respect to the carboxyl group of the substrate, transaminases have been broadly classified into α-TAs and ω-TAs [7], [9]. The first ones require the presence of a carboxylic acid group in the α-position to the keto or amine functionality, allowing only the α-aminoacid formation [6], [7], [11]. In contrast, ω-transaminases can convert aliphatic ketones and amines without a carboxylate group in the α-position [14]. An important subgroup of ω-TAs are amine transaminases (ATAs), which can accept substrates that completely lack a carboxylate group, which is highly attractive into the industrial point of view since it confers them the potential of synthesizing chiral primary amines from the corresponding prochiral ketones [13].

The most well-known and employed ATAs are biologically active as dimers or higher oligomers, and they require the coordination of PLP in the active site to perform transamination [8], [15]. Transamination reaction is divided in two half reactions: oxidative deamination of the amino donor and reductive amination of the amine acceptor [1], [3] (Figure 4.1). In these half reactions, PLP acts as a molecular shuttle transporting the amino group [7], [8], [16]. Concretely, a

ping-pong bi-bi mechanism takes place [4], [11], [17]. PLP, which forms a Schiff base with an active site lysine, is firstly aminated resulting in the formation of pyridoxamine-5'-phosphate (PMP), while the respective keto product of the amino donor is released [3], [11], [16]. After that, the amino group from PMP is transferred to the acceptor molecule producing the aminated product and regenerating PLP for the next catalytic cycle [11], [16].

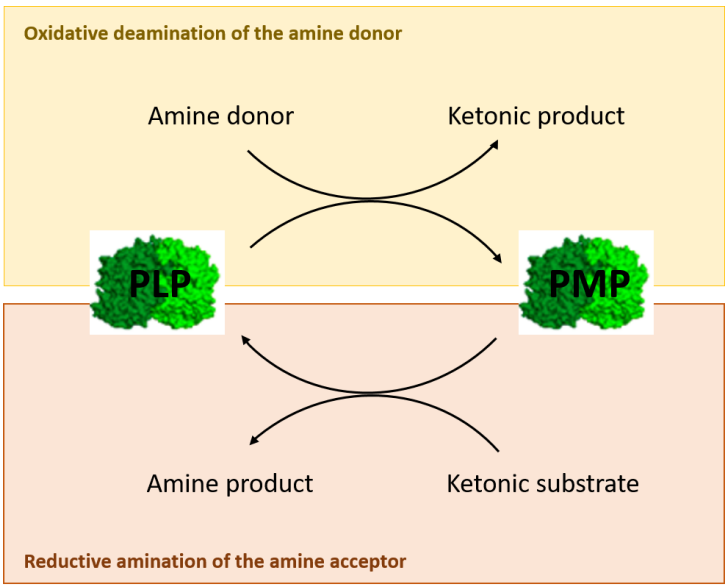

Figure 4.1 Reaction mechanism of the most well-kown transaminases. PLP, coordinated in the active center acts as a molecular shuttle transporting the amino group in two different half-reactions. Source: Börner 2016 [8].

Focusing now on pyruvate decarboxylase (E.C.4.1.1.1), it is a thiamine pyrophosphate and Mg^{2+} ion-dependent enzyme that catalyzes the non-oxidative decarboxylation of pyruvate yielding acetaldehyde and carbon dioxide [18]–[23]. PDC is a key enzyme in the glycolytic pathway and ethanol fermentation [24]–[27] since, together with alcohol dehydrogenase (ADH), which reduces acetaldehyde to ethanol with the help of the co-substrate NADH, enables the conversion of pyruvate to ethanol [19], [28]. In nature it can be widely found in plants, yeast and fungui, it is absent in animals and rare in prokaryotes [24], [29], [30]. Currently, only six bacterial PDCs has been described, even though they have attracted extensive attention in the development of new ethanologenic strains [23], [31]. These mentioned PDCs are from *Acetobacter pasteurianus* (ApPDC), *Gluconoacetobacter diazotrophicus* (GdPDC), *Gluconobacter oxydans* (GoPDC), *Zymobacter palmae* (ZpPDC), *Zymomonas mobilis* (ZmPDC) and *Sarcina*

ventriculi (SvPDC) [23]. In addition to its key role on ethanol fermentation, PDC is also commercially attractive because it is able to catalyze carboligation reactions such as the synthesis of R-phenylacetylcarbinol (R-PAC), a key pharmaceutical precursor of ephedrine and pseudoephedrine [25], [32], [33].

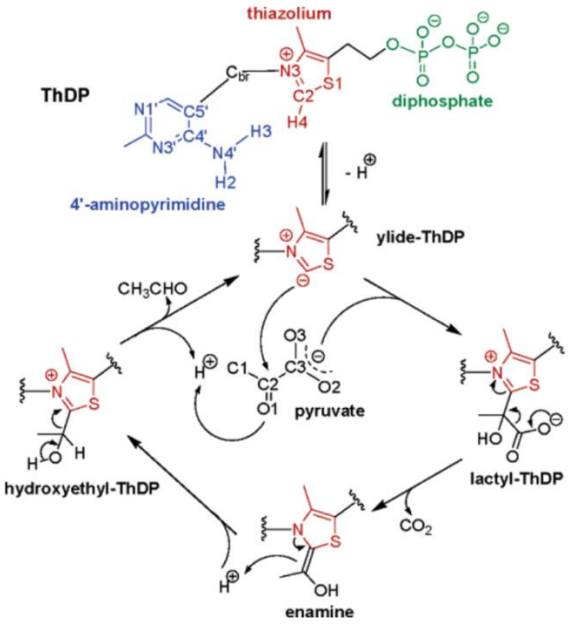

Figure 4.2 PDC reaction mechanism. TPP (ThDP in the figure) forms an ylide that attacks the pyruvate C2 atom forming lactyl-TPP. Then, CO_2 is released and an enamine is formed. Finally, by a proton addition, hydroxyethyl-TPP and releases acetaldehyde. Source: Lie 2005 [34].

Pyruvate decarboxylase belongs to the TPP-dependent enzymes group, which are characterized for the use of the diphosphorilated form of vitamin B1 (thiamin diphosphate, TPP) as a cofactor, and are mainly involved in the decarboxylation of α-ketoacids [27], [30], [34]. TPP, as well as Mg^{2+}, have a major importance in PDC structural stabilization and enzymatic activity. Most of described PDCs are homotetramers with a subunit molecular weight of about 60 kDa [26], [28]. Cofactor TPP is pH-dependently bounded at the interface created by two monomers that form an already functional dimer. Two of these dimers assemble into the tetramer in the quaternary structure [21]. Mg^{2+} ions also assist in anchoring TPP to the protein by forming an octahedral coordination sphere [34]. Thiamine diphosphate also plays a major role in the catalytic mechanism (Figure 4.2). It contains a thiazolium ring, which is able to form a nucleophilic anion called ylide-TPP. This ylide attacks the pyruvate C2 atom forming lactyl-TPP and, after that, carbon dioxide is released while an enamine is formed. Finally, hydroxyethyl-TPP is formed by a

proton addition to the enamine and releases acetaldehyde regenerating, at the same time, ylide-TPP [28], [35].

As a previous step before constructing the cascade reactions of transaminase with PDC for the synthesis of the chiral amines 3-amino-1-phenylbutane (3-APB) and 1-phenyl-ethylamine (1-PEA), some characterization studies were carried out taking into account all the bibliographically reported knowledge about both enzymes. In addition, since four different transaminases were kindly donated to the research group (Table 4.1), preliminary reaction screenings were performed to select which ones would be used in further studies. Deeper theoretical bases about this reaction mechanism will be provided in chapter 5.

Table 4.1 Transaminases available in the present thesis and their corresponding microorganisms.

Transaminase	Microorganism
Ate-TA	*Aspergillus terreus*
Ate-TA_T247S	*Aspergillus terreus*
Cvi-TA	*Chromobacterium violaceum*
Vfl-TA	*Vibrio fluvialis*

4.2. Materials and Methods

4.2.1. Chemicals and enzymes

All chemicals were purchased from Sigma-Aldrich (St. Louis, MO, USA). Four transaminases from *Aspergillus terreus* (Ate-TA, Ate-TA_T247S), *Chromobacterium violaceum* (Cvi-TA) and *Vibrio fluvialis* (Vfl-TA) were kindly donated by DSM/InnoSyn in the form of *Escherichia coli* cell-free extracts (CFE), containing between 40 and 55 $mg \cdot mL^{-1}$ of total protein. In the case of CFE of Ate-TA and Ate-TA_T247S around 70 % of the total protein was transaminase, while this percentage was 47 % for Cvi-TA and 35 % for Vfl-TA. Pyruvate decarboxylase (PDC) from *Zimobacter palmae* was produced by high cell density cultures as it has been described in chapter 3. CFEs of this strain were obtained by sonication with a Vibracell® VC50 (Sonic and Materials®, Newton, CT, USA) with four times 15 s pulses (50 W) and 2 min intervals in ice between each pulse. Centrifugation was performed (10000 g, 10 min) to remove the resulting cell debris. ZpPDC CFEs contained 10 $mg \cdot mL^{-1}$ of total protein, from which around 40 % was PDC.

4.2.2. Enzymatic activity assays

4.2.2.1. Transaminase activity assay

Transaminase activity assay was based on the acetophenone formation measurement at 340 nm and 30ºC from α-Methylbenzylamine and pyruvic acid. The assay was performed in 1 mL reaction mixture, consisting of potassium phosphate buffer 100 mM and pH 7.5 containing 0.1 mM PLP, 22.5 mM α-Methylbenzylamine and 5 mM sodium pyruvate. Coefficient of molar extinction (ε) of acetophenone is 0.28 $mM^{-1} \cdot cm^{-1}$ and one transaminase activity unit corresponds to the amount of enzyme that produces 1 µmol acetophenone per minute at 30ºC. Absorbance measurements were performed using a SPECORD® 200 PLUS (Analytik Jena) spectrophotometer.

4.2.2.2. Pyruvate decarboxylase activity assay

PDC activity was determined by coupling the pyruvate decarboxylation with alcohol dehydrogenase (ADH) and following NADH oxidation at 340 nm and 25ºC, whose coefficient of molar extinction (ε) is 6.22 $mM^{-1} \cdot cm^{-1}$. The reaction mixture contained 33 mM sodium pyruvate, 0.11 mM NADH, 3.5 $U \cdot mL^{-1}$ ADH from *Saccharomyces cerevisiae* (Sigma-Aldrich), 0.1 mM TPP and 0.1 mM $MgCl_2$ in citrate buffer 200 mM and pH 6. One unit of PDC activity corresponds to the amount of pyruvate decarboxylase that converts 1 µmole of pyruvate to acetaldehyde per minute. Absorbance measurements were performed using a SPECORD® 200 PLUS (Analytik Jena) spectrophotometer.

4.2.3. Influence of pH on enzyme activity and stability

The optimum pH for each enzyme was found out by performing enzymatic activity assays at different pHs. Assay buffer was prepared replacing the standard assay buffer by citrate buffer 100 mM (pH from 4.5 to 6), potassium phosphate buffer 100 mM (pH 6.5 – 8) and bicarbonate buffer 100mM (pH higher than 8).

Enzyme stability was determined by preparing a 5 % v v^{-1} solution of the cell lysates containing the enzymes in the mentioned buffers, at different pHs, and maintaining the solutions at 25ºC and mild agitation. Aliquots were taken at different times and enzyme activity was measured.

4.2.4. Influence of cofactors on PDC activity

PDC wet biomass obtained by fermentation was resuspended in citrate buffer 200 mM and pH 6 at a concentration of 200 g L^{-1}. After that, biomass was disrupted by sonication with a Vibracell® VC50 (Sonic and Materials®, Newton, CT, USA) with four times 15 s pulses (50 W) and 2 min intervals in ice between each pulse. Centrifugation was performed (10000 g, 10 min) to remove the resulting cell debris. The resulting CFE were 50-times diluted in different pH buffers and in the presence or absence of 1 mM TPP and $MgCl_2$. For pHs from 4 to 6, citrate buffer 100 mM was used, from 6.5 to 8 potassium phosphate buffer 100 mM and for higher pH values bicarbonate buffer 100 mM. Samples were incubated at room temperature (25 ^oC) and mild agitation for 10 minutes and activity was measured.

To study PDC ability to recover its activity after being subjected to high pHs, CFE were prepared as previously described but using buffers in a pH range from 8 to 10. After measuring its initial PDC activity, they were 10-fold diluted in citrate buffer 200 mM and pH 6 with the presence of 1 mM TPP and $MgCl_2$. After incubating the mixture for 30 minutes at 25 ^oC, activity was measured again.

4.2.5. Transaminase screening

Reactions were performed in 15-mL Falcon tubes with 3 mL reaction mixture consisting of 5 % v v^{-1} transaminase cell lysate, 25 % v v^{-1} PDC cell lysate, 1 mM pyridoxal 5'-phospate (PLP), 0.1 mM thiamine pyrophosphate (TPP), 0.1 mM $MgCl_2$, 200 mM alanine and 10 mM of each ketonic substrate (4-PB and AP) in 150 mM of potassium phosphate buffer of the optimum pH of each transaminase. Samples were placed in a Multitherm shaker (Benchmark Scientific) at 30^oC and 1000 rpm and after 24 h the presence or absence of 3-APB and 1-PEA was detected by HPLC. Control reactions were performed substituting PDC cell lysate with distillate water.

4.2.6. Ketonic substrates and amines analysis by HPLC

All amine and ketonic substrates concentrations were measured by HPLC analysis in an UltiMate 3000 (Dionex) equipped with a variable wavelenght detector. Compounds were separated on a reversed-phase CORTECS C18+ 2.7 µm 4.6× 150 mm column (Waters Milford, MA, USA). After

acidifying reaction samples with 3 M hydrochloric acid to deactivate the enzymes, 15 µL were injected at a 0.7 mL·min^{-1} flow rate and 30ºC. In the case of 4-PB to 3-APB reaction, samples were eluted using a gradient from 30 to 55 % solvent B —consisting of 0.095 % v v^{-1} in MeCN/H_2O 4:1 v v^{-1}— to solvent A — consisting of 0.1 % v v^{-1} TFA in H_2O— over 13 minutes and compounds were detected at a 254 nm wavelength. In the case of AP to 1-PEA the gradient started at 15 % solvent B instead of 30 % and compounds were detected at a 210 nm wavelength.

4.3. Results and discussion

4.3.1. Searching pH compromise conditions

Constructing a one-pot multienzymatic system implies the combination of several biocatalysts with their individual optimal operational conditions, thus requiring a selection of reaction conditions compatible with all the biocatalysts involved [36], [37]. In order to find a compromise to combine the several reactions in an optimal way, a powerful tool is a good separate enzyme characterization [38]. Finding an optimum pH range is not only critical during reaction cascades construction but also challenging, since pH is an intrinsic characteristic with major effects on enzyme activity and stability [39].

In this sense, suitable compromise conditions had to be found for the one-pot multienzymatic synthesis of chiral amines. For this reason, pH effect on enzymatic activity and kinetic stability were individually studied in each transaminase as well as in pyruvate decarboxylase.

4.3.1.1. Activity profiles towards pH

Aiming to establish the optimum pH of PDC and the four different TAs, individual activity profiles towards pH were constructed and they are shown in Figure 4.3. These kind of profiles are not only useful to find conditions in which enzymes show the maximum activity, but also to study their tolerance in front of pH changes, which facilitates the selection of suitable compromise conditions.

Regarding transaminases, Cvi-TA and Vfl-TA showed narrow profiles, both reaching the maximum activity at pH 7.5. On the contrary, transaminases from *Aspergillus terreus (*Ate-TA_T244S and Ate-TA) showed widener profiles with optimum pH at 7 and 6, respectively. Despite it is usual to find out optimum transaminase pHs higher than 8, especially in the case of

Cvi-TA and Vfl-TA [40], [41], the optimum conditions found in this study have also been reported [42]. PDC reached its maximum activity at pH 6.5 but its activity dependency towards pH was not as strong as for transaminases in the tested range, maintaining more than 80 % of the maximum activity from pH 5 to 7.5. Even though the lowest activity was detected at pH 8.5, it only represented a 35 % less than the maximum. It has been widely reported that ZpPDC, as the majority of the most known PDCs, has a pH-dependent quaternary structure for which the optimal conditions are between pH 6 and 6.7 [20], [24], [30]. At pH values above pH 8, destabilization of the tetramer PDC structure starts to take place [19], [30], [43], reason why an activity decrease was detected from pH 7.5 and pH conditions higher than 8.5 were not tested. More studies centered on ZpPDC activity in relationship to its pH and cofactor-dependent structure will be exposed in section 4.3.2.

Out from the activity profiles obtained, it can be concluded that transaminase activity in all cases was highly affected by pH conditions compared to the PDC. For this reason, the compromise pH conditions would be defined by the optimum pH for each transaminase.

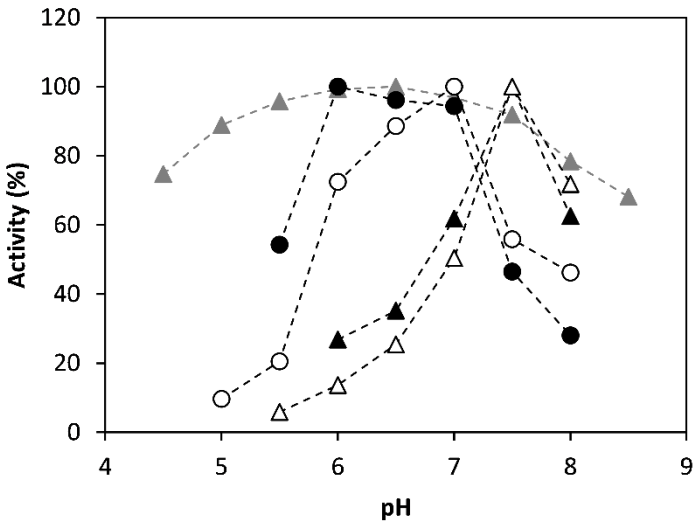

Figure 4.3 pH activity profile of pyruvate decarboxylase and the four transaminases. (▲) PDC. (●) Ate-TA. (○) Ate-TA_T247S. (▲) Cvi-TA. (△) Vfl-TA. Assays were performed at different pHs, with citrate buffer 100 mM (pH 4.5 – 6), potassium phosphate buffer 100 mM (pH 6.5 – 8) and bicarbonate buffer 100 mM (pH >8). Temperatures: 25^{o}C for PDC and 30^{o}C for TAs.

4.3.1.2. Enzyme stability vs pH

Besides optimum pH, enzyme stability must also be taken into account in the establishment of compromise conditions. Several authors have pointed out that activity maintenance through a biocatalytic process is related to two kinds of stability: i) thermodynamic (or conformational) stability and ii) kinetic (or long term) stability. The first one refers to the resistance of protein conformation to reversible unfolding, while the second one measures the time before an irreversible inactivation occurs [10], [44]–[46]. Therefore, kinetic stability under certain conditions represents a key enzyme feature for successful biocatalytic process implementation [46].

Long term stabilities of PDC and the four TAs were studied under different pH conditions. On the one hand, it was necessary to ensure that all enzymes would resist the compromise conditions established in section 4.3.1.1. On the other, kinetic stability represents a key information for further experiments involving incubation phases in different pH conditions such as enzyme immobilization.

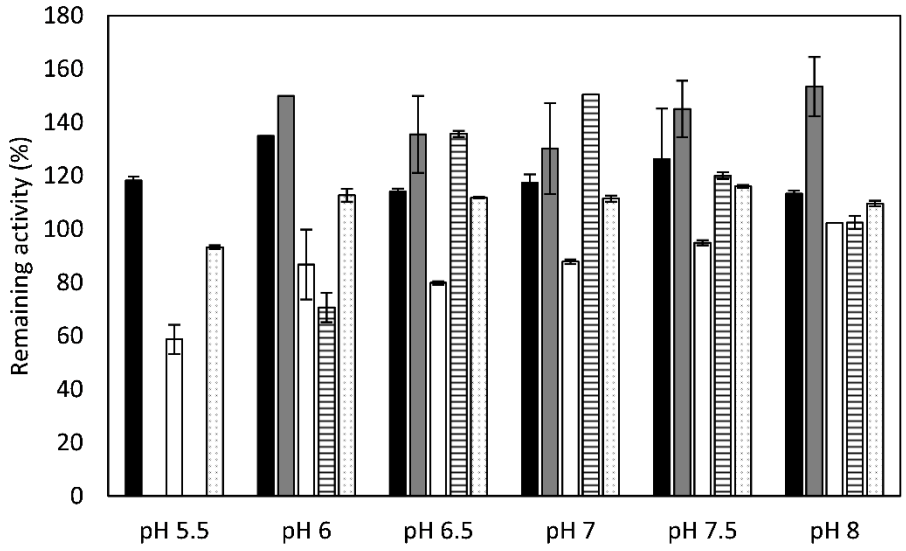

Figure 4.4 TAs and PDC stability at different pH conditions after 8 hours incubation. (black) PDC (dark grey) Ate-TA (white) Ate-TA_T274S (striped) Cvi-TA (dotted) Vfl-TA. Enzymes were incubated at 25^{o}C and mild agitation at different pHs: with citrate buffer 100 mM (pH 5.5 – 6) and potassium phosphate buffer 100 mM (pH 6.5 – 8).

In Figure 4.4, remaining activity after 8 hours is shown for all enzymes at a pH range from 5.5 to 8. It should be noticed that in most of the cases in which the enzymes were stable, an activity increase was observed, obtaining remaining activities higher than 100 % after 8 hours. This effect can be observed for PDC in all tested pHs, for Ate-TA and Vfl-TA in all pHs except for 5.5 and for Cvi-TA under pH 6.5, 7 and 7.5. Even though several authors also reported this activation over time in the case of transaminases [10], [47], it has only been related to few reasons. Since most transaminases are homodimers and the active site is formed by both enzyme subunits, a proposed explanation for this hyperactivation was a complete dimerization to form active enzyme [47].

Except for pH 5.5, both PDC and the four transaminases showed a high stability after 8 hours in the studied pH range. Therefore, it was proved that establishing the compromise pH in the optimum for each transaminase is adequate for the interest multienzymatic system, since enzyme deactivation should not occur, at least due to the pH conditions, neither in any TA nor in PDC.

Another common measure for kinetic stability is the half-life time, which is defined as the necessary time to reduce the activity to the half when enzymes are incubated under specific conditions [44]. In Table 4.2 half-lives for PDC and TAs are shown. Pyruvate decarboxylase showed a half-life higher than 24 hours in all the pH range tested. Regarding transaminases, they were more sensitive at low pH conditions but, in general, they did not lose half of their activity before 24 hours for pH conditions above 6.

Table 4.2 Half-life time of the four transaminases and PDC under the different pH conditions tested. Enzymes were incubated at 25^{o}C and mild agitation at different pHs: citrate buffer 100 mM (pH 5 – 6) and potassium phosphate buffer 100 mM (pH 6.5 – 8).

	Half-life (h)				
	PDC	*Cvi-TA*	*Vfl-TA*	*Ate-TA*	*Ate-TA_T247S*
pH 5	> 24	< 0.5	2	0.5	4
pH 5.5	> 24	< 0.5	> 24	< 4	8
pH 6	> 24	< 24	> 24	> 24	> 24
pH 6.5	> 24	> 24	> 24	> 24	24
pH 7	> 24	> 24	> 24	> 24	> 24
pH 7.5	> 24	> 24	> 24	> 24	> 24
pH 8	> 24	24	> 24	> 24	> 24

4.3.2. Effect of cofactors on PDC activity

Zymobacter palmae PDC (ZpPDC) has the same quaternary structure as described in the case of other bacterial PDCs or the well-known PDC from Brewer's yeast [19], [48]. It consists of a tetramer built up of four identical monomers of around 60 kDa [19]. Each two monomers are tightly bound forming a functional dimer, which is the minimal catalytically active unit [21], and two of them assemble forming a dimer of dimers [21], [48]. As it has already been mentioned during the chapter introduction, TPP is non-covalently anchored to the monomer interface by a Mg^{2+} ion, playing a major role on structure stabilization and on the biocatalytic mechanism of the enzyme [19]–[22], [34], [35], [48]. Thus, the additional presence of TPP and Mg^{2+} must be taken into account in the development of a biocatalytic process in which PDC is involved [20], [27].

Cofactor binding to the protein and thus quaternary structure stabilization is directly related to pH conditions [19], [20], [43]. For this reason, a characterization relating pH and cofactor presence was performed with the ZpPDC previously obtained by fermentation (see chapter 3). As it was mentioned in materials and methods, PDC was obtained from cell disruption in citrate buffer 200 mM and pH 6 without any additional cofactor supplementation. The mentioned lysate was 50-times diluted at different pH buffers in the presence or absence of both cofactors and, after 10-minutes incubation, PDC remaining activity was measured. As it is shown in Figure 4.5, in the pH range from 4.5 to 7, ZpPDC conserves a 90 % or more of the initial activity even though an excess of cofactors is not added. At pH 7.5 and 8, around 60 % and 20 % of the maximum activity was respectively detected without cofactors, while in the same case but in higher pH conditions the entire activity was lost. This tendency could be related to the previously reported cofactor dissociation at pH above 7.5 due to the TPP release from the enzyme [19], [43]. However, more than 90 % of the initial activity was observed by the addition of an excess of cofactors until pH 9. Therefore, medium supplementation with TPP and Mg^{2+} may have broken the dissociation equilibrium of TPP binding and extended the maintenance of ZpPDC in a biocatalytically-active form to higher pH conditions.

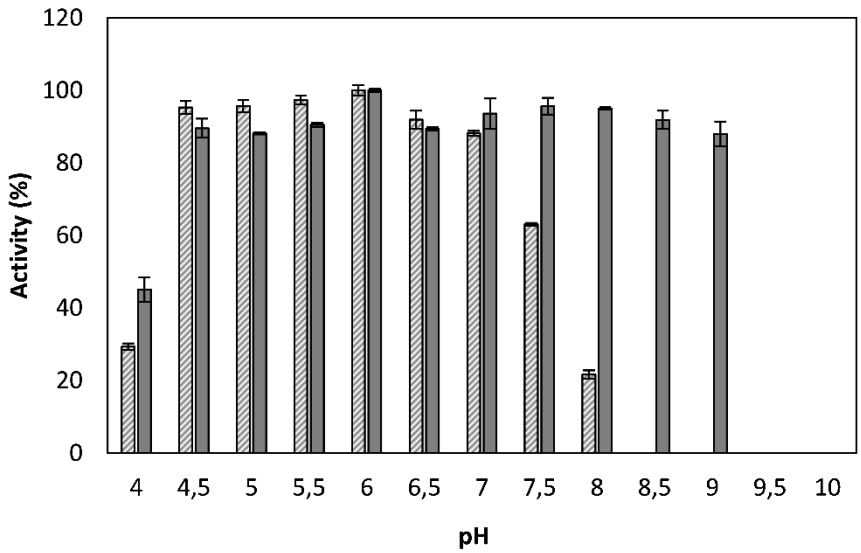

Figure 4.5 Remaining PDC activity after incubation at different pHs and in presence or absence of cofactors (1 mM TPP and 1 mM $MgCl_2$). PDC activity was tested after incubation during 10 min at 25^{o}C and mild agitation at different pHs in absence of cofactors (striped) or in presence of cofactors (grey). Incubation buffers: citrate buffer 100 mM (pH 4 – 6), potassium phosphate buffer 100 mM (pH 6.5 – 8) and bicarbonate buffer 100 mM (pH >8). Percentages were calculated in respect to the maximum activity, which corresponds to pH 6 with the presence of cofactors.

According to several authors the pH-dependent protein dissociation can be reversible [43]. For this reason a new experiment was carried out to study if PDC activity could be recovered after subjecting the enzyme into non-favorable conditions. The study started with different samples of ZpPDC extract in buffers of a pH range from 8 to 10 and without any cofactor supplementation. After not detecting any significant PDC activity due to the high pH, all samples were 10-fold diluted into citrate buffer 200 mM and pH 6 with 1 mM TPP and 1 mM $MgCl_2$ and incubated 30 minutes at room temperature. Then, activity measurements (Table 4.3) revealed that nearly 100 % of the maximum activity could be recovered at pH 8 to 9. In higher pHs no activity was detected, hence ZpPDC suffered an irreversible denaturation.

Table 4.3 ZpPDC ability of recovering its activity after being subjected to pH higher than 8, in which protein dissociation takes place. Initial activity corresponds to the detected at pH buffers from 8 to 10 (bicarbonate buffer 100 mM). Activity after recovery is the one detected after changing the conditions to acetate buffer 100 mM pH6 and 1 mM of TPP and Mg^{2+}. Temperature 25ºC and mild agitation.

pH	Initial activity (%)	Activity after recovery (%)
Blank (6.0)	97.56 ± 2.60	100.00 ± 0.00
8.0	21.66 ± 1.14	90.83 ± 0.41
8.5	0.00 ± 0.00	97.05 ± 4.42
9.0	0.00 ± 0.00	94.07 ± 6.53
9.5	0.00 ± 0.00	0.00 ± 0.00
10.0	0.00 ± 0.00	0.00 ± 0.00

4.3.3. Transaminase screening

After enzyme characterization to establish compromise conditions, a preliminary reaction screening study was carried out to select which of the transaminases were appropriate to construct the enzymatic cascade with PDC. As it has been mentioned in section 4.3.1.1, TAs are more sensitive to pH changes. For this reason, the optimum pH for each transaminase was used (pH 6.0 Ate-TA, pH 7.0 Ate-TA_T247S and pH 7.5 for Cvi-TA and Vfl-TA). First of all, 3-APB synthesis was studied (see Scheme 4.1). Reactions were prepared coupling 5 % v v^{-1} of each transaminase with 5-fold more concentration of the ZpPDC cell-free extract (30 $U \cdot mL^{-1}$ reaction). To ensure an entire structure stability on PDC (see section 4.3.2), its cofactors (TPP and $MgCl_2$) were added at 0.1 mM concentration. In the same way, transaminase cofactor pyridoxal-5'-phosphate (PLP) addition is also required in this kind of reactions [49], reason why it was included at 1 mM concentration. Regarding substrates, 10 mM of the ketone (4-phenyl-2-butanone, 4-PB) was added since it is the maximum possible value due to its solubility, while 20-times more alanine concentration was used. This excess of amine donor has been reported to facilitate equilibrium shift to amine formation [49]. At the same time, blank reactions without PDC were carried out to compare the difference between constructing or not the cascade reaction.

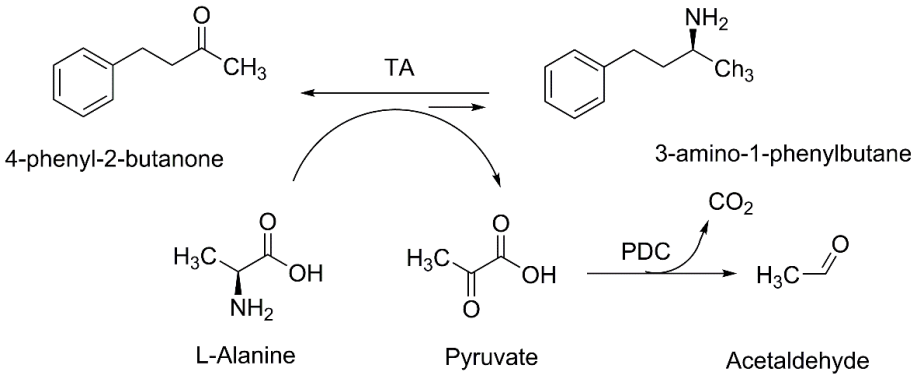

Scheme 4.1 One-pot cascade reaction for 3-amino-1-phenylbutane (3-APB) synthesis catalyzed by transaminase and pyruvate decarboxylase.

Screening results for 3-APB synthesis are exposed in Table 4.4. After 24 hours incubation, when no PDC was added, slight amounts of 3-APB were detected only in the experiments performed with Cvi-TA and Vfl-TA. On the other hand, when transaminases were coupled with PDC, Cvi-TA and Vfl-TA reaction samples showed significant amounts of 3-APB, which suggested that the coupling of the decarboxylation reaction leads to an equilibrium shift towards amine formation. Thus, Cvi-TA and Vfl-TA were selected for further experiments and the transaminases from *Aspergillus terreus* were discarded. Low reaction yields have been reported when Ate-TAs are used for catalyzing reaction with aromatic ketonic substrates, especially if the ketone is located next to the aromatic ring, since they preferably convert aliphatic substrates [50].

Table 4.4 Transaminase screening for 3-APB synthesis. Each transaminase reaction was performed at its optimum pH. Reactions without PDC were also performed to compare the effect of adding or not PDC. Reaction time 24 h; temperature 30^{o}C; 4-PB 10 mM; alanine 200 mM; TA 5 % v v^{-1}; PDC 25 % v v^{-1}.

Enzyme	PDC presence	pH	[APB] (mM)
Ate-TA	+	6,0	0.0
	-		0.0
Ate-TA_T247S	+	7,0	0.0
	-		0.0
Cvi-TA	+	7,5	6.2
	-		0.6
Vfl-TA	+	7,5	5.9
	-		1.0

After selecting Cvi-TA and Vfl-TA for the 3-APB synthesis, screening was also performed for the 1-PEA case (Scheme 4.2). The same conditions explained before were applied. For a better comparison between the two synthesis reactions studied, also 10 mM of ketonic substrate (Acetophenone, AP) was used, even though its solubility is higher (30 mM).

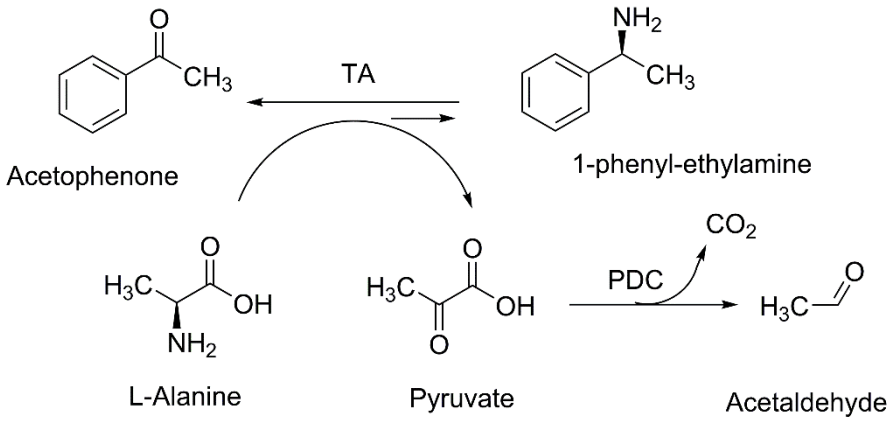

Scheme 4.2 One-pot cascade reaction for 1-phenyl-ethylamine (1-PEA) synthesis catalyzed by transaminase and pyruvate decarboxylase.

Screening results (Table 4.5) revealed 1-PEA presence when Cvi-TA and Vfl-TA were used. However, final amine concentrations obtained with Cvi-TA were not significant and it was no difference between adding and not PDC. This negative results could be related to a reported inhibitory effect of acetophenone, which completely inhibited Cvi-TA at concentrations higher than 3.5 mM [47]. Regarding Vfl-TA, around 50 % yield was obtained when a reaction cascade was carried out. Since an effective equilibrium shift took place when Vfl-TA was used, this transaminase was selected for further experiments on 1-PEA synthesis.

Table 4.5 Transaminase screening for 1-PEA synthesis. Each transaminase reaction was performed at its optimum pH. Reactions without PDC were also performed to compare the effect of adding or not PDC. Reaction time 24 h; temperature 30^{o}C; AP 10 mM; alanine 200 mM; TA 5 % v v^{-1}; PDC 25 % v v^{-1}.

Enzyme	PDC presence	pH	[PEA] (mM)
Ate-TA	+	6.0	0.0
	-		0.0
Ate-TA_T247S	+	7.0	0.0
	-		0.0
Cvi-TA	+	7.5	0.2
	-		0.2
Vfl-TA	+	7.5	5.1
	-		0.4

4.4. Conclusions

Optimum pH conditions for four different transaminases and ZpPDC were found and it was concluded that TAs are more affected by pH changes than PDC. For this reason, the compromise conditions to build up cascade reactions are defined by the TAs optimum pHs (Ate-TA pH 6, Ate-TA_T247S pH 7, Cvi-TA pH 7.5 and Vfl-TA pH 7.5). Stability studies revealed that all enzymes have a high long-time stability not only in the established pH compromise conditions but also in a pH range from 6 to 8. In PDC characterization in relationship with the presence/absence of its cofactors, it was concluded that TPP and Mg^{2+} addition is critical for ZpPDC activity maintenance, especially in high pHs, which are the conditions in which enzyme dissociation takes place. PDC dissociation has shown to be reversible in the pH range from 8 to 9. Finally, in a preliminary transaminase screening, effective 3-APB synthesis was detected in reactions catalyzed by Cvi-TA and Vfl-TA, while effective 1-PEA synthesis was only carried out by Vfl-TA. In all cases, PDC presence was critical for an appropriate equilibrium shifting that enables amine production.

4.5. References

[1] F. Guo and P. Berglund, “Transaminase biocatalysis: optimization and application,” *Green Chem.*, vol. 19, no. 2, pp. 333–360, Jan. 2017.

[2] B.-Y. Hwang and B.-G. Kim, “High-throughput screening method for the identification of active and enantioselective ω-transaminases,” *Enzyme Microb. Technol.*, vol. 34, no. 5, pp. 429–436, Apr. 2004.

[3] M. S. Malik, E.-S. Park, and J.-S. Shin, “Features and technical applications of ω-transaminases,” *Appl. Microbiol. Biotechnol.*, vol. 94, no. 5, pp. 1163–1171, Jun. 2012.

[4] I. Slabu, J. L. Galman, R. C. Lloyd, and N. J. Turner, “Discovery, Engineering, and Synthetic Application of Transaminase Biocatalysts,” *ACS Catal.*, vol. 7, no. 12, pp. 8263–8284, 2017.

[5] S. A. Kelly *et al.*, “Application of ω-Transaminases in the Pharmaceutical Industry,” *Chem. Rev.*, vol. 118, pp. 349–367, 2017.

[6] D. Ghislieri and N. J. Turner, “Biocatalytic Approaches to the Synthesis of Enantiomerically Pure Chiral Amines,” *Top. Catal.*, vol. 57, no. 5, pp. 284–300, Mar. 2014.

[7] S. Mathew and H. Yun, “ω-Transaminases for the Production of Optically Pure Amines and Unnatural Amino Acids,” *ACS Catal.*, vol. 2, pp. 993–1001, 2012.

[8] T. Börner *et al.*, “Explaining Operational Instability of Amine Transaminases: Substrate-Induced Inactivation Mechanism and Influence of Quaternary Structure on Enzyme−Cofactor Intermediate Stability,” *ACS Catal.*, vol. 7, pp. 1259–1269, 2016.

[9] J. S. Shin, H. Yun, J. W. Jang, I. Park, and B. G. Kim, “Purification, characterization, and molecular cloning of a novel amine:pyruvate transaminase from Vibrio fluvialis JS17,” *Appl. Microbiol. Biotechnol.*, vol. 61, no. 5–6, pp. 463–471, Jun. 2003.

[10] S. Chen, H. Land, P. Berglund, and M. S. Humble, “Stabilization of an amine transaminase for biocatalysis,” *J. Mol. Catal. B Enzym.*, vol. 124, pp. 20–28, Feb. 2016.

[11] M. D. Patil, G. Grogan, A. Bommarius, and H. Yun, “Recent advances in ω-transaminase-mediated biocatalysis for the enantioselective synthesis of chiral amines,” *Catalysts*, vol. 8, no. 7. 2018.

[12] F. Steffen-Munsberg *et al.*, “Bioinformatic analysis of a PLP-dependent enzyme superfamily suitable for biocatalytic applications,” *Biotechnol. Adv.*, vol. 33, pp. 566–604, 2015.

[13] A. Gomm and E. O’Reilly, “Transaminases for chiral amine synthesis,” *Curr. Opin. Chem. Biol.*, vol. 43, pp. 106–112, Apr. 2018.

[14] K. E. Cassimjee, M. S. Humble, H. Land, V. Abedi, and P. Berglund, “Chromobacterium violaceum ω-transaminase variant Trp60Cys shows increased specificity for (S)-1-phenylethylamine and 4’-substituted acetophenones, and follows Swain–Lupton

parameterisation," *Org. Biomol. Chem.*, vol. 10, no. 28, pp. 5466–5470, Jun. 2012.

[15] S. Chen, J. C. Campillo-Brocal, P. Berglund, and M. S. Humble, "Characterization of the stability of Vibrio fluvialis JS17 amine transaminase," *J. Biotechnol.*, vol. 282, pp. 10–17, Sep. 2018.

[16] D. Koszelewski, K. Tauber, K. Faber, and W. Kroutil, "ω-Transaminases for the synthesis of non-racemic α-chiral primary amines," *Trends in Biotechnology*, vol. 28, no. 6. pp. 324–332, Jun-2010.

[17] U. Kaulmann, K. Smithies, M. E. B. Smith, H. C. Hailes, and J. M. Ward, "Substrate spectrum of ω-transaminase from Chromobacterium violaceum DSM30191 and its potential for biocatalysis," *Enzyme Microb. Technol.*, vol. 41, no. 5, pp. 628–637, Oct. 2007.

[18] S. E. Lowe' and J. G. Zeikus', "Purification and characterization of pyruvate decarboxylase from Sarcina ventriculi," *J. Gen. Microbiol.*, vol. 138, pp. 803–807, 1992.

[19] S. König, M. Spinka, and S. Kutter, "Allosteric activation of pyruvate decarboxylases. A never-ending story?," *J. Mol. Catal. B Enzym.*, vol. 61, no. 1–2, pp. 100–110, 2009.

[20] D. Gocke *et al.*, "Comparative characterisation of thiamin diphosphate-dependent decarboxylases," *J. Mol. Catal. B Enzym.*, vol. 61, pp. 30–35, 2009.

[21] K. Tittmann, A. Balakrishnan, Y. Gao, P. Moorjani, N. S. Nemeria, and F. Jordan, "Bifunctionality of the thiamin diphosphate cofactor: Assignment of tautomeric/ionization states of the 4'-aminopyrimidine ring when various intermediates occupy the active sites during the catalysis of yeast pyruvate decarboxylase," *J. Am. Chem. Soc.*, vol. 134, no. 8, pp. 3873–3885, 2012.

[22] L. J. Van Zyl, W.-D. Schubert, M. I. Tuffin, and D. A. Cowan, "Structure and functional characterization of pyruvate decarboxylase from Gluconacetobacter diazotrophicus," *BMC Struct. Biol.*, vol. 14, no. 21, pp. 1–13, 2014.

[23] L. Buddrus, E. S. V. Andrews, D. J. Leak, M. J. Danson, V. L. Arcus, and S. J. Crennell, "Crystal structure of an inferred ancestral bacterial pyruvate decarboxylase," *Acta Crystallogr. Sect. F Struct. Biol. Commun.*, vol. 74, no. 3, pp. 179–186, Mar. 2018.

[24] K. C. Raj, L. A. Talarico, L. O. Ingram, and J. A. Maupin-furlow, "Cloning and Characterization of the Zymobacter palmae Pyruvate Decarboxylase Gene (pdc) and Comparison to Bacterial Homologues," *Appl. Environ. Microbiol.*, vol. 68, no. 6, pp. 2869–

2876, 2002.

[25] A. S. Demir, P. Ayhan, and S. Betül Sopaci, “Thiamine pyrophosphate dependent enzyme catalyzed reactions: Stereoselective C-C bond formations in water,” *Clean - Soil, Air, Water*, vol. 35, no. 5, pp. 406–412, 2007.

[26] D. Dobritzsch, S. König, G. Schneider, and G. Lu, “High resolution crystal structure of pyruvate decarboxylase from Zymomonas mobilis. Implications for substrate activation in pyruvate decarboxylases.,” *J. Biol. Chem.*, vol. 273, no. 32, pp. 196–204, 1998.

[27] P. Arjunan *et al.*, “Crystal structure of the thiamin diphosphate-dependent enzyme pyruvate decarboxylase from the yeast Saccharomyces cerevisiae at 2.3 angstrom resolution,” *J. Mol. Biol.*, vol. 256, no. 3, pp. 590–600, 1996.

[28] O. P. Ward and A. Singh, “Enzymatic asymmetric synthesis by decarboxylases,” *Curr. Opin. Biotechnol.*, vol. 11, pp. 520–526, 2000.

[29] K. Chandra Raj, L. Ingram, and J. Maupin-Furlow, “Pyruvate decarboxylase: a key enzyme for the oxidative metabolism of lactic acid by Acetobacter pasteurianus,” *Arch. Microbiol.*, vol. 176, no. 6, pp. 443–451, Dec. 2001.

[30] J. M. Candy and R. G. Duggleby, “Structure and properties of pyruvate decarboxylase and site-directed mutagenesis of the Zymomonas mobilis enzyme,” *Biochim. Biophys. Acta - Protein Struct. Mol. Enzymol.*, vol. 1385, pp. 323–338, 1998.

[31] L. J. Van Zyl, M. P. Taylor, K. Eley, M. Tuffin, and D. a. Cowan, “Engineering pyruvate decarboxylase-mediated ethanol production in the thermophilic host Geobacillus thermoglucosidasius,” *Appl. Microbiol. Biotechnol.*, vol. 98, no. 3, pp. 1247–1259, 2014.

[32] H. Yun and B.-G. Kim, “Enzymatic production of (R)-phenylacetylcarbinol by pyruvate decarboxylase from Zymomonas mobilis,” *Biotechnol. Bioprocess Eng.*, vol. 13, no. 3, pp. 372–376, Jun. 2008.

[33] A. K.-L. Chen, M. Breuer, B. Hauer, P. L. Rogers, and B. Rosche, “pH shift enhancement of Candida utilis pyruvate decarboxylase production,” *Biotechnol. Bioeng.*, vol. 92, no. 2, pp. 183–188, Oct. 2005.

[34] M. A. Lie, L. Celik, K. A. Jørgensen, and B. Schiøtt, “Cofactor activation and substrate binding in pyruvate decarboxylase. Insights into the reaction mechanism from molecular dynamics simulations,” *Biochemistry*, vol. 44, no. 45, pp. 14792–14806, 2005.

[35] A. Shrestha, S. Dhamwichukorn, and E. Jenwitheesuk, “Bioinformation Modeling of pyruvate decarboxylases from ethanol producing bacteria Bioinformation,” *Bioinformation*, vol. 4, no. 8, pp. 378–384, 2010.

[36] E. Ricca, B. Brucher, and J. H. Schrittwieser, “Multi-Enzymatic Cascade Reactions: Overview and Perspectives,” *Adv. Synth. Catal.*, vol. 353, no. 13, pp. 2239–2262, Sep. 2011.

[37] K. Rosenthal and S. Lütz, “Recent developments and challenges of biocatalytic processes in the pharmaceutical industry,” *Curr. Opin. Green Sustain. Chem.*, vol. 11, pp. 58–64, Jun. 2018.

[38] P. A. Santacoloma, G. Sin, K. V Gernaey, and J. M. Woodley, “Multienzyme-Catalyzed Processes: Next-Generation Biocatalysis,” *Org. Process Res. Dev.*, vol. 15, pp. 203–212, 2011.

[39] Y. Zhang, Q. Wang, and H. Hess, “Increasing Enzyme Cascade Throughput by pH-Engineering the Microenvironment of Individual Enzymes,” *ACS Catal.*, vol. 7, pp. 2047–2051, 2017.

[40] U. Schell, R. Wohlgemuth, and J. M. Ward, “Synthesis of pyridoxamine 5′-phosphate using an MBA:pyruvate transaminase as biocatalyst,” *J. Mol. Catal. B Enzym.*, vol. 59, no. 4, pp. 279–285, Aug. 2009.

[41] J.-S. Shin and B.-G. Kim, “Asymmetric synthesis of chiral amines with ?-transaminase,” *Biotechnol. Bioeng.*, vol. 65, no. 2, pp. 206–211, Oct. 1999.

[42] M. S. Humble *et al.*, “Crystal structures of the Chromobacterium violaceumω-transaminase reveal major structural rearrangements upon binding of coenzyme PLP,” *FEBS J.*, vol. 279, no. 5, pp. 779–792, Mar. 2012.

[43] A. D. Gounaris, I. Turkenkopf, S. Buckwald, and A. Young, “Pyruvate decarboxylase - Protein dissociation into subunits under conditions in which thiamine pyrophosphate is released,” *J. Biol. Chem.*, vol. 246, no. 5, pp. 1302–1309, 1971.

[44] K. M. Polizzi, A. S. Bommarius, J. M. Broering, and J. F. Chaparro-Riggers, “Stability of biocatalysts,” *Curr. Opin. Chem. Biol.*, vol. 11, no. 2, pp. 220–225, Apr. 2007.

[45] P. V. Iyer and L. Ananthanarayan, “Enzyme stability and stabilization—Aqueous and non-aqueous environment,” *Process Biochem.*, vol. 43, no. 10, pp. 1019–1032, Oct. 2008.

[46] V. Stepankova, S. Bidmanova, T. Koudelakova, Z. Prokop, R. Chaloupkova, and J. Damborsky, “Strategies for stabilization of enzymes in organic solvents,” *ACS Catalysis*, vol. 3, no. 12. American Chemical Society, pp. 2823–2836, 06-Dec-2013.

[47] K. E. Cassimjee, M. S. Humble, V. Miceli, C. Granados Colomina, and P. Berglund, “Active Site Quantification of an ω-Transaminase by Performing a Half Transamination Reaction,” *ACS Catal.*, vol. 1, pp. 1051–1055, 2011.

[48] L. Buddrus, E. S. V Andrews, D. J. Leak, M. J. Danson, V. L. Arcus, and S. J. Crennell, “Crystal structure of pyruvate decarboxylase from Zymobacter palmae,” *Acta Crystallogr. Sect. F Struct. Biol. Commun.*, vol. 72, pp. 700–706, 2016.

[49] P. Tufvesson, J. Lima-Ramos, J. S. Jensen, N. Al-Haque, W. Neto, and J. M. Woodley, “Process considerations for the asymmetric synthesis of chiral amines using transaminases,” *Biotechnol. Bioeng.*, vol. 108, no. 7, pp. 1479–1493, 2011.

[50] A. Łyskowski *et al.*, “Crystal Structure of an (R)-Selective ω-Transaminase from Aspergillus terreus,” *PLoS One*, vol. 9, no. 1, p. e87350, 2014.

5. Asymmetric chiral amine synthesis by the cascade reaction of TA and PDC

5.1. Introduction

Chiral amines are molecules of high industrial interest because of their broad range of applications [1]. They have been widely used as chiral auxiliaries, resolving agents and building blocks for the synthesis of natural and unnatural compounds [1], [2]. They can be broadly found in numerous active pharmaceutical ingredients (APIs), agrochemicals, bioactive natural products and pharmaceutical building blocks, reason why the development of biocatalytic strategies for their synthesis has been identified as a key research priority in the pharmaceutical, agrochemical and chemical industries [3]–[5].

Chiral amines have been classically synthesized using chemical methods and efforts are still being addressed to obtain new chemical procedures operationally simple, preferably one-step and allowing high chemo-, regio-, diastero- and enantiocontrol [6]. The most well-recognized chemical method for chiral amine synthesis is via hydrogenation of a Schiff base, but there are several others such as diasteroisomeric crystallization, C-H insertion or nucleophilic addition [2], [7]–[9]. However, most of these chemical approaches use toxic transition metal catalysts linked to sophisticated ligands working at high pressure, which causes environmental issues. Moreover, these catalysts often show insufficient stereoselectivity in a single catalytic step, leading to the necessity of an additional recrystallization to accomplish the pharmaceutical requirements [8], [10]. In contrast, enzyme reactions own mild reaction conditions and high stereoselectivity, thus highly enantiopure compounds can be easily achieved. For this reason, biocatalytic approaches for the production of chiral amines have received considerable attention as an alternative [2], [4], [8].

Multiple biocatalytic approaches have been developed for the synthesis of optically pure amines involving the use of several enzymes, including hydrolases, amine dehydrogenases, imine reductases, ammonia lyases, monoamine oxidases, reductive aminases and amine transaminases [3]–[5], [7]. The most commonly used strategy in industry is kinetic resolution, consisting in the enantioselective transformation of a starting racemic amine [9], [11]. Therefore, an enantioenriched product is obtained by using an enzyme which acts with enantiopreference towards the non-desirable isomer in the racemic mixture [7]. Even though a wide range of chiral amines have been obtained with kinetic resolution, it has as a main disadvantage a theoretical maximum yield of 50% of the desired isomer [7], [10], [12]. To

overcome this disadvantage, the use of ω-transaminases has received a major attention because these enzymes allow a direct amine synthesis from prostereogenic ketones [5], [13].

Asymmetric synthesis of chiral amines starting from the corresponding prochiral ketones in combination with a suitable amine donor molecule (see Scheme 5.1) theoretically offers a potentially 100% yield and an excellent enantioselectivity depending on the transaminase used [5], [11], [12], [14]. However, the major challenges facing this technique are product inhibition and specially an unfavorable equilibrium towards amine formation [3], [4], [12], [15].

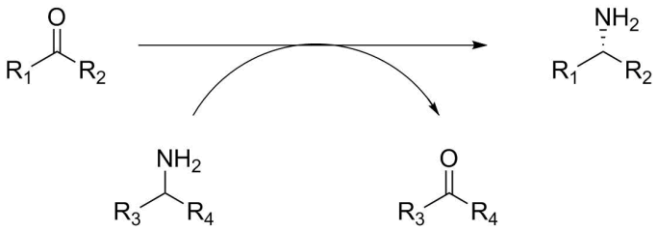

Scheme 5.1 Asymmetric synthesis of chiral amines starting from the corresponding prochiral ketone. An appropriate amine donor transfers its amino group to the prochiral ketone and is transformed to the corresponding ketonic by-product while the interest amine is produced.

To suppress the reverse reaction and shift the equilibrium, reagents can be used in different stoichiometries [9]. Applying an excess of amine donor represents the simplest equilibrium shifting strategy, with which some successful amine synthesis cases have been reported [15]–[17]. Nevertheless, the applicability of this method is limited by the initial reaction equilibrium, the substrate solubility and a possible enzyme inhibition [15], [17]. For this reason, more popular equilibrium shift strategies are based on the in-situ removal of the reaction by-product in order to prevent the reverse reaction from competing and compromising conversion/yield [3]. An option is the extraction of ketone product by organic solvent, taking advantage of the different polarities of amines and ketones. Even though several biphasic reaction systems (either liquid-solid or liquid-liquid) are available, this strategy has some drawbacks such as the poor distinction between substrate and product or the destabilization of proteins by organic solvents [15]. Alternatively, the use of amine donors leading to volatile ketones has been studied. The use of ispropylamine as amine donor has increasingly been regarded as it is an easy-obtainable cheap reactant with which acetone is formed as by-product. Then, acetone is highly volatile and

it can be easily removed by applying reduced pressure or nitrogen sweeping at the regular temperature [12], [15], [17], [18].

Despite the described alternative amino donors, alanine is still the most used owing to its widespread acceptance by enzymes [7]. When alanine is used as amino donor, pyruvate is formed as by-product and, in this sense, several biocatalytic strategies has been proposed for its removal. Even though the use of several enzymes in one pot is not always desirable because of the overall cost increase that can suppose [19], combining transaminase with other enzymatic routes allows the shortening of reaction routes, a reduction of chemical waste and the achievement of a high atom-efficiency [15]. A widely applied method consists in coupling TA with lactate dehydrogenase (LDH), which converts pyruvate to lactate [7], [12], [16], [17], [20]. This transformation involves the expense of NADH, thus an additional enzyme is needed for cofactor recycling. In most cases, glucose dehydrogenase (GDH) and glucose are added for this purpose [16], [17], [20]. GDH transforms glucose, which acts as a reducing agent, to gluconic acid, while NADH is produced again from the NAD^+ generated during LDH reaction. Therefore, the overall process becomes more complex since it requires three enzymes, a reducing agent must be added and a pH control is recommended because a shift on pH takes place when high gluconic acid amounts are produced [16], [17]. Another extensively employed pyruvate removing option is the use of alanine dehydrogenase (AlaDH), which converts pyruvate back to alanine, having the double effect of also regenerating the amine donor [7], [12]. This reaction takes place with the expenses of ammonia and NADH, which means that a cofactor recycling system must also be considered [16], [20]. To avoid the need of expensive cofactors and recycling systems, two methods have been described involving the use of a single enzyme for pyruvate removing. On the one hand, acetolactate synthase can be used to condense two molecules of pyruvate to acetolactate, which, after a spontaneous decarboxylation, yields acetoin and CO_2 [17], [21]. On the other, pyruvate decarboxylase can be used to directly transform pyruvate to acetaldehyde and CO_2 [7], [11], [12], [17], [20]. All the mentioned biocatalytic approaches for pyruvate removing are summarized in Scheme 5.2.

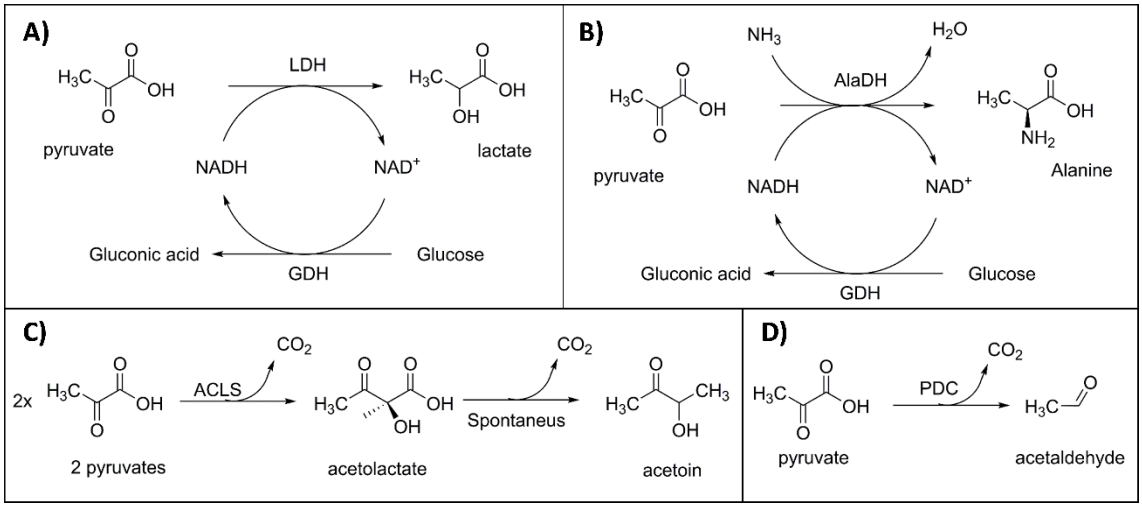

Scheme 5.2 Pyruvate removal systems based on the construction of enzymatic cascades. A) Lactate dehydrogenase (LDH) converts pyruvate to lactate with the expense of NADH, which is recycled by the glucose dehydrogenase (GDH) reaction. B) Alanine dehydrogenase (AlaDH) recycles the amine donor by transforming pyruvate to alanine with the expense on NADH, which is recycled by the GDH reaction. C) Acetolactate synthase (ACLS) condenses two pyruvates to acetolactate, which is spontaneously decarboxylated to acetoin. D) Pyruvate decarboxylase (PDC) decarboxylates pyruvate to acetaldehyde.

In the present thesis, asymmetric synthesis of two model chiral amines has been studied according to the strategies illustrated in Scheme 5.3: i) 3-amino-1-phenylbutane (3-APB) from the prochiral ketone 4-phenyl-2-butanone (4-PB) and ii) 1-phenyl-ethylamine (1-PEA) from acetophenone (AP). In both cases, alanine was used as amine donor and pyruvate decarboxylase (PDC) was coupled with the TA as a pyruvate removing system for shifting the equilibrium. As it has been mentioned, PDC transforms pyruvate to acetaldehyde and CO_2. Therefore, in addition of not needing expensive cofactors with the consequent need for a recycling system, an irreversible equilibrium shift can be obtained due to the loss of the carbon dioxide by-product [7], [12], [20]. The main drawback of this system is related to acetaldehyde formation. Even though it is an easily removable by-product due to its high volatility, it can be aminated leading ethylamine formation, which would suppose an undesired competition with the prochiral ketone that also would consume alanine [16], [17].

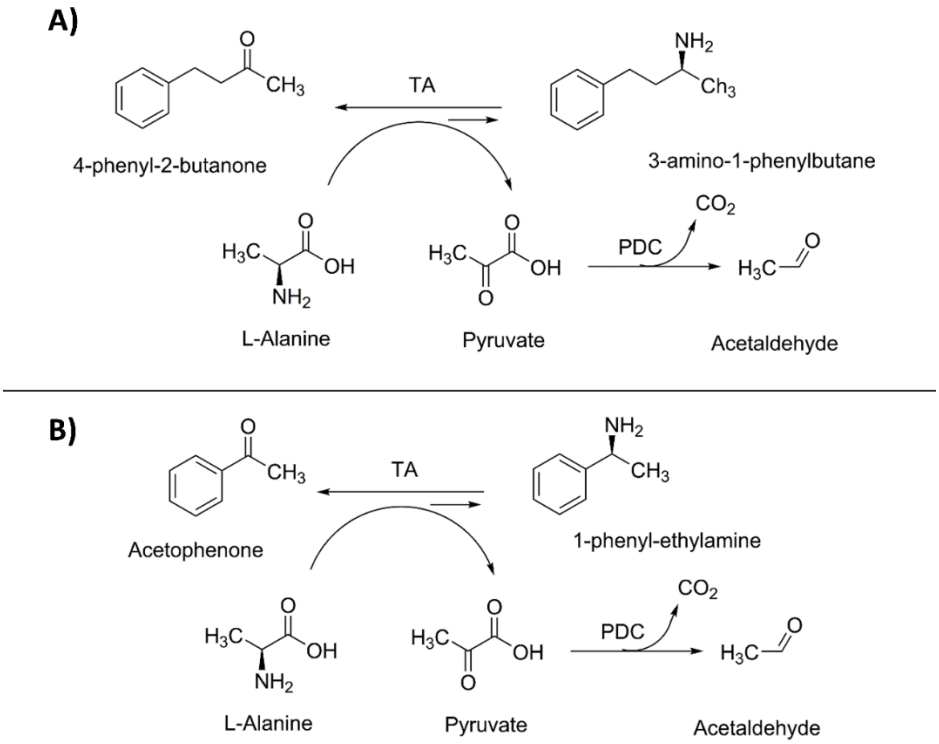

Scheme 5.3 Asymmetric synthesis of two model chiral amines using pyruvate decarboxylase system for pyruvate removing. A) 3-amino-1-phenylbutane (3-APB) synthesis from its prochiral ketone 4-phenyl-2-butanone (4-PB) and alanine as amino donor. B) 1-phenyl-ethylamine (1-PEA) synthesis from its prochiral ketone acetophenone (AP) and alanine as amino donor.

5.2. Materials and methods

5.2.1. Chemicals and enzymes

All chemicals were purchased from Sigma-Aldrich (St. Louis, MO, USA). Four transaminases from *Aspergillus terreus* (Ate-TA, Ate-TA_T247S), *Chromobacterium violaceum* (Cvi-TA) and *Vibrio fluvialis* (Vfl-TA) were kindly donated by DSM/InnoSyn in the form of *Escherichia coli* cell-free extracts (CFE), containing between 40 and 55 $mg \cdot mL^{-1}$ of total protein. In the case of CFE of Ate-TA and Ate-TA_T247S around 70 % of the total protein was transaminase, while this percentage was 47 % for Cvi-TA and 35 % for Vfl-TA. Pyruvate decarboxylase (PDC) from *Zimobacter palmae* was produced by high cell density cultures of a recombinant *E. coli* strain obtained by the research group as it has been described in chapter 3. CFEs of this strain were obtained by sonication with a Vibracell® VC50 (Sonic and Materials®, Newton, CT, USA) with four times 15 s pulses (50 W) and 2 min intervals in ice between each pulse. Centrifugation was

performed (10000 g, 10 min) to remove the resulting cell debris. ZpPDC CFEs contained 10 $mg \cdot mL^{-1}$ of total protein, from which around 40 % was PDC.

5.2.2. Asymmetric synthesis of chiral amines with transaminase and pyruvate decarboxylase

All biocatalytic reactions were performed in potassium phosphate buffer 150 mM and pH 7.5 containing 1 mM pyridoxal-5'-posphate (PLP), 0.1 mM thiamine pyrophosphate (TPP) and 0.1 mM $MgCl_2$. A transaminase cell lysate concentration of 5 % $v \cdot v^{-1}$ was coupled with 25 % $v \cdot v^{-1}$ PDC cell lysate in 15-mL Falcon tubes containing 3 mL working volume and kept at 30^{o}C and 1000 rpm for 8 hours in a Multitherm shaker (Benchmark Scientific). Reactant concentrations were 10 mM ketonic substrate and 200 mM alanine.

5.2.3. Temperature and amine donor concentration effect on chiral amines synthesis

To study the temperature effect on amine synthesis all reaction conditions mentioned were maintained while temperature was shifted to 15^{o}C or 40^{o}C. In the alanine concentration effect studies, reactions were performed increasing the amine donor concentration to 400 mM and 600 mM.

5.2.4. Reaction medium engineering

The effect of adding DMSO or glycerol in the reaction medium was studied. In a first screening, reactions were performed as described in section 5.2.2 but including 5 %, 10 % or 15 % of the mentioned cosolvents. Initial and final ketonic substrates and amines concentrations were measured to calculate the respective reaction yields. Reactions with those medium compositions which did not show negative effects on yield were deeper studied. In this cases, ketonic substrate concentrations were increased to the maximum allowed by the ketone solubility into the new conditions.

5.2.5. Enzymatic activity assays

5.2.5.1. Transaminase activity assay

Transaminase activity assay was based on the acetophenone formation measurement at 340 nm and 30ºC from α-Methylbenzylamine and pyruvic acid. The assay was performed in 1 mL reaction mixture, consisting of potassium phosphate buffer 100 mM and pH 7.5 containing 0.1 mM PLP, 22.5 mM α-Methylbenzylamine and 5 mM sodium pyruvate. Coefficient of molar extinction (ε) of acetophenone is 0.28 $mM^{-1} \cdot cm^{-1}$ and one transaminase activity unit corresponds to the amount of enzyme that produces 1 µmol acetophenone per minute at 30ºC. Absorbance measurements were performed using a SPECORD® 200 PLUS (Analytik Jena) spectrophotometer.

5.2.5.2. Pyruvate decarboxylase activity assay

PDC activity was determined by coupling the pyruvate decarboxylation with alcohol dehydrogenase (ADH) and following NADH oxidation at 340 nm and 25ºC, whose coefficient of molar extinction (ε) is 6.22 $mM^{-1} \cdot cm^{-1}$. The reaction mixture contained 33 mM sodium pyruvate, 0.11 mM NADH, 3.5 UA mL^{-1} ADH from *Saccharomyces cerevisiae* (Sigma-Aldrich), 0.1 mM TPP and 0.1 mM $MgCl_2$ in citrate buffer 200 mM and pH 6. One unit of PDC activity corresponds to the amount of pyruvate decarboxylase that converts 1 µmole of pyruvate to acetaldehyde per minute. Absorbance measurements were performed using a SPECORD® 200 PLUS (Analytik Jena) spectrophotometer.

5.2.6. Analytical methods

5.2.6.1. Ketonic substrates and amines analysis by HPLC

All amine and ketonic substrates concentrations were measured by HPLC analysis in an UltiMate 3000 (Dionex) equipped with a variable wavelenght detector. Compounds were separated on a reversed-phase CORTECS C18+ 2.7 µm 4.6× 150mm column (Waters Milford, MA, USA). After acidifying reaction samples with 3 M hydrochloric acid to deactivate the enzymes, 15 µL were injected at a 0.7 $mL \cdot min^{-1}$ flow rate and 30ºC. In the case of 4-PB to 3-APB reaction, samples were eluted using a gradient from 30 to 55 % solvent B —consisting of 0.095 % ($v \cdot v^{-1}$) in MeCN/H_2O 4:1 ($v \cdot v^{-1}$) — to solvent A — consisting of 0.1 % ($v \cdot v^{-1}$) TFA in H_2O— over 13 minutes and compounds were detected at a 254 nm wavelength. In the case of AP to 1-PEA the gradient

started at 15 % solvent B instead of 30 % and compounds were detected at a 210 nm wavelength.

5.2.6.2. Enantiomeric excess determination

At the end of the reaction the entire volume was acidified with 3 M hydrochloric acid and centrifuged to remove the precipitate proteins. After that, a first extraction step was performed with dichloromethane and the organic phase was discarded. After basifying the aqueous phase with NaOH, a second extraction was carried out with the same solvent. The new organic phase was dried with anhydrous sodium sulphate and concentrated by distillation in a Heidolph VV 2000 rotary evaporator. Amines of interest (3-APB or 1-PEA) were separated from the remaining impurities by a silica column using 1:10 methanol in dichloromethane with 2 % triethylamine as mobile phase.

The enantiomeric excess was determined by nuclear magnetic resonance (NMR) in the NMR service of the same university (SeRMN UAB), using (*R*)-(-)-1,1'-binaphtyl-2,2'-hydrogenphosphate (BHP) as a chiral solvating agent (CSA). An equimolar quantity of the CSA was used if not stated otherwise. The ^{1}H-NMR spectra were acquired with a Bruker AVANCE-III 600 MHz NMR Spectrometer (Bruker Biospin, Rheinstetten, Germany) in $CDCl_3$ at 298 K.

5.3. Results and discussion

5.3.1. Synthesis of 3-APB by the cascade reaction of transaminase and pyruvate decarboxylase.

As it has already been mentioned, 3-amino-1-phenylbutane (3-APB) asymmetric synthesis by TAs coupled with PDC as pyruvate removal system was studied (see Scheme 5.3 A). In chapter 4, four different transaminases and the ZpPDC produced by fermentation in the present work (chapter 3) were characterized to found compromise pH conditions. After that, in a first screening study, transaminases from *Chromobacterium violaceum* (Cvi-TA) and *Vibrio fluvialis* (Vfl-TA) were selected as the most adequate for this reaction under pH 7.5 conditions.

The mentioned cascade reaction was deeply studied with Cvi-TA and Vfl-TA and compared with the respective one-enzyme systems. Time courses of the reactions are presented in Figure 5.1 (A and C) as well as enzyme activity profiles (B and D). Results showed that an effective amine synthesis only took place by the cascade systems (TA + PDC). In comparison to reactions

performed without pyruvate removal system, 10-fold higher 3-APB concentration was achieved with Cvi-TA/PDC and 6-fold higher with Vfl-TA/PDC. Even though the same final amine concentration was achieved with both transaminases (around 6 mM), Cvi-TA showed a 1.75-fold higher initial reaction rate (4.95 $mM \cdot h^{-1}$) than Vfl-TA (2.83 $mM \cdot h^{-1}$). Regarding stability profiles (Figure 5.1 B and D), while Cvi-TA activity sharply decreased towards reaction time, suffering a 90 % deactivation after two hours, Vfl-TA showed a better operational stability, suffering firstly an hyperactivation and ending the reaction with a 20 % remaining activity after 8 hours. It can be also observed that when no PDC was coupled and thus almost no amine was formed, TAs activities remained more stable. This low operational stability in TAs when transamination takes place has widely been reported [22] and recently related by other authors to an irreversible inactivation step that proceeds once the TA:PMP complex dissociates into free PMP and apoenzyme [23].

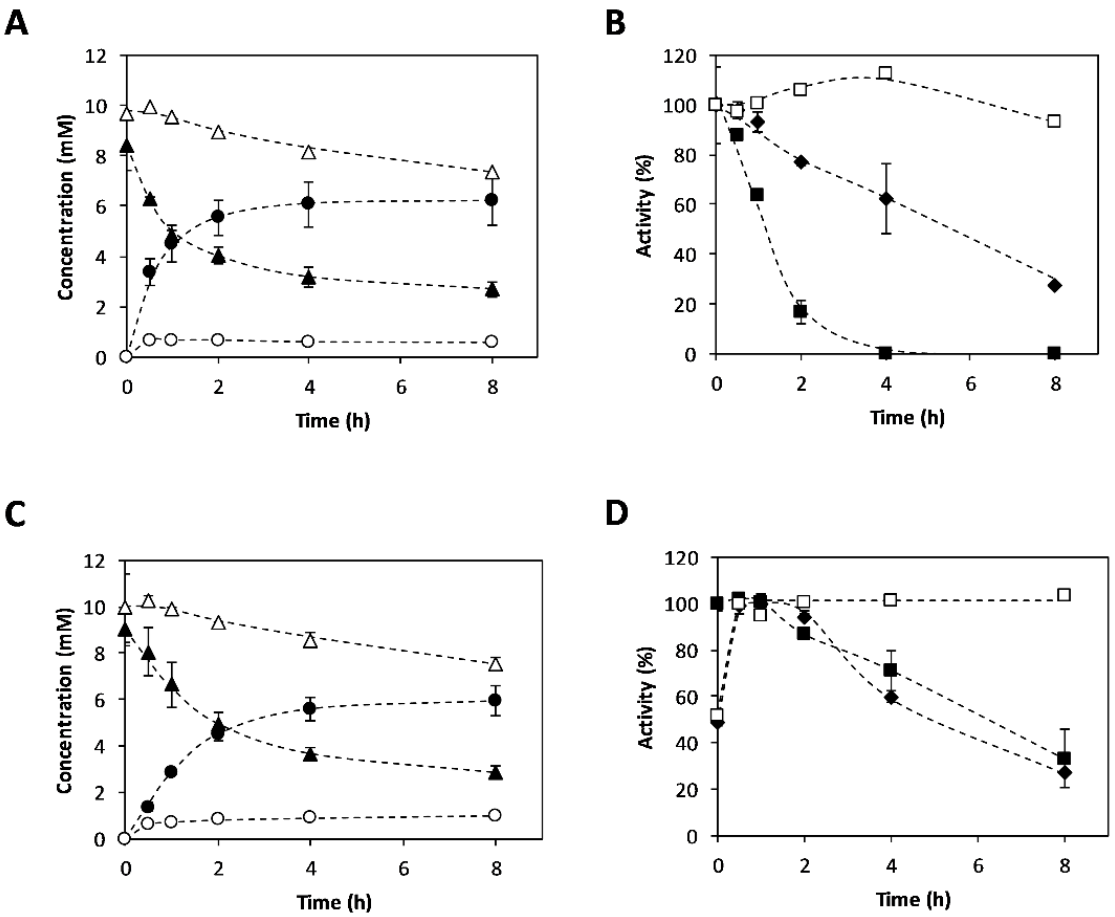

Figure 5.1 Reaction time courses of 3-APB synthesis and operational enzymatic stability. A) and C) are the reaction time courses performed with Cvi-TA (A) and Vfl-TA (C): (●) 3-APB concentration in cascade reactions; (○) 3-APB concentration in reactions without PDC; (▲) PB concentration in cascade reactions;

(△)PB concentration in reactions without PDC. Operational stability of Cvi-TA (B) and Vfl-TA (D), as well as PDC when cascade reactions were performed: (■) Transaminase activity in cascade reactions. (□) Transaminase activity in reactions without PDC. (◆) PDC activity. Temperature 30 ^{o}C; pH 7.5; 4-PB 10 mM; Alanine 200 mM; TA 5 % v v^{-1}; PDC 25 % v v^{-1}.

The same conversion percentages (Table 5.1) were achieved with the two different transaminases when coupled with PDC, which were around 3-fold higher than when no pyruvate decarboxylase was added. Moreover, the obtained yields in both coupled reactions were similar to the achieved conversion, which reflects a high reaction selectivity towards the target product (88.70 ± 10.24 % and 86.10 ± 12.89 % for the Cvi-TA/PDC system and the Vfl-TA/PDC system, respectively). When no PDC was added, also similar conversion with both TAs were reached (23.00 ± 9.45 % and 22.94 ± 8.84 % for the Cvi-TA system and the Vfl-TA system, respectively). However, yields were significantly lower compared to the conversions, resulting in very low selectivities: < 35% and < 60% (Table 5.1) for Cvi-TA and Vfl-TA, respectively. These results indicated that, when no decarboxylation reaction is coupled, side-reactions catalyzed by the TA are boosted.

Table 5.1 Process metrics of 3-APB synthesis by the cascade reaction of TA and PDC. Final 3-APB concentration, conversion, yield and selectivity of the cascade reactions performed with Cvi-TA or Vfl-TA coupled with PDC and compared with their respective one-enzyme reactions. Reaction time 8h; temperature 30^{o}C; pH 7.5; 4-PB 10 mM; Alanine 200 mM; TA 5 % v v^{-1}; PDC 25 % v v^{-1}.

Enzyme	Reaction	Final [APB] (mM)	Conversion (%)	Yield (%)	Selectivity (%)	STY ($mmol \cdot L^{-1} \cdot h^{-1}$)
Cvi-TA	TA and PDC	6.20 ± 0.98	72.04 ± 3.12	64.22 ± 10.14	88.70 ± 10.24	0.78 ± 0.12
	TA	0.58 ± 0.00	23.00 ± 9.45	6.11 ± 0.98	34.07 ± 18.27	0.07 ± 0.00
Vfl-TA	TA and PDC	5.92 ± 0.64	71.03 ± 2.99	60.77 ± 6.58	86.10 ± 12.89	0.74 ± 0.08
	TA	1.01 ± 0.05	22.94 ± 8.84	10.45 ± 2.00	57.43 ± 30.84	0.13 ± 0.01

Chiral amine synthesis using the Vfl-TA/ZpPDC system was reported by Höhne *et al* [11], which synthesized several amines including 3-APB. However, a conversion of 45 % was obtained in that case, even though reaction was performed with 5 mM ketone and 110 mM L-alanine [11]. Therefore, in the present work, process metrics of the TA/PDC system have been improved.

However, better conversions were achieved in studies in which Vfl-TA was coupled with other co-product removal systems such as alanine dehydrogenase (AlaDH) or lactate dehydrogenase (LDH) [24]. The use of Cvi-TA coupled with PDC has not been reported, thus the effectiveness of the system with this enzyme has been proved in the present study. Nevertheless, Cvi-TA has been applied in the mentioned AlaDH and LDH system, achieving conversions of 16 % and 86 % respectively [25].

5.3.2. Reaction conditions optimization

Even though many potential biocatalytic processes have been suggested in literature, its implementation to industrial scale supposes great efforts on the achievement of several safety, legal, economic and environmental aspects [26]. Enzyme reactions are frequently hampered by unfavorable thermodynamics that may be addressed by the modulation of the applied conditions. These conditions can be usually so different from those found in nature [27], thus biocatalyst related issues, such as enzyme inhibition or instability, must be also taken into account [28]. In addition, industry will always tend to reduce production steps as long as it is possible. In this sense, enzymes are often used as crude cell extracts, as is the case of the present work, in order to avoid additional purification steps. A main disadvantage of this enzyme form is the presence of protein impurities that can catalyze possible side-reactions and negatively affect process selectivity [29].

Taking into account all the mentioned issues, efforts must be made to appropriately optimize the processes to achieve reasonable metrics to industrial implementation. In the present section, deeper studies on 3-APB asymmetric synthesis were performed to modulate conditions in a way that yield could be maximized.

5.3.2.1. Temperature effect on 3-APB synthesis

In a first approach to optimize the cascade reaction system, temperature effect was studied. On the one hand, temperature was shifted to 40ºC with the aim to increase reaction rate and enhance volatile by-products elimination (acetaldehyde and CO_2) [30]. On the other hand, temperature was decreased to 15ºC to improve enzyme stability and thus prevent an early reaction stop due to enzyme deactivation. In the mentioned temperatures, both substrate and product were stable.

Synthesis profiles are shown in Figure 5.2 (A and C) and related to temperature effect on operational stabilities (B and D). When temperature was increased to 40°C, 1.45-fold higher initial reaction rates were obtained for both TAs/PDC systems compared to cascade reactions performed at 30°C (7.2 $mM \cdot h^{-1}$ Cvi-TA and 5.8 $mM \cdot h^{-1}$ Vfl-TA). However, lower 3-APB concentrations were achieved (around 4.5 mM in both cases). In addition, a decrease on product concentration was detected after 4 hours reaction, which was slightly more pronounced with Vfl-TA. Thus, temperature increase may have led to boost undesired side reactions involving the target product.

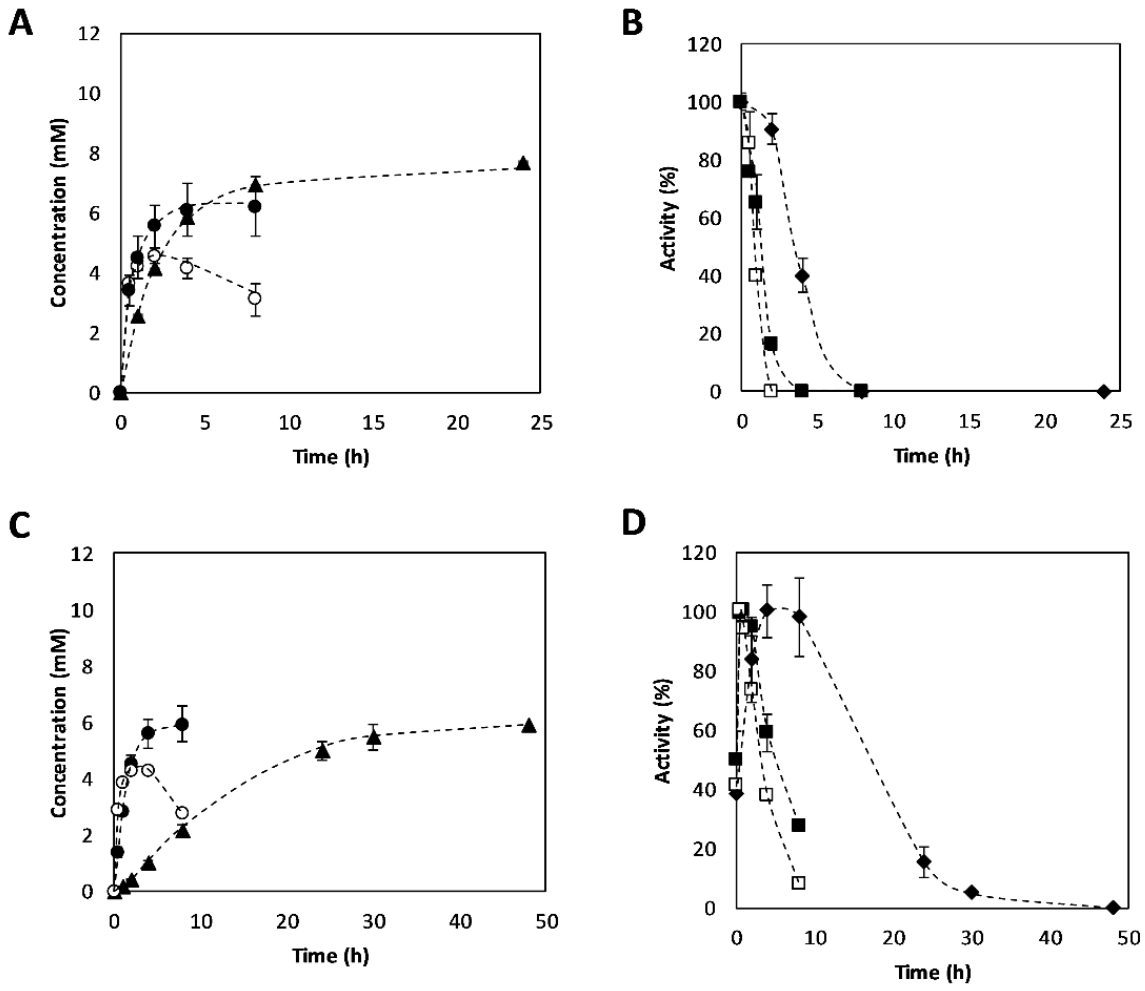

Figure 5.2 Temperature effect on 3-APB synthesis and on operational enzymatic stability. A) and C) show the reaction time courses performed with Cvi-TA (A) or Vfl-TA (C) and PDC at 15°C (▲), 30°C (●) and 40°C (○). B) and D) show operational stability of Cvi-TA (B) and Vfl-TA (D) during the cascade reactions performed at 15°C (◆), 30°C (■) and 40°C (□). pH 7.5; 4-PB 10 mM; Alanine 200 mM; TA 5 % v v^{-1}; PDC 25 % v v^{-1}.

Temperature increase also negatively affected enzyme operational stabilities (Figure 5.2 B and D), especially in Vfl-TA. In the case of Cvi-TA, stability profile suffered a sharper decrease at 40ºC in comparison with 30ºC and total deactivation was slightly earlier detected. Regarding Vfl-TA, after 8 hours, it was practically deactivated while at 30ºC it still conserved around 20% of the initial activity. Other authors have reported similar results in the synthesis of chiral amines from pro-chiral ketones using commercial transaminases. When ATA-103, ATA-113, ATA-114 and ATA-117 were applied for asymmetric amination of 4-phenyl 2-butanone, lower conversions were obtained with ATA-114, ATA-117 and ATA-103 after 24 hours when temperature was increased from 30 to 40ºC, probably due to a decrease in enzyme stability. Only with commercial ATA-113 conversion was increased from 61 to 82 % after temperature increasing which could be related to a higher operational stability of this transaminase towards temperature [31]. As it was expected, both Cvi-TA and Vfl-TA increased their operational stability when temperature was decreased to 15ºC. Nevertheless, this enhanced stability was associated to lower reaction rates (2.1 $mM \cdot h^{-1}$ CviTA and 0.28 $mM \cdot h^{-1}$ VflTA), which enlarged reaction times to 24 hours and 48 hours respectively.

As it is shown in Table 5.2, temperature shift was only favorable in the case of Cvi-TA at 15ºC in terms of selectivity, whose high value indicates that undesired side reactions were suppressed. However, an only 10% increase on yield was obtained compared to the results at 30ºC while space-time-yield suffered a 60% decrease. Regarding Vfl-TA, STY loss at 15ºC was even more severe due to the high reaction time combined with a decrease in terms of conversion, yield and selectivity. Regarding the results concerning the 40ºC, low selectivity percentages, which did not surpass 50%, together with the significant difference between conversions and yields, indicate again the presence of undesired side reactions. Altogether lead to the conclusion that 30ºC was the best option to perform the cascade reactions.

Table 5.2 Process metrics of 3-APB synthesis with the cascade reaction at different temperatures. Final 3-APB concentration, reaction time, conversion, yield, selectivity and space-time yield of the cascade reaction of Cvi-TA/Vfl-TA and PDC at different temperature conditions. pH 7.5; 4-PB 10 mM; Alanine 200 mM; TA 5 % v v^{-1}; PDC 25 % v v^{-1}.

Enzyme	Temperature (°C)	Final [APB] (mM)	Reaction time (h)	Conversion (%)	Yield (%)	Selectivity (%)	STY ($mmol \cdot L^{-1} \cdot h^{-1}$)
Cvi-TA	15	7.68 ± 0.05	24	73.71 ± 0.51	75.40 ± 0.48	102.31 ± 1.35	0.32 ± 0.00
	30	6.20 ± 0.98	8	72.04 ± 3.12	64.22 ± 10.14	88.70 ± 10.24	0.78 ± 0.12
	40	3.08 ± 0.54	8	61.72 ± 1.34	30.22 ± 5.32	48.80 ± 7.55	0.38 ± 0.07
Vfl-TA	15	5.92 ± 0.50	48	71.78 ± 1.29	52.21 ± 4.40	80.89 ± 5.38	0.12 ± 0.01
	30	5.92 ± 0.64	8	71.03 ± 2.99	60.77 ± 6.58	86.10 ± 12.89	0.74 ± 0.08
	40	2.30 ± 0.45	8	48.35 ± 2.08	24.11 ± 4.71	46.46 ± 7.14	0.29 ± 0.06

5.3.2.2. Amine donor concentration

The next step for achieving a cascade reaction optimization consisted in studying the effect of amine donor concentration on reaction yield. Although certain limitations such as enzyme inhibition, substrate solubility and downstream complexity must be taken into account [15], [28], [32], offering an excess of amino donor is a widely reported strategy to force an equilibrium shift in transaminations [4], [9], [15], [28], [32]. When L-alanine is used as amine donor, at least 10-fold excess is recommendable [32], reason why the chosen initial concentration was 200 mM, which correspond to a 20-fold excess in respect to the ketonic substrate (10 mM). A study on alanine excess effect to reaction yield has been reported for the case of 1-N-Boc-3-aminopyrrolidine synthesis by the cascade reaction of Vfl-TA and PDC. In the mentioned work, a significant increase on yield was produced when an alanine excess higher than 22-fold was used [11]. For this reason, in this study, initial lower amino donor concentrations than 200 mM (20-fold excess) were not tested and reactions were performed in a 40-fold and a 60-fold excess.

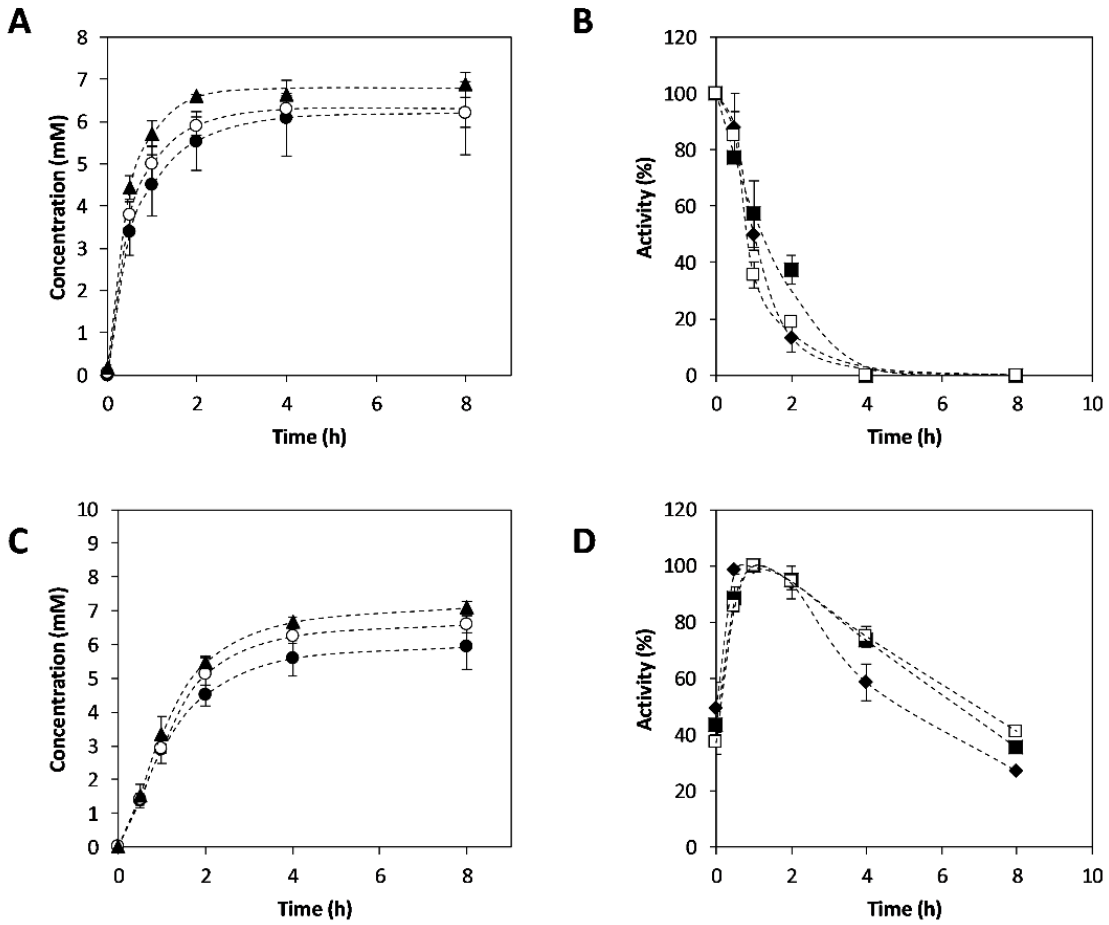

Figure 5.3 Alanine concentration effect on 3-APB synthesis and on operational enzymatic stability. A) and C) show the reaction time courses performed with Cvi-TA (A) or Vfl-TA (C) and PDC using 200 mM (●), 400 mM (○) and 600 mM (▲) alanine concentration. B) and D) show operational stability of Cvi-TA (B) and Vfl-TA (D) during the cascade reactions performed at 200 mM (◆), 400 mM (■) and 600 mM (□) initial alanine concentration. Temperature 30^{o}C; pH 7.5; 4-PB 10 mM; TA 5 % v v^{-1}; PDC 25 % v v^{-1}.

Figure 5.3 shows a comparison of reaction time courses at different initial alanine concentrations (200 mM, 400 mM, and 600 mM) both using Cvi-TA/PDC (A) and Vfl-TA/PDC (C). In both different transaminases, initial reaction rates were higher when alanine concentration was increased from 200 to 600 mM, thus the alanine concentration increase did not have any inhibitory effect on transaminases. Nevertheless, no significant changes were observed in operational stabilities (Figure 5.3 B and D).

Final 3-APB concentrations achieved at 400 mM and 600 mM alanine concentration were not significantly higher than the ones obtained with 200 mM (Table 5.3). An around 10 % higher yield could be considered when amine donor excess was increased to 60-fold (600 mM alanine)

in comparison with applying a 20-fold excess (200 mM alanine), which agrees with the previously mentioned 1-N-Boc-3-aminopyrrolidine case [11]. The similarity between yield and conversion percentages, as well as the high selectivity values, indicates that the alanine increase did not enhance the emergence of side reactions. Although higher alanine concentrations did not show a negative effect on reaction, the low yield increase in relationship with the high additional alanine used for it led to the conclusion that the initially planned amine donor excess of 20-fold is the most suitable strategy.

Table 5.3 Process metrics of 3-APB synthesis with the cascade reaction of TA and PDC performed at different initial alanine concentrations. Final 3-APB concentration, conversion, yield and selectivity of the cascade reactions performed with Cvi-TA or Vfl-TA coupled with PDC at different initial alanine concentrations. Temperature 30^{o}C; pH 7.5; 4-PB 10 mM; TA 5 % v v^{-1}; PDC 25 % v v^{-1}.

Enzyme	Initial [Alanine] (mM)	Final [APB] (mM)	Conversion (%)	Yield (%)	Selectivity (%)	STY (mmol·L^{-1}·h^{-1})
Cvi-TA	200	6.20 ± 0.98	72.04 ± 3.12	64.22 ± 10.14	88.70 ± 10.24	0.78 ± 0.12
	400	6.22 ± 0.35	76.43 ± 3.57	59.54 ± 3.33	78.27 ± 8.01	0.78 ± 0.04
	600	6.88 ± 0.06	77.81 ± 1.58	71.73 ± 1.64	92.19 ± 0.25	0.86 ± 0.01
Vfl-TA	200	5.92 ± 0.64	71.03 ± 2.99	60.77 ± 6.58	86.10 ± 12.89	0.74 ± 0.08
	400	6.60 ± 0.25	78.37 ± 4.38	68.44 ± 2.62	87.78 ± 8.24	0.82 ± 0.03
	600	7.08 ± 0.18	80.04 ± 6.23	73.21 ± 2.00	91.83 ± 4.64	0.89 ± 0.02

5.3.3. Reaction medium engineering: study on cosolvent addition into the medium

Widely-used approaches on biocatalytic processes optimization are based on reaction medium engineering. In general, performing reactions in aqueous medium is preferred because of its lower environmental impact. However, a common limitation of aqueous systems is the low solubility of some substrates in water, which hampers the achievement of high product concentrations [32]. In this sense, cosolvents are often used not only to increase substrate load [32]–[34] but also because of their positive stabilization effect on enzymatic structures [15], [22], [35], even though its presence may complicate downstream processes or could result in an enzymatic activity decrease [22], [32].

In the present section, medium engineering by cosolvent addition was applied for the cascade reaction of the two selected transaminases and PDC. Two different cosolvents were selected as possible candidates for medium modification: DMSO and glycerol. On the one hand, the use of

DMSO has widely been reported in asymmetric amine synthesis by ω-transaminases [10], [22], [24], [31], [36], [37]. The use of this cosolvent at a concentration range from 5 % to 15 % into 3-APB synthesis not only improved conversion in several transaminase cases but also increased its estereoselectivity [31], even though detrimental effects have also been reported in the Vfl-TA case [24]. DMSO has been presented as a promising additive for Cvi-TA stabilization too, but it may have a negative effect on its activity [22]. On the other hand, glycerol has been extensively used as a protein preservative during enzyme storage [38]. Even though its use on asymmetric synthesis is not common, glycerol showed the ability of preventing Cvi-TA denaturation, which may be helpful for the operational stability maintenance during reaction [22].

A preliminary reaction screening was carried out adding into the reaction medium DMSO or glycerol at 5 %, 10 % and 15 % concentration. The effect of these medium modifications to reaction yields are exposed in Figure 5.4, both in the case of cascade reactions performed with Cvi-TA (A) and Vfl-TA (B).

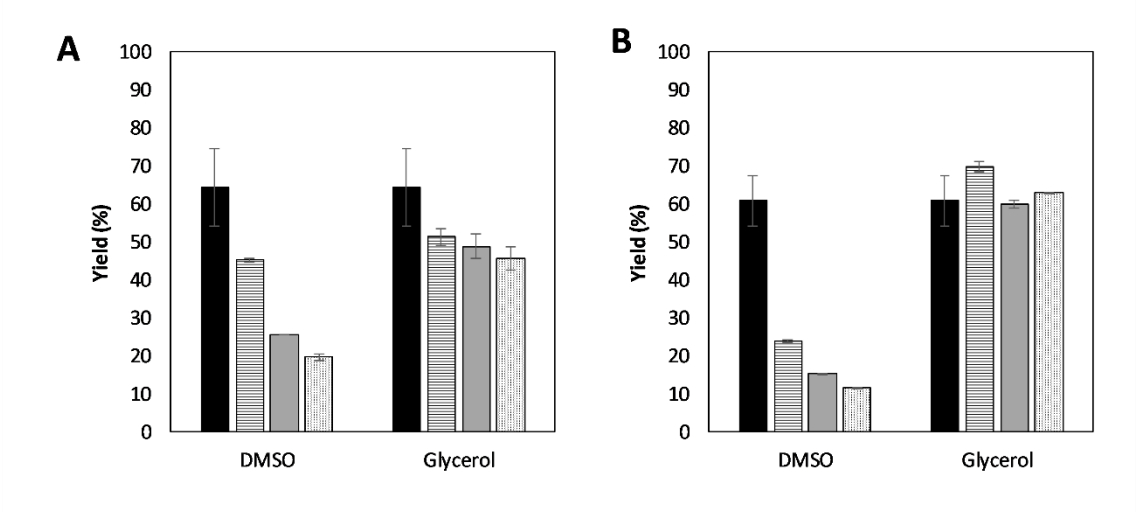

Figure 5.4 Effect of DMSO and glycerol presence on 3-APB synthesis. Reaction yields obtained by adding 0% (black), 5% (striped), 10% (grey) and 15% (dotted) of DMSO or glycerol into the medium in cascade reactions with Cvi-TA (A) or Vfl-TA (B) coupled with PDC. Reaction conditions were the same established in previous sections (pH 7.5; temperature 30ºC; [4-PB] 10 mM; [L-Alanine] 200 mM; TA 5 % v v^{-1}; PDC 25 % v v^{-1}; reaction time 8 hours).

In general, DMSO had a negative effect, especially in the Vfl-TA reaction, which suffered a 60 % loss on yield just with the addition of 5 % DMSO. As it has been mentioned, this detrimental

effects of DMSO on conversion have already been reported for this enzyme [24]. In contrast, even though only one third of the aqueous conditions yield was obtained when more than 10 % DMSO was applied in Cvi-TA reaction, the consequences of adding 5 % cosolvent concentration were not that negative, since 70 % of the initial yield was obtained. Therefore, a 5 % DMSO in the medium was selected as a possible modification in the case of Cvi-TA reaction. In the presence of the mentioned DMSO concentration, 4-PB solubility increased from 10 mM to 20 mM, which offered the possibility of starting the reaction at higher initial substrate concentration.

Regarding glycerol addition to the medium, a 20-30 % decrease on Cvi-TA reaction yield took place while it did not suppose any yield loss in Vlf-TA case. Then, the possibility of using glycerol as a cosolvent was also selected. The yield decreases obtained with Cvi-TA could be related to the activity loss due to the cosolvent presence reported by Chen 2016 [22], who explored the effect of DMSO and glycerol concentration on Cvi-TA activity. In that work, the first one had a more negative effect since with a 10 % of glycerol more than 80 % of the activity without cosolvent was obtained, while with a 10 % DMSO this percentage did not arrive to 50 % [22]. By selecting 10 % glycerol into the medium, initial 4-PB concentration could be increased from 10 mM to 15 mM due to the enhanced solubility.

5.3.3.1. Cascade reaction of Cvi-TA and PDC with DMSO into the medium

After selecting 5 % DMSO in Cvi-TA, cascade reaction with this enzyme and this medium composition was more deeply studied. Because of the cosolvent presence more ketonic substrate amount could be solubilized, thus 4-phenyl-2-butanone initial concentration was increased to 20 mM. However, the obtained synthesis profile (Figure 5.5 A) was so similar in respect to the reaction in aqueous conditions (section 5.3.1) even though the initial reaction rate was slightly lower (3.83 $mM \cdot h^{-1}$ with DMSO and 4.95 $mM \cdot h^{-1}$ without it). Having increased the initial substrate concentration when DMSO was added into the medium, a higher initial reaction rate would be expectable. However, the mentioned reaction took place with lower Cvi-TA activity, which could be both associated to DMSO effect and/or a probable substrate inhibition. Also an identical transaminase deactivation profile (Figure 5.5 B) to the one obtained in the aqueous system was obtained, which consisted in a total deactivation after 4 hours. Therefore, DMSO could neither improve Cvi-TA reaction performance nor enzyme stability.

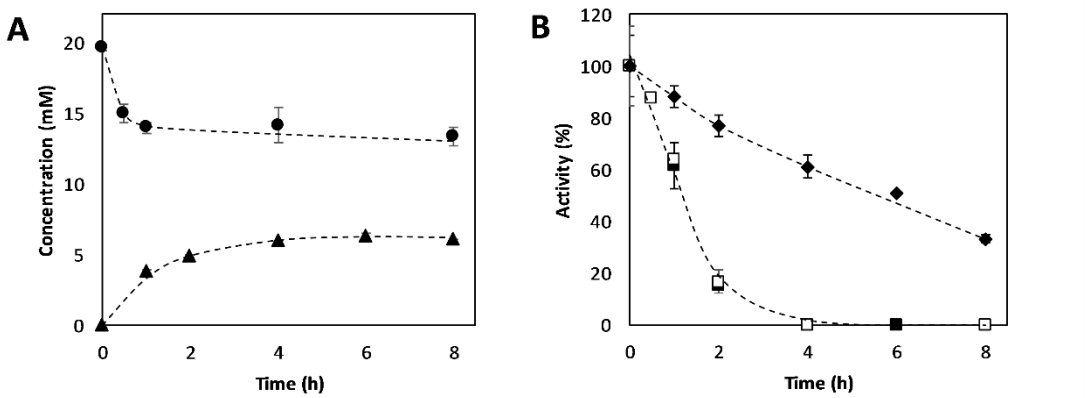

Figure 5.5 Effect of DMSO presence on 3-APB synthesis by the cascade reaction of Cvi-TA and PDC. A) Reaction time course: (▲) 3-APB concentration (mM), (●) 4-PB concentration (mM). B) Transaminase (■) and PDC (◆) operational stability during reaction. For a better evaluation of DMSO effect on TA stability, Cvi-TA deactivation profile when reaction was performed in aqueous medium is also presented (□) (pH 7.5; temperature 30ºC; [4-PB] 20 mM; [L-Alanine] 200 mM; TA 5 % v v^{-1}; PDC 25 % v v^{-1}).

Even though the same final 3-APB concentration was achieved (6 mM), reaction finished with half of the conversion and yield (32.15 ± 3.30 % and 30.99 ± 0.08 % respectively) in comparison with reactions without DMSO (72.40 ± 3.12 % and 64.22 ± 10.14 % respectively) because the initial 4-PB concentration had been doubled (see Table 5.4). This conversion decrease can be explained by the lower activity of Cvi-TA under these conditions. It has been reported that this transaminase, in the presence of 5% DMSO, shows a 60% of its activity in optimum conditions [22]. Since, in addition of not improving operational stability, more ketonic substrate was needed to obtain the same final amine concentration as in the aqueous system, the strategy of adding DMSO was discarded.

Table 5.4 Effect of DMSO presence on 3-APB synthesis by the cascade reaction of Cvi-TA and PDC. Initial 4-PB concentration, final 3-APB concentration, conversion, yield and selectivity of cascade reactions performed with Cvi-TA in aqueous medium and in the presence of 5% DMSO (pH 7.5; temperature 30°C; [4-PB] 20 mM; [L-Alanine] 200 mM).

[DMSO] (%)	Initial [PB] (mM)	Final [APB] (mM)	Conversion (%)	Yield (%)	Selectivity (%)
0	10	6.20 ± 0.98	72.04 ± 3.12	64.22 ± 10.14	88.70 ± 10.24
5	20	6.08 ± 0.02	32.15 ± 3.30	30.99 ± 0.08	97.45 ± 10.28

5.3.3.2. Effect of glycerol addition to the cascade reaction of Cvi-TA/Vf-TA and PDC

Also medium modification by glycerol addition effect was studied both for the case of using Cvi-TA and Vfl-TA into the cascade reaction with PDC. In this case, regarding the high tolerance of the enzymes towards this cosolvent, 10 % concentration was added. Higher concentrations were not regarded with the aim of modifying the least medium rheology and also because significant activity loses on Cvi-TA have been reported [22]. In this case, glycerol showed less solubilization power than DMSO and initial 4-PB concentration could only be increased to 15 mM.

As it is exposed in Figure 5.6 A, glycerol presence could not modify 3-APB synthesis profile in the cascade reaction performed with Cvi-TA in respect to the obtained without cosolvents (section 5.3.1), even though it enhanced transaminase operational stability maintaining 50 % of the initial activity after 4 hours (see Figure 5.6 B). As it occurred with DMSO, reaction rate did not increase with the higher substrate concentration, which could be explained with the aforementioned reported effects of glycerol to Cvi-TA.

In contrast, in the case of Vfl-TA, 10% glycerol not only enhanced stability but also changed reaction profile (Figure 5.6 C and D). Synthesis took place with an initial rate of less than the half previously obtained in the reactions in aqueous medium (1.10 $mM \cdot h^{-1}$ with glycerol and 2.83 $mM \cdot h^{-1}$ without it). However, after 8 hours, around 70% of the maximum activity was still maintained, unlike the case of aqueous medium, in which only 25% of the maximum activity was observed at this time. Therefore, reaction was extended several more hours, which led to a final concentration of more than 10 mM. This represents the highest reported 3-APB concentration asymmetrically synthetized by a transaminase using the PDC system for co-product elimination. It can also be mentioned that the use of glycerol enhanced PDC stability in all cases.

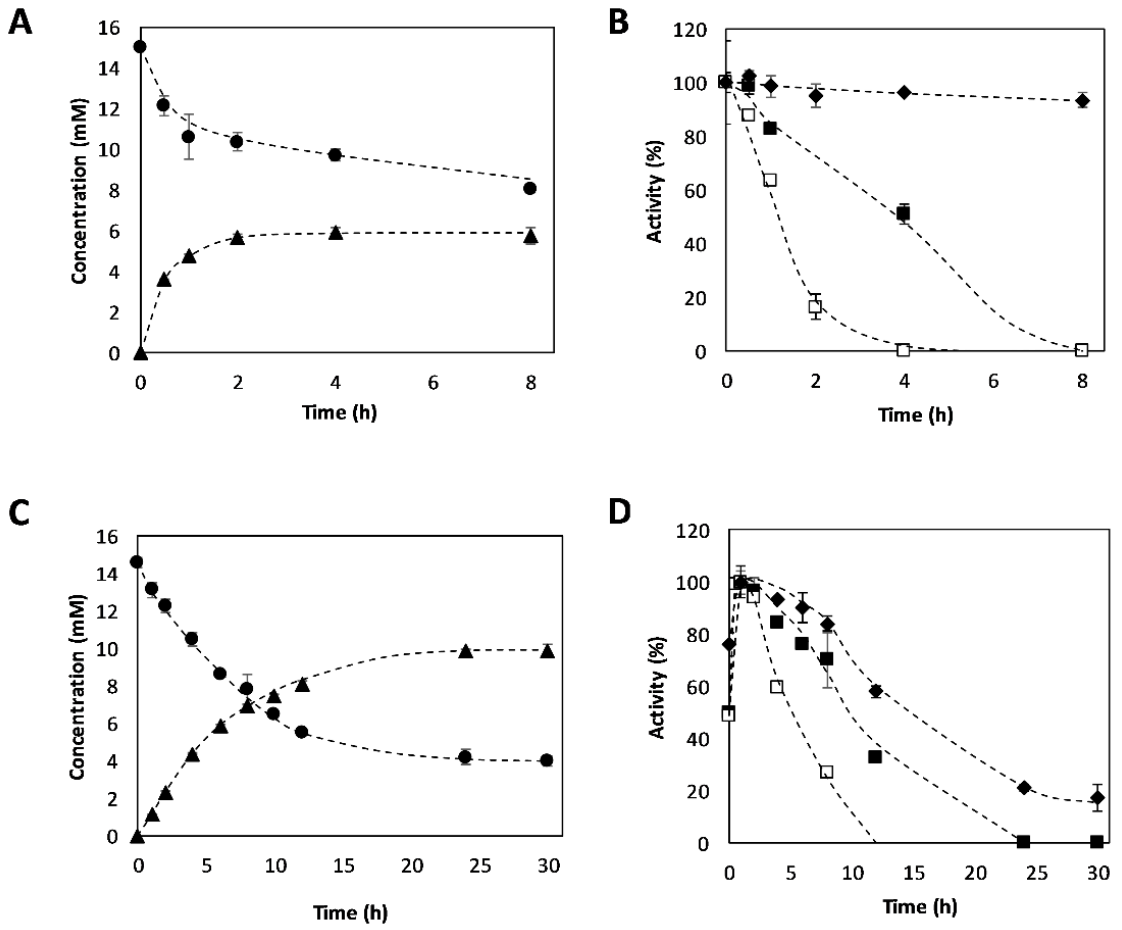

Figure 5.6 Effect of 10% glycerol presence on 3-APB synthesis by the cascade reaction of TA and PDC. Reaction time courses of reactions performed with Cvi-TA (A) or Vfl-TA (C): (▲) 3-APB concentration (mM), (●) 4-PB concentration (mM). Figures B and D correspond to operational stability profiles of the reactions performed with Cvi-TA and Vfl-TA respectively: (■) transaminase activity towards time, (◆) PDC activity towards time. For a better understanding of glycerol effect on TA stability, Cvi-TA (B) and Vfl-TA (D) deactivation profiles when reactions were performed in aqueous medium are also presented (□) (pH 7.5; temperature 30ºC; [4-PB] 15 mM; [L-Alanine] 200 mM; TA 5 % v v^{-1}; PDC 25 % v v^{-1}).

Regarding that final 3-APB concentration did not increase in Cvi-TA reaction when 10% glycerol was added, a decrease on conversion and yield was expectable because the initial substrate concentration was higher (see Table 5.5). Therefore, this optimization strategy was discarded for Cvi-TA since increasing the substrate expense, as well as the medium complexity, is not desirable if the results do not justify it. On the other hand, in Vfl-TA reaction with 10% glycerol, conversion and yield were maintained (72.34 ± 1.97 % and 68.16 ± 0.07 % respectively) since the final amine concentration achieved was proportional to the increase on initial substrate concentration (see Table 5.5). However, reaction time was larger, which led to a reduction on

space-time yield (0.34 ± 0.01 mmol·L^{-1}·h^{-1} with glycerol, 0.74 ± 0.08 mmol·L^{-1}·h^{-1} without glycerol), but this drawback could be compensated by the increase on biocatalyst yield, which was 1.7-fold higher in comparison to the reaction in aqueous medium (14.83 ± 0.30 mmol·mg TA^{-1} with glycerol, 8.61.74 ± 0.93 mmol·mg TA^{-1} without glycerol). Therefore, taking into account that two particularly important process metrics in the industrial point of view [39] were enhanced, 10% glycerol addition into the medium was considered a promising strategy for cascade reaction optimization when Vfl-TA is used.

Table 5.5 Effect of glycerol presence on process metrics of 3-APB synthesis. Initial 4-PB concentration, final 3-APB concentration, conversion, yield, space-time yield (STY) and biocatalyst yield (BY) obtained in cascade reactions of Cvi-TA/Vfl-TA and PDC in aqueous medium and in the presence of 10% glycerol (pH 7.5; temperature 30ºC; [L-Alanine] 200 mM).

Enzyme	[Glycerol] (%)	Initial [PB] (mM)	Final [APB] (mM)	Conversion (%)	Yield (%)	STY (mmol·L^{-1}·h^{-1})	BY (mmol·mg TA^{-1})
Cvi-TA	0	10	6.20 ± 0.98	72.04 ± 3.12	64.22 ± 10.14	0.78 ± 0.12	5.01 ± 0.79
	10	15	5.76 ± 0.40	48.28 ± 1.01	37.11 ± 2.55	0.72 ± 0.05	4.65 ± 0.32
Vfl-TA	0	10	5.92 ± 0.64	71.03 ± 2.99	60.77 ± 6.58	0.74 ± 0.08	8.61 ± 0.93
	10	15	10.20 ± 0.21	72.34 ± 1.97	68.16 ± 0.07	0.34 ± 0.01	14.83 ± 0.30

5.3.4. Synthesis of 1-PEA by the cascade reaction of TA and PDC

As it has been previously mentioned (see introduction in section 5.1), asymmetric synthesis of 1-PEA using transaminase coupled with PDC for pyruvate removing was also studied (Scheme 5.3 B). Unlike the case of 3-APB, positive results on the preliminary screening were only obtained with Vfl-TA (see section 4.3.3), thus Cvi-TA was discarded in this section.

As it can be observed in the reaction time course (Figure 5.7 A), 1-PEA synthesis only took place when Vfl-TA was coupled with PDC. Specifically, reaction took place with a maximum rate of 0.65 mM·h^{-1}. This lower rate in comparison to 3-APB case (2.83 mM·h^{-1}) enlarged reaction more than 8 hours, but after 24 h similar final amine concentration was achieved (5.13 mM). In the same way as in previous reactions, transaminase suffered an initial activation, reaching a maximum after 2 hours. After that, a progressive activity loss was observed in the cascade system, while the activity was entirely maintained when PDC was not coupled. Therefore, this reaction was also affected by the low transaminase operational stability.

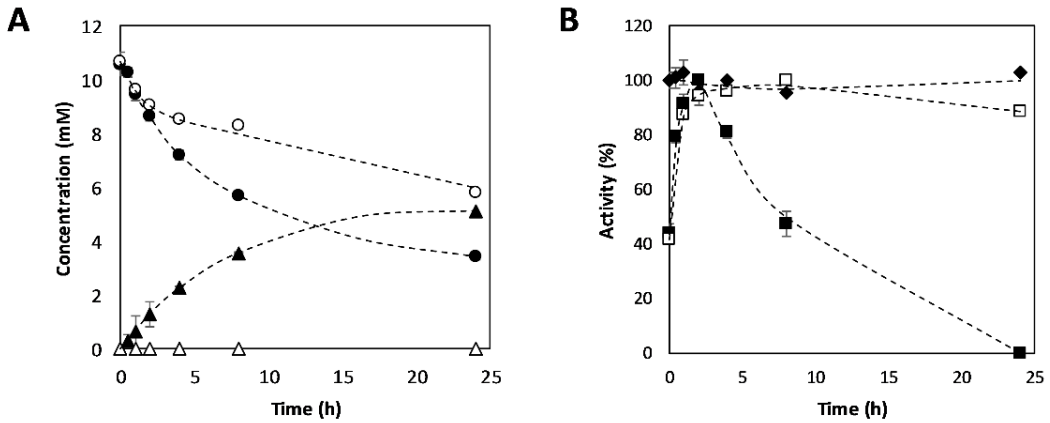

Figure 5.7 Reaction time courses of 1-PEA synthesis and operational enzymatic stability. A) Reaction time course performed with Vfl-TA: (▲) 1-PEA concentration in cascade reaction; (△) 1-PEA concentration in reaction without PDC; (●) AP concentration in cascade reaction; (○) AP concentration in reaction without PDC. B) Operational stability of Vfl-TA, as well as PDC when cascade reactions were performed: (■) Transaminase activity in cascade reactions. (□) Transaminase activity in reactions without PDC. (◆) PDC activity. Temperature 30 ^{o}C; pH 7.5; AP 10 mM; Alanine 200 mM; Vfl-TA 5 % v v^{-1}; PDC 25 % v v^{-1}.

At the end, a final reaction yield of 48.51 ± 0.06 % was achieved but the obtained conversion was higher, reaching 67.75 ± 0.87 % (see Table 5.6). However, acetophenone consumption was observed when PDC was not added and thus synthesis did not take place, leading to a conversion of 45.57 ± 0.57 %. Therefore, the low selectivity could be related not only to side reactions but also to a substrate evaporation. When a blank reaction without any enzyme was prepared, an around 25 % acetophenone consumption was observed after 24 hours, which reinforces the hypothesis of substrate evaporation presence.

Asymmetric synthesis of 1-PEA using PDC as a co-product removing system has not been reported. Vfl-TA has been used for 1-PEA synthesis in combination with alanine dehydrogenase for pyruvate removing, but no significant results were obtained [40]. In contrast, by using whole cells expressing Vfl-TA and coupling it with LDH system, a final concentration of 6.7 mM 1-PEA was reached starting with 30 mM acetophenone, which represents a 22.3 % yield [41]. Vfl-TA has also been coexpressed in *E. coli* with acetolactate synthase (ALS) to construct an entire cascade with this pyruvate removing system. In that case, starting from an AP concentration of 10 mM, a 30 % yield was obtained when reaction was performed with the whole cells [42].

Table 5.6 Process metrics of 1-PEA synthesis by the cascade reaction of Vfl-TA and PDC. Final 1-PEA concentration (24 hours), conversion, yield and selectivity of the cascade reactions performed with Vfl-TA coupled with PDC and compared with the respective one-enzyme reaction. Reaction time 24 h; temperature 30ºC; pH 7.5; AP 10 mM; Alanine 200 mM; TA 5 % v v^{-1}; PDC 25 % v v^{-1}.

Reaction	Final [PEA] (mM)	Conversion (%)	Yield (%)	Selectivity (%)
TA and PDC	5.13 ± 0.01	67.75 ± 0.87	48.51 ± 0.06	71.61 ± 0.84
TA	0.00 ± 0.00	45.57 ± 0.57	0.00 ± 0.00	0.00 ± 0.00

5.3.4.1. Optimization approaches applied to 1-PEA case.

As in the 3-APB synthesis case (see section 5.3.2.1), increasing the temperature to 40ºC doubled the initial reaction rate in comparison with applying 30ºC (see Figure 5.8 A). However, even though the product consumption occurred in the 3-APB case was not observed with 1-PEA, reaction stopped when a concentration of only 2.17 mM had been reached, which represents less than the half obtained with 30ºC (5.13 mM). This low reaction efficiency could be related again with an earlier enzyme deactivation due to the increased temperature (see Figure 5.8 B). In contrast, when cascade reaction was performed at low temperature (15ºC) a slower initial rate was observed (0.15 mM·h^{-1}), which led to a longer reaction time. Despite the increased operational stability, similar final 1-PEA concentration as at 30ºC was obtained.

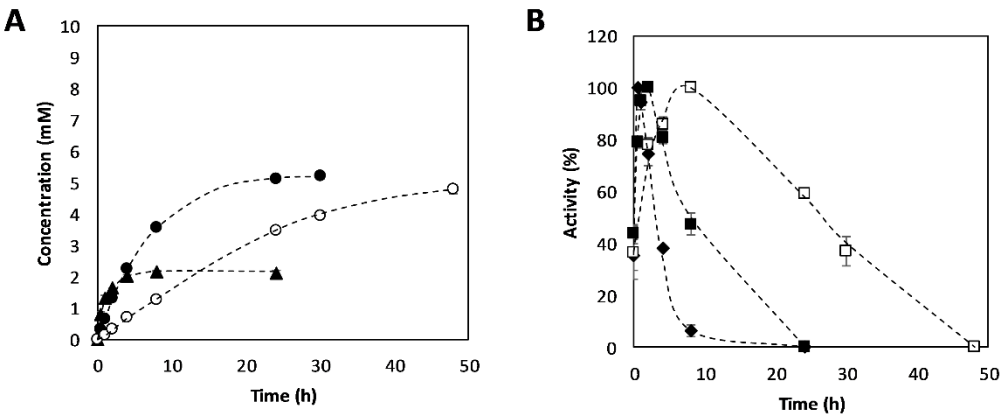

Figure 5.8 Temperature effect on 1-PEA synthesis and on operational enzymatic stability. (A) 1-PEA concentration towards time in the cascade reaction of Vfl-TA and PDC at 15ºC (○), 30ºC (●) and 40ºC (▲). (B) Vfl-TA operational stability during the cascade reactions performed at 15ºC (□), 30ºC (■) and 40ºC (◆). pH 7.5; AP 10 mM; Alanine 200 mM; TA 5 % v v^{-1}; PDC 25 % v v^{-1}.

Therefore, changing the temperature did not contribute to a reaction optimization. As it is exposed in Table 5.7, lowering the temperature supposed an increase on selectivity (from 71.61 ± 0.84 % at 30°C to 93.60 ± 3.28 % at 15°C), which could be related both to a less substrate evaporation and to a reduction of side-reactions. However, the enlargement of the reaction time without a yield increase resulted in a decrease on space-time yield (from 0.21 ± 0.00 mmol·L^{-1}·h^{-1} at 30°C to 0.10 ± 0.00 mmol·L^{-1}·h^{-1} at 15°C), which was 50 % lower. In contrast, performing the cascade reaction at 40°C, slightly increased STY (from 0.21 ± 0.00 mmol·L^{-1}·h^{-1} at 30°C to 0.27 ± 0.00 mmol · L^{-1} · h^{-1} at 40°C), but yield was much lower (from 48.51 ± 0.06 % at 30°C to 20.29 ± 0.75 % at 40°C) and worse selectivity results were obtained (from 71.61 ± 0.84 % at 30°C to 42.84 ± 2.18 % at 40°C).

Table 5.7 Process metrics of 1-PEA synthesis with the cascade reaction at different temperatures. Final 1-PEA concentration, reaction time, conversion, yield, selectivity and space-time yield (STY) of the cascade reaction of Vfl-TA and PDC at different temperature conditions. pH 7.5; AP 10 mM; Alanine 200 mM; TA 5 % v v^{-1}; PDC 25 % v v^{-1}.

Temperature (°C)	Final [PEA] (mM)	Reaction time (h)	Conversion (%)	Yield (%)	Selectivity (%)	STY (mmol·L^{-1}·h^{-1})
15	4.79 ± 0.13	48	48.73 ± 0.40	45.60 ± 1.22	93.60 ± 3.28	0.10 ± 0.00
30	5.13 ± 0.01	24	67.75 ± 0.87	48.51 ± 0.06	71.61 ± 0.84	0.21 ± 0.00
40	2.17 ± 0.02	8	47.41 ± 0.67	20.29 ± 0.75	42.84 ± 2.18	0.27 ± 0.00

Regarding the effect of amino-donor/amine-acceptor ratio, doubling the initial alanine concentration did not suppose any change on conversion, yield or selectivity (see Table 5.8). In the case of adding 600 mM alanine, a 20 % increase on selectivity was observed (from 71.61 ± 0.84 % at 200 mM alanine to 92.61 ± 6.29 % at 600 mM alanine), thus it contributed to a side-reaction reduction. However, considering that the final amine concentration was maintained, this 3-fold increase on alanine expense was not considered worthy.

Table 5.8 Process metrics of 1-PEA synthesis with the cascade reaction of TA and PDC performed at different initial alanine concentrations. Final 1-PEA concentration (24 hours), conversion, yield and selectivity of the cascade reactions performed with Vfl-TA coupled with PDC at different initial alanine concentrations. Temperature 30^{o}C; pH 7.5; AP 10 mM; TA 5 % v v^{-1}; PDC 25 % v v^{-1}.

Initial [Alanine] (mM)	Final [PEA] (mM)	Conversion (%)	Yield (%)	Selectivity (%)
200	5.13 ± 0.01	67.75 ± 0.87	48.51 ± 0.06	71.61 ± 0.84
400	4.95 ± 0.36	68.16 ± 0.84	47.07 ± 2.21	69.02 ± 2.39
600	5.33 ± 0.40	53.78 ± 5.36	49.47 ± 1.58	92.61 ± 6.29

5.3.4.2. Reaction medium engineering

Reaction medium engineering was applied in the same way as in the 3-APB case (see section 5.3.3). Preliminary reaction screening was performed with the same cosolvents (DMSO and glycerol) at different concentrations (5%, 10% or 15%) and a noticeable negative effect of DMSO to Vfl-TA was again observed (see Figure 5.9). When a 5 % DMSO was added to the medium, only 13 % yield was achieved and its value decreased when higher DMSO concentrations were applied. Therefore, this cosolvent was discarded. Regarding the use of glycerol, unlike the case of 3-APB, in which it did not suppose any yield loss (section 5.3.3), reaction suffered around 20-30% losses in all concentration cases in respect to reaction in aqueous medium. However, taking into account the successful results obtained with 3-APB reaction when glycerol was added (section 5.3.3.2), 10 % glycerol was selected for further experiments. In this case, substrate solubility was the same in 10 % glycerol as in aqueous medium (30 mM). In previous reactions, AP was added at 10 mM. However, in this case, expecting the same Vfl-TA stability increase as when glycerol was added in 3-APB reaction, AP concentration was increased to the maximum.

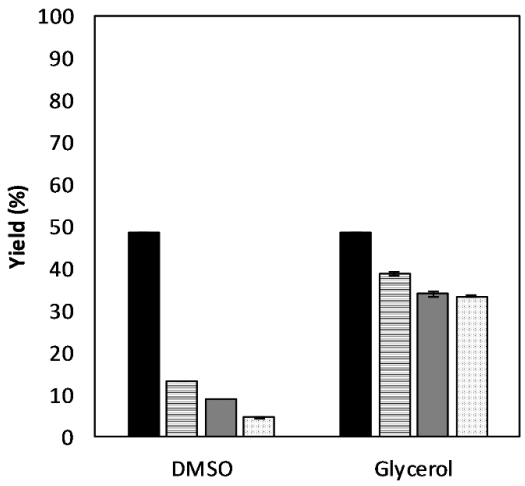

Figure 5.9 Effect of DMSO and glycerol presence on 1-PEA synthesis. Reaction yields obtained after 24 hours by adding 0% (black), 5% (striped), 10% (grey) and 15% (dotted) of DMSO or glycerol into the medium in cascade reaction with Vfl-TA coupled with PDC. Reaction conditions were the same established in previous sections (pH 7.5; temperature 30ºC; [AP] 10 mM; [L-Alanine] 200 mM).

As is expectable when initial substrate concentration is higher, reaction took place with higher initial rate in comparison with the aqueous system (0.98 $mM \cdot h^{-1}$ with glycerol and 0.65 $mM \cdot h^{-1}$ without it), which led to higher final 1-PEA concentration after 24 hours (8.96 mM) (see Figure 5.10 A). Operational stability shown in Figure 5.10 B revealed that glycerol delayed the maximum transaminase activity achievement and its subsequent deactivation, reason why higher final amine concentration may have been achieved.

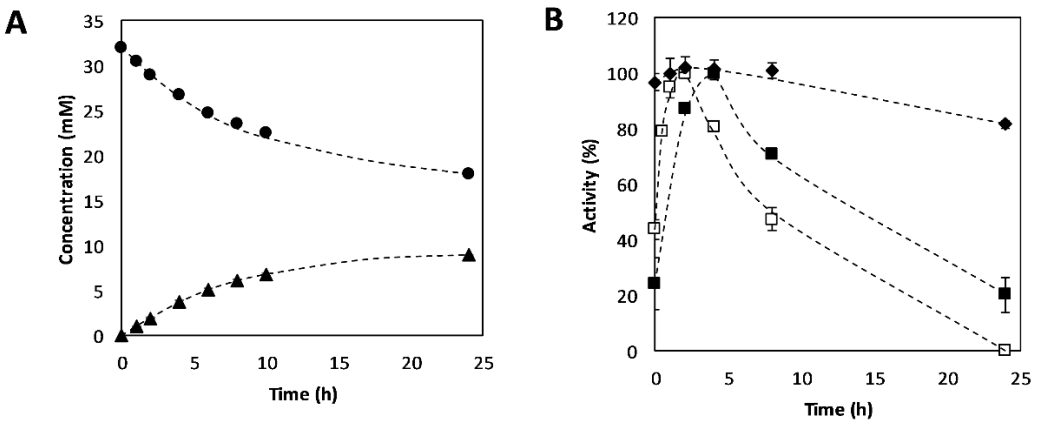

Figure 5.10 Effect of 10% glycerol presence on 1-PEA synthesis by the cascade reaction of Vfl-TA and PDC. (A) Reaction time course of asymmetric 1-PEA synthesis with the cascade reaction with Vfl-TA adding into

the medium 10% of glycerol: (▲) 1-PEA concentration (mM), (●) AP concentration (mM). (B) Operational stability profile of the reaction: (■) transaminase activity towards time, (◆) PDC activity towards time. For a better understanding of glycerol effect on TA stability, Vfl-TA deactivation profile when reaction was performed in aqueous medium is also represented (□)(pH 7.5; temperature 30ºC; [4-PB] 15 mM; [L-Alanine] 200 mM).

Since the increase on initial substrate concentration was higher than the final amine concentration increase in comparison with reactions in aqueous medium, a reduction on conversion (43.56 ± 0.44 % with glycerol, 67.75 ± 0.87 % without glycerol) and yield (28.08 ± 0.26 % with glycerol, 48.51 ± 0.06 % without glycerol) was obtained at the end (see Table 5.9). However, total reaction time did not increase in comparison with the reaction in aqueous system, which led to an around 2-fold higher space-time yield (from 0.21 ± 0.00 $mmol \cdot L^{-1} \cdot h^{-1}$ to 0.37 ± 0.02 $mmol \cdot L^{-1} \cdot h^{-1}$). Moreover, as it also happened with 3-APB case (see section 5.3.3.2) the use of 10 % glycerol into the medium increased the biocatalyst yield 1.7-fold (from 7.47 ± 0.01 $mmol \cdot mg\ TA^{-1}$ to 13.04 ± 0.06 $mmol \cdot mg\ TA^{-1}$). Therefore, medium modification by glycerol addition was again considered a promising optimization strategy that enhanced some important process metrics.

Table 5.9 Effect of glycerol presence on process metrics of 1-PEA synthesis. Initial AP concentration, final 1-PEA concentration, conversion, yield, space-time yield (STY) and biocatalyst yield (BY) obtained in cascade reactions of Vfl-TA and PDC in aqueous medium and in the presence of 10 % glycerol (pH 7.5; temperature 30ºC; [L-Alanine] 200 mM).

[Glycerol] (%)	Initial [AP] (mM)	Final [PEA] (mM)	Conversion (%)	Yield (%)	STY ($mmol \cdot L^{-1} \cdot h^{-1}$)	BY ($mmol \cdot mg\ TA^{-1}$)
0	10	5.13 ± 0.01	67.75 ± 0.87	48.51 ± 0.06	0.21 ± 0.00	7.47 ± 0.01
10	30	8.96 ± 0.05	43.56 ± 0.44	28.08 ± 0.26	0.37 ± 0.02	13.04 ± 0.06

5.3.5. Amine purification and enantiomer excess determination

As it has been previously introduced (see section 5.1), one of the key advantages of biocatalysis towards chemical processes on chiral amine production is that highly enantiopure products can be achieved due to enzyme stereoselectivity, although it may not be possible in every case [2], [8]. Even though the growing interest on entantioselective synthesis has enhanced the

development of new methods for determining enantiomeric excess (ee), nuclear magnetic resonance (NMR) spectroscopy continues to be one of the most important methods for analyzing chiral molecules [43], [44]. In this methods, the mixture of enantiomers firstly needs to be converted into a diastereoisomeric mixture by the use of a chiral auxiliary. Diastereoisomeric composition can be then measured by NMR and directly related to the enantiomeric composition of the original mixture [45]. A very common and powerful technique consists in the use of chiral solvating agents (CSA) as chiral auxiliaries [46]. CSAs are optically pure compounds that bind to the compounds through intermolecular forces. Since the association constants of the enantiomers with the CSA are often different, the two enantiomers show different time-averaged solvation environments that can also cause differences in the chemical shifts in the NMR spectrum [43].

From the point of view of biocatalysis, although NMR provides simple procedures for ee determining, it has as a main drawback the requirement of a high product purity, which is not always easily achieved due to the complexity of enzymatic reaction mixtures. For this reason, in the present work, a previous step for chiral amine ee determination was to develop an effective purification procedure. In this regard, chromatography in silica-gel columns still represents a widely used purification tool for the analysis of organic compounds. This method consist in loading the mixture to a column packed with highly adsorbent silica gel powder and then developing the column with the appropriate solvent [47]. Individual compounds are differently retained based on their adsorption and desorption into the silica gel and can be then collected in different eluent fractions at the end of the column.

5.3.5.1. Amines purification

Just as the first reaction studies were focused on 3-APB synthesis, the development of an efficient procedure for ee determination also started with this chiral amine. In order to have a model to compare with, NMR spectrum of a commercial racemic mixture of 3-APB was obtained by the Universitat Autònoma de Barcelona NMR service (SeRMN) and it is shown in Figure 5.11. After that, crude reaction samples were analyzed in the same manner. The impossibility of distinguishing the peaks corresponding to 3-APB spectrum in these samples proved that a previous purification process was needed.

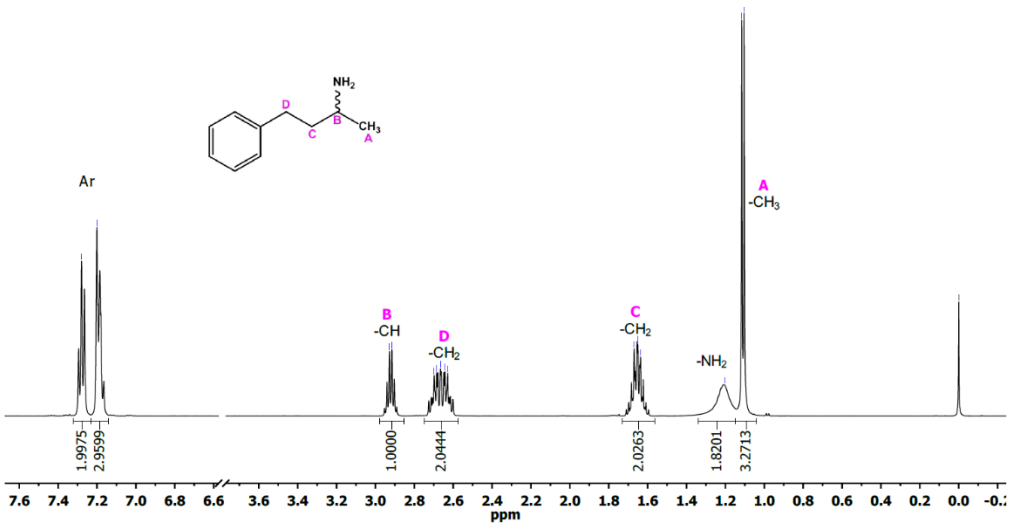

Figure 5.11 NMR spectrum of a commercial racemic mixture of 3-amino-1-phenylbutane.

In a first purification attempt, a double extraction was planned (see Scheme 5.4). After stopping reactions by adding HCl in a final concentration of 600 mM, all the proteins precipitated and they could be easily removed by centrifugation. Then, it was estimated that the resulting supernatant, in addition to the interest amine, could at least contain unreacted PB and alanine, the produced acetaldehyde, cofactors of both enzymes and the salts present in the buffer. Taking advantage of the low pH resulting from HCl addition (pH 1.1), a first extraction was carried out with dichloromethane (DCM). After discarding organic phase, which was supposed to contain PB, acetaldehyde and the transaminase cofactor PLP, aqueous phase was basified to pH 12.7 and a second extraction was performed with the same solvent. This time, the new aqueous phase was discarded, since it was supposed to contain alanine and the PDC cofactor TPP together with all the salts, while the amine may have been purified to the organic phase. This organic phase was analyzed by HPLC and, besides the amine presence, it was also proved that PB had been removed, even though the absence of other by-products was not sure. After that, the second organic phase was dried with anhydrous sodium sulfate to completely remove water and distilled in a rotary evaporator.

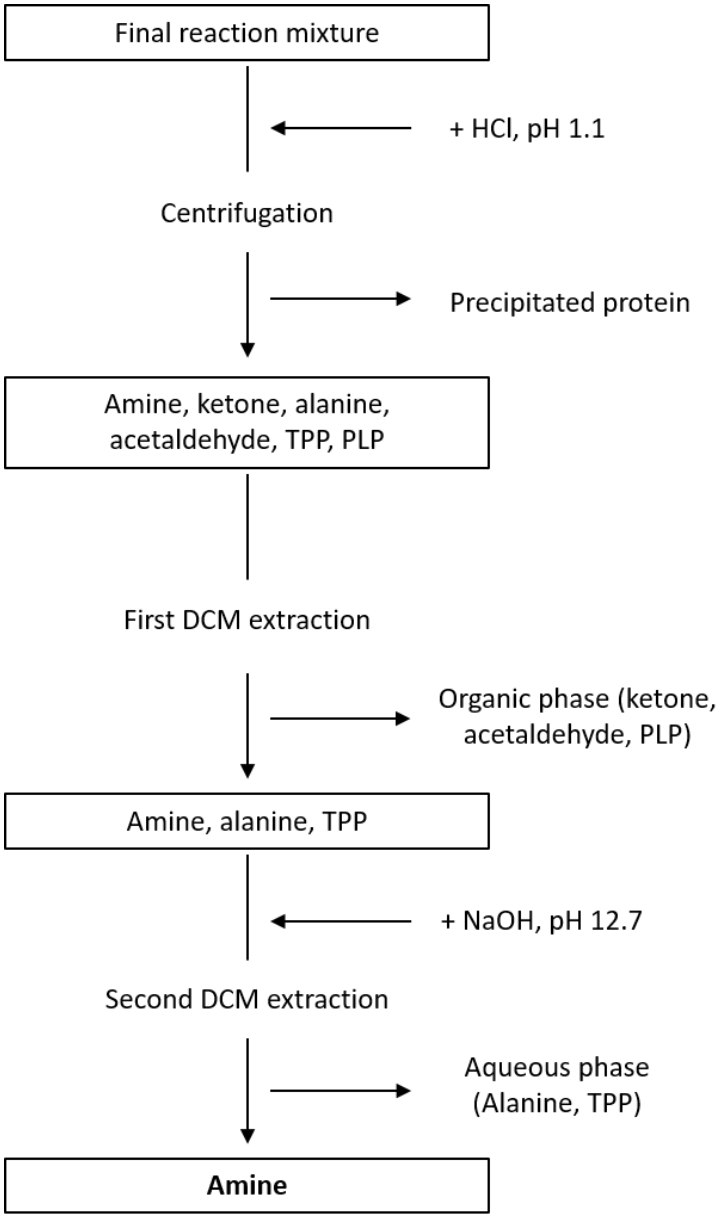

Scheme 5.4 Double extraction procedure planned for amine purification.

However, NMR spectrums revealed that samples were not pure enough (see Figure 5.12), neither in reactions performed with Cvi-TA nor with Vfl-TA. The presence of undesired by-products, which could proceed both from the cell free extracts used and from undesired side-reactions, forced the addition of more purification steps.

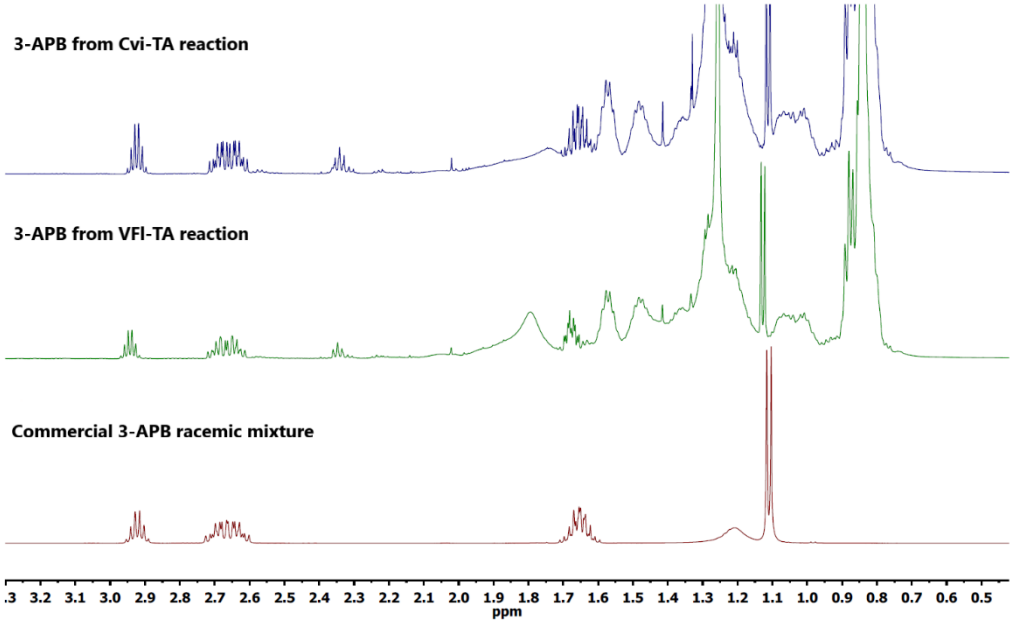

Figure 5.12 NMR spectra of the samples obtained after the double extraction procedure performed with crude reaction mixtures either performed using Cvi-TA and Vfl-TA.

A liquid-solid chromatography using a silica-gel column was planned. A key point for the development of an effective adsorption chromatography procedure is to find out the appropriate solvent mixture that will be used as eluent. In these regards, thin-layer chromatography (TLC) was carried out. TLC is performed on a sheet coated with a thin layer of the adsorbent. After applying the sample on the plate, eluent (or mobile phase) is drawn up the plate via capillary action and separation is achieved because the different analytes ascent at different rates [48]. An appropriate solvent mixture would be the one with which the interest compound migrates enough into TLC plate, but without totally ascending until the end. This mentioned requirements could be achieved with a 1:10 mixture of methanol in dichloromethane (DCM) with a 2% of triethylamine (TEA). In Figure 5.13, the resulting TLC is shown. To detect where 3-APB was deposited, a pattern sample was loaded using commercial 3-APB and, to visualize the results, ninhydrine was used, which reacts with amine compounds colorimetrically revealing, this way, the plates.

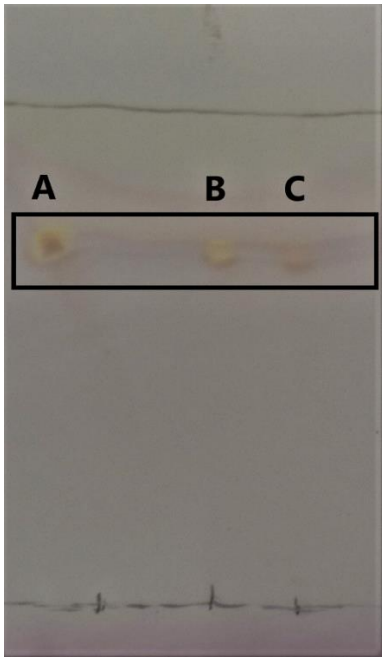

Figure 5.13 Thin layer chromatography of the second organic phase of the double extraction performed using 1:10 methanol in DCM with 2% triethylamine. A) Commercial racemic mixture of 3-APB. B) Sample extracted from a reaction mixture obtained using Cvi-TA. B) Sample extracted from a reaction mixture obtained using Vfl-TA.

The next step consisted in using the found solvent mixture to purify the amine in a silica column, which would allow the obtainment of appropriate sample amounts to perform the NMR spectra. After performing the double extraction mentioned before and drying the second organic phase with anhydrous sodium sulfate, volume was reduced by evaporation to 0.2 mL. Chromatography was carried out with the resulting sample using 1:10 methanol in DCM with 2 % of TEA and small fractions were being collected. A drop of each fraction was loaded to a TLC plate and this was revealed with ninhydrin to detect which fractions contained the amine. An additional TLC was carried out with the samples that contained the amine to prove its purity. However, when the performed TLC was observed in UV light, unknown impurities were detected in some fractions. For this reason, not all of the fractions that contained 3-APB could be collected for its further analysis, which decreased the purification yield. Starting from samples of 43.0 ± 2.0 mg, the 3-APB purified amount was 8.5 ± 1.5 mg, which represents a global yield of 19.6 ± 2.6 %. Nevertheless, when an NMR spectrum of the samples was obtained (Figure 5.14), it was demonstrated that 3-APB purity was enough to compare it with the commercial spectrum. Since the only interest of the purification procedure was to be able to determine the ee by NMR, it was considered valid even though the global purification yield was low.

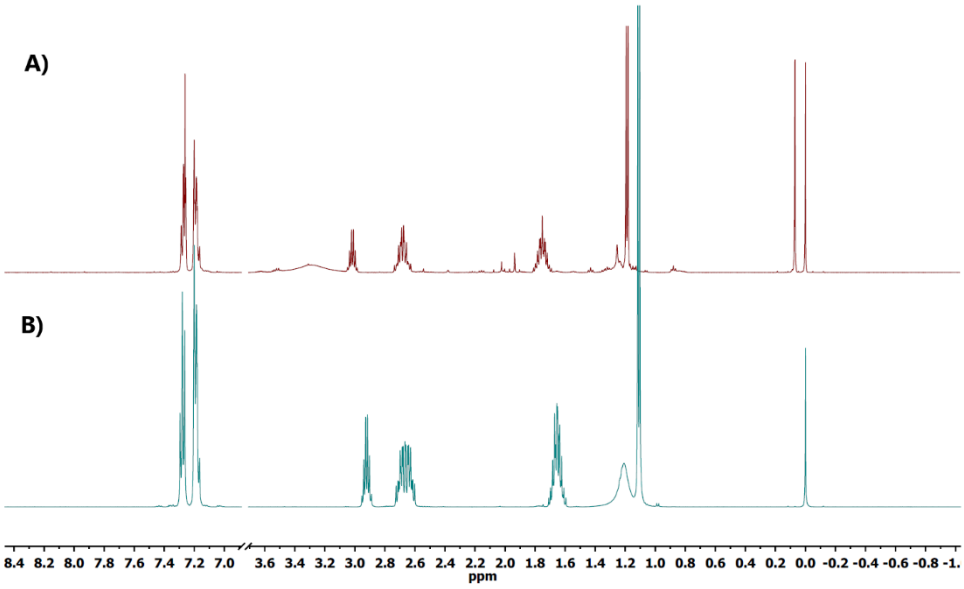

Figure 5.14 NMR spectrum of the product obtained after all the purification procedure. A) NMR spectrum of 3-APB purified from a reaction sample. B) NMR spectrum of a commercial racemic mixture of 3-APB.

For the determination of the entantiomeric excess of the product obtained during 1-PEA synthesis reaction, an NMR spectrum of a commercial racemic mixture of this chiral amine was obtained as in the previous case (see Figure 5.15). Due to the similarity on amine structure, as well as on reaction mixture composition in comparison with 3-APB synthesis, the same purification procedure was applied. As it will be shown in further results, a sufficiently purified product to be analyzed by NMR could be obtained with the developed purification process.

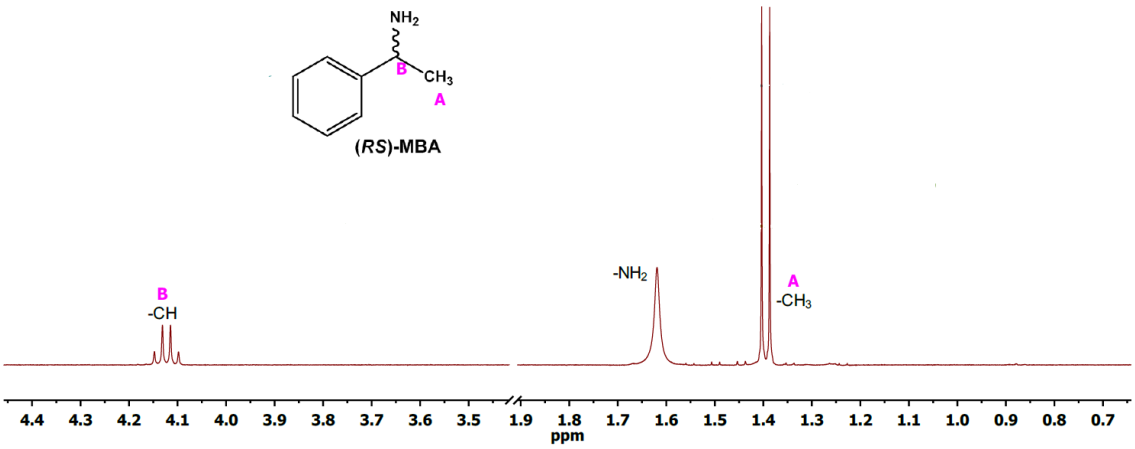

Figure 5.15 NMR spectrum of a commercial racemic mixture of 1-phenyl-ethylamine (1-PEA).

5.3.5.2. Enantiomeric excess determination

Once samples could be sufficiently purified, further NMR analysis were carried out to determine enantiomeric excess. As it has been mentioned, a common method for ee determination consists in the use of a CSA, which forms two different diastereoisomeric complexes with the different enantiomers that can be distinguished in NMR spectra. In this case, *R*)-(-)-1,1'-binaphtyl-2,2'-hydrogenphosphate (BHP) was selected as CSA, since its use for ee determination of chiral amines has been previously reported [49]. Firstly, diastereoisomerization with commercial 3-APB racemic mixture was carried out. As it can be observed in Figure 5.16 (A), some peaks were doubled and efficiently separated as a consequence of the interaction with BHP. In order to find out which one corresponded to each initial enantiomer, commercial enantiopure (S)-3-APB was added to the sample. As it can be observed in Figure 5.16 (B), the peak in the right augmented its area, thus it corresponded to enantiomer S.

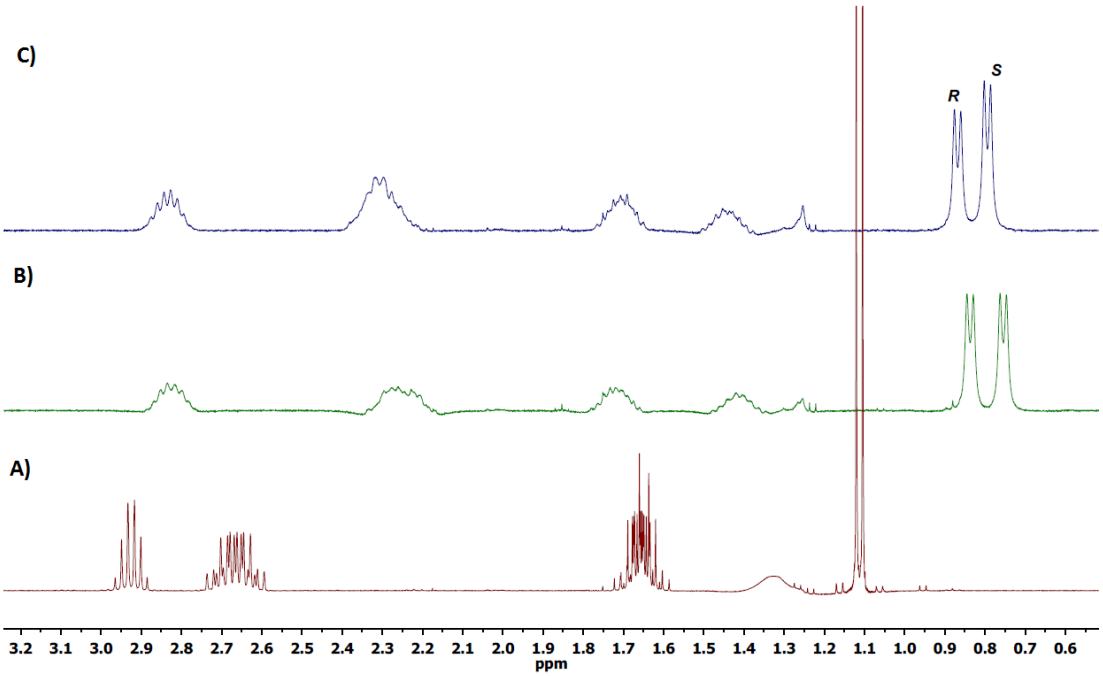

Figure 5.16 Diastereoisomerization of a commercial 3-APB racemic mixture using R)-(-)-1,1'-binaphtyl-2,2'-hydrogenphosphate (BHP) as a chiral solvating agent (CSA). A) Initial spectrum of commercial 3-APB racemic mixture. B) Spectrum of commercial 3-APB racemic mixture after the addition of BHP, resulting in a peak separation. C) Spectrum of commercial 3-APB racemic mixture after the addition of BHP and commercial (S)-3-APB to differentiate the two enantiomers after peak separation.

After proving that BHP is an adequate CSA for 3-APB enantiomer separation in NMR, reaction samples were analyzed by the same method. By integrating the resulting peaks, the percentage of each enantiomer in samples could be obtained to calculate the corresponding ee. In Table 5.10, ee is shown both for reactions catalyzed by Cvi-TA/PDC and Vfl-TA/PDC. In addition, the product obtained in reactions catalyzed by Vfl-TA/PDC with 10% glycerol into the medium, which had led to the most successful results, was also analyzed. Both Cvi-TA/PDC and Vfl-TA/PDC systems showed high stereoselectivity reaching enantiomeric excesses of 92.00 ± 1.15 % and 89.33 ± 1.76 % for (S)-3-APB respectively. The addition of glycerol into the medium did not significantly change the ee and a percentage of 88.00 ± 1.15 % was obtained. Similar ee was reported for Vfl-TA by Höhne *et al* [11], which synthesized 3-APB using the same cascade system with ZpPDC and obtained an ee of 88.5%. Also Vfl-TA stereoselectivity was similar in works where it was coupled with alanine dehydrogenase (AlaDH) or lactate dehydrogenase (LDH) (84 % (S) and 89 % (S) respectively) [24]. In the case of Cvi-TA, its use for 3-APB synthesis has been reported using the AlaDH and LDH pyruvate removing systems and, in both cases, low stereoselectivity results were obtained [25], therefore improved enantiopurity was reached in the present work.

Table 5.10 Enantiomeric excess of 3-APB obtained in reactions catalyzed by Cvi-TA and Vfl-TA, as well as the obtained in the case of using Vfl-TA with 10% glycerol into the medium.

Transaminase	Medium	ee (%S)
Cvi-TA	Aqueous	92.00 ± 1.15
Vfl-TA	Aqueous	89.33 ± 1.76
Vfl-TA	10% glycerol	88.00 ± 1.15

The same CSA was used for the diastereoisomerization of 1-PEA. As it is shown in

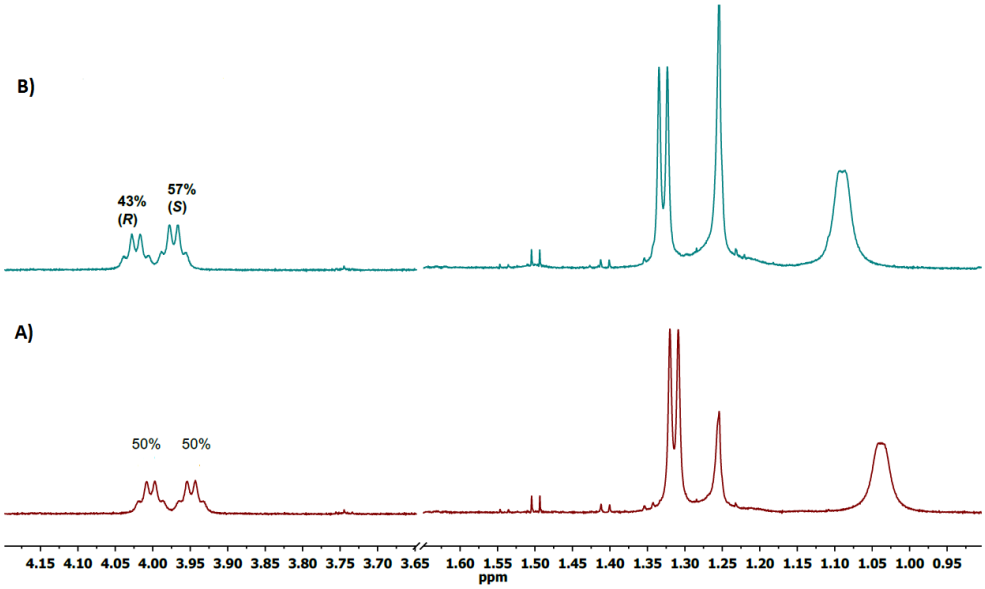

Figure ***5.17*** A, BHP was able to separate some peaks in NMR spectrum performed with the commercial 1-PEA racemic mixture. After the addition of enantiopure commercial (S)-1-PEA, it was observed that, as in the case of 3-APB, the left peak corresponded to enantiomer R and the right one to enantiomer S (

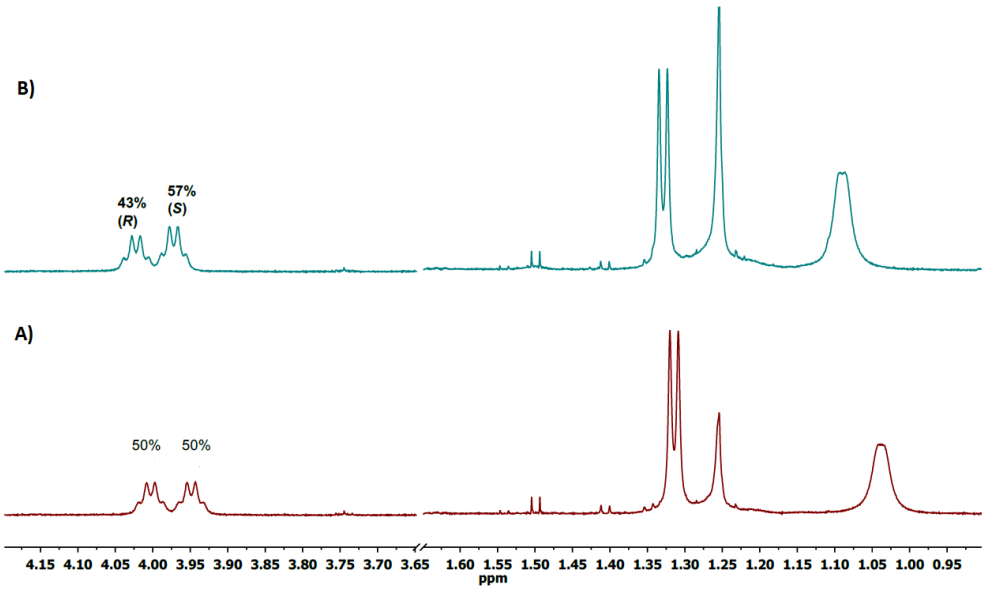

Figure ***5.17*** B). After this characterization, samples proceeding form 1-PEA synthesis reactions using Vfl-TA/PDC in aqueous medium and with 10 % glycerol were analyzed with this method. However, a peak separation was not observed in any case, which was explained by a high purity for one enantiomer that made not possible to observe the peak for the minority one. When commercial (S)-1-PEA was added to the samples, non-conclusive results were obtained due also to the ability of detecting only one peak. For this reason, commercial racemic mixture was added and the peak corresponding to (S)-enantiomer was higher, which led to the conclusion that reaction products were (S)-1-PEA. Since it was not possible to quantify the percentage of each

enantiomer, it was qualitatively assumed that enantiomeric excesses of >99 % had been reached. This high ee has also been reported in 1-PEA synthesis reactions using Vfl-TA coupled with AlaDH, even though in that case conversion values were so low [40].

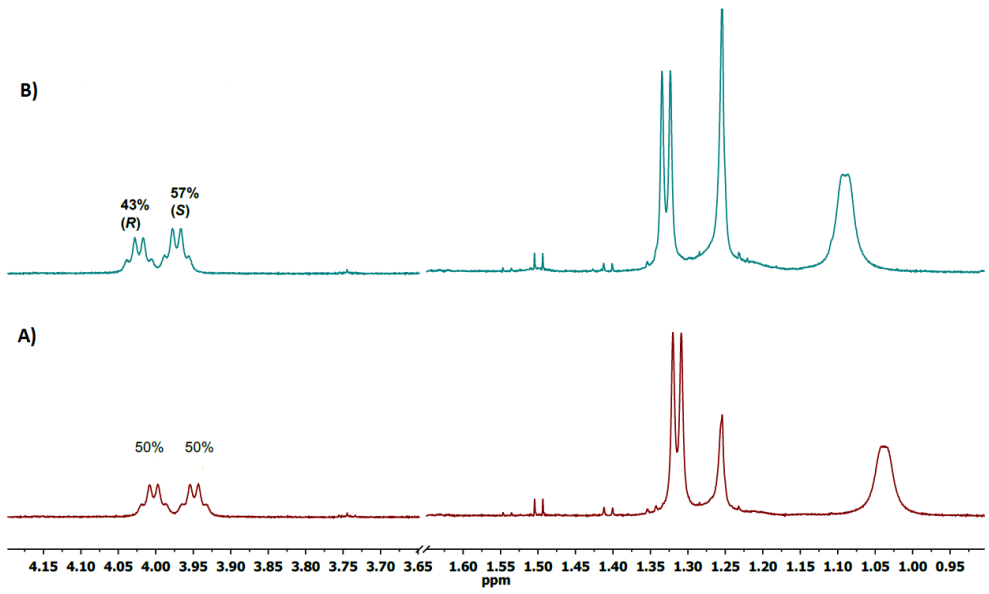

Figure 5.17 Diastereoisomerization of a commercial 1-PEA racemic mixture using R)-(-)-1,1'-binaphtyl-2,2'-hydrogenphosphate (BHP) as a chiral solvating agent (CSA). A) Spectrum of commercial 1-PEA racemic mixture after the addition of BHP, resulting in a peak separation. B) Spectrum of commercial 1-PEA racemic mixture after the addition of BHP and commercial (S)-1-PEA to differentiate the two enantiomers after peak separation.

5.4. Conclusions

Synthesis of 3-APB was efficiently carried out coupling Cvi-TA and Vfl-TA with PDC, which acts as a pyruvate removal system. In both cases, yields higher than 60% were reached, even though low operational stabilities were observed. During the further optimization approaches, it was concluded that 30^{o}C and a 20-fold excess of amine-donor were the best conditions among the tested values. After that, in reaction medium engineering approaches, final product concentration could be increased to around 10 mM by the application of 10 % glycerol into the medium in reactions catalyzed by Vfl-TA/PDC. This concentration, which represents a 1.7-fold increase in comparison with reactions performed in aqueous system, is the highest reported in 3-APB synthesis using PDC for pyruvate removing. Regarding 1-PEA synthesis, around 50 % yield

was obtained after 24 h by coupling Vfl-TA with PDC. After applying the same optimization and medium engineering approaches as in the case of 3-APB, improvements were also achieved also when 10% glycerol was added into the medium. In this case, a final 1-PEA concentration of around 9 mM was reached, which also represents a 1.7-fold increase in comparison to aqueous system. Finally, enantiomeric excess of the products could be determined by NMR using BHP as a CSA. Previous to the analysis, sufficient purification could be reached by the development of a procedure based on a double extraction followed by a chromatography step. In the case of 3-APB synthesis, high enantiopurity was achieved for enantiomer S (around 90 % ee) both using Cvi-TA and Vfl-TA. The addition of 10 % glycerol into the medium did not suppose significant changes in ee. Even better stereoselectivity was observed in the case of 1-PEA, since ee of >99 % in enantiomer S was reached.

5.5. References

[1] S. Arrasate, E. Lete, and N. Sotomayor, "Synthesis of enantiomerically enriched amines by chiral ligand mediated addition of organolithium reagents to imines," *Tetrahedron: Asymmetry*, vol. 12, no. 14, pp. 2077–2082, Aug. 2001.

[2] D. Ghislieri and N. J. Turner, "Biocatalytic Approaches to the Synthesis of Enantiomerically Pure Chiral Amines," *Top. Catal.*, vol. 57, no. 5, pp. 284–300, Mar. 2014.

[3] A. Gomm and E. O'Reilly, "Transaminases for chiral amine synthesis," *Curr. Opin. Chem. Biol.*, vol. 43, pp. 106–112, Apr. 2018.

[4] A. P. Green, N. J. Turner, and E. O'Reilly, "Chiral Amine Synthesis Using ω-Transaminases: An Amine Donor that Displaces Equilibria and Enables High-Throughput Screening," *Angew. Chemie Int. Ed.*, vol. 53, no. 40, pp. 10714–10717, Sep. 2014.

[5] S. Schätzle, F. Steffen-Munsberg, A. Thontowi, M. Höhne, K. Robins, and U. T. Bornscheuer, "Enzymatic Asymmetric Synthesis of Enantiomerically Pure Aliphatic, Aromatic and Arylaliphatic Amines with (R)-Selective Amine Transaminases," *Adv. Synth. Catal.*, vol. 353, no. 13, pp. 2439–2445, Sep. 2011.

[6] T. C. Nugent and M. El-Shazly, "Chiral amine synthesis - Recent developments and trends for enamide reduction, reductive amination, and imine reduction," *Adv. Synth. Catal.*, vol. 352, no. 5, pp. 753–819, 2010.

[7] S. A. Kelly *et al.*, "Application of ω-Transaminases in the Pharmaceutical Industry," *Chem.*

Rev., vol. 118, pp. 349–367, 2017.

[8] M. S. Malik, E.-S. Park, and J.-S. Shin, "Features and technical applications of ω-transaminases," *Appl. Microbiol. Biotechnol.*, vol. 94, no. 5, pp. 1163–1171, Jun. 2012.

[9] M. Breuer *et al.*, "Industrial Methods for the Production of Optically Active Intermediates," *Angew. Chemie Int. Ed.*, vol. 43, no. 7, pp. 788–824, Feb. 2004.

[10] F. G. Mutti, C. S. Fuchs, D. Pressnitz, J. H. Sattler, and W. Kroutil, "Stereoselectivity of Four (R)-Selective Transaminases for the Asymmetric Amination of Ketones," *Adv. Synth. Catal.*, vol. 353, no. 17, pp. 3227–3233, Nov. 2011.

[11] M. Höhne, S. Kühl, K. Robins, and U. T. Bornscheuer, "Efficient asymmetric synthesis of Chiral amines by combining transaminase and pyruvate decarboxylase," *ChemBioChem*, vol. 9, no. 3, pp. 363–365, 2008.

[12] S. Mathew and H. Yun, "ω-Transaminases for the Production of Optically Pure Amines and Unnatural Amino Acids," *ACS Catal.*, vol. 2, pp. 993–1001, 2012.

[13] G. Zheng and J. Xu, "New opportunities for biocatalysis : driving the synthesis of chiral chemicals," *Curr. Opin. Biotechnol.*, vol. 22, pp. 784–792, 2011.

[14] P. Tufvesson, J. S. Jensen, W. Kroutil, and J. M. Woodley, "Experimental determination of thermodynamic equilibrium in biocatalytic transamination," *Biotechnol. Bioeng.*, vol. 109, no. 8, pp. 2159–2162, 2012.

[15] F. Guo and P. Berglund, "Transaminase biocatalysis: optimization and application," *Green Chem.*, vol. 19, no. 2, pp. 333–360, Jan. 2017.

[16] M. Fuchs, J. E. Farnberger, and W. Kroutil, "The Industrial Age of Biocatalytic Transamination," *European J. Org. Chem.*, vol. 2015, no. 32, pp. 6965–6982, 2015.

[17] D. Koszelewski, K. Tauber, K. Faber, and W. Kroutil, "ω-Transaminases for the synthesis of non-racemic α-chiral primary amines," *Trends in Biotechnology*, vol. 28, no. 6. pp. 324–332, Jun-2010.

[18] W. Kroutil *et al.*, "Asymmetric Preparation of prim-, sec-, and tert-Amines Employing Selected Biocatalysts," *Org. Process Res. Dev.*, vol. 17, pp. 751–759, 2013.

[19] K. Fesko, K. Steiner, R. Breinbauer, H. Schwab, M. Schürmann, and G. A. Strohmeier, "Investigation of one-enzyme systems in the ω-transaminase-catalyzed synthesis of chiral amines," *J. Mol. Catal. B Enzym.*, vol. 96, pp. 103–110, Dec. 2013.

[20] E. Ricca, B. Brucher, and J. H. Schrittwieser, “Multi-Enzymatic Cascade Reactions: Overview and Perspectives,” *Adv. Synth. Catal.*, vol. 353, no. 13, pp. 2239–2262, Sep. 2011.

[21] J. D. Stewart, “Dehydrogenases and transaminases in asymmetric synthesis,” *Curr. Opin. Chem. Biol.*, vol. 5, no. 2, pp. 120–129, Apr. 2001.

[22] S. Chen, H. Land, P. Berglund, and M. S. Humble, “Stabilization of an amine transaminase for biocatalysis,” *J. Mol. Catal. B Enzym.*, vol. 124, pp. 20–28, Feb. 2016.

[23] T. Börner *et al.*, “Explaining Operational Instability of Amine Transaminases: Substrate-Induced Inactivation Mechanism and Influence of Quaternary Structure on Enzyme-Cofactor Intermediate Stability,” *ACS Catal.*, vol. 7, no. 2, pp. 1259–1269, 2017.

[24] F. G. Mutti *et al.*, “Amination of Ketones by Employing Two New (S)-Selective ω-Transaminases and the His-Tagged ω-TA from Vibrio fluvialis,” *European J. Org. Chem.*, vol. 2012, no. 5, pp. 1003–1007, Feb. 2012.

[25] D. Koszelewski, M. Göritzer, D. Clay, B. Seisser, and W. Kroutil, “Synthesis of optically active amines employing recombinant ω-transaminases in E. coli cells,” *ChemCatChem*, vol. 2, no. 1, pp. 73–77, 2010.

[26] P. Tufvesson, J. Lima-Ramos, M. Nordblad, and J. M. Woodley, “Guidelines and Cost Analysis for Catalyst Production in Biocatalytic Processes,” *Org. Process Res. Dev.*, vol. 15, pp. 266–74, 2011.

[27] J. M. Woodley, “Protein engineering of enzymes for process applications,” *Curr. Opin. Chem. Biol.*, vol. 17, pp. 310–316, 2013.

[28] M. T. Gundersen, R. Abu, M. Schürmann, and J. M. Woodley, “Amine donor and acceptor influence on the thermodynamics of x-transaminase reactions,” *Tetrahedron: Asymmetry*, vol. 26, pp. 567–570, 2015.

[29] W. Böhmer *et al.*, “Highly efficient production of chiral amines in batch and continuous flow by immobilized ω-transaminases on controlled porosity glass metal-ion affinity carrier,” *J. Biotechnol.*, vol. 291, pp. 52–60, Feb. 2019.

[30] M. D. Patil, G. Grogan, A. Bommarius, and H. Yun, “Recent advances in ω-transaminase-mediated biocatalysis for the enantioselective synthesis of chiral amines,” *Catalysts*, vol. 8, no. 7. 2018.

[31] D. Koszelewski, I. Lavandera, D. Clay, D. Rozzell, and W. Kroutil, “Asymmetric synthesis of optically pure pharmacologically relevant amines employing ω-transaminases,” *Adv. Synth. Catal.*, vol. 350, no. 17, pp. 2761–2766, 2008.

[32] P. Tufvesson, J. Lima-Ramos, J. S. Jensen, N. Al-Haque, W. Neto, and J. M. Woodley, “Process considerations for the asymmetric synthesis of chiral amines using transaminases,” *Biotechnol. Bioeng.*, vol. 108, no. 7, pp. 1479–1493, 2011.

[33] H. Kohls, F. Steffen-Munsberg, and M. Höhne, “Recent achievements in developing the biocatalytic toolbox for chiral amine synthesis,” *Curr. Opin. Chem. Biol.*, vol. 19, no. 1, pp. 180–192, 2014.

[34] R. Abu and J. M. Woodley, “Application of Enzyme Coupling Reactions to Shift Thermodynamically Limited Biocatalytic Reactions,” *ChemCatChem*, vol. 7, no. 19, pp. 3094–3105, Oct. 2015.

[35] R. Fernandez-Lafuente, “Stabilization of multimeric enzymes: Strategies to prevent subunit dissociation,” *Enzyme Microb. Technol.*, vol. 45, no. 6–7, pp. 405–418, Dec. 2009.

[36] M. D. Truppo, J. D. Rozzell, J. C. Moore, and N. J. Turner, “Rapid screening and scale-up of transaminase catalysed reactions,” *Org. Biomol. Chem.*, vol. 7, no. 2, pp. 395–398, Dec. 2009.

[37] K. Deepankumar *et al.*, “Enhancing Thermostability and Organic Solvent Tolerance of ω-Transaminase through Global Incorporation of Fluorotyrosine,” *Adv. Synth. Catal.*, vol. 356, no. 5, pp. 993–998, Mar. 2014.

[38] S. N. Timasheff, “Control of Protein Stability and Reactions by Weakly Interacting Cosolvents: The Simplicity of the Complicated,” in *Advances in protein chemistry*, 1998, pp. 355–432.

[39] D. J. Pollard and J. M. Woodley, “Biocatalysis for pharmaceutical intermediates : the future is now,” *Trends Biotechnol.*, vol. 25, no. 2, pp. 66–73, 2006.

[40] D. Koszelewski, I. Lavandera, D. Clay, G. M. Guebitz, D. Rozzell, and W. Kroutil, “Formal asymmetric biocatalytic reductive amination,” *Angew. Chemie - Int. Ed.*, vol. 47, no. 48, pp. 9337–9340, 2008.

[41] J.-S. Shin and B.-G. Kim, “Asymmetric synthesis of chiral amines with ω-transaminase,” *Biotechnol. Bioeng.*, vol. 65, no. 2, pp. 206–211, Oct. 1999.

[42] H. Yun and B.-G. Kim, “Asymmetric Synthesis of (S)-α-Methylbenzylamine by Recombinant Escherichia coli Co-Expressing Omega-Transaminase and Acetolactate Synthase,” *Biosci. Biotechnol. Biochem.*, vol. 72, no. 11, pp. 3030–3033, Nov. 2008.

[43] T. J. Wenzel and J. D. Wilcox, “Chiral reagents for the determination of enantiomeric excess and absolute configuration using NMR spectroscopy,” *Chirality*, vol. 15, no. 3, pp. 256–270, 2003.

[44] K. D. Klika, M. Budovská, and P. Kutschy, “NMR spectral enantioresolution of spirobrassinin and 1-methoxyspirobrassinin enantiomers using (S)-(-)-ethyl lactate and modeling of spirobrassinin self-association for rationalization of its self-induced diastereomeric anisochromism (SIDA) and enantiomer,” *J. Fluor. Chem.*, vol. 131, no. 4, pp. 467–476, Apr. 2010.

[45] D. Parker, “NMR Determination of Enantiomeric Purity,” *Chem. Rev*, vol. 91, pp. 1441–1457, 1991.

[46] C. Estivill, P. M. Ivanov, M. Pomares, M. Sánchez-Arís, and A. Virgili, “α,α’-Bis(trifluoromethyl)-9,10-anthracenedimethanol: Enantioselective synthesis and bidentate complexes with benzenedimethanols,” *Tetrahedron Asymmetry*, vol. 15, no. 9, pp. 1431–1436, 2004.

[47] P. B. Bhore and V. V. Khanvilkar, “Silica gel: a keystone in chromatographic techniques,” *Int. J. Pharm. Sci. Res.*, vol. 10, no. 1, pp. 12–22, 2019.

[48] A. A. Bele and A. Khale., “An overview on thin layer chromatography,” *Int. J. Pharm. Sci. Res.*, vol. 2, no. 2, pp. 256–267, 2011.

[49] L. Yang, T. Wenzel, R. T. Williamson, M. Christensen, W. Schafer, and C. J. Welch, “Expedited Selection of NMR Chiral Solvating Agents for Determination of Enantiopurity,” *ACS Cent. Sci.*, vol. 2, pp. 332–340, 2016.

6. TA and PDC immobilization

6.1. Introduction

In the previous chapter, the low operational stability of transaminases was identified as a key drawback for process implementation. As it has been previously mentioned (see chapter 4), operational stability of enzymes depends both on storage stability (related to long-term stability) and on their ability to tolerate various reaction environments (related to thermodynamic stability) [1]. In the case of multimeric enzymes, as is the case of TA and PDC, one of the enzyme inactivation mechanism is the dissociation of the enzyme subunits or the loss of their correct assembly structure [2]. In this regards, transaminase inactivation has been related to the cofactor dissociation during reaction, which destabilizes its structure [3]. For this reason, it makes sense to focus research efforts on enzyme stabilization methods. A common way for enhancing operational stability is reaction medium engineering [1], which has been already explored in Chapter 5. At the same time, another strategy for preventing this multimeric enzyme dissociation is immobilization [2].

Enzyme immobilization consists in physically localizing the biocatalysts in a certain region of space [4], making them perform as an heterogeneous catalyst [5]. It involves their confining or association to an insoluble support/matrix, in which the catalytic activities are retained in a way that they can be easily decoupled from the liquid carrying the reagents and products [4], [6], [7]. Enzyme immobilization can change the biocatalyst and its microenvironment, which has been related to some enzyme improvements, such as enhanced selectivity, decreased inhibitions and, specially, higher stability [2], [8]. Taking into account that the mentioned subunit dissociation and protein unfolding are the main steps on enzyme inactivation, rigidly fixing enzymes into a support will prevent these structure changes, which will therefore enhance stability [9], [10]. Other widely accepted advantages of immobilization include enzyme reutilization, easy separation from reaction mixture, which facilitates product recovery and purification, and applications in continuous processes [4], [8], [11]–[13]. However, an immobilized system may not always be beneficial, especially when the free enzyme is cheap and the process is already developed [8]. In addition to the increased costs, other potential disadvantages are a possible reduce in activity and diffusional limitations [4].

Several methods of immobilization are available and, although different classifications have been proposed, they have been generally categorized as (see Figure 6.1): i) binding to a carrier material via adsorption or covalent bounds, ii) cross-linking via short molecular cross-linkers and

iii) retention in permeable materials, such as gels, membranes or fibers [4]–[6], [14]. When biocatalyst consists of whole cells or organelles, physical entrapment is the most used technique, whereas single enzymes are more often bound to carriers or cross-linked [8]. In case of choosing enzyme binding to carriers, a variety of organic or inorganic supports are available [15]. The choice of the support and the technique depends on the nature of the enzyme and its ultimate application [7]. Some desirable features of a support are an economical price, inertness, non-toxicity, maximum biocatalyst loading, operational durability, ease of immobilization or physical strength [6], [7], [10]. Although there are several classes of organic supports, those based on macromolecular sugars such as starch, cellulose or chitosan has become so popular. Among them, agarose has attracted special interest because, in addition of its low cost, it is very hydrophilic, compatible with many activation (functionalization) strategies, readily available with a large variety of pore sizes and resistant to mechanical stirring. Moreover, the particle size may be modulated, from mm to µm range, depending on the final application [10].

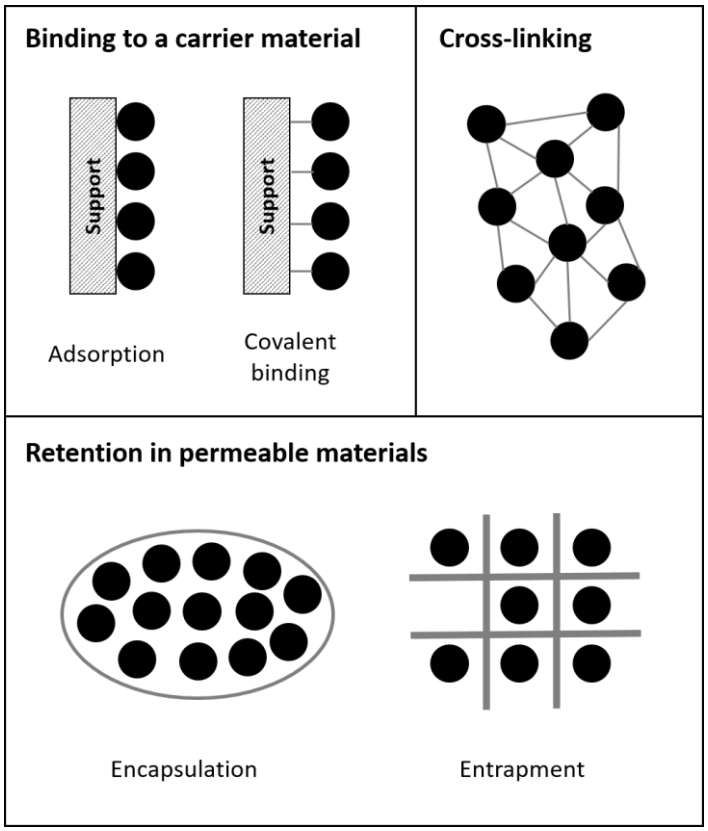

Figure 6.1 Common immobilization methods, classified into: i) binding to a carrier material, ii) cross-linking and iii) retention in permeable materials.

In the present chapter, both transaminase and PDC immobilization by means of covalent binding into agarose-based supports was studied. Covalent binding has as the main advantages the avoiding of enzyme leaching to the reaction medium and a better control of the binding chemistry during immobilization [5], [13], [16]. Attaching enzyme molecules to a rigid support through covalent linkages should prevent conformational changes highly stabilizing, this way, the biocatalyst [17]. These covalent bonds can be formed taking advantage of different functional groups such as amino, carboxyl or phenol [7]. In this sense, exopy-functionalized supports provide an easy immobilization of enzymes through the reaction of epoxy-groups with amino, thiol and phenolic groups, which are nucleophilic groups of high abundance in the protein surface [16]–[19]. Epoxy groups present high stability, which makes possible to perform long-term incubations under alkaline conditions in order to get an intense multipoint covalent attachment [17], [19]. On the other hand, carboxy groups can be also used for immobilization since there are present in majority surface residues (Asp and Glu) [10], [20]. An immobilization method that uses this approach is monoaminomethyl-N-aminoethyl agarose (agarose functionalized with monoaminomethyl-N-aminoethyl groups), commonly known as MANA-agarose. The amino groups present in this kind of supports can react with the mentioned carboxy groups and form covalent bounds using carbodiimide.

6.2. Materials and methods

6.2.1. Chemicals and enzymes

All chemicals were purchased from Sigma-Aldrich (St. Louis, MO, USA). Transaminases from *Chromobacterium violaceum* (Cvi-TA) and *Vibrio fluvialis* (Vfl-TA) were kindly donated by DSM/InnoSyn in the form of *Escherichia coli* cell-free extracts (CFE), containing between 40 and 55 mg·mL^{-1} of total protein. In the case of CFE of Cvi-TA, around 47 % of the total protein was transaminase, while this percentage was 35 % for Vfl-TA. Pyruvate decarboxylase (PDC) from *Zimobacter palmae* was produced by high cell density cultures of a recombinant *E. coli* strain as it has been described in Chapter 3. CFEs of this strain were obtained by sonication with a Vibracell® VC50 (Sonic and Materials®, Newton, CT, USA) with four times 15 s pulses (50 W) and 2 min intervals in ice between each pulse. Centrifugation was performed (10000 g, 10 min) to remove the resulting cell debris. ZpPDC CFEs contained 10 mg· mL^{-1} of total protein, from which around 40 % was PDC. Amino functionalized agarose 4BCL (MANA-agarose) was purchased from Agarose Bead Technologies® (ABT®, Madrid, Spain). Epoxy-agarose was functionalized as it will

be further described using commercial agarose from Agarose Bead Technologies® (ABT®, Madrid, Spain).

6.2.2. Immobilization in MANA-agarose

Enzyme immobilization in MANA-agarose was carried out in potassium phosphate buffer 50 mM and pH 6.2. Immobilization mixtures consisted of 10% MANA-agarose, which has a density of 1.03 $g \cdot mL^{-1}$, in respect to the entire volume if it is not stated elsewhere; and a blank sample was always prepared in parallel by changing the volume corresponding to MANA-agarose for distilled water. After washing the support with the immobilization buffer, the desired enzymatic load and the corresponding enzyme cofactors in each case were solved in the mentioned mixture and incubated at 25ºC and mild agitation conditions to perform a first ionic attachment phase. Samples were taken periodically to measure supernatant, suspension and blank activities. When no variations were detected in the supernatant activity, covalent attachment was forced by adding N-(3-Dimethylaminopropyl)-N'-ethylcarbodiimide (CDI) at a final concentration of 25 mM and incubated during 2 hours at the same conditions. After that, NaCl was added at 1 M final concentration and incubated one hour more to remove the enzyme that did not form covalent bounds.

6.2.3. Immobilization in epoxy-agarose

Agarose was epoxy-functionalized according to the group protocols, consisting in mixing, in a 1:1:1 volume proportion, agarose beads 6 % BCL with a 0.6 M solution of NaOH and 1,4-butanediol diglicidyl ether with the presence of 2 $mg \cdot mL^{-1}$ $NaBH_4$; and incubating it during 8 hours at 25ºC and mild agitation. After washing it with abundant distillate water, a support with around 80 mmol $epoxy \cdot g^{-1}$ was obtained [33]. Immobilization was carried out in potassium phosphate buffer 1 M and pH 8. Immobilization mixtures consisted of 10 % ($v\ v^{-1}$) epoxy-agarose, which has a density of 1.03 $g \cdot mL^{-1}$, in respect to the entire volume; and a blank sample was always prepared in parallel by changing the volume corresponding to epoxy-agarose for distilled water. The desired initial enzymatic load and the corresponding enzyme cofactors in each case were dissolved to the immobilization mixture and it was incubated at 25ºC and mild agitation. Samples of supernatant, suspension and blank were taken periodically to measure enzyme activities. When no variation was detected in the supernatant activity, a 0.2 M final

concentration of 2-mercaptoethanol was added and it was incubated during 4 hours at 4ºC to block the epoxy groups that had not react with any protein-surface group.

6.2.4. Immobilization metrics

In order to obtain immobilization time courses, samples were periodically taken to measure the activity of the whole suspension (SUSP), the supernatant (SN) and the blank. In some occasions, total protein concentration of supernatant samples was found by Bradford's method and their percentage in the interest enzyme by protein electrophoresis. Out from these results, concentration of the interest enzyme could be calculated. In the case of transaminases, this mentioned concentration was used to find immobilization yield according to Equation 6.1. In the equation, TA concentration refers to mg TA per mL of support.

$$Immobilization\ yield\ (\%) = \frac{Offered\ [TA]\ (mg \cdot mL^{-1}) - Final\ SN\ [TA]\ (mg \cdot\ mL^{-1})}{Offered\ [TA]\ (mg \cdot mL^{-1})} \cdot 100$$

Equation 6.1

In the case of PDC, activity results were used to obtain the final immobilization metrics. Immobilization yield and retained activity were calculated with Equation 6.2 and Equation 6.3 respectively. All the activities in the equations are expressed in units per mL of support.

$$Immobilization\ yield\ (IY)\ (\%) = \frac{Initial\ SUSP\ (U \cdot mL^{-1}) - Final\ SN\ (U \cdot mL^{-1})}{Initial\ SUSP\ (U \cdot mL^{-1})} \cdot 100$$

Equation 6.2

$$Retained\ activity\ (RA)\ (\%) = \frac{Final\ SUSP\ (U \cdot mL^{-1}) - Final\ SN\ (U \cdot mL^{-1})}{Initial\ SUSP\ (U \cdot mL^{-1})} \cdot 100$$

Equation 6.3

6.2.5. Analytical methods

6.2.5.1. Transaminase activity assay

Transaminase activity assay was based on the acetophenone formation measurement at 340 nm and 30ºC from α-Methylbenzylamine and pyruvic acid. The assay was performed in 1 mL reaction mixture, consisting of potassium phosphate buffer 100 mM and pH 7.5 containing 0.1 mM PLP, 22.5 mM α-Methylbenzylamine and 5 mM sodium pyruvate. To measure the activity in suspension samples, the total assay volume was doubled. Coefficient of molar extinction (ε) of acetophenone is 0.28 $mM^{-1} \cdot cm^{-1}$ and one transaminase activity unit corresponds to the amount of enzyme that produces 1 µmol acetophenone per minute at 30ºC. Absorbance measurements were performed using a SPECORD® 200 PLUS (Analytik Jena) spectrophotometer. For suspension samples measurements, magnetic agitation provided by the same equipment was used.

6.2.5.2. Pyruvate decarboxylase activity assay

PDC activity was determined by coupling the pyruvate decarboxylation with alcohol dehydrogenase (ADH) and following NADH oxidation at 340 nm and 25ºC, whose coefficient of molar extinction (ε) is 6.22 $mM^{-1} \cdot cm^{-1}$. The reaction mixture contained 33 mM sodium pyruvate, 0.11 mM NADH, 3.5 UA mL^{-1} ADH from *Saccharomyces cerevisiae* (Sigma-Aldrich), 0.1 mM TPP and 0.1 mM $MgCl_2$ in citrate buffer 200 mM and pH 6. To determine the activity of suspension samples, total assay volume was doubled. One unit of PDC activity corresponds to the amount of pyruvate decarboxylase that converts 1 µmole of pyruvate to acetaldehyde per minute. Absorbance measurements were performed using a SPECORD® 200 PLUS (Analytik Jena) spectrophotometer. In the case of suspension samples, magnetic stirring provided by the same equipment was used.

6.2.5.3. Total protein content

Total intracellular protein content present in samples was determined with the Bradford Method using Coomassie Protein Assay Reagent Kit (Thermo Scientific®) and Bovine Serum Albumin (BSA) as standard. The assays were performed in 96-microwell plates and Thermo Scentific® Multiskan FC equipment was used for the absorbance reading. Analyses were carried out in duplicate.

6.2.5.4. SDS-Page electrophoresis

To determine the percentage of enzyme among the rest of intracellular soluble proteins present in the samples, a NuPAGE electrophoresis system (Invitrogen®, Carlsbad, CA, USA) was used. Lysates were obtained as previously described. A volume of 10µL sample was mixed with 5µL *NuPAGE™ LDS Sample Buffer* (4X), 2µL *NuPAGE™ Reducing Agent* (10X) and 3µL deionized water. After 10 min incubation at 70ºC samples were charged to NuPAGE 12 % Bis-Tris electrophoresis gel and it was run using MES-SDS as running buffer at 200 V during 40 minutes. After that, the gel was fixed with a solution containing 40 % v v^{-1} and 10% v v^{-1} acetic acid in water and stained with *Bio-Safe™ Coomassie Stain* (BIO-RAD). Pictures were taken with a *Gel Doc EZ Imaging System* (Bio-Rad®) and analyzed with *Image Lab™ 6.0 Software* (Bio-Rad®).

6.3. Results and discussion

6.3.1. Transaminase immobilization in MANA-agarose

Enzyme immobilization in MANA-agarose is based on the interaction between the amino groups contained into the support and the carboxylic ones of the enzyme surface. Firstly, ionic adsorption phase takes place. To enable this ionic adsorption, during the immobilization process a low ionic strength must be maintained. Moreover, pH conditions must be lower than the support pK to positively charge it, but higher than enzyme pK to ensure that it has an overall negative charge. Since MANA-agarose has a pK 6.8 [20] and a pK 5.4 for Vfl-TA has been reported [21], it was initially decided to perform the immobilization in potassium phosphate buffer 50 mM and pH 6.2. Even though Cvi-TA characterization is not bibliographically described, sequence and structure similarities in both enzymes have been described [1], reason why the same initial immobilization conditions were selected. After ionic adsorption, carbodiimide (CDI) can be used as an activating agent of the enzyme carboxylic groups to transform the ionic forces to more stable covalent bounds [22]. Following the experience of previous MANA immobilizations in the research group, carbodiimide was applied at 25 mM concentration during 2 hours. Finally, the enzyme that has not been covalently attached to MANA-agarose, can be removed by increasing the medium ionic pressure by adding a high salt concentration.

6.3.1.1. Study of the immobilization process at low and high enzymatic load

Initial characterization studies were performed for the immobilization of both Cvi-TA and Vfl-TA in MANA-agarose. According to the supplier (see section 6.2.1), the used support contained between 40 and 60 μmol of aminoethyl per mL of gel, which means a binding capacity of around 30 mg BSA immobilized per mL of support. For this reason, TAs were firstly offered at a relative low enzymatic load in respect to the mentioned data (around 13 mg of total protein per mL support). Afterwards, the initial enzymatic charge was increased to around 70 mg total protein per mL support, with the aim of progressively increase the load until its maximum. Immobilization time-courses are shown in Figure 6.2 and Figure 6.3 respectively.

Due to the typical transaminase hyperactivation already observed in previous chapters (chapter 4 and chapter 5) and also reported by other authors [23], [24], taking conclusions from the immobilization time-courses is a difficult task. In the case of Cvi-TA immobilization at low enzymatic load (Figure 6.2 A), a 40 % increase on suspension activity immediately took place at the beginning and it remained stable during the ionic phase. Hyperactivation also occurred in blank samples in a slower way but, at the end of ionic phase, activity was 60% higher than the initial. On the contrary, supernatant activity decreased around 40%, but due to the described enzymatic activity variations it could not be concluded that this percentage also corresponded to the fraction of offered transaminase attached to the support. Regarding Vfl-TA immobilization (Figure 6.2 B), a total activity loss on supernatant activity was observed after 0.5 h of ionic phase, which may be an indicative of immobilization. However, as in the case of Cvi-TA, only qualitative conclusions can be made since suspension and blank suffered a hyperactivation and nearly triplicated the initial activity in only half an hour. After ionic phase, the 2-hour incubation with 25 mM EDAC had a negative effect on Cvi-TA because activity decreased in a similar way both into suspension and blank in all cases. In Vfl-TA immobilization, EDAC did not have the same repercussion, since blank samples did not lose activity during this incubation. Both Cvi-TA and Vfl-TA suffered a notable activity loss when 1 M NaCl was added to the medium. In the case of Cvi-TA, the negative effect of NaCl led to final activity of suspension and blank of around 10 % of the offered one. In contrast, Vfl-TA activity decrease was not that pronounced and, at the end, both suspension and blank showed higher activity than in the beginning of the process. In both enzyme cases no activity was detected in the supernatant after NaCl incubation, which may be an indicative of a totally efficient of covalent bound formation with CDI addition.

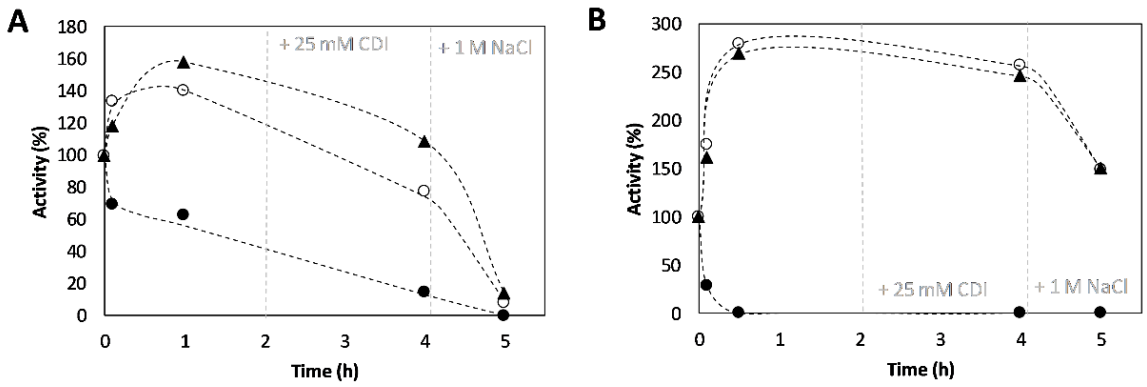

Figure 6.2 Time courses of transaminase immobilizations in MANA-agarose at low initial enzymatic load (13 mg total protein per mL support). A) Cvi-TA immobilization at low enzymatic load. B) Vfl-TA immobilization at low enzymatic load. (●) Supernatant; (○) Suspension; (▲) Blank. Immobilizations performed in potassium phosphate buffer 50 mM and pH 6.2 at 25 ^{o}C.

Regarding the interpretation difficulties of TA immobilization profiles constructed with enzymatic activity, when the offered enzymatic load was increased to 70 mg total protein per mL support, total protein concentration of the supernatant was also analyzed through the time (see Figure 6.3). In the case of Cvi-TA (Figure 6.3 A), total protein concentration immediately decreased and then it remained stable until the end, indicating that ionic attachment took place and all the initially attached protein was immobilized at the end without any leakage. The same conclusion was obtained with Vfl-TA (Figure 6.3 B), even though in this case ionic phase was slightly slower. However, in both Cvi-TA and Vfl-TA, it can also be observed that not all protein was immobilized, which was expectable since higher load than the maximum recommended by the supplier was offered. Therefore, higher initial enzymatic loads were not considered.

On the other hand, immobilization profiles obtained by following the activity were again difficult to discuss due to TAs hyperactivation. In Cvi-TA immobilization (Figure 6.3 A), suspension and blank nearly doubled their activity during ionic attachment in a similar manner. However, supernatant suffered a 50 % activity increase and remained stable before carbodiimide addition. In the same way that transaminase hyperactivation has been associated to a time-dependent dimer formation [23], several authors have pointed out that monomer dissociation could be one of the deactivation causes in multimeric enzymes [2], [24]. Due to this deactivation mechanism, transaminase may show a direct dependence between enzyme concentration and stability [2]. Therefore, activity loss on the supernatant in low enzymatic load (see Figure 6.2 A) could have been related to less transaminase concentration because of the enzyme attachment to the

support, even though it is not possible to quantify it. Supernatant hyperactivation at high enzymatic load could indicate a higher Cvi-TA presence. As it happened when 13 mg protein per mL support were offered, carbodiimide and especially NaCl negatively affected Cvi-TA activity and, at the end, both suspension and blank presented around 30 % of the initially offered activity. Regarding Vfl-TA, (Figure 6.3 B), supernatant activity decreased a 30 % during the ionic phase, but again, because of the high enzymatic activity variability, it is not possible to confirm that it corresponded to the transaminase fraction attached to the MANA-agarose. After that, immobilization finished in a similar way than with lower enzymatic charge. NaCl had a high repercussion on Vfl-TA, even though, at the end, suspension and blank finished the process with higher activity than the offered.

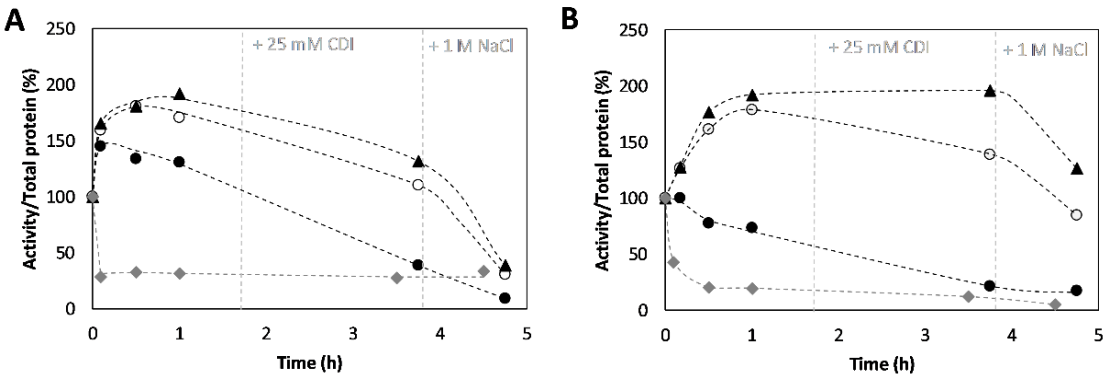

Figure 6.3 Time courses of transaminase immobilizations in MANA-agarose at high initial enzymatic load (70 mg total protein per mL support). A) Cvi-TA immobilization at high enzymatic load. B) Vfl-TA immobilization at high enzymatic load. (●) Supernatant activity; (○) Suspension activity; (▲) Blank activity; (◆) Total protein concentration of the supernatant. Immobilizations performed in potassium phosphate buffer 50 mM and pH 6.2 at 25 ^{o}C.

To obtain a better characterization of the resulting immobilized derivatives, further analysis were performed with the immobilizations at high initial enzymatic load (70 mg total protein per mL support). For both Cvi-TA and Vfl-TA, supernatant samples from the beginning of the process and from the end were taken. In order to study the amount of transaminase attached to the MANA-agarose, total protein concentration analysis and protein electrophoresis were performed. Total protein concentration of the mentioned samples, as well as their transaminase content in % are shown in Table 6.1. The amount of transaminase loaded to the support was calculated by the difference between the initial supernatant samples and the final ones. As it

can be concluded from results in the mentioned table, in both transaminase cases MANA-agarose was loaded to its maximum capacity (around 40 mg total protein per mL support), because protein presence was detected at the end in the supernatant. In the case of Cvi-TA, the increase on transaminase percentage at the end indicates that this transaminase had less affinity for the MANA-agarose than other proteins present in the cell-free extract. Taking into account the initially offered Cvi-TA (30.40 mg/mL) and the amount detected in the final supernatant, it was calculated that the final derivative contained 22.14 mg of Cvi-TA per mL, which means that the immobilization yield was 72.80 %. In contrast, Vfl-TA concentration decreased at the end of the immobilization, then it had higher preference for the support than the other proteins. Nevertheless, since Vfl-TA CFE had lower transaminase concentration, the final transaminase load was similar (20.33 mg Vfl-TA per mL support) even though immobilization yield was nearly 90 %.

Table 6.1 Protein characterization of supernatant samples at the beginning and at the end of transaminase immobilization in MANA-agarose offering a high initial enzymatic load (65 mg total protein per mL support). Total protein concentrations were obtained by performing Bradford's method. Transaminase fraction in % of the same samples were estimated by protein electrophoresis. From these values, TA concentration of each sample could be calculated.

Enzyme	Supernatant sample	Total protein concentration ($mg \cdot mL^{-1}$)	TA fraction (%)	Attached TA[a] ($mg \cdot mL\ support^{-1}$)	Immobilization yield (%)[b]
Cvi-TA	Initial	64.94 ± 1.17	46.83 ± 1.93	22.14	72.80
	Final	13.64 ± 1.81	60.65 ± 2.45		
Vfl-TA	Initial	65.52 ± 4.11	35.33 ± 0.29	20.33	87.81
	Final	12.68 ± 1.60	22.25 ± 0.35		

[a] Estimated by calculating TA concentration of each sample and taking the difference between initial and final samples.

[b] Calculated with the obtained TA concentration of initial and final samples.

Covalent immobilization of the two studied transaminases in amino activated supports has not been bibliographically reported. In previous researches in the same group, an immobilization attempt of a not-described transaminase in MANA-agarose was carried out [25]. However, no activity decrease in supernatant was observed during the procedure, which led to the conclusion that immobilization was not taking place. Neto 2015 [26] used the amino-based supports Sepabeads® EC-EA and Relizyme® EA-403 to immobilize a transaminase from *Aspergillus terreus*. In that case, immobilization yields of around 80% were obtained even though immobilization was only performed by ionic interaction without forming covalent bounds [26].

6.3.1.2. Process optimization to obtain a highly active immobilized derivative

After proving that transaminase immobilization in MANA-agarose effectively took place, optimizations were necessary to obtain a highly active derivative. As it was observed in the immobilization time courses (Figure 6.2 and Figure 6.3), NaCl had a negative effect on transaminase activity, since a sharp decrease on suspension profiles was observed both in the case of Cvi-TA and Vfl-TA. For this reason, stability assays were performed with the aim of reducing the NaCl concentration. In order to reproduce immobilization procedure conditions the two transaminases were incubated in the same immobilization buffer (potassium phosphate 50 mM and pH 6.2) but with no support. After one-hour incubation, which would correspond to the ionic adsorption phase, activity was measured. Taking into account the hyper activation observed in the immobilization profiles (Figure 6.3), it was considered that the maximum possible activity had been achieved at this time. After that, a 2-hours incubation with 25 mM carbodiimide was carried out and its effect on enzyme activity was studied. As it is shown in

Table ***6.2***, both transaminases were negatively affected by the CDI presence, especially Cvi-TA, which suffered between 30 and 40% deactivation.

After incubating the enzymes in carbodiimide, different NaCl concentrations were applied to study its effect on activity. Considering that 1 M NaCl led to low final derivative activities (see section 6.3.1.1), this concentration was decreased to 500 mM, 250 mM and 100 mM. In the case of Cvi-TA, which was the transaminase more affected by the high ionic strength, a considerable activity decrease was still detected with 500 mM NaCl (see Table 6.2). Even though a 10% activity decrease was observed when 250 mM was applied, it was considered that this concentration would be enough to detach the protein that had not formed covalent bounds without a considerable enzyme deactivation. The same concentration was selected in the case of Vfl-TA since it did not show any repercussion.

To prove that this NaCl concentration is adequate to remove the protein not attached with covalent bounds, ionic adsorption phase was again reproduced. However, instead of adding carbodiimide, 250 mM NaCl were directly applied. By analyzing the total protein concentration at the beginning, after ionic phase and at the end, it was observed that the applied ionic strength was enough to detach all the protein in all cases. Therefore, the MANA-immobilization used in further experiments would include this optimization.

Table 6.2 Optimization of transaminase immobilization process in MANA-agarose focusing on the effect of different salt concentration on enzyme activity.

Enzyme	[NaCl] (mM)	Remaining activity (%)		
		t= 1h[a]	t= 3h[b]	t= 4h[c]
Cvi-TA	500	100.00	59.80 ± 0.06	37.37 ± 1.98
	250	100.00	67.58 ± 0.99	60.59 ± 8.9
	100	100.00	70.97 ± 1.37	73.29 ± 0.97
Vfl-TA	500	100.00	79.51 ± 3.71	70.52 ± 1.59
	250	100.00	75.66 ± 2.11	81.03 ± 2.47
	100	100.00	81.16 ± 0.12	84.97 ± 1.78

[a] Activity after ionic attachement phase to MANA-agarose

[b] Activity after incubation with 25 mM carbodiimide

[c] Activity after incubation with the different NaCl concentrations.

6.3.2. Transaminase immobilization in epoxy-agarose

Epoxy-activated supports contain oxirane groups that are able to react with protein amino groups but also with surface exposed residues having different nucleophilic groups such as hydroxyl or thiol [16], [18], [27]. The approximation between oxirane groups and the enzyme functional groups allows a nucleophilic attach that leads to stable covalent bounds formation. This process is favored at neutral and alkaline conditions [17], [27], [28], reason why in this case phosphate buffer 1 M and pH 8 was chosen for the immobilization. Additionally, after covalent bounds formation, the unreacted epoxy groups can be blocked by incubating the derivative with aminated compounds [25]. In this case, following the group experience in this kind of immobilizations, 2-mercaptoethanol was used.

Just as in the case of TA immobilizations in MANA-agarose, first immobilization attempts were carried out at relatively low enzymatic load (13 mg of total protein per mL support). After that, offered enzymatic load was increased to 65 mg of total protein per mL support. The obtained immobilization time-courses are reviewed in Figure 6.4. As it already happened during transaminase immobilization in MANA-agarose, the typical time-dependent TA hyperactivation hampered the conclusions obtaining. Regarding Cvi-TA immobilization at low enzymatic load (Figure 6.4 A), enzyme immobilization led to a more activated biocatalyst since a higher activity increase was detected in the suspension in comparison to the blank samples, while a 20% activity decrease was observed in the supernatant. However, after 2-mercaptoethanol addition, suspension suffered a deactivation that did not happen in the blank and supernatant samples. Therefore, support blockage phase had a negative effect on immobilized enzyme. After

recovering the immobilized derivative, this showed the same activity as the whole suspension at the end of the process but it cannot be concluded that all transaminase had been immobilized because supernatant samples also showed activity. When the initial load was increased to 70 mg per mL support (Figure 6.4 C), a similar supernatant profile was obtained. However, hyperactivation of the suspension and blank was not that notable, even though higher activity in the suspension than in the blank was again detected. Support blockage also affected immobilized enzyme this time, but the detected activity decrease was not that sharp. In this case, the final recovered derivative, presented a 40% of the whole suspension activity at the end of the process. However, due to the high variability in transaminase activity and regarding the results obtained at low enzymatic load, it cannot be concluded that this fraction corresponded to the immobilization yield.

During Vfl-TA immobilization at low enzymatic load (Figure 6.4 B), transaminase hyperactivation was much more pronounced than in the Cvi-TA case, since a 5-fold increase in the blank and a 6-fold increase in suspension were detected after 2 hours. Moreover, in this case, supernatant activity did not decrease but it was doubled. The high difference between suspension and supernatant activity may be an indicative of immobilization but in any case the attached fraction can be quantified. Epoxy blockage phase did not have any negative repercussion on transaminase but a 50 % increase on supernatant activity was observed. This increase, coupled with the fact that the recovered immobilized derivative showed half of the activity detected in the last suspension samples, may lead to the conclusion that part of the enzyme was detached after the blocking phase. When the offered enzyme was higher (see Figure 6.4 D), hyperactivation was lower and no difference was observed between suspension and blank. Regarding supernatant, an initial activity decrease was detected but, after the blockage with 2-mercaptoethanol, an increase was again observed and the final suspension activity exceeded the initial offered load. Activity of the recovered derivative represented less than the half of this final suspension activity, which lead again to the conclusion that not all transaminase was attached to epoxy-agarose but immobilization yield could not be calculated due to the high activity variations observed.

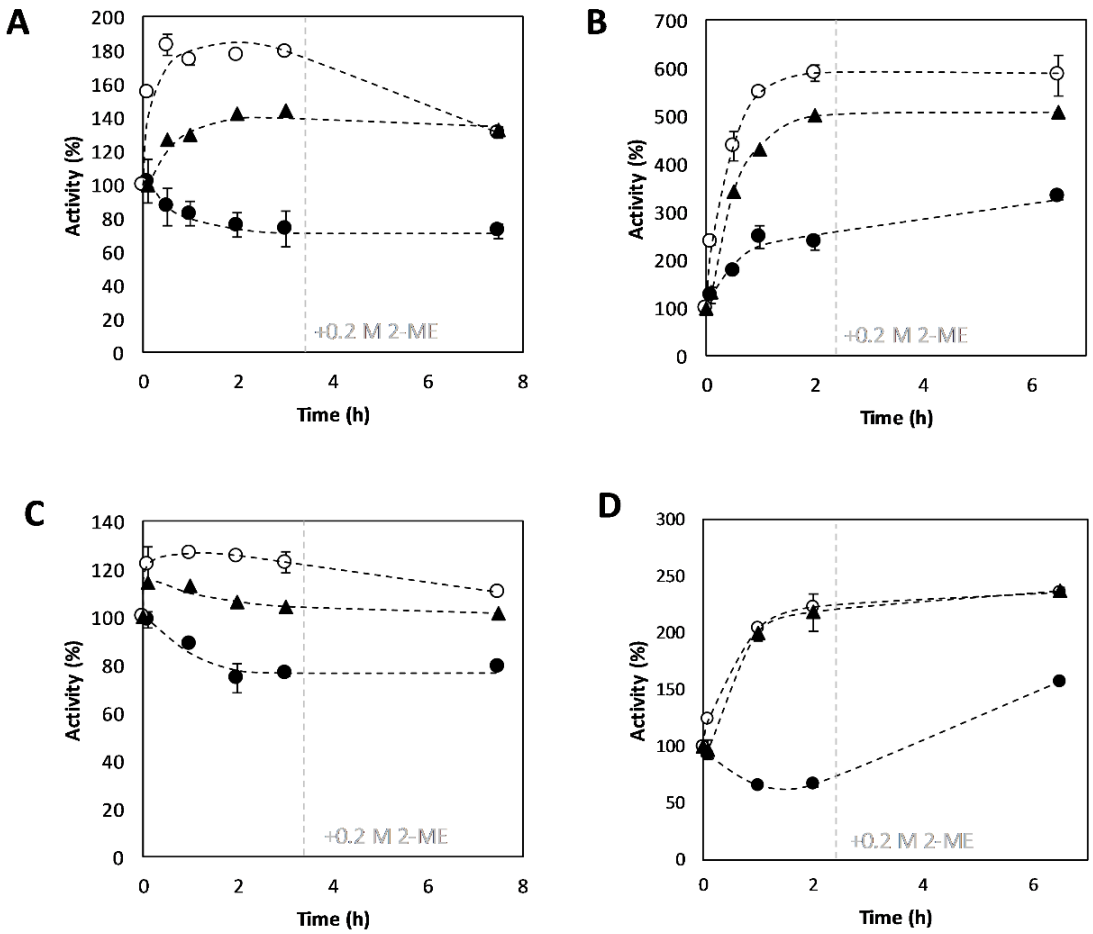

Figure 6.4 Time courses of transaminase immobilizations in epoxy-agarose at low (13 mg of total protein per mL support) and high (70 mg of total protein per mL support) initial enzymatic load. Immobilizations performed in potassium phosphate buffer 1 M and pH 8 at 25°C. A) Cvi-TA immobilization at low enzymatic load. B) Vfl-TA immobilization at low enzymatic load. C) Cvi-TA immobilization at high enzymatic load. D) Vfl-TA immobilization at high enzymatic load. (●) Supernatant; (○) Suspension; (▲) Blank.

Like in the case of transaminase immobilization in MANA-agarose (see section 6.3.1), the not-conclusive results obtained with the immobilization time courses led to the necessity of carrying out a protein characterization of the immobilizations at high enzymatic load. Total protein concentration of initial and final supernatant samples was analyzed by Bradford's method and transaminase fraction was estimated by performing an electrophoresis gel. As it is shown in Table 6.3, a maximum load of around 40 mg total protein per mL epoxy-agarose was achieved in both cases (45.00 $mg \cdot mL^{-1}$ in the case of Cvi-TA and 46.80 $mg \cdot mL^{-1}$ in the case of Vfl-TA). Regarding Cvi-TA immobilization, it was observed that the percentage of this transaminase in the supernatant increased at the end, which is an indicative that it had less

affinity for the support than other proteins present in the CFE. In contrast, Vfl-TA fraction remained stable, which means that the attachment took place proportionally. For this reason, Vfl-TA immobilization yield was 1.26-fold higher than in the Cvi-TA case. However, since Cvi-TA CFE contained more transaminase, the final enzymatic load in mg TA per mL support was similar for the both obtained derivatives (17.33 mg·mL^{-1} in the case of Cvi-TA and 16.62 mg·mL^{-1} in the case of Vfl-TA).

Table 6.3 Protein characterization of supernatant samples at the beginning and at the end of transaminase immobilization in epoxy-agarose offering a high initial enzymatic load (70 mg total protein per mL support). Total protein concentrations were obtained by Bradford's method. Transaminase fraction in % of the same samples were estimated by protein electrophoresis. From these values, TA concentration of each sample could be calculated.

Enzyme	Supernatant sample	Total protein concentration (mg·mL^{-1})	TA fraction (%)	Attached TA[a] (mg·mL support^{-1})	Immobilization yield (%)[b]
Cvi-TA	Initial	64.94 ± 1.17	46.83 ± 1.93	17.33	56.97
	Final	19.97 ± 1.29	65.53 ± 1.01		
Vfl-TA	Initial	65.52 ± 4.11	35.33 ± 0.29	16.62	71.79
	Final	18.71 ± 1.63	34.90 ± 1.01		

[a] Estimated by calculating TA concentration of each sample and taking the difference between initial and final samples.
[b] Calculated with the obtained TA concentration of initial and final samples.

Only few transaminase immobilizations in epoxy-activated supports have been reported but in any case agarose-based. Cvi-TA has been immobilized in bisepoxyde-activated aminoalkyl supports, obtaining a 100 % immobilization yield and reporting a final derivative containing 100 mg of pure enzyme per g support [16]. Regarding Vfl-TA, it has been reported its immobilization in epoxy-functionalized cellulose. In that case, the enzymatic load was similar as in the present study, being attached 40 mg protein per g support and with 90 % of retained activity [29]. The same enzymatic load was also reported during immobilization of Januvia TA in the commercial epoxy-based support Sepabeads® EXE120, but in this case 45% retained activity was detected [30]. Finally, in a previous thesis of the same research group, a transaminase was immobilized in Eupergit® CM obtaining a 70 % immobilization yield with only 20 % retained activity [25].

6.3.3. PDC immobilization in MANA-agarose

After effectively immobilizing the two transaminases in MANA-agarose, the same method was used to immobilize PDC. As it was already mentioned in section 6.3.1, pH conditions of the immobilization in MANA-agarose must be lower than the pKa of the support to positively charge it and higher than the protein isoelectric point to ensure a negative overall charge. Since ZpPDC presents and isoelectric point of 4.93, immobilization was initially planned in potassium phosphate buffer 25 mM and pH 6. Just as the case of TAs immobilization, initially planned protocols consisted in a first ionic attachment phase followed by a 2-hours incubation with 25 mM carbodiimide to induce the covalent binding. Finally, 1 hour incubation at high ionic pressure ensures the removing of the protein that does not form covalent bounds.

6.3.3.1. Initial PDC immobilization attempts in MANA-agarose

PDC immobilization studies in MANA-agarose started by offering a low enzymatic charge (10 U per mL support). As it is shown in the time-course A of Figure 6.5, all the supernatant activity disappeared in half an hour, which means that PDC was quickly adsorbed to the support. After that, carbodiimide was added and, after 2-hours incubation, ionic pressure was increased to remove the protein that had not formed covalent bounds. The absence of supernatant activity at the end means that all the enzyme was covalently attached to MANA agarose, thus a 100 % immobilization yield was obtained. However, an activity decrease was observed both in the suspension and in the blank after the ionic adsorption phase, which may be associated to a stability loss due to carbodiimide or NaCl presence into the immobilization buffer. Therefore, the process ended with a retained activity of 55.3 % due to the mentioned activity decrease.

When the initial offered activity was doubled (Figure 6.5 B), both supernatant and blank showed lower enzyme deactivation after ionic adsorption phase, which may be due to the stabilization effect associated to the increase on protein concentration commonly described in multimeric proteins [2]. Nevertheless, protein detachment was detected after incubation with carbodiimide, which meant a final immobilization yield of 47.3 % and a retained activity of around 25 %. Altogether, led to a final immobilized derivative with the same activity as the obtained when 10 U·mL support^{-1} were offered. Finally, initial enzymatic load was increased to 70 U per mL support (Figure 6.5 C), but the enzyme detachment was even more pronounced.

Even though an IY of 31.9 % was obtained, no retained activity was detected, resulting in a completely inactive derivative.

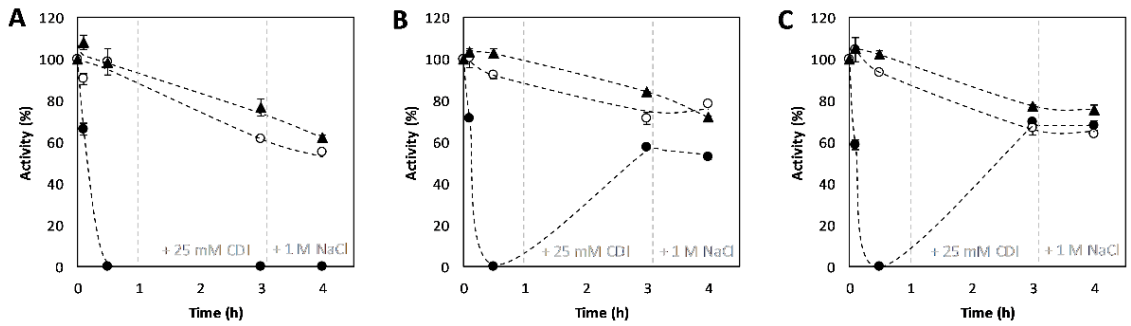

Figure 6.5 Time courses of PDC immobilizations in MANA-agarose at different initial enzymatic loads. Immobilizations performed in potassium phosphate buffer 25 mM and pH 6 at 25ºC. A) PDC immobilization in an initial enzymatic load of 10 U per mL of MANA-agarose. B) PDC immobilization in an initial enzymatic load of 20 U per mL of MANA-agarose. C) PDC immobilization in an initial enzymatic load of 70 U per mL of MANA-agarose. (●) Supernatant; (○) Suspension; (▲) Blank.

An explanation about why PDC was detaching from the support after adding CDI when high initial enzymatic loads were offered is difficult to find. Carbodiimides are reagents that have been frequently used for protein modification, since they interact with protein carboxylic groups making them more sensitive to nucleophilic attach [31]. During MANA immobilization, the mentioned CDI effect allows a proper interaction between protein carboxylic groups and supports amine groups [32], [33], therefore it is necessary to form covalent bounds. However, during this immobilization step, pH conditions must be controlled because it has been reported a high CDI instability in low pHs due to an hydrolysis process [31]. In the immobilization procedure followed in this case (see materials and methods, section 6.2), CDI was added at the immobilization mixture from a previously prepared stock solution. To avoid a pH increase, previously to the addition, the stock solution pH is readjusted with HCl to maintain the immobilization conditions. However, it must be taken into account the low ionic strength of the immobilization mixture, which may have not been enough to maintain the pH, leading to lower pH values when CDI from the stock solution was added. Since, according to Gilles 1990 [31], carbodiimide stability deeply decreases at pH<6, it was decided to adjust the immobilization conditions to ensure that CDI was in its optimum state. In further experiments, pH conditions were more deeply controlled. In addition, a new immobilization buffer was chosen with slightly

higher pH and ionic strength in order to protect immobilization mixture to the possible variations mentioned when CDI is added.

Following the new planned indications, immobilizations were repeated in potassium phosphate buffer 50 mM and pH 6.2. During immobilization at 10 U·mL^{-1} initial enzymatic load (Figure 6.6 A), PDC was quickly adsorbed to MANA-agarose and, after that, no activity was detected in the supernatant, which means that immobilization took place with 100 % yield. Moreover, unlike in the previous conditions tested, suspension did not suffer the same activity decrease as the blank. Therefore, immobilization could have enhanced PDC stability and a final retained activity of almost 90 % was achieved. When 20 U per mL support were offered (Figure 6.6 B), which is the initial load in which detachment was already observed in previous experiments, 100 % immobilization yield was also observed with a similar retained activity as by offering 10 U·mL^{-1} (82.4 %). Thus, the process had been improved with the new buffer and, for this reason, further experiments with higher enzymatic load were performed. However, by offering 100 U per mL support, PDC detachment was again observed even though the enzyme had been rapidly adsorbed (Figure 6.6 C). After carbodiimide incubation, supernatant activity increased to around 70 % of the offered activity, which meant a final immobilization yield of 32.9 %. Although some stability improvement was observed in the suspension profile in comparison with the blank, the final retained activity was 15.1 %. In conclusion, the slight increase on pH and ionic strength, helped to improve immobilization process, but the achievement of a derivative with high enzymatic charge was still not possible.

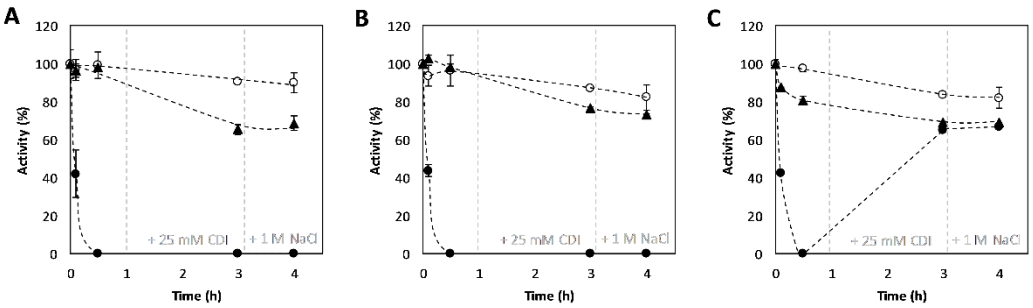

Figure 6.6 Time courses of PDC immobilizations in MANA-agarose at different initial enzymatic loads. Immobilizations performed in potassium phosphate buffer 50 mM and pH 6.2 at 25ºC. A) PDC immobilization in an initial enzymatic load of 10 U per mL of MANA-agarose. B) PDC immobilization in an initial enzymatic load of 20 U per mL of MANA-agarose. C) PDC immobilization in an initial enzymatic load of 100 U per mL of MANA-agarose. (●) Supernatant; (○) Suspension; (▲) Blank.

6.3.3.2. Simultaneous purification and immobilization of PDC

During an investigation performed in the same research group, MANA-agarose was used as ionic exchange matrix in FPLC column for the same ZpPDC purification. In the mentioned research, it was found that at pH 5 the amount of positively charged proteins in the lysate increased, while PDC still had an overall negative charge. For this reason, contaminant proteins were less adsorbed to the support and a purification factor of 4 could be achieved [34]. Following these successful results, an innovative two-step process to simultaneously purify and immobilize PDC was developed in the present thesis. The new procedure consisted in a first ionic adsorption phase performed with acetate buffer 50 mM and pH 5, followed by a wash in the same buffer to remove the contaminant proteins. After that, to avoid the mentioned carbodiimide instability, a buffer exchange to potassium phosphate buffer 50 mM and pH 6.2 was carried out before its addition.

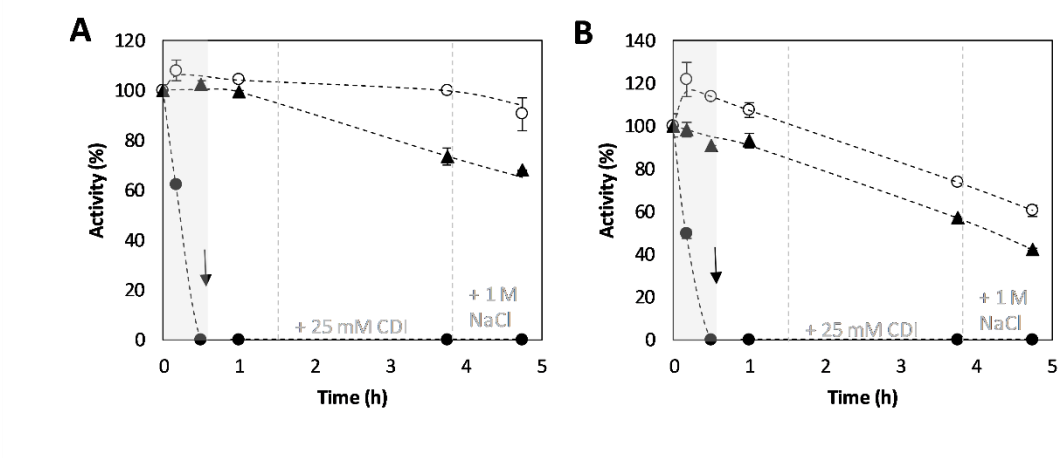

Figure 6.7 Simultaneous purification and immobilization of PDC in MANA-agarose. A) PDC purification and immobilization by offering an initial enzymatic load of 15 U per mL of MANA-agarose. B) PDC purification and immobilization by offering an initial enzymatic load of 150 U per mL of MANA-agarose. (●) Supernatant; (○) Suspension; (▲) Blank. The arrow indicates the buffer exchange from acetate buffer 50 mM and pH 5 to potassium phosphate buffer 50 mM and pH 6.2. Temperature 25ºC.

By offering 15 U per mL of support (Figure 6.7 A), PDC was rapidly adsorbed to MANA-agarose since no activity was detected to the supernatant. Neither after CDI incubation nor after increasing the ionic pressure, activity appeared to the supernatant. Thus, an immobilization yield of 100% was obtained at the end demonstrating that it was possible to efficiently purify and immobilize PDC at the same time by the developed method. In addition, stability was improved

by immobilization because final retained activity was around 90 % while, during the process, the blank sample lost around 40 % of its initial activity. Regarding the successful results, offered activity was 10-fold increased with the aim of obtaining a highly activated derivative as well as to study if the PDC detachment previously detected after CDI addition in high enzymatic loads (see Figure 6.6) took place this time. As it can be observed in Figure 6.7 B, PDC was efficiently immobilized with 100 % yield but, at the end of the process, retained activity of around 60 % was obtained, even though suspension showed slightly better stability than the blank. It can also be observed that the sharpest activity decrease was produced after the incubations with carbodiimide and NaCl. Therefore, at higher initial load, PDC is more affected by the covalent bound formation and the subsequent increase of ionic strength to remove the resting protein attached by adsorption.

6.3.3.3. PDC immobilized derivative obtainment at maximum activity load

Despite the decreased retained activity obtained when the new simultaneous purification and immobilization process was carried out at 150 U per mL support, further experiments were performed to increase the enzymatic load to the maximum possible. In previous experiments, CFEs had been diluted to pH 5 acetate buffer with a 10 % v v^{-1} of MANA-agarose (see materials and methods). However, to offer the maximum possible initial protein concentration but maintaining the 10 % proportion of support in respect to the reaction mixture CFEs had to be directly obtained in acetate buffer 50 mM and pH 5 and were directly offered at the mentioned proportion to MANA-agarose. After finishing the ionic phase without detecting any activity into the supernatant, the immobilized derivative was recovered and new CFE was offered again at the same proportion the necessary times until supernatant did not lose the entire activity. From this preliminary experiment, it was concluded that the maximum charge that could be adsorbed to the support was around 3000 U of PDC per mL MANA-agarose. The next step consisted in following the entire immobilization process directly offering the found maximum load, even though the 10 % proportion was not maintained, since the total CFE volume required was several times higher. As it can be observed in Figure 6.8, ionic adsorption phase lasted more than in previous cases, which can be associated to the increase on volume proportion necessary to achieve the 3000 U per mL support, which is the maximum activity load found in previous experiments. After that, no more activity was detected in the supernatant, neither after buffer exchange nor incubation with carbodiimide and NaCl. Therefore, an immobilization yield of 100 % was obtained. However, activity decrease after carbodiimide addition was even deeper

than in the case of 150 U per mL support offered, which led to a final retained activity of only 20 %.

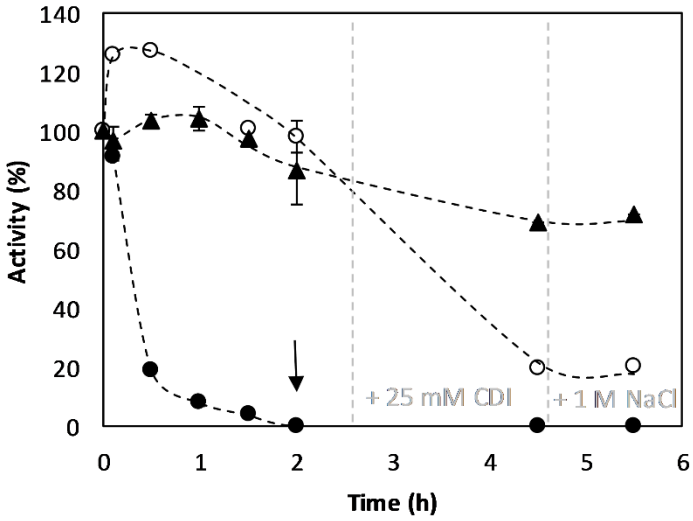

Figure 6.8 Simultaneous purification and immobilization of PDC in MANA-agarose by offering the maximum initial enzymatic load (3000 U per mL of MANA-agarose). (●) Supernatant; (○) Suspension; (▲) Blank. The arrow indicates the buffer exchange from acetate buffer 50 mM and pH 5 to potassium phosphate buffer 50 mM and pH 6.2.

Aiming to obtain an optimum immobilized derivative with the maximum activity possible but offering the less initial enzymatic load, further experiments were performed. Regarding that worse retained activity results were obtained at higher enzymatic loads, several initial enzyme amounts were offered per mL of MANA-agarose. As it is shown in Figure 6.9, retained activity linearly decreased by increasing the initial charge. As it is specified in the same figure, these results are translated to final derivatives with not more than 600-700 U per mL of support. Since the maximum final specific activity obtained was by offering 2000 U per mL support, it was concluded that it was not worthy to offer higher initial loads. For this reason, this value was fixed as optimum and used for the preparation of derivatives in further experiments concerning immobilized PDC.

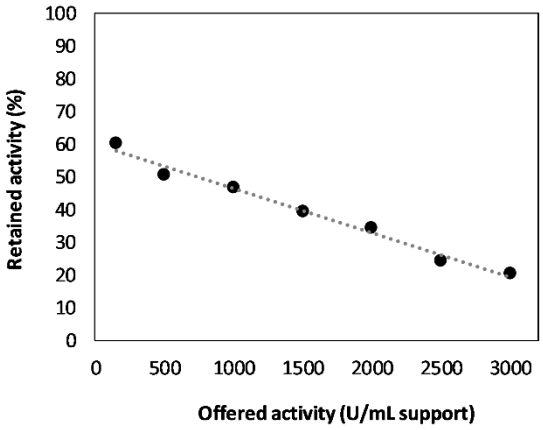

Offered activity (U/mL support)	Final derivative activity (U/mL support)
150	78.7
500	252.5
1000	468.3
1500	587.5
2000	684.2
2500	601.4
3000	621.9

Figure 6.9 Effect of different offered initial activities to the final derivative retained activity percentage. In the table, the final derivative activity in each case is shown.

6.3.3.4. Immobilization process optimization

Since the final retained activity was still so low further optimizations were planned. Activity in the supernatant was not being detected in any case at the end, thus derivative activity loss could not be associated to enzyme leakage. The low retained activity couldn't neither be due to diffusional limitations, since during ionic phase 100 % of the offered activity was always maintained in the suspension. Therefore, a loss on the derivative activity was the reason of these non-optimum values. Carbodiimide effect on PDC stability was studied by adding 25 mM CDI to a 2000 $U \cdot mL^{-1}$ solution of PDC in potassium phosphate buffer 50 mM and pH 6.2. As it can be observed in Figure 6.10 (A) PDC activity remained at its 100 % for 1.5 h and a 20 % decrease was detected after 2 hours. Even though the detected activity decrease did not correspond to the activity loss in the immobilized derivatives, it was decided to perform the procedure but decreasing the CDI incubation phase to 1 hour (see Figure 6.10 B). Nevertheless, shorten the mentioned phase did not show any improvement of PDC immobilization. Therefore, the activity loss when high enzymatic loads are offered is an effect of the interaction between the enzyme, the support and the carbodiimide.

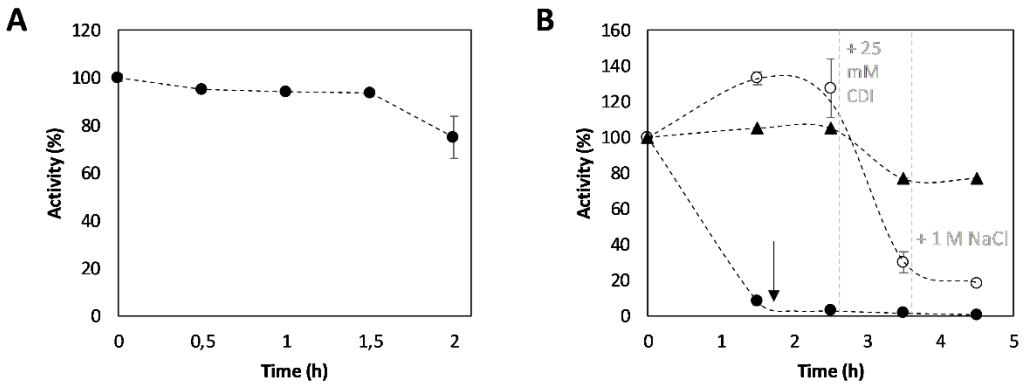

Figure 6.10 A) PDC stability profile in the presence of carbodiimide. A concentration of 25 mM CDI was added to a 2000 $U \cdot mL^{-1}$ solution of PDC in potassium phosphate buffer 50 mM and pH 6.2. B) PDC simultaneous purification and immobilization in MANA-agarose shortening the CDI incubation phase to 1 hour. (●) Supernatant; (○) Suspension; (▲) Blank. The arrow indicates the buffer exchange from acetate buffer 50 mM and pH 5 to potassium phosphate buffer 50 mM and pH 6.2.

6.3.4. PDC immobilization in epoxy-agarose

Just as transaminases were immobilized in epoxy-agarose, the same method was used for PDC immobilization. As it has already been mentioned in section 6.3.2, covalent bound formation between support oxirane groups and different enzyme functional groups is favored at neutral and alkaline conditions. For this reason, as well as with the aim to reproduce the same protocol, which would supply valuable information for possible future coimmobilization approaches, immobilization was again performed in potassium phosphate buffer 1 M pH 8.

In general, working with PDC at basic pH conditions is not recommended since, as it has been explained in Chapter 4, it suffers a pH-dependent quaternary structure destabilization [35]–[37]. However, in the same chapter, it was demonstrated that in the presence of its cofactors (TPP and $MgCl_2$) this destabilization could be avoided. Even though cofactors were added into the immobilization mixture at 1 mM concentration, as it can be observed in the immobilization time-course presented in Figure 6.11, both supernatant, suspension and blank suffered an around 70 % activity loss after 3 hours. Since the previous stability studies had been performed in 100 mM phosphate buffer (see chapter 4), stability loss was associated to the increase on ionic strength. Therefore, the incompatibility of the enzyme with the immobilization method requirements, lead to the conclusion that it was not possible to immobilize ZpPDC in epoxy-agarose, reason why this kind of support was discarded.

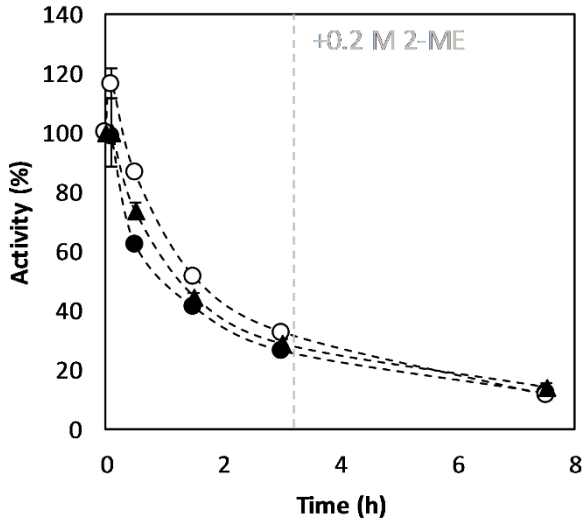

Figure 6.11 Time course of PDC immobilization in epoxy agarose at low enzymatic load (10 U per mL of support) in potassium phosphate buffer 1 M and pH 8 at 25ºC. (●) Supernatant; (○) Suspension; (▲) Blank.

6.4. Conclusions

Immobilization of the two transaminases was carried out in MANA-agarose and in epoxy-agarose. In all immobilization profiles, transaminases showed its typical hyperactivation, reason why immobilization results had to be followed with the protein concentration. Immobilized derivatives of Cvi-TA and Vfl-TA in MANA-agarose were obtained with a maximum total protein load of 40 mg per mL of support. In the case of Cvi-TA, they contained 22.14 mg of TA per mL, which corresponds to an immobilization yield of 72.80 %. In the case of Vfl-TA, they contained 20.33 mg of TA per mL, which corresponds to an immobilization yield of 87.81 %. Regarding derivatives in epoxy-agarose, even though similar maximum total protein could be attached, they contained slightly lower transaminase amounts. Cvi-TA derivatives contained 17.33 mg TA·mL^{-1}, corresponding to 56.97 % yield, while Vfl-TA derivatives contained 16.62 mg TA·mL^{-1}, which corresponds to 71.79 % yield.

Regarding PDC immobilization, epoxy-agarose support was discarded because of the low PDC stability in the required immobilization conditions. In contrast, immobilization could be performed in MANA-agarose following the same procedure as in TAs case, but enzyme detachment after CDI incubation was detected when initial enzymatic load was increased. This drawback could be overcome by developing a simultaneous purification and immobilization procedure based on pH decrease followed by a buffer exchange to ensure CDI stability. Even

though a maximum enzymatic load of 3000 U per mL of MANA-agarose could be offered, it was established that the maximum worthy to offer was 2000 $U \cdot mL^{-1}$ since at high enzymatic charges deactivation during CDI incubation was detected. A final derivative of around 700 $U \cdot mL^{-1}$ was obtained.

6.5. References

[1] S. Chen, J. C. Campillo-Brocal, P. Berglund, and M. S. Humble, "Characterization of the stability of Vibrio fluvialis JS17 amine transaminase," *J. Biotechnol.*, vol. 282, pp. 10–17, Sep. 2018.

[2] R. Fernandez-Lafuente, "Stabilization of multimeric enzymes: Strategies to prevent subunit dissociation," *Enzyme Microb. Technol.*, vol. 45, no. 6–7, pp. 405–418, Dec. 2009.

[3] T. Börner *et al.*, "Explaining Operational Instability of Amine Transaminases: Substrate-Induced Inactivation Mechanism and Influence of Quaternary Structure on Enzyme−Cofactor Intermediate Stability," *ACS Catal.*, vol. 7, pp. 1259–1269, 2016.

[4] E. Katchalski-Katzir, "Immobilized enzymes - learning from past successes and failures," *Trends Biotechnol.*, vol. 11, no. 11, pp. 471–478, 1993.

[5] W. Böhmer *et al.*, "Highly efficient production of chiral amines in batch and continuous flow by immobilized ω-transaminases on controlled porosity glass metal-ion affinity carrier," *J. Biotechnol.*, vol. 291, pp. 52–60, Feb. 2019.

[6] V. L. Sirisha, A. Jain, and A. Jain, *Enzyme Immobilization: An Overview on Methods, Support Material, and Applications of Immobilized Enzymes*, 1st ed., vol. 79. Elsevier Inc., 2016.

[7] S. F. D'Souza, "Immobilized enzymes in bioprocess," *Curr. Sci.*, vol. 77, no. 1, pp. 69–79, 1999.

[8] W. Hartmeier, "Immobilized biocatalysts - From simple to complex systems," *Trends Biotechnol.*, vol. 3, no. 6, pp. 149–153, 1985.

[9] A. Klibanov, "Enzyme Stabilization by Immobilization," *Methods Enzymol.*, vol. 137, no. C, pp. 584–598, 1988.

[10] P. Zucca, R. Fernandez-Lafuente, and E. Sanjust, “Agarose and Its Derivatives as Supports for Enzyme Immobilization,” *Molecules*, vol. 21, pp. 1577–1599, 2016.

[11] B. A. Kikani, S. Pandey, and S. P. Singh, “Immobilization of the a-amylase of Bacillus amyloliquifaciens TSWK1-1 for the improved biocatalytic properties and solvent tolerance,” *Bioprocess Biosyst Eng*, vol. 36, pp. 567–577, 2013.

[12] M. D. Patil, G. Grogan, A. Bommarius, and H. Yun, “Recent advances in ω-transaminase-mediated biocatalysis for the enantioselective synthesis of chiral amines,” *Catalysts*, vol. 8, no. 7. 2018.

[13] H. Mallin, U. Menyes, T. Vorhaben, M. Höhne, and U. T. Bornscheuer, “Immobilization of two (R)-Amine Transaminases on an Optimized Chitosan Support for the Enzymatic Synthesis of Optically Pure Amines,” *ChemCatChem*, vol. 5, no. 2, pp. 588–593, 2013.

[14] I. Chibata, “Biocatalysis: immobilized cells and enzymes,” *J. Mol. Catal.*, vol. 1986, pp. 63–86, 1986.

[15] I. Slabu, J. L. Galman, R. C. Lloyd, and N. J. Turner, “Discovery, Engineering, and Synthetic Application of Transaminase Biocatalysts,” *ACS Catal.*, vol. 7, no. 12, pp. 8263–8284, 2017.

[16] E. Abaházi *et al.*, “Covalently immobilized Trp60Cys mutant of ω-transaminase from Chromobacterium violaceum for kinetic resolution of racemic amines in batch and continuous-flow modes,” *Biochem. Eng. J.*, vol. 132, pp. 270–278, Apr. 2018.

[17] C. Mateo, V. Grazu, J. M. Palomo, F. Lopez-Gallego, R. Fernandez-Lafuente, and J. M. Guisan, “Immobilization of enzymes on heterofunctional epoxy supports,” *Nat. Protoc.*, vol. 2, no. 5, pp. 1022–1033, May 2007.

[18] C. Mateo, O. Abian, R. Fernandez–Lafuente, and J. M. Guisan, “Increase in conformational stability of enzymes immobilized on epoxy-activated supports by favoring additional multipoint covalent attachment,” *Enzyme Microb. Technol.*, vol. 26, no. 7, pp. 509–515, Apr. 2000.

[19] A. A. Mendes, H. F. de Castro, G. S. S. Andrade, P. W. Tardioli, and R. de L. C. Giordano, “Preparation and application of epoxy–chitosan/alginate support in the immobilization of microbial lipases by covalent attachment,” *React. Funct. Polym.*, vol. 73, no. 1, pp. 160–167, Jan. 2013.

[20] R. Fernandez-Lafuente *et al.*, “Preparation of activated supports containing low pK

amino groups. A new tool for protein immobilization via the carboxyl coupling method," *Enzyme Microb. Technol.*, vol. 15, no. 7, pp. 546–550, 1993.

[21] J. S. Shin, H. Yun, J. W. Jang, I. Park, and B. G. Kim, "Purification, characterization, and molecular cloning of a novel amine:pyruvate transaminase from Vibrio fluvialis JS17," *Appl. Microbiol. Biotechnol.*, vol. 61, no. 5–6, pp. 463–471, Jun. 2003.

[22] M. Pešić, C. López, G. Álvaro, and J. López-Santín, "A novel immobilized chloroperoxidase biocatalyst with improved stability for the oxidation of amino alcohols to amino aldehydes," *J. Mol. Catal. B Enzym.*, vol. 84, pp. 144–151, 2012.

[23] K. E. Cassimjee, M. S. Humble, V. Miceli, C. Granados Colomina, and P. Berglund, "Active Site Quantification of an ω-Transaminase by Performing a Half Transamination Reaction," *ACS Catal.*, vol. 1, pp. 1051–1055, 2011.

[24] S. Chen, H. Land, P. Berglund, and M. S. Humble, "Stabilization of an amine transaminase for biocatalysis," *J. Mol. Catal. B Enzym.*, vol. 124, pp. 20–28, Feb. 2016.

[25] A. M. Cárdenas-Fernández, "Inmovilización de transaminasas y amonio liasas y su aplicación en síntesis de compuestos aminados. Memoria para optar al grado de doctor en Biotecnología por la Universitat Autònoma de Barcelona," Universitat Autònoma de Barcelona, 2012.

[26] W. Neto, M. Schürmann, L. Panella, A. Vogel, and J. M. Woodley, "Immobilisation of omega-transaminase for industrial application: Screening and characterisation of commercial ready to use enzyme carriers," *J. Mol. Catal. B Enzym.*, vol. 117, pp. 54–61, 2015.

[27] M. García-Bofill, P. W. Sutton, M. Guillén, and G. Álvaro, "Enzymatic synthesis of vanillin catalysed by an eugenol oxidase," *Appl. Catal. A Gen.*, vol. 582, Jul. 2019.

[28] E. Katchalski-Katzir and D. M. Kraemer, "Eupergit® C, a carrier for immobilization of enzymes of industrial potential," *J. Mol. Catal. B Enzym.*, vol. 10, pp. 157–176, 2000.

[29] S. P. de Souza *et al.*, "Cellulose as an efficient matrix for lipase and transaminase immobilization," *RSC Adv.*, vol. 6, no. 8, pp. 6665–6671, Jan. 2016.

[30] M. D. Truppo, H. Strotman, and G. Hughes, "Development of an Immobilized Transaminase Capable of Operating in Organic Solvent," *ChemCatChem*, vol. 4, no. 8, pp. 1071–1074, 2012.

[31] M. A. Gilles, A. Q. Hudson, and C. L. Borders, “Stability of water-soluble carbodiimides in aqueous solution,” *Anal. Biochem.*, vol. 184, no. 2, pp. 244–248, 1990.

[32] L. M. Vázquez, “Co-inmovilización de la cloroperoxidasa y la fructosa-6-fosfato aldolasa para su utilización en la síntesis de pre-D-fagomina,” Universitat Autònoma de Barcelona, 2019.

[33] M. Pešić, “Biocatalyst and bioprocess engineering for the synthesis of aminopolyols by enzymatic oxidation and aldol addition,” Universitat Autònoma de Barcelona, 2012.

[34] N. Alcover, A. Carceller, G. Álvaro, and M. Guillén, “Zymobacter palmae pyruvate decarboxylase production process development: Cloning in Escherichia coli, fed-batch culture and purification,” *Eng. Life Sci.*, vol. 19, no. 7, pp. 502–512, 2019.

[35] A. D. Gounaris, I. Turkenkopf, S. Buckwald, and A. Young, “Pyruvate decarboxylase - Protein dissociation into subunits under conditions in which thiamine pyrophosphate is released,” *J. Biol. Chem.*, vol. 246, no. 5, pp. 1302–1309, 1971.

[36] D. Gocke *et al.*, “Comparative characterisation of thiamin diphosphate-dependent decarboxylases,” *J. Mol. Catal. B Enzym.*, vol. 61, pp. 30–35, 2009.

[37] S. König, M. Spinka, and S. Kutter, “Allosteric activation of pyruvate decarboxylases. A never-ending story?,” *J. Mol. Catal. B Enzym.*, vol. 61, no. 1–2, pp. 100–110, 2009.

7. Application of immobilized Enzymes in chiral amine synthesis by TA and PDC

7.1. Introduction

Making a final review of the present thesis, different aspects of a biocatalytic process development can be observed through the chapters. After obtaining the necessary enzymes, with the development of a new strain and its cultivation process in the case of PDC, their characterization was carried out. A well understanding of the enzymes is an essential initial step to appropriately plan reaction conditions and to take into account all conditions that the enzymes need to effectively work. In the asymmetric chiral amine synthesis mechanism studied in this work, the needs of both TA and PDC had to be taken into account. In that sense, cofactor role on both TA and PDC stability and reaction mechanisms is one of the main factors that should be considered. Transaminases are PLP-dependent enzymes which catalyze the transfer of an amino group from an amino donor to an amino acceptor [1]–[6], in this particular case, from alanine to 4-PB or AP, which are the ketonic substrates of the target reactions. Therefore, besides important aspects such as reaction conditions, another factor to take into account was the inclusion of PLP, even though its repercussion on reaction mechanism was initially not deeply studied. On the other hand, PDC is a TPP and Mg^{2+} ion-dependent enzyme that catalyzes the non-oxidative decarboxylation of pyruvate to acetaldehyde and carbon dioxide [7]–[12]. In this case, it is responsible of removing the produced pyruvate during transamination from the medium in order to force an equilibrium shift that allowed a propper chiral amine synthesis. As it was already described, cofactors in PDC are pH-dependently bounded at the interface of the PDC subunits and have a major role on the catalytic mechanism [10], [13]–[15]. For this reason, studies considering cofactor repercussion on PDC activity were already performed during Chapter 4.

After the first characterizations, which allowed the election of the transaminases to work with, as well as the establishment of compromise conditions between TA and PDC, reactions were deeper studied and some optimizations were proposed. However, one of the major drawbacks that hampered the yield improvement was the low operational stability presented by transaminases. For this reason, it would be important to analyze which mechanisms are mainly involved on activity loss during reaction. Since the used transaminases are active in a dimer form and they require the coordination of PLP in the active site to perform transaminations [16], [17], activity loss during reaction could be related both to conformational changes and to its

relationship with the cofactor. Regarding conformational destabilization, dissociation of enzyme subunits has been identified as a first deactivation step. Then, the second step involves changes in their tertiary structure [18], [19]. Therefore, to maintain enzyme stability, a first target is to maintain enzyme conformational structure. One approach, which was already carried out during chapter 5, is to apply medium engineering and search additives that protect multimeric proteins against stress-induced dissociation [17], [18]. Even though in some cases process metrics were improved by adding glycerol into the reaction medium, operational stability could be still improved. For this reason, it was decided to immobilize enzymes (see chapter 6), since immobilization represents another widely used strategy for protein stabilization [20]. Covalent immobilization was chosen because attaching proteins to a rigid support through covalent bounds should prevent the mentioned conformational changes, as well as reduce enzyme leaking [21]–[24].

On the other hand, to understand the role of cofactor PLP on operational stability, it is interesting to focus on the mechanism of transaminations. As it was already introduced in Chapter 2, transamination reaction is divided in two half reactions: oxidative deamination of the amino donor and reductive amination of the amine acceptor [1], [3]. PLP, which is linked to an active site lysine through a Schiff base, acts as a molecular shuttle transporting the amino group [16], [25]–[29]. This cofactor is firstly aminated resulting in the formation of pyridoxamine-5'-phosphate (PMP), while the respective keto product of the amino donor is released [3], [28], [30], [31]. After that, the amino group from PMP is transferred to the acceptor molecule producing the aminated product and regenerating PLP for the next catalytic cycle [28], [30]. Whereas PLP is covalently bound to the active site, the intermediate PMP interacts with the apoenzyme via non-covalent interactions. Therefore, dissociation constant of E:PMP is much higher than E-PLP [26]. According to Börner 2016 [16] the stability problem is related to the formation of this mentioned dissociation of the enzyme and PMP. The formed apoenzyme presents an increased tendency of unfolding and irreversible inactivation through aggregation. Besides conformational changes prevention, immobilization also supposes a powerful tool against the mentioned aggregation, since the protein rigidifying that it provides avoids the interaction between unfolded enzymes.

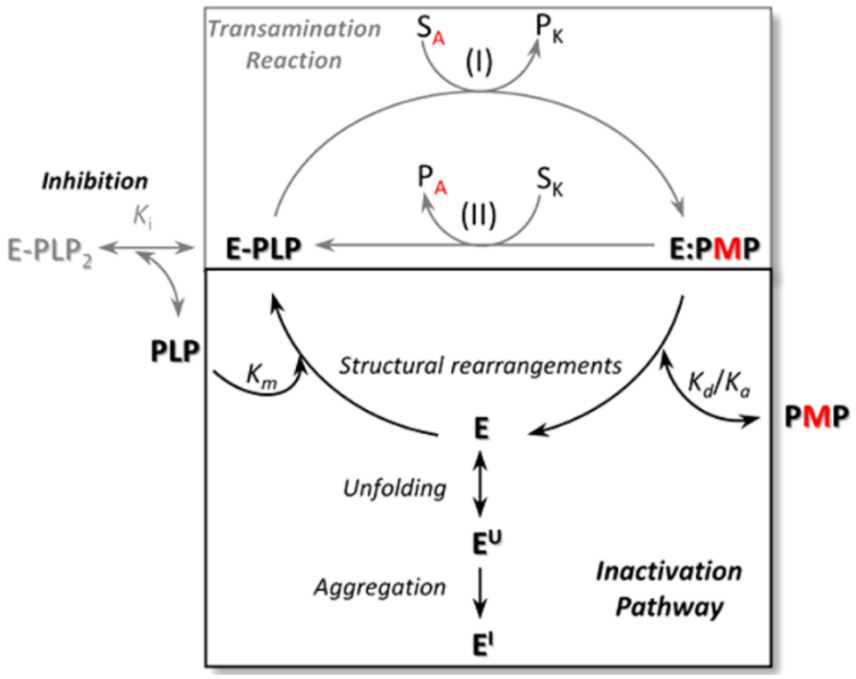

Figure 7.1 Transaminase deactivation mechanism during reaction proposed by Börner 2016. Part of the PMP dissociates from the enzyme. Some of the formed apoenzyme can associate again with PLP, but part of it suffers an unfolding that leads to irreversible aggregation. Source: Börner 2016 [16].

In this final thesis chapter, immobilized derivatives obtained during chapter 6 will be applied in reaction to test its efficiency on operational stability enhancement. In addition, the availability of a PDC immobilized derivative opens doors to plan a new process strategy based on recycling the biocatalysts for several reaction cycles. As it was introduced in chapter 6, widely accepted advantages of immobilization include easy separation from reaction mixture, which, in addition to facilitate product recovery and purification, also allows enzyme reutilization [20], [21], [30], [32], [33].

7.2. Materials and methods

7.2.1. Chemicals and enzymes

All chemicals were purchased from Sigma-Aldrich (St. Louis, MO, USA). Transaminases from *Chromobacterium violaceum* (Cvi-TA) and *Vibrio fluvialis* (Vfl-TA) were kindly donated by DSM/InnoSyn in the form of *Escherichia coli* cell-free extracts (CFE), containing between 40 and 55 mg·mL^{-1} of total protein. In the case of CFE of Cvi-TA, around 47 % of the total protein was transaminase, while this percentage was 35 % for Vfl-TA. Pyruvate decarboxylase (PDC) from

Zymobacter palmae was produced by high cell density cultures of a recombinant *E. coli* strain as it has been described in Chapter 3. CFEs of this strain were obtained by sonication with a Vibracell® VC50 (Sonic and Materials®, Newton, CT, USA) with four times 15 s pulses (50 W) and 2 min intervals in ice between each pulse. Centrifugation was performed (10000 g, 10 min) to remove the resulting cell debris. ZpPDC CFEs contained 10 mg· mL^{-1} of total protein, from which around 40 % was PDC. Amino functionalized agarose 4 BCL (MANA-agarose) was purchased from Agarose Bead Technologies® (ABT®, Madrid, Spain). Epoxy-agarose was functionalized as it will be further described using commercial agarose from Agarose Bead Technologies® (ABT®, Madrid, Spain).

7.2.2. Immobilization methods

7.2.2.1. TA immobilization in MANA-agarose

TA immobilization in MANA-agarose was carried out according to the studies performed in chapter 6. In the case of both Cvi-TA and Vfl-TA, immobilization was performed in potassium phosphate buffer 50 mM and pH 6.2 containing 1 mM PLP; and immobilization mixtures consisted of 10 % MANA-agarose in respect to the entire volume. After washing the support with the immobilization buffer, a volume of 1 mL of CFE per mL of MANA-agarose and the mentioned immobilization mixture was incubated at 25ºC and mild agitation conditions to perform a first ionic attachment phase. Samples were taken periodically to measure supernatant, suspension and blank activities. When no variations were detected in the supernatant activity, covalent attachment was forced by adding N-(3-Dimethylaminopropyl)-N'-ethylcarbodiimide (CDI) at a final concentration of 25 mM and incubated during 2 hours at the same conditions. After that, NaCl was added at 250 mM final concentration and incubated one hour more to remove the enzyme that did not form covalent bounds.

7.2.2.2. TA immobilization in epoxy-agarose

Immobilizations in epoxy-agarose were also performed according to the results obtained during chapter 6. Previously to immobilization, agarose beads 6 % BCL were epoxy-functionalized according to the group protocols, consisting in mixing, in a 1:1:1 proportion, agarose beads with a 0.6 M solution of NaOH and 1,4-butanediol diglicidyl ether with the presence of 2 mg·mL^{-1}

$NaBH_4$; and incubating it during 8 hours at 25ºC and mild agitation. After washing it with abundant distillate water, a support with around 80 mmol epoxy·g^{-1} was obtained. Immobilization was carried out in potassium phosphate buffer 1 M and pH 8 containing 1 mM PLP. Immobilization mixtures consisted of 10 % epoxy-agarose in respect to the entire volume and 1 mL of Cvi-TA/Vfl-TA CFE was offered per mL of epoxy-agarose. These mixtures were incubated at 25ºC and mild agitation. Samples of supernatant, suspension and blank were taken periodically to measure enzyme activities. When no variation was detected in the supernatant activity, 0.2 M of 2-mercaptoethanol was added and it was incubated during 4 hours at 4ºC to block the epoxy groups that had not reacted with any protein-surface group.

7.2.2.3. PDC immobilization in MANA-agarose

PDC was immobilized following the simultaneous purification and immobilization developed during chapter 6. A first ionic attachment phase was carried out in acetate buffer 50 mM and pH 5; and 2000 U PDC per mL of support were offered. After a 2 hours incubation at 25ºC and mild agitation, supernatant was removed and the obtained derivative was washed with acetate buffer 50 mM and pH 5 to remove the proteins that had not been attached to the support. Then, supernatant was replaced by potassium phosphate buffer 50 mM and pH 6.2 containing 25 mM CDI to start covalent bound formation phase. After one hour incubation, 1 M NaCl was added and the mixture was incubated one more hour to remove protein non-covalently linked to MANA-agarose.

7.2.3. Reactions with immobilized enzymes

All biocatalytic reactions were performed in potassium phosphate buffer 150 mM and pH 7.5 containing 1 mM pyridoxal 5'-posphate (PLP), 0.1 mM thiamine pyrophosphate (TPP) and 0.1 mM $MgCl_2$. Reactions were adjusted to contain the same TA concentration in mg TA per mL reaction as when free enzymes were used in chapter 5 (1.52 mg·mL^{-1} in Cvi-TA case; 1.16 mg·mL^{-1} in Vfl-TA case). When only immobilized TA was used, it was coupled with 25 % v v^{-1} PDC cell lysate. In the case of using both enzymes immobilized, the corresponding immobilized PDC volume was added so that derivatives volume did not suppose more than 10 % v v^{-1} of the entire reaction mixture. Before applying the immobilized derivatives in reaction, they were saturated with PLP, to avoid the undesired attachment of the reaction cofactor neither to MANA-agarose nor to epoxy-agarose.

Reactions took place in screw-capped 30 mL bottles with a 10 mL working volume and they were agitated in an orbital shaker at 30ºC and 300 rpm. Reactant concentrations were 10 mM ketonic substrate (4-PB or AP) and 200 mM alanine.

7.2.4. Analytical methods

7.2.4.1. Transaminase activity assay

Transaminase activity assay was based on the acetophenone formation measurement at 340 nm and 30ºC from α-Methylbenzylamine and pyruvic acid. The assay was performed in 1 mL reaction mixture, consisting of potassium phosphate buffer 100 mM and pH 7.5 containing 0.1 mM PLP, 22.5 mM α-Methylbenzylamine and 5 mM sodium pyruvate. To measure the activity in samples where the enzyme was immobilized, the total assay volume was doubled. Coefficient of molar extinction (ε) of acetophenone is 0.28 $mM^{-1} \cdot cm^{-1}$ and one transaminase activity unit corresponds to the amount of enzyme that produces 1 μmol acetophenone per minute at 30ºC. Absorbance measurements were performed using a SPECORD® 200 PLUS (Analytik Jena) spectrophotometer. For measurements with immobilized enzymes, magnetic agitation provided by the same equipment was used.

7.2.4.2. Pyruvate decarboxylase activity assay

PDC activity was determined by coupling the pyruvate decarboxylation with alcohol dehydrogenase (ADH) and following NADH oxidation at 340 nm and 25ºC, whose coefficient of molar extinction (ε) is 6.22 $mM^{-1} \cdot cm^{-1}$. The reaction mixture contained 33 mM sodium pyruvate, 0.11 mM NADH, 3.5 $U \cdot mL^{-1}$ ADH from *Saccharomyces cerevisiae* (Sigma-Aldrich), 0.1 mM TPP and 0.1 mM $MgCl_2$ in citrate buffer 200 mM and pH 6. To determine the activity of immobilized samples, total assay volume was doubled. One unit of PDC activity corresponds to the amount of pyruvate decarboxylase that converts 1 μmole of pyruvate to acetaldehyde per minute. Absorbance measurements were performed using a SPECORD® 200 PLUS (Analytik Jena) spectrophotometer. In the case of samples where the enzyme was immobilized, magnetic stirring provided by the same equipment was used.

7.2.4.3. Total protein content

Total intracellular protein content present in samples was determined with the Bradford Method using Coomassie Protein Assay Reagent Kit (Thermo Scientific®) and Bovine Serum Albumin (BSA) as standard. The assays were performed in 96-microwell plates and Thermo Scentific® Multiskan FC equipment was used for the absorbance reading. Analyses were carried out in duplicate.

7.2.4.4. SDS-Page electrophoresis

To determine the percentage of enzyme among the rest of intracellular soluble proteins present in the samples, a NuPAGE electrophoresis system (Invitrogen®, Carlsbad, CA, USA) was used. Lysates were obtained as previously described. A volume of 10 µL sample was mixed with 5 µL *NuPAGE™ LDS Sample Buffer* (4X), 2µL *NuPAGE™ Reducing Agent* (10X) and 3 µL deionized water. After 10 min incubation at 70ºC samples were charged to NuPAGE 12 % Bis-Tris electrophoresis gel and it was run using MES-SDS as running buffer at 200 V during 40 minutes. After that, the gel was fixed with a solution containing 40 % v v^{-1} and 10 % v v^{-1} acetic acid in water and stained with *Bio-Safe™ Coomassie Stain* (BIO-RAD). Pictures were taken with a *Gel Doc EZ Imaging System* (Bio-Rad®) and analyzed with *Image Lab™ 6.0 Software* (Bio-Rad®).

7.2.4.5. Ketonic substrates and amines analysis by HPLC

All amine and ketonic substrates concentrations were measured by HPLC analysis in an UltiMate 3000 (Dionex) equipped with a variable wavelenght detector. Compounds were separated on a reversed-phase CORTECS C18+ 2.7 µm 4.6× 150 mm column (Waters Milford, MA, USA). After acidifying reaction samples with 3 M hydrochloric acid to deactivate the enzymes, 15 µL were injected at a 0.7 mL·min^{-1} flow rate and 30ºC. In the case of 4-PB to 3-APB reaction, samples were eluted using a gradient from 30 to 55 % solvent B —consisting of 0.095 % (v v^{-1}) in MeCN/H_2O 4:1 (v v^{-1}) — to solvent A — consisting of 0.1 % (v v^{-1}) TFA in H_2O— over 13 minutes and compounds were detected at a 254 nm wavelength. In the case of AP to 1-PEA the gradient started at 15 % solvent B instead of 30 % and compounds were detected at a 210 nm wavelength.

7.3. Results and discussion

7.3.1. Effect of immobilization on TA operational stability

Aiming to test if immobilization is useful to enhance TAs operational stability, the previously obtained immobilized transaminase derivatives (see chapter 6) were tested in reaction. In order to ensure that all the possible changes on results were due to TA immobilization, reactions were carried out with free PDC. A key point to obtain comparable results was to apply the same enzymatic load as in reactions with the free enzyme. Because of the high variability of transaminase activity due to their hyperactivation through the time, the mentioned comparison was carried out in terms of mg TA per mL reaction instead of units per mL. In Table 7.1, a summary of calculations performed to obtain the % of derivative to apply in each case is shown. As it has been mentioned in previous chapters (see chapter 4 and 5) all the reactions with free enzymes were carried out applying a 5% v v^{-1} of the CFEs. Taking into account the total protein concentration of the CFEs (Cvi-TA 64.94 mg·mL^{-1}; Vfl-TA 65.52 mg·mL^{-1}) and their TA content (Cvi-TA 46.83 %; Vfl-TA 35.33 %), it was estimated that the transaminase concentration in reactions with free enzymes was 1.52 mg·mL^{-1} in the case of Cvi-TA and 1.16 mg·mL^{-1} in the case of Vfl-TA. Considering the TA load of each derivative, already obtained in chapter 6 and presented again in Table 7.1, the % of immobilized TA to apply in each case was calculated and presented in the last column. In all cases, the percentage ranged between 5 and 9 %. However, it must be mentioned that the TA percentage to apply is always higher in the case of epoxy-agarose, since lower TA amounts could be loaded in this kind of support.

Table 7.1 Percentage of immobilized TA to apply in reactions and data used to calculate it in each case. [free TA] corresponds to TA concentration (mg/mL) in reactions previously performed using free enzymes. TA load is the TA content of each immobilized derivative expressed in mg TA per mL of each support used. [Derivative] corresponds to the derivative concentration in % v v^{-1} to apply in each case to obtain a reaction mixture with the same mg TA per mL as in reactions with free enzymes.

Enzyme	[free TA] (mg·mL^{-1})	Immobilization method	TA load (mg TA·mL support^{-1})	[Derivative] (% v v^{-1} reaction)
Cvi-TA	1.52	MANA-agarose	22.14	6.9
		epoxy-agarose	17.33	8.8
Vfl-TA	1.16	MANA-agarose	20.33	5.7
		epoxy-agarose	16.62	6.9

7.3.1.1. Synthesis of 3-APB using immobilized transaminases and free PDC

Synthesis of 3-APB reaction was the first to be tested using Cvi-TA and Vfl-TA immobilized both in MANA-agarose and epoxy-agarose; and ZpPDC in the free form. All reaction conditions were maintained, including % v v^{-1} of PDC, in exception of the % in volume of immobilized transaminase, already explained. As it was already mentioned, immobilization may prevent subunit dissociation, which has been defined as a first step on enzyme inactivation [18]. In addition, protein rigidifying produced during immobilization may also be highly effective on stability improvement, since it prevents the loss of protein assembly [19]. Finally, enzyme immobilization may also protect the previously explained TA coordination with the cofactor PLP or, at least, reduce the bibliographically described conformational changes produced during its loss [16], [17].

As it can be observed in Figure 7.2 A, immobilizing Cvi-TA both in MANA-agarose and epoxy-agarose did not have any significant repercussion on 3-APB synthesis. Reactions took place with similar initial rates as in the case of using free enzymes (4.95 $mM \cdot h^{-1}$ free TA; 4.42 $mM \cdot h^{-1}$ TA in MANA-agarose; 4.99 $mM \cdot h^{-1}$ TA in epoxy-agarose). In the same way, similar operational stability profiles were obtained (see Figure 7.2 B) and Cvi-TA activity suffered a sharp decrease in all cases that resulted in enzyme deactivation in 4 hours.

Regarding reactions performed with immobilized Vfl-TA, as it is shown in Figure 7.2 C, 3-APB synthesis took place with lower reaction rates than with free transaminase (2.83 $mM \cdot h^{-1}$ free TA; 0.80 $mM \cdot h^{-1}$ TA in MANA-agarose; 0.52 $mM \cdot h^{-1}$ TA in epoxy-agarose), which enlarged reaction time from 8 hours to 24 h. Moreover, at the end, around 25 % lower 3-APB concentrations were reached (5.92 mM free enzyme; 4.83 mM in MANA-agarose; 4.37 mM in epoxy-agarose). These reaction rate decreases led to the conclusion that, even though the same Vfl-TA mg per mL reaction was used all time, when the enzyme was immobilized, less activity was being applied. The lower activity could be both associated to a partial enzyme deactivation during immobilization or to diffusional limitations. However, it was not possible to detect the mentioned limitations because of the TA hyperactivation observed during immobilization time-courses (see chapter 6). Focusing on operational stability (Figure 7.2 D), in the case of Vfl-TA immobilized in epoxy-agarose, the same profile as in the reaction with free enzymes was obtained. However, when Vfl-TA immobilized in MANA-agarose was used, the initial hyperactivation did not take place and deactivation started at the beginning of the reaction. It must be mentioned that, even though reaction rate decreased after 8 hours, at this time and until the end, deactivation kept taking place, which may be associated to the presence of

undesired-side reactions catalyzed by the transaminases. For instance, it has been described that Vfl-TA may use the produced acetaldehyde and the alanine excess to produce ethanamine [34]. By-product formation may have been the major responsible of the activity loss from the time in which 3-APB synthesis rate started to decrease until the end.

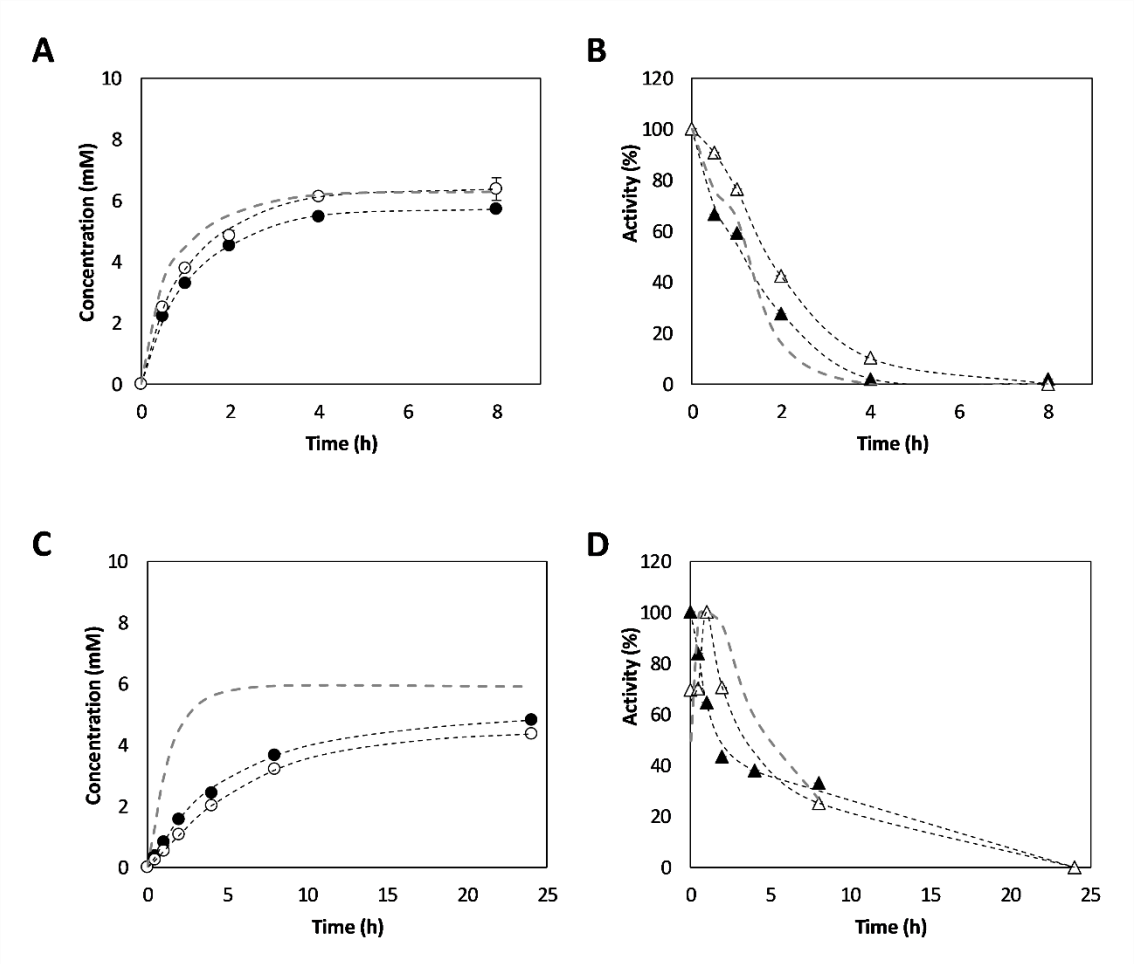

Figure 7.2 Effect of immobilizing transaminases on 3-APB synthesis by the cascade reaction of TA and PDC. A) and C) show 3-APB concentration towards time in the cascade reactions performed with Cvi-TA (A) or Vfl-TA (C) immobilized in MANA-agarose (●) and in epoxy-agarose (○). B) and D) show operational stability of Cvi-TA (B) and Vfl-TA (D) immobilized in MANA-agarose (▲) and in epoxy-agarose (△). The dotted grey lines correspond to the results obtained during reactions with free transaminase in all cases. Temperature 30 ^{o}C; pH 7.5; 4-PB 10 mM; Alanine 200 mM; PDC in CFE form 25 % v v^{-1}.

Final process metrics of all the performed reactions with immobilized TA derivatives are summarized in Table 7.2 and compared with the results obtained during reactions with free enzymes. In the case of Cvi-TA, only slightly lower conversion and yield results were obtained when this transaminase was immobilized in MANA-agarose, but the differences were not

considered significant since they did not arrive to 10 % neither in comparison with reaction with free enzymes nor with Cvi-TA immobilized in epoxy-agarose. Also the same selectivity percentages were reached in all cases. Despite the TA immobilization, it must be taken into account that PDC was still applied in CFE form, therefore reaction mixture complexity did not decrease enough to see any repercussion on selectivity. Finally, STY and BY were also maintained in all immobilization forms, since reaction time was the same in all cases and reaction had the same Cvi-TA content in mg respectively.

Table 7.2 Process metrics of 3-APB synthesis by the cascade reaction of immobilized TA and free PDC. Final 3-APB concentration, conversion, yield, selectivity, space-time yield (STY) and biocatalyst yield (BY) of the cascade reactions performed with Cvi-TA or Vfl-TA immobilized both in MANA-agarose and epoxy-agarose and free PDC. Temperature 30 ºC; pH 7.5; 4-PB 10 mM; Alanine 200 mM; PDC in CFE form 25 % v v^{-1}.

Transaminase	Immobilization method	Final [APB] (mM)	Reaction time (h)	Conversion (%)	Yield (%)	Selectivity (%)	STY ($mmol \cdot L^{-1} \cdot h^{-1}$)	BY ($mmol \cdot mg\ TA^{-1}$)
Cvi-TA	free enzyme	6.20 ± 0.98	8	72.04 ± 3.12	64.22 ± 10.14	88.70 ± 10.24	0.78 ± 0.12	5.01 ± 0.79
	MANA-agarose	5.70 ± 0.03	8	61.93 ± 0.08	54.60 ± 0.27	88.17 ± 0.54	0.71 ± 0.00	4.60 ± 0.02
	epoxy-agarose	6.38 ± 0.37	8	73.59 ± 0.38	61.31 ± 2.35	83.34 ± 3.63	0.79 ± 0.05	5.15 ± 0.30
Vfl-TA	free enzyme	5.92 ± 0.64	8	71.03 ± 2.99	60.77 ± 6.58	86.10 ± 12.89	0.74 ± 0.08	8.61 ± 0.93
	MANA-agarose	4.83 ± 0.02	24	47.48 ± 0.90	43.34 ± 0.16	91.32 ± 1.40	0.20 ± 0.00	7.02 ± 0.03
	epoxy-agarose	4.37 ± 0.11	24	50.54 ± 0.54	42.05 ± 1.04	83.19 ± 1.17	0.18 ± 0.00	6.35 ± 0.16

Regarding reactions performed with Vfl-TA, significant changes were observed when this enzyme was immobilized, but it was no difference between immobilizing it in MANA-agarose or in epoxy-agarose. Conversions with immobilized Vfl-TA were around 50 % while yields of approximately 40 % were reached. These values supposed respectively 0.3-fold and 0.25-fold lower values in comparison with reactions with free Vfl-TA (around 70 % conversion and 60 % yield). As in the case of Cvi-TA, selectivity values did not suffer significant changes, which was associated to the same reasons explained before. However, due to the increase on reaction time when Vfl-TA was immobilized (from 8 to 24 h), STY reached both with MANA-agarose and epoxy-agarose was around 0.20 $mmol \cdot L^{-1} \cdot h^{-1}$, which represents the approximately 30 % of the STY achieved with free Vfl-TA. Finally, the 25 % lower final concentration obtained with immobilized derivatives, led to the same decrease on BY, since reactions were adjusted to contain equivalent TA concentration in mg per mL reaction.

7.3.1.2. Synthesis of 1-PEA using immobilized transaminases and free PDC.

In the same way, the effect of immobilizing TA on operational stability was also tested in 1-PEA synthesis. During the preliminary transaminase screening in chapter 4, only Vfl-TA was selected for this reaction and CviTA was discarded since no significant 1-PEA synthesis was detected using this enzyme. In Figure 7.3 reaction time courses are shown, as well as operational stability profiles. As it happened in the case of 3-APB synthesis, reaction took place with lower reaction rates when Vfl-TA was immobilized (0.65 $mM \cdot h^{-1}$ free Vfl-TA; 0.45 $mM \cdot h^{-1}$ in MANA-agarose; 0.47 $mM \cdot h^{-1}$ in epoxy-agarose), suggesting again that immobilized derivatives were less active than the free form (see section 7.3.1.1). Even though this time the lower rates did not enlarge reaction time, at the end, around 50 % lower 1-PEA concentrations were reached in comparison with the reaction performed with free transaminase (5.13 mM free Vfl-TA; 2.43 mM in MANA-agarose; 2.28 mM in epoxy-agarose). Regarding stability profiles (Figure 7.3 B), a negative repercussion of immobilization on operational stability was observed. While, in reactions with free enzymes, Vfl-TA suffered an initial hyperactivation of around 4 hours and then progressively lost its activity, when the immobilized derivative in MANA-agarose was used, the enzyme started at its maximum activity and sharply lost it in around four hours. Deactivation rate was even higher in reactions of Vfl-TA immobilized in epoxy-agarose. In this case, as it happened during 3-APB synthesis, the initial hyperactivation occurred but it did much faster than with free enzymes, since the maximum activity was reached after half an hour and TA completely lost its activity after 2 hours.

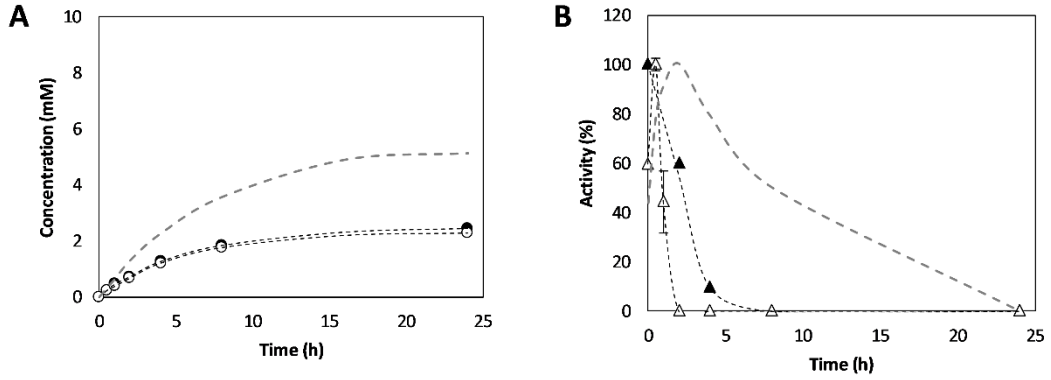

Figure 7.3 Effect of immobilizing Vfl-TA on 1-PEA synthesis by the cascade reaction of TA and PDC. A) 1-PEA concentration towards time in the cascade reactions performed with Vfl-TA immobilized in MANA-agarose (●) and in epoxy-agarose (○). B) Operational stability of Vfl-TA immobilized in MANA-agarose (▲) and in epoxy-agarose (△). The dotted grey lines correspond to the results obtained during reactions with free transaminase in all cases. Temperature 30 °C; pH 7.5; 4-PB 10 mM; Alanine 200 mM; PDC in CFE form 25 % v v^{-1}.

As it is shown in Table 7.3, the lower final 1-PEA concentrations reached with immobilized Vfl-TA lead to around 50% reductions in conversion and yield in comparison with reactions with free enzymes, both by immobilizing with MANA-agarose and with epoxy-agarose. However, selectivity was maintained and even a slightly more than 10 % increment was observed in reactions catalyzed by the MANA-agarose derivative. In the same way conversion and yield decreased, also STY and BY suffered a 50 % reduction in comparison with free enzymes, since reaction time and enzyme concentration in mg per mL were the same when both MANA-agarose and epoxy-agarose derivatives were used.

Table 7.3 Process metrics of 1-PEA synthesis by the cascade reaction of immobilized Vfl-TA and free PDC. Final 1-PEA concentration, conversion, yield, selectivity, space-time yield (STY) and biocatalyst yield (BY) of the cascade reactions performed with Vfl-TA immobilized both in MANA-agarose and epoxy-agarose; and free PDC. Temperature 30 °C; pH 7.5; 4-PB 10 mM; Alanine 200 mM; PDC in CFE form 25 % v v^{-1}.

Immobilization method	Final [PEA] (mM)	Conversion (%)	Yield (%)	Selectivity (%)	STY ($mmol \cdot L^{-1} \cdot h^{-1}$)	BY ($mmol \cdot mg\ TA^{-1}$)
free enzyme	5.13 ± 0.01	67.75 ± 0.87	48.51 ± 0.06	71.61 ± 0.84	0.21 ± 0.00	7.47 ± 0.01
MANA-agarose	2.43 ± 0.01	30.74 ± 1.38	25.55 ± 0.34	83.27 ± 4.84	0.10 ± 0.00	3.53 ± 0.01
epoxy-agarose	2.28 ± 0.07	36.79 ± 2.49	26.56 ± 1.09	72.72 ± 7.88	0.10 ± 0.00	3.32 ± 0.10

After having synthesized the both target chiral amines (3-APB and 1-PEA) with transaminases immobilized in MANA-agarose and epoxy-agarose, it was concluded that the same results can be obtained independently from the immobilization method. For this reason, it was decided to select one of the two immobilization methods for further studies. MANA-agarose was prioritized for two main reasons. On the one hand, as it was previously described, lower amounts of this derivative are required to achieve the same results since its enzymatic load is higher (Table 7.1). On the other hand, in chapter 6, it was observed that it was not possible to immobilize ZpPDC in epoxy-agarose but it was in MANA-agarose. In the point of view of possible future coimmobilization approaches, MANA-agarose is the method that would allow to simultaneously immobilize the both enzymes of the cascade.

7.3.2. Effect of PLP on TA operational stability

As it was observed in the previous section, immobilizing transaminases do not suppose any relevant improve on operational stability. Moreover, MANA-agarose was selected as the most adequate immobilization method because, as it was already explained, less derivative percentage is required for the same results with epoxy-agarose and because PDC could only be immobilized with this method. As it has been commented, enzyme activity loss during reaction can be associated to several mechanisms. In the specific case of TAs, cofactor PLP, which is essential for its transamination activity, can also play a key role on inactivation through reaction. According to Börner 2016 [16], PLP is firmly anchored in the TAs, active center formed by amino acids proceeding from both subunits. However, after the first half-reaction (see chapter Introduction) the enzyme-PMP complex present weaker bounds that can be dissociated. Even though coordination between enzyme and PLP can be recovered depending on cofactor availability, when this dissociation occurs, the free enzyme without cofactor, firstly unfolds reversibly and then aggregates irreversibly, which would explain the loss on operational stability. When enzymes are immobilized, aggregation is not possible. Moreover, during reactions performed at section 7.3.1, protein precipitates were never detected, therefore the covalent bounding to the supports supposed an effective immobilization without enzyme leakage. Regarding protein unfolding and enzyme-PMP dissociation, may have been reduced by immobilizing enzymes, but not totally suppressed. For this reason, in the present section, more studies focusing on the role of PLP were performed.

7.3.2.1. Effect of increasing PLP concentration on 3-APB synthesis using immobilized TA

Considering the described hypothesis about TA deactivation by the cofactor loss, new reactions were performed using both Cvi-TA and Vfl-TA immobilized in MANA-agarose. However, at the time in which reactions started to slow down (2 h in Cvi-TA; 4 h in Vfl-TA), PLP additions were performed in order to increase 1 mM its concentration. These additions were repeated every two hours to ensure its availability all the time. As it can be observed in Figure 7.4 A, when the described addition was carried out in reactions catalyzed by Cvi-TA, reaction could be slightly enlarged resulting in a 1.2-fold higher final 3-APB concentration (6.78 mM with PLP additions; 4.83 mM without). In the case of Vfl-TA (Figure 7.4 B), the effect was more difficult to appreciate because of the larger reaction time. However, at the end, also a 1.2-fold increase on final 3-APB concentration could also be observed (5.55 mM with PLP additions; 4.83 mM without).

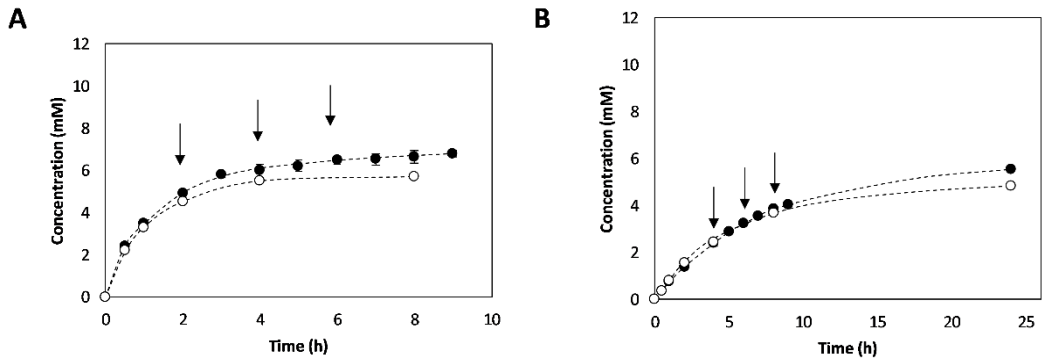

Figure 7.4 Effect of PLP additions on 3-APB synthesis with TAs immobilized in MANA-agarose and free PDC. A) Reactions performed with Cvi-TA. B) Reactions performed with Vfl-TA. (●) Reactions with PLP additions. (○) Reactions without PLP additions. Arrows indicate the times in which 1 mM PLP additions were performed. Temperature 30 °C; pH 7.5; 4-PB 10 mM; Alanine 200 mM; PDC 25 % v v^{-1}.

After detecting that increasing PLP concentration had some effect on 3-APB synthesis, new reactions were prepared but, at this time, they were started at higher PLP concentration. In Figure 7.5, the effect of starting reactions with both transaminases immobilized in MANA-agarose at 5 mM PLP concentration is shown and compared with the previous reactions, in which the initial PLP concentration was 1 mM. Different from the last described strategy, applying higher PLP concentration from the beginning did not have any effect on reactions catalyzed by Cvi-TA (see Figure 7.5 A) and the same profile was obtained. Moreover, in the case of using Vfl-TA (see Figure 7.5 B) a slightly negative effect was observed since reaction took place with lower reaction rate in comparison with using 1 mM PLP (0.56 $mM \cdot h^{-1}$ starting at 5 mM PLP; 0.80 $mM \cdot h^{-1}$ starting at 1 mM PLP) and lower final 3-APB concentration was obtained (4.04 mM starting at 5 mM PLP; 4.83 mM starting at 1 mM PLP). Contradictory effects have been reported on TA activity and stability when using different PLP concentrations, since it was observed that increasing PLP concentration enhances stability but has inhibitory effects that negatively affect productivity [16].

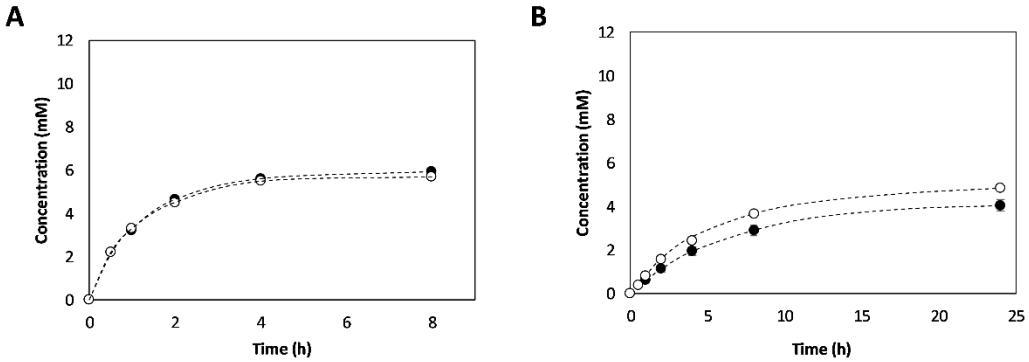

Figure 7.5 Effect of increasing the initial PLP concentration to 5 mM on 3-APB synthesis with TAs immobilized in MANA-agarose and free PDC. A) Reactions performed with Cvi-TA. B) Reactions performed with Vfl-TA. (●) Reactions with 5 mM PLP. (○) Reactions with 1 mM PLP. Temperature 30 ºC; pH 7.5; 4-PB 10 mM; Alanine 200 mM; PDC 25 % v v^{-1}.

A summary of final process metrics obtained in the described reactions with variations concerning PLP is shown in Table 7.4, where are also compared with the results obtained in previous reactions with Cvi-TA and Vfl-TA immobilized in MANA-agarose (see section 7.3.1). In reactions performed with Cvi-TA, as it was already mentioned, PLP additions every 2 hours led to slightly higher 3-APB concentration, reason why the obtained yield is also higher in comparison with the other strategies (61.55 % PLP additions; 54.60 % initial reaction; 56.45 % starting at 5 mM PLP). However, the same conversion as in the other cases was obtained, leading to higher selectivity. Finally, STY was also 1.2-fold higher when PLP additions were performed in respect to the initial reaction and reaction with 5 mM PLP; and BY was also increased, since reactions contained the same mg Cvi-TA per mL all the time. Regarding Vfl-TA case, reaction time was maintained when PLP additions were performed but, as it has been mentioned, the 1.2-fold increase on final 3-APB concentration also took place. In contrast, 15 % lower 3-APB concentration was reached when PLP was increased to 5 mM from the beginning. These variations on final product concentration are reflected on yield values (51.74 % PLP additions; 43.34 % initial reaction; 36.32 % starting at 5 mM PLP), even though the increase on selectivity observed for Cvi-TA in reactions with PLP additions did not take place this time. Moreover, when reaction started with 5 mM PLP selectivity decreased in respect to the other two cases (around 70 % at 5 mM PLP; around 90 % in the other cases), so PLP increase might have enhanced undesired side reactions. This time, STY variations were not that significant, while the expected variations on BY considering the final 3-APB concentrations were obtained.

Table 7.4 Process metrics of 3-APB with TAs immobilized in MANA-agarose and free PDC under different PLP concentrations. Both Cvi-TA and Vfl-TA results are presented at 1 mM PLP concentration, starting at 1 mM and making periodic PLP additions and at 5 mM PLP. Temperature 30 ^{o}C; pH 7.5; 4-PB 10 mM; Alanine 200 mM; PDC 25 % v v^{-1}.

Transaminase	Descritpion	Final [APB] (mM)	Reaction time (h)	Conversion (%)	Yield (%)	Selectivity (%)	STY ($mmol \cdot L^{-1} \cdot h^{-1}$)	BY ($mmol \cdot mg\ TA^{-1}$)
Cvi-TA	1 mM PLP	5.70 ± 0.03	8	61.93 ± 0.08	54.60 ± 0.27	88.17 ± 0.54	0.71 ± 0.00	4.60 ± 0.02
	PLP additions	6.78 ± 0.13	9	61.72 ± 1.06	61.55 ± 1.20	99.79 ± 3.65	0.85 ± 0.02	5.48 ± 0.11
	5 mM PLP	5.93 ± 0.00	8	59.16 ± 4.36	56.45 ± 0.00	95.94 ± 7.07	0.74 ± 0.00	4.79 ± 0.00
Vfl-TA	1 mM PLP	4.83 ± 0.02	24	47.48 ± 0.90	43.34 ± 0.16	91.32 ± 1.40	0.20 ± 0.00	7.02 ± 0.03
	PLP additions	5.55 ± 0.03	24	58.57 ± 1.17	51.74 ± 0.03	88.37 ± 1.71	0.23 ± 0.00	8.07 ± 0,05
	5 mM PLP	4.04 ± 0.26	24	49.38 ± 3.01	36.32 ± 1.84	73.61 ± 0.77	0.17 ± 0.01	5.88 ± 0.38

7.3.2.2. TA activity recovery by a post-reaction PLP incubation

Even though chiral amine synthesis could be slightly enhanced by periodically adding PLP into reaction mixture, the improvement on process metrics was not considered worthy in respect to the higher operation complexity that supposed. However, the obtained results demonstrated that part of the transaminase activity loss was due to PLP dissociation, thus it may be recovered by enzyme incubation with its cofactor after reaction. In previous studies from the same research group, PLP was removed from the PLP-dependent enzyme serine hydroxymethyl transferase (SHMT). After incubating again with different cofactor concentration, an immediate activity recovery of between 60 and 80 % was observed in all cases [35]. To prove the same effect on Cvi-TA and Vfl-TA, the two immobilized derivatives of these transaminases in MANA-agarose were applied in reaction to deactivate them. After that, they were incubated at 25^{o}C and mild agitation in potassium phosphate buffer 150 mM and pH 7.5 containing 0 mM, 1 mM and 5 mM PLP and activity was measured to detect any activity recovery.

In Figure 7.6, % activity recovery in respect to the one before its deactivation during reaction is shown both for the case of Cvi-TA (A) and Vfl-TA (B) at the beginning of their incubation with PLP and after 2 hours incubation. As it can be observed, in both cases some activity could be recovered just by resuspending the immobilized derivatives in fresh buffer, which may be associated to a protein refolding when more optimal conditions in comparison with the ones present at the end of reaction are applied again. In the case of Cvi-TA, 25 % of the initial activity was immediately detected and it increased to 40 % after two hours, while in the case of Vfl-TA around 50 % of the initial activity was detected and it was maintained after the 2 hours incubation. When incubation was carried out with 1 mM PLP, around 60 % of the activity was

immediately detected with Cvi-TA and after 2 h was completely recovered. However, with Vfl-TA, around 90 % of the activity was initially recovered but a slight loss of activity was detected through the time. Finally, hyperactivation was observed in both enzymes when 5 mM PLP was applied. In the case of Cvi-TA, 50 % higher than the initial activity was observed and, at the end, this initial activity was nearly triplicated. In the case of Vfl-TA, the 5 mM PLP enabled an entire activity recovery in immediate form and activity was nearly doubled after 2 hours.

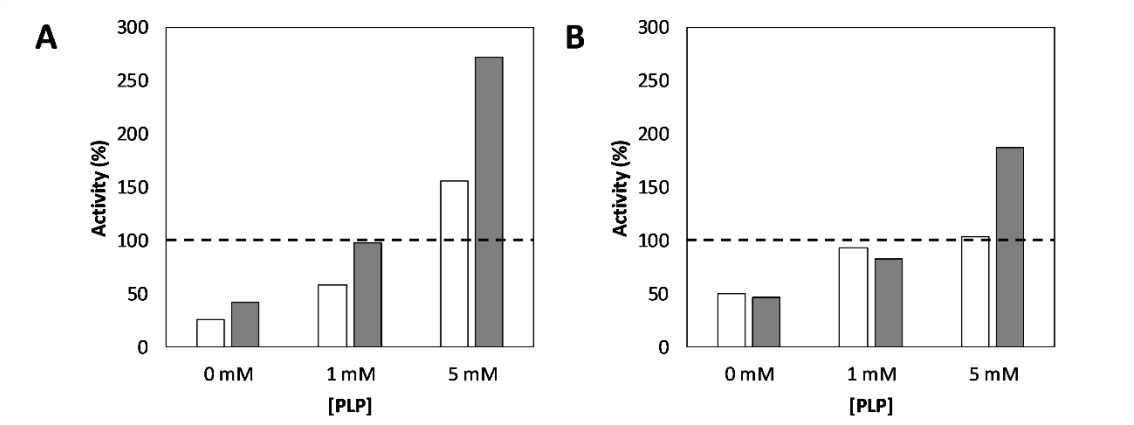

Figure 7.6 Transaminase activity recovery after its total deactivation during reaction by incubation with different PLP concentrations. White bars represent the % activity recovery at the beginning of the incubation (time 0 hours). Grey bars represent the % activity recovery at the end of the incubation (time 2 hours). A) Recovery performed with Cvi-TA. B) Recovery performed with Vfl-TA. Potassium phosphate buffer 150 mM and pH 7.5; temperature 25ºC; mild agitation conditions. To calculate the percentages initial activity before deactivation in reaction was taken as a reference.

After the 2-hours incubations with different PLP concentrations, immobilized derivatives were recovered, washed with potassium phosphate buffer and activity was measured again. As it can be observed in Table 7.5 the obtained activity recoveries for Cvi-TA samples that had been incubated without PLP and with 1 mM PLP agreed with the measured after 2 hours incubation. However, even though with 5 mM PLP the initial activity had been triplicated, after the wash, the double of the initial activity could be observed. In the same line, Vfl-TAs activity recoveries agreed with the obtained at 2 hours incubation in exception of the samples incubated with 5 mM PLP. In this case, while during PLP incubation activity was doubled, after the wash it was only 30% higher than the initial one. Because of the high activity variations typically obtained with transaminases, it was concluded that a two hours incubation of the derivatives after reaction

with PLP had an activity recovery effect, even though this recovery could not be precisely quantified.

Table 7.5 Final transaminase activity recovery after its total deactivation during reaction by incubation with different PLP concentrations. Activities measure after recovering the derivatives from the incubation mixtures and washing them with potassium phosphate buffer 150 mM and pH 7.5. To calculate the percentages initial activity before deactivation in reaction was taken as a reference.

Enzyme	[PLP] (mM)	Activity recovery (%)
Cvi-TA	0	41,7
	1	106,3
	5	198,8
Vfl-TA	0	46,1
	1	91,2
	5	130,8

7.3.3. Chiral amine synthesis with TA and PDC immobilized in MANA-agarose

As it was introduced during chapter 6, immobilization of the enzymes makes them perform as heterogeneous catalysts [22], which provides several advantages on process. On the one hand, using immobilized enzymes allows an operation on continuous [21], [30], [32]. On the other, it enables its efficient and immediate recovery after reaction and enzymatic activity can be exploited in multiple catalytic cycles [36]. In the previous sections it was observed that immobilization itself does not improve TAs operational stability, which supposes a drawback for TA reusability. However, protein retention in a solid support prevents its aggregation avoiding, this way, part of the enzyme irreversible deactivation. Moreover, it was proved that PLP loss play a major role on TA activity loss during reaction. Thanks to immobilization, the enzyme could be recovered after reaction and, by an incubation in the presence of fresh PLP, part of the initial activity could be recovered. These promising results opened doors to perform several reaction cycles, since between each cycle TA activity may be recovered by alternate them with PLP incubation phases. Nevertheless, before this mentioned approach, it was convenient to study the possibility to perform reactions with both TA and PDC immobilized in order to simultaneously reuse both enzymes of the enzymatic cascade.

During section 7.3.1 it was already exposed the way in which reactions were adjusted to contain the same TA amounts in mg per mL reaction as when free enzymes were used. The resulting TA percentages were maintained in this case and the corresponding immobilized PDC percentage to do not surpass a 10% of derivatives in respect to the total reaction volume was added in each case. Using higher derivatives percentages is not considered convenient in order to maintain the medium rheology. Due to this adjustment and considering that the obtained PDC derivatives had around 650 U per mL of MANA-agarose, the final activity per mL of reaction was slightly lower in comparison with reactions performed with free PDC. However it was prioritized to maintain TA concentration, since it was the enzyme that more drawbacks had supposed due to its low operational stability. Decreasing TA concentration was not considered convenient, because in that case an even lower operational stability would have been expectable. In contrast, PDC had not shown significant stability problems neither in reactions with free enzymes nor when TA was immobilized; and equilibrium was always properly shifted, suggesting that PDC was never limiting reactions. Therefore, in reactions performed with Cvi-TA, which contained 6.9 % v v^{-1} of this enzyme, a 3.1 % v v^{-1} of PDC was applied, while in reactions with Vfl-TA, with 5.7 % v v^{-1} of TA, the PDC percentage was 4.3 % vv^{-1}. In addition to the slight reduction on PDC load in reactions, it was detected that, between reactions with immobilized PDC, variation on activity was high. Since the mentioned activity variations did not ensure the same reaction performance as the initial reactions with free enzymes, to perform an adequate comparison, a control reaction was always carried out in parallel. In the mentioned control reactions, carried out with free enzymes, PDC amount was adjusted to have the same U per mL reaction as the immobilized-enzymes reaction case studied every time.

7.3.3.1. Synthesis of 3-APB with both TAs and PDC immobilized

Following the line of all studies performed in the present thesis, the first reaction studied with all the enzymes of the cascade immobilized was 3-APB synthesis. In Figure 7.7, results obtained when reaction was carried out with Cvi-TA are shown. As it can be observed, enzyme immobilization led to a lower initial reaction rate in comparison with the control reaction (1.87 $mM \cdot h^{-1}$ immobilized enzymes; 2.83 $mM \cdot h^{-1}$ free enzymes). However, reaction with free enzymes slowed down before, reason why after 4 hours and until the end of the reactions (8 hours) both profiles were identical. As a result, the same conversion, yield and selectivity were obtained immobilizing or not the enzymes. Therefore, the same final 3-APB concentration was

also obtained (4.1 mM) even though it was lower than the usually obtained in previous reactions (around 6 mM), probably due to the lower PDC activity.

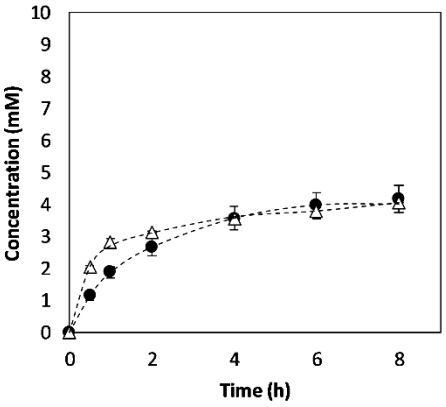

	Free enzymes	Immobilized enzymes
Conversion (%)	50.47 ± 1.55	49.30 ± 4.00
Yield (%)	40.03 ± 0.45	40.23 ± 5.60
Selectivity (%)	79.41 ± 3.33	81.19 ± 4.76

Figure 7.7 Time course synthesis of 3-APB catalyzed by free and immobilized PDC and Cvi-TA. (●) 3-APB synthesis in reactions performed with both enzymes immobilized in MANA-agarose. (△) 3-APB synthesis in control reaction, performed with free enzymes. In the table, conversion, yield and selectivity of both cases are shown. Temperature 30 ^{o}C; pH 7.5; 4-PB 10 mM; Alanine 200 mM. Reaction with immobilized enzymes contained 6.9 % v v^{-1} of immobilized Cvi-TA and 3.1 % v v^{-1} of immobilized PDC. Reaction with free enzymes was adjusted to have the same mg·mL^{-1} TA and the same U·mL^{-1} PDC as the immobilized reaction.

When Vfl-TA was used (Figure 7.8), also a decrease on initial reaction rate was observed (0.59 mM·h^{-1} immobilized enzymes; 1.05 mM·h^{-1} free enzymes). However, at the end, similar final 3-APB concentrations were obtained, even though it was slightly higher in reactions with free enzymes (3.6 mM immobilized enzymes; 3.9 mM free enzymes). Again, probably due to the lower PDC activity, amine concentrations were lower than the obtained during the first reactions with free enzymes. Regarding final conversions and yields, they were again similar immobilizing or not the enzymes due to the similar 3-APB concentrations reached, even though a slight decrease on selectivity was observed in the case of immobilizing the enzymes.

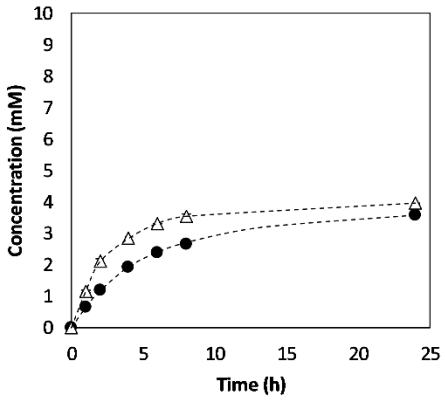

	Free enzymes	Immobilized enzymes
Conversion (%)	43.75 ± 3.62	48.39 ± 1.57
Yield (%)	41.77 ± 4.24	35.68 ± 0.54
Selectivity (%)	95.33 ± 1.81	73.78 ± 1.27

Figure 7.8 Time course synthesis of 3-APB catalyzed by free and immobilized PDC and Vfl-TA. (●) 3-APB synthesis in reactions performed with both enzymes immobilized in MANA-agarose. (△) 3-APB synthesis in the control reaction, performed with free enzymes. In the table, conversion, yield and selectivity of both cases are shown. Temperature 30 ^{o}C; pH 7.5; 4-PB 10 mM; Alanine 200 mM. Reaction with immobilized enzymes contained 5.7 % v v^{-1} immobilized Vfl-TA and 4.3 % v v^{-1} immobilized PDC. Reaction with free enzymes was adjusted to have the same mg·mL^{-1} TA and the same U·mL^{-1} PDC as the immobilized reaction.

A comparison between immobilizing all the enzymes and only immobilizing TA is shown in Table 7.6. Final process metrics of the mentioned cases appear coupled with the reaction with free enzymes taken as a control in each case, since variations were detected when PDC activity was reduced. In general, it could be concluded that immobilization did not suppose any significant variation when Cvi-TA was used, neither only immobilizing Cvi-TA nor immobilizing both enzymes. As it was already commented on section 7.3.1.1, slight differences on process metrics when only Cvi-TA was immobilized were not considered significant because they did not surpass a 10%. The metrics differences were even lower between reactions with all the enzymes of the cascade immobilized and their corresponding control reactions. Probably due to variations on PDC activity, a reduction of final 3-APB concentration from around 6 mM to around 4 mM could be observed when all the enzymes used were immobilized in comparison with only immobilizing TA. As a consequence, all process metrics in exception of selectivity, which was always maintained, suffered an around 30 % reduction.

Regarding Vfl-TA results, as it was already commented in section 7.3.1.1, immobilizing only the TA had a significant effect, since reaction time was enlarged and final 3-APB was reduced from

around 6 mM, in the free form, to around 5 mM, with immobilized TA. These changes were reflected on their corresponding process metrics, as it was discussed in the mentioned section. When all enzymes were immobilized, also a decrease of 3-APB final concentration was observed but the difference between immobilized and free enzymes was not that high as in the previous case. While with only immobilizing transaminase 3-APB concentration was around 20% lower from its control reaction, immobilizing both TA and PDC, the decrease in comparison with the corresponding control was around 10%. Moreover, when reaction with free enzymes contained less PDC activity, reaction time was enlarged to 24 hours, thus the PDC variation had a higher repercussion on reaction than the immobilization of PDC. Therefore, the decrease on process metrics when all enzymes were immobilized in respect to only immobilizing TA were associated to the lower PDC activity.

Table 7.6 Comparison between the effect on 3-APB synthesis metrics of immobilizing only TA and immobilizing both TA and PDC. Both for Cvi-TA and Vfl-TA the corresponding control reactions are presented, consisting in reactions with free enzymes adjusted to contain the same TA in mg·mL^{-1} and the same PDC activity per mL reaction. Temperature 30 °C; pH 7.5; 4-PB 10 mM; Alanine 200 mM.

Transaminase	Descritpion	Final [APB] (mM)	Reaction time (h)	Conversion (%)	Yield (%)	Selectivity (%)	STY (mmol·L^{-1}·h^{-1})	BY (mmol·mg TA^{-1})
Cvi-TA	TA immobilized	5.70 ± 0.03	8	61.93 ± 0.08	54.60 ± 0.27	88.17 ± 0.54	0.71 ± 0.00	4.60 ± 0.02
	Control	6.20 ± 0.98	8	72.04 ± 3.12	64.22 ± 10.14	88.70 ± 10.24	0.78 ± 0.12	5.01 ± 0.79
	TA + PDC immob.	4.16 ± 0.42	8	49.31 ± 4.00	40.23 ± 5.60	81.19 ± 4.76	0.52 ± 0.05	3.36 ± 0.34
	Control	4.04 ± 0.01	8	50.47 ± 1.55	40.03 ± 0.45	79.41 ± 3.33	0.51 ± 0.00	3.26 ± 0.01
Vfl-TA	TA immobilized	4.83 ± 0.02	24	47.48 ± 0.90	43.34 ± 0.16	91.32 ± 1.40	0.20 ± 0.00	7.02 ± 0.03
	Control	5.92 ± 0.64	8	71.03 ± 2.99	60.77 ± 6.58	86.10 ± 12.89	0.74 ± 0.08	8.61 ± 0.93
	TA + PDC immob.	3.57 ± 0.05	24	48.39 ± 1.56	35.68 ± 0.54	73.78 ± 1.27	0.15 ± 0.00	5.19 ± 0.08
	Control	3.94 ± 0.29	24	43.75 ± 3.62	41.77 ± 4.24	95.33 ± 1.81	0.16 ± 0.01	5.73 ± 0.43

7.3.3.2. Synthesis of 1-PEA with both TAs and PDC immobilized

After the studies on 3-APB synthesis, both Vfl-TA and PDC immobilized derivatives were applied on the synthesis of 1-PEA, the other target chiral amine of the present thesis. Reaction profiles of the mentioned reaction case and its corresponding control, as well as a comparison of conversions, yields and selectivities, are shown in Figure 7.9. As it already happened when 3-APB synthesis was performed with Vfl-TA and PDC both immobilized, initial reaction rate was 1.7-fold higher in the control reaction with free enzymes than in reaction with all immobilized (0.40 mM·h^{-1} immobilized enzymes; 0.68 mM·h^{-1} free enzymes). Moreover, as it also happened

in the mentioned 3-APB synthesis case, this time reaction was also not enlarged and ended up with similar final 1-PEA concentration, even though it was slightly higher in control reaction (2.3 mM immobilized enzymes; 2.7 mM free enzymes). Therefore, conversion, yield and selectivity did not suffer any significant changes immobilizing or not the enzymes.

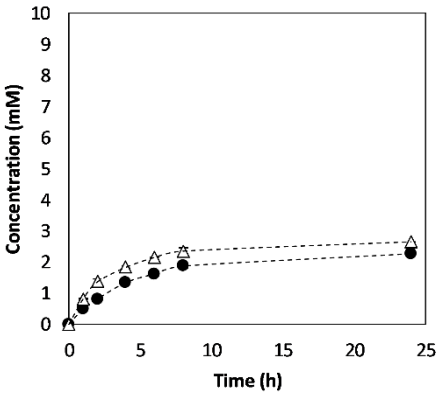

	Free enzymes	Immobilized enzymes
Conversion (%)	30.56 ± 0.02	31.25 ± 0.28
Yield (%)	26.53 ± 0.25	24.29 ± 0.40
Selectivity (%)	86.81 ± 0.75	77.75 ± 2.00

Figure 7.9 Effect of immobilizing both Vfl-TA and PDC on 1-PEA synthesis. (●) Reaction profile of reactions performed with both enzymes immobilized in MANA-agarose. (△) Reaction profile of the control reaction, performed with free enzymes. In the table, conversion, yield and selectivity of both cases are shown. Temperature 30 ^{o}C; pH 7.5; AP 10 mM; Alanine 200 mM. Reaction with immobilized enzymes contained 5.7 % v v^{-1} immobilized Vfl-TA and 4.3 % v v^{-1} immobilized PDC. Reaction with free enzymes was adjusted to have the same mg·mL^{-1} TA and the same U·mL^{-1} PDC as the immobilized reaction.

The comparison between immobilizing only TA and immobilizing also PDC is shown in Table 7.7. For the mentioned comparison, as it was done in the previous section, each reaction results appear coupled with the corresponding control reaction performed with free enzymes and adjusted to contain the same PDC activity per mL reaction. As it happened with 3-APB synthesis, immobilizing the TA had a high repercussion on 1-PEA synthesis, even though reaction time did not increase. As a result, the half of the amine concentration was obtained in comparison with reaction with free enzymes (2.4 mM Vfl-TA immobilized; 5.1 mM free enzymes). However, the same concentration was obtained when all the enzymes were in the immobilized form (2.3 mM), even though in the control with lower PDC concentration the final 1-PEA obtained was around 2.7 mM. Therefore, it is true that PDC reduction could hamper 1-PEA synthesis, but TA immobilization had a higher repercussion, since reaction only immobilizing Vfl-TA contained more PDC and the same results were obtained. Consequently, no variations on process metrics

could be detected between reactions with only Vfl-TA immobilized, with both Vfl-TA and PDC immobilized and with free enzymes but with less PDC activity. The mentioned metrics, in exception of selectivity, which it was maintained in all cases, were reduced to the half in comparison to the initially obtained with reactions in the free form.

Table 7.7 Comparison between the effect on 1-PEA synthesis metrics of immobilizing only TA and immobilizing both TA and PDC. The corresponding control reactions are presented, consisting in reactions with free enzymes adjusted to contain the same TA concentration in mg·mL^{-1} and the same PDC activity per mL reaction. Temperature 30 °C; pH 7.5; AP 10 mM; Alanine 200 mM.

Descritpion	Final [PEA] (mM)	Reaction time (h)	Conversion (%)	Yield (%)	Selectivity (%)	STY (mmol·L^{-1}·h^{-1})	BY (mmol·mg TA^{-1})
TA immobilized	2.43 ± 0.01	24	30.74 ± 1.38	25.55 ± 0.34	83.27 ± 4.84	0.10 ± 0.00	3.53 ± 0.01
Control	5.13 ± 0.01	24	67.75 ± 0.87	48.51 ± 0.06	71.61 ± 0.84	0.21 ± 0.00	7.47 ± 0.01
TA + PDC immob.	2.25 ± 0.02	24	31.25 ± 0.28	24.29 ± 0.40	77.75 ± 2.00	0.09 ± 0.00	3.28 ± 0.02
Control	2.65 ± 0.02	24	30.56 ± 0.02	26.53 ± 0.25	86.82 ± 0.75	0.11 ± 0.00	3.86 ± 0.04

7.3.4. TA and PDC immobilized derivatives application in reaction cycles

After proving that it was possible to perform the cascade reactions with both TA and PDC immobilized in MANA-agarose, the next step was to study the reusability of the mentioned derivatives in several reaction cycles. A key factor for enzyme reusability is operational stability. In this sense, PDC was not considered to suppose any drawback since it had presented a good operational stability through all the different reaction approaches studied in the present thesis. Regarding TA, which presents a low operational stability, it was already proved that, after losing its entire activity, it is possible to recover it by an incubation with fresh PLP (see section 7.3.2.2). Therefore, to perform several reaction cycles, it would be convenient to recover the derivatives and incubate them during 2 hours in a fresh solution of 5 mM PLP in potassium phosphate buffer 150 mM and pH 7.5. Moreover, to obtain results to compare with, control reactions were carried out in parallel, consisting in reactions with free enzymes in which, at the end of each cycle, PLP was also added at 5 mM concentration. After the 2-hour incubation, ketonic substrate was again adjusted to 10 mM to simulate the following cycle. Generally, enzyme derivatives stopped being reused when the obtained yield was lower than 10 %.

7.3.4.1. 3-APB synthesis in reaction cycles with immobilized TA and PDC

In Figure 7.10, reaction cycles with Cvi-TA are shown (graph A) and coupled with the respective control reaction (graph B). As it was expected because of the application of the same conditions, in the first cycle, the same results as in section 7.3.3.1 were obtained, consisting in lower reaction rates than the blank with free enzymes and a final 3-APB concentration of around 4 mM. However, the second cycle took place with around 60% lower reaction rate (1.47 $mM \cdot h^{-1}$ cycle 1; 0.62 $mM \cdot h^{-1}$ cycle 2) and half of the final 3-APB obtained in the first cycle was reached. In the following two cycles, only slight reductions in reaction rates were detected and the differences between the obtained 3-APB amounts were not considered significant (2.02 mM cycle 2; 1.95 mM cycle 3; 1.80 mM cycle 4). Finally, reaction profile varied more significantly in the fifth cycle and around 35% less product was obtained. Even though the differences between cycle 5 and cycle 6 were not that high, enzyme reuse was stopped after the sixth cycle since final 3-APB concentration did not arrive to 1 mM, which would correspond to a 10 % reaction yield. Focusing on the control reaction performed in parallel (see Figure 7.10 B), the same reaction profile as the first cycle was obtained, even though initial rate was slightly higher. After 8 hours, the PLP incubation and the addition of more 4-PB to simulate a second cycle did not suppose more 3-APB synthesis. Therefore, reusing enzymes in several reaction cycles is only possible using them in immobilized form.

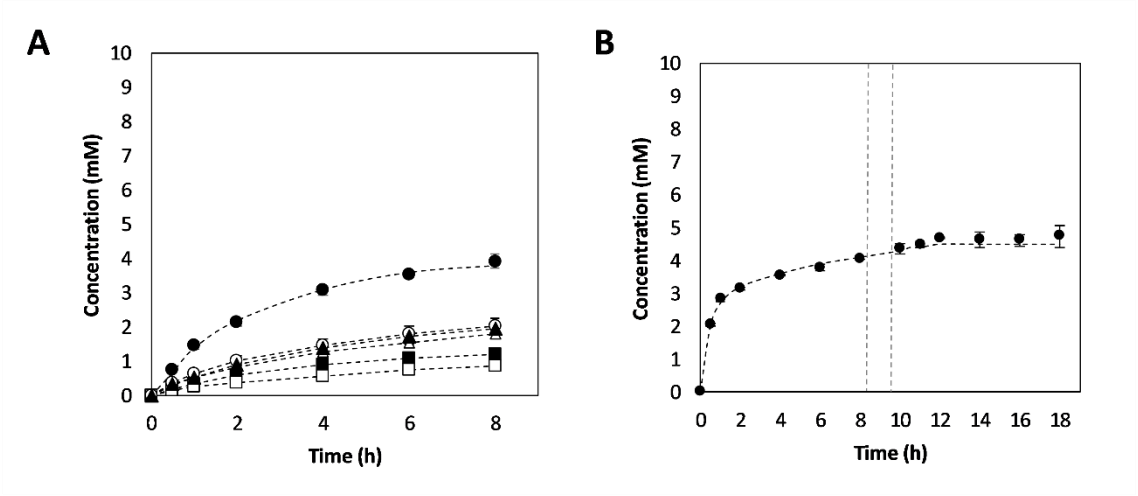

Figure 7.10 Synthesis of 3-APB in several reaction cycles using Cvi-TA and PDC both immobilized in MANA-agarose. A) Reaction profiles through the performed cycles. (●) Cycle 1; (○) Cycle 2; (▲) Cycle 3; (△) Cycle 4; (■) Cycle 5; (□) Cycle 6. B) Reaction profile of the control reaction performed with free enzymes with the same mg TA per mL reaction and U PDC per mL reaction. The second cycle was simulated by adding 5 mM PLP and increasing 4-PB concentration to 10 mM again. Temperature 30 °C; pH 7.5; 4-PB

10 mM; Alanine 200 mM; Between cycles, activity recovery phases were performed by a 2-hour incubation with 5 mM PLP.

To better understand enzyme behaviors in the different cycles in Figure 7.11 enzyme activities at the beginning and at the end of each cycle are represented. It must be taken into account that, between cycles, 2-hours incubations with PLP were carried out. As it can be observed, Cvi-TA lost all its activity at the end of all the cycles. However, the activity could be entirely recovered two times, reason why, starting cycle 2 and cycle 3, Cvi-TA had the same activity as at the beginning of the whole process. After that, only around 40 % of the initial activity could be recovered and these value progressively decreased in the next cycles. Regarding PDC, it can be observed that it maintained its operational stability during the first cycle. However, the first PLP incubation negatively affected its stability and, at the beginning of cycles 2, 3 and 4, it presented an activity of between 30 % and 40 % compared to the initial one.

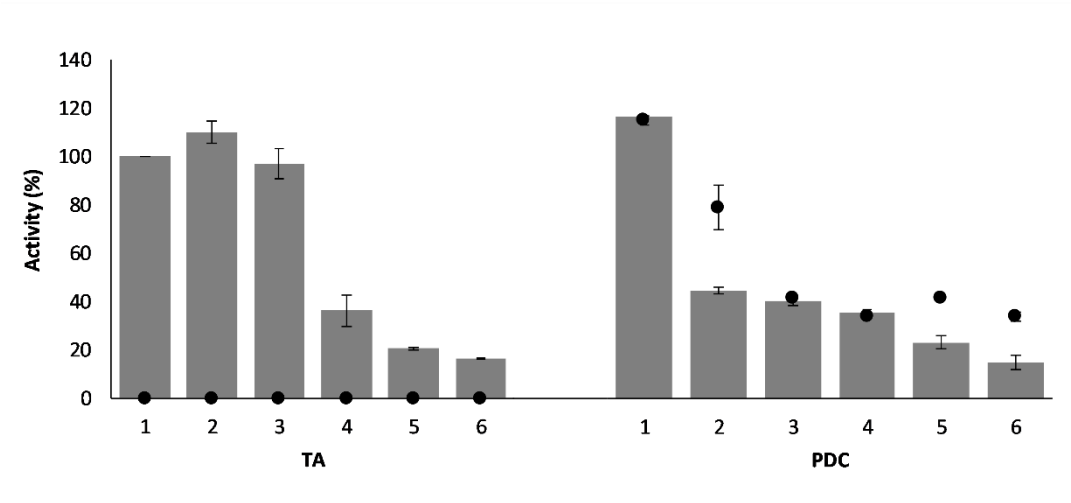

Figure 7.11 Cvi-TA and PDC activities at the beginning and at the end of each 3-APB synthesis reaction cycle. (bars) Activity at the beginning of the cycle (t=0 h). (●) Activity at the end of the cycle (t=8 h). Temperature 30 ^{o}C; pH 7.5; 4-PB 10 mM; Alanine 200 mM; Cvi-TA 6.9 % v v^{-1}; PDC 3.1 % v v^{-1}. Between cycles, activity recovery phases were performed by a 2-hour incubation with 5 mM PLP.

As it can be observed in Figure 7.12, these lower initial PDC activities, coincided with a deep initial reaction rate and significantly lower final yield, which was maintained at around 20 % in the three mentioned cycles. Since the second and the third cycles started with the entire TA activity, it could be considered that PDC activity loss was the key factor that negatively affected reaction. Even in the fourth cycle, in which TA activity could not be entirely recovered, it could

be considered that PDC hampered more 3-APB synthesis than TA, since similar results than the previous two cycles were obtained. Nevertheless, in cycle 5 both TA and PDC started with the 20 % of the initial activity and this values was even lower at the sixth. Then, the significant yield decrease in these cycles may be associated both to the low Cvi-TA and PDC activities.

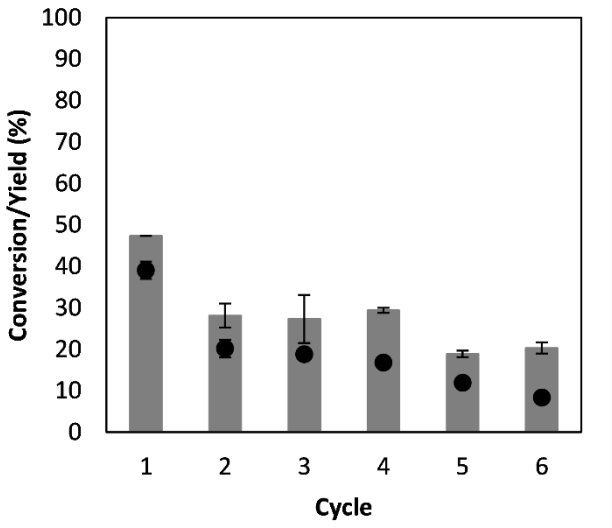

Figure 7.12 Conversion and yield of each 3-APB synthesis reaction cycle performed with immobilized Cvi-TA and PDC. (bars) Conversion. (●) Yield. Temperature 30 ^{o}C; pH 7.5; 4-PB 10 mM; Alanine 200 mM; Cvi-TA 6.9 % v v^{-1}; PDC 3.1 % v v^{-1}. Between cycles, activity recovery phases were performed by a 2-hour incubation with 5 mM PLP.

Results obtained by applying Vfl-TA derivatives in reaction cycles are shown in Figure 7.13 Even though when this transaminase was immobilized reaction time was enlarged to 24 hours, it was decided to shorten reaction cycles to 8 hours. The reason for these shortening was that, as it could be observed in the first reaction profile obtained in section 7.3.3.1 (Figure 7.8), after 8 hours, reaction had already started to slow down and, consequently, 3-APB increment between 8 and 24 h did not even arrive to 1 mM. Thus, it was not considered worthy to enlarge reaction 24 hours, with its corresponding consequences on operational stability, since with a second 8-hours cycle, higher 3-APB concentration may probably be reached than waiting until 24 hours.

As it was expected and can be observed in Figure 7.13 A, the first reaction cycle took place with the expected initial reaction rate according to the results obtained when reaction was initially tested with both enzymes immobilized (0.57 mM·h^{-1}) and, after 8 hours, 3-APB concentration of 2.65 mM was reached. However, as it happened with Cvi-TA, reaction rate was significantly reduced at the second cycle and half of the final amine concentration was achieved in

comparison with cycle 2. In the following cycles, concentration was decreasing 0.2 mM each time, which could be considered not significant. However, since 3-APB concentration was already low, it supposed a yield in the 4th cycle that did not arrive to 10 %. Therefore, this time, enzymes were reused two less cycles than in the case of Cvi-TA. Focusing on the control reaction (Figure 7.13 B), it can be observed how, even the incubation with PLP and the 4-PB addition to reach again 10 mM, reaction continued since, as it has already been commented, Vfl-TA reactions last more than 8 hours. However, after around 12 hours, reaction stopped and no additional 3-APB synthesis was observed. Therefore, it was considered again that reaction cycles could be only performed with immobilized derivatives.

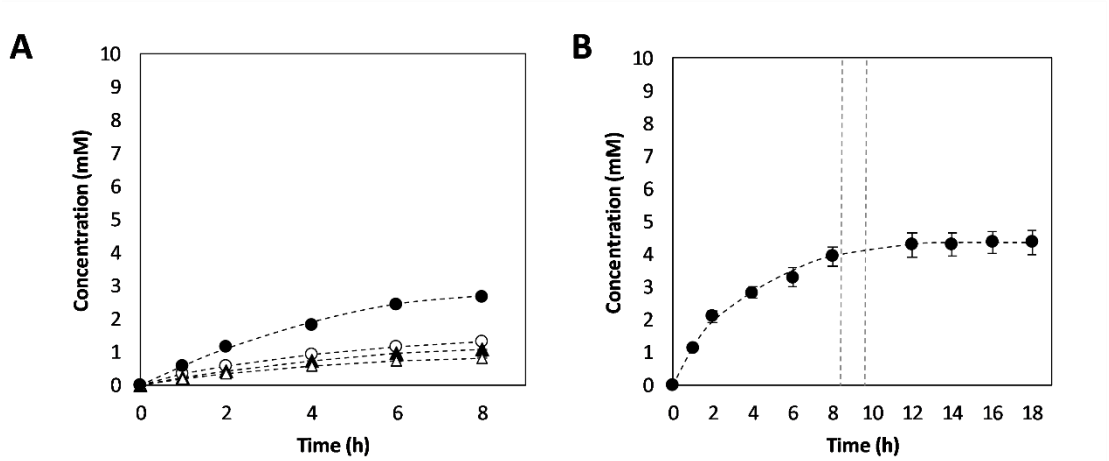

Figure 7.13 Synthesis of 3-APB in several reaction cycles using Vfl-TA and PDC both immobilized in MANA-agarose. A) Reaction profiles through the performed cycles. (●) Cycle 1; (○) Cycle 2; (▲) Cycle 3; (△) Cycle 4. B) Reaction profile of the control reaction performed with free enzymes with the same mg TA per mL and the same U PDC per mL of reaction. The second cycle was simulated by adding 5 mM PLP and increasing 4-PB concentration to 10 mM again. Temperature 30 ^{o}C; pH 7.5; 4-PB 10 mM; Alanine 200 mM. Between cycles, activity recovery phases were performed by a 2-hour incubation with 5 mM PLP.

This time, activity measures of each cycle (Figure 7.14) revealed that Vfl-TA maintained around 25 % of the initial activity at the end of the first reaction cycle. However, unlike the case of Cvi-TA, with PLP incubation, only 40 % of the initial activity could be recovered. Then, activity was completely lost and, after the second recovery phase, activity increased again to 40 %. After losing again the entire activity, the last cycle could start with the 30 % of the initial activity. Regarding PDC, this time a significant activity loss was observed before incubation with PLP, since the first cycle ended up with around 50 % of the initial PDC activity. Even though the stability was maintained the next two cycles, it decreased again at the last cycle. It must be

mentioned that some fluctuations were observed in the described PDC activity measures. For this reason, it was considered that in cycles 2 and 3 PDC maintained around 50 % of the activity all time. Even though, similarly as in the Cvi-TA, PDC behavior was in concordance with yield decrease (Figure 7.15), this decrease cannot be entirely associated with PDC, since a considerable loss of TA activity also occurred.

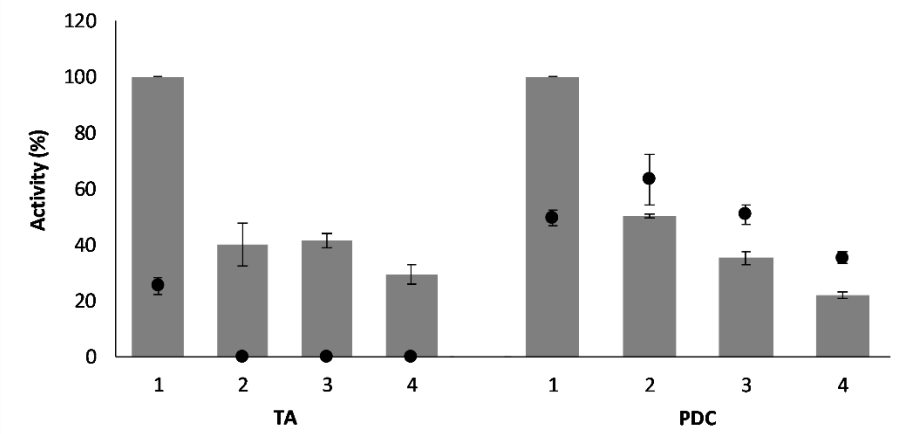

Figure 7.14 Vfl-TA and PDC activities at the beginning and at the end of each 3-APB synthesis reaction cycle. (bars) Activity at the beginning of the cycle (t=0 h). (●) Activity at the end of the cycle (t=8 h). Temperature 30 °C; pH 7.5; 4-PB 10 mM; Alanine 200 mM; Vfl-TA 5.7 % v v^{-1}; PDC 4.3 % v v^{-1}. Between cycles, activity recovery phases were performed by a 2-hour incubation with 5 mM PLP.

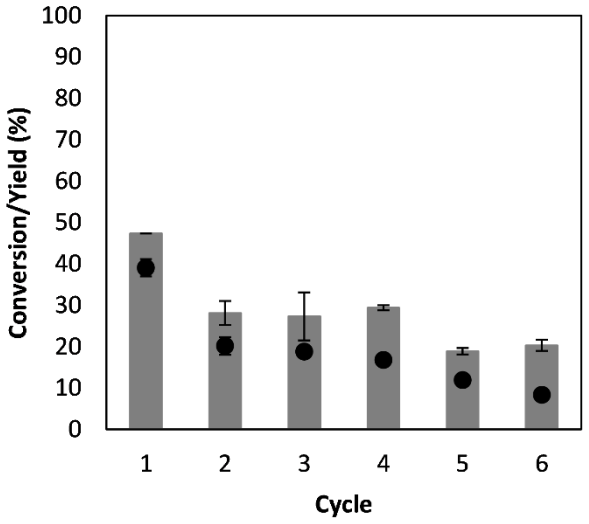

Figure 7.15 Conversion and yield of each 3-APB synthesis reaction cycle performed with immobilized Vfl-TA and PDC. (bars) Conversion. (●) Yield. Temperature 30 °C; pH 7.5; 4-PB 10 mM; Alanine 200 mM;

Vfl-TA 5.7 % v v^{-1}; PDC 4.3 % v v^{-1}. Between cycles, activity recovery phases were performed by a 2-hour incubation with 5 mM PLP.

7.3.4.2. 1-PEA synthesis in reaction cycles with immobilized TA and PDC

Synthesis of 1-PEA was also performed using the planned reaction cycle mechanism with both Vfl-TA and PDC immobilized in MANA-agarose. As in the case of 3-APB synthesis, reaction time was shorten to 8 hours following the criteria described in the previous section. Moreover, the same strategy of recovering TA activity by alternating cycles with PLP incubations was followed; and also a control reaction was carried out in parallel.

As it can be observed in Figure 7.16 A, also this time Vfl-TA was reused four times. Cycle 1 took place with an initial rate of 0.45 mM·h^{-1} and a final 1-PEA concentration of 2.01 mM. As it was usual in previous reaction cycles studies, a 50 % decrease on the mentioned values took place at cycle 2. It is true that yield in the second cycle was already lower than 10 % but, considering that yield was already low in the first cycle and that the decreasing tendency was similar than the obtained during 3-APB synthesis, it was considered appropriate to enlarge the process two more cycles. After the second cycle, reduction on rate and final product concentration were more progressive and, at the end of the 4th cycle, yield was around 5 %. As it was expected following the examples of previous reaction cycles, in control reaction (Figure 7.16 B) 1-PEA additional synthesis was not detected in the second simulated cycle.

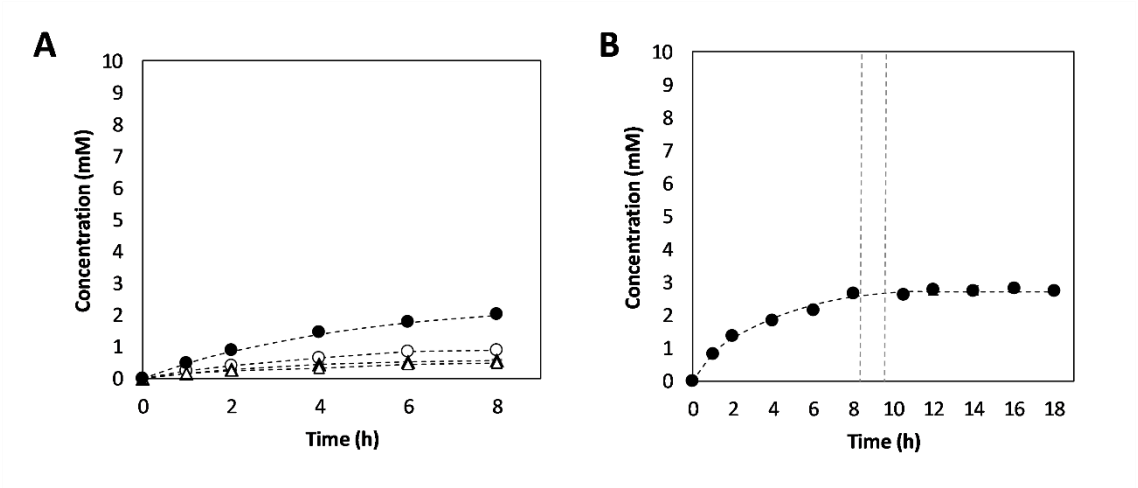

Figure 7.16 Synthesis of 1-PEA in several reaction cycles using Vfl-TA and PDC both immobilized in MANA-agarose. A) Reaction profiles through the performed cycles. (●) Cycle 1; (○) Cycle 2; (▲) Cycle 3;

(△) Cycle 4. B) Reaction profile of the control reaction performed with free enzymes and containing the same TA concentration in mg·mL^{-1} and PDC activity in U·mL^{-1} reaction. The second cycle was simulated by adding 5 mM PLP and increasing 4-PB concentration to 10 mM again. Temperature 30 ^{o}C; pH 7.5; AP 10 mM; Alanine 200 mM. Between cycles, activity recovery phases were performed by a 2-hour incubation with 5 mM PLP.

Regarding transaminase activity (Figure 7.17), as it happened during 3-APB synthesis with Vfl-TA, the enzyme maintained part of its initial activity at the end of cycle 1 and, after that, only part of it could be recovered, in this case around 50 %. At the end of the following cycles, the entire activity was lost and the 50 % could be recovered. Regarding PDC activity, its behavior was similar than in the 3-APB synthesis with Vfl-TA case. This enzyme lost a significant part of its activity during the first cycle and, after that, around 50 % of the initial activity was maintained until cycle 4, when a slightly more significant decrease was observed. Again, the deepest decrease on process metrics (Figure 7.18) coincided with a significant lost on TA and PDC activities. Therefore, both Vfl-TA and PDC may have hampered 1-PEA synthesis from cycle 2.

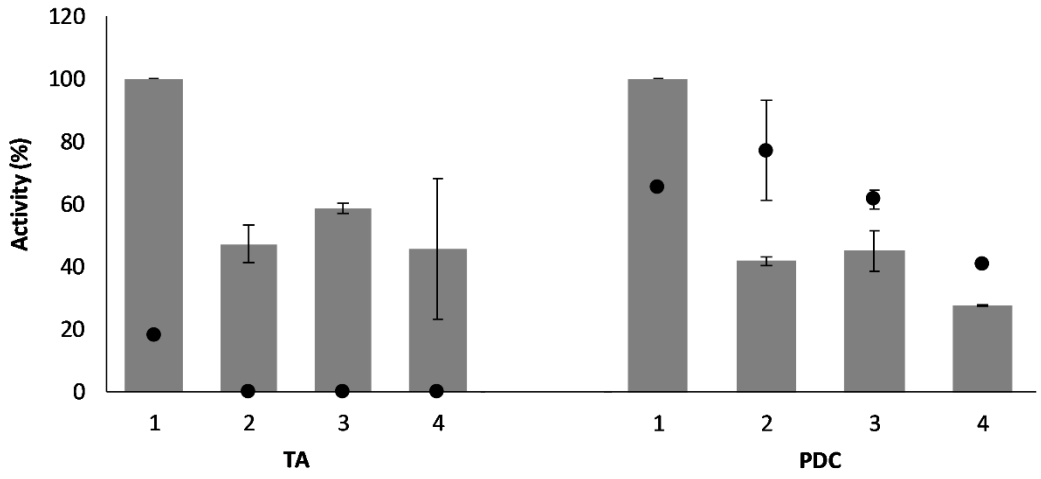

Figure 7.17 Vfl-TA and PDC activities at the beginning and at the end of each 1-PEA synthesis reaction cycle. (bars) Activity at the beginning of the cycle (t=0 h). (●) Activity at the end of the cycle (t=8 h). Temperature 30 ^{o}C; pH 7.5; AP 10 mM; Alanine 200 mM; Vfl-TA 5.7 % v v^{-1}; PDC 4.3 % v v^{-1}. Between cycles, activity recovery phases were performed by a 2-hour incubation with 5 mM PLP.

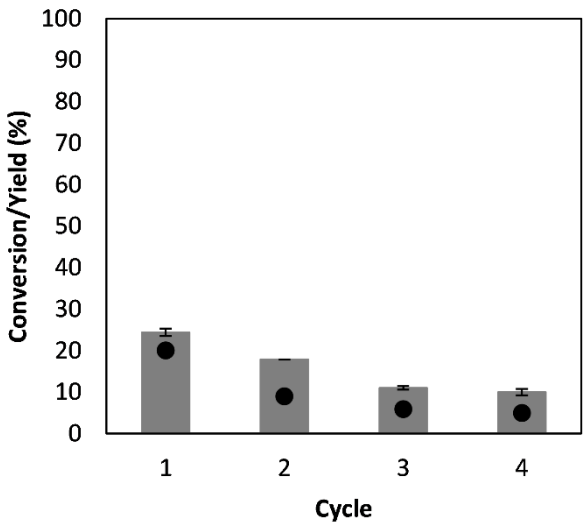

Figure 7.18 Conversion and yield of each 1-PEA synthesis reaction cycle performed with immobilized Vfl-TA and PDC. (bars) Conversion. (●) Yield. Temperature 30 ºC; pH 7.5; AP 10 mM; Alanine 200 mM; Vfl-TA 5.7 % v v^{-1}; PDC 4.3 % v v^{-1}. Between cycles, activity recovery phases were performed by a 2-hour incubation with 5 mM PLP.

7.3.5. Comparison between process strategies

In order to evaluate the advantages that working in reaction cycles with immobilized enzymes could suppose, a comparison of the most relevant process approaches of the entire thesis was performed. In Table 7.8 overall process metrics obtained in 3-APB synthesis with reaction cycles appear compared with the most relevant results obtained during reactions with soluble enzymes performed in chapter 5. In the case of Cvi-TA, reaction cycles are compared with reaction with free enzymes in aqueous medium. Therefore, it must be taken into account that, when enzymes were immobilized, slightly lower PDC activity could be added, which in section 7.3.3.1 was identified as a limitation that led to lower reaction yield. However, due to the possibility of recycling six times the enzymes, it can be observed that the 3-APB total amount was doubled with reaction cycles, even though reaction time was 6-times higher in comparison with reaction with free enzymes. Therefore, STY suffered a deep decrease, but biocatalyst yield was also doubled, which means that more advantage can be taken of Cvi-TA when it is immobilized. However, it must be taken into account that also PLP is expended between cycles, thus a deeper reflection about if the mentioned expense is worthy should be considered. Regarding that PDC stability through the cycles supposed a higher drawback than Cvi-TA (Figure 7.11 and Figure 7.12), a possible alternative approach would be reaction cycles in which Cvi-TA immobilized derivatives are used but PDC is added in the soluble form and is replaced every cycle. In that

case, in addition to the complexity that immobilizing supposes, PDC expense would be so high (25 % vv^{-1} of CFE in each reaction) and from the 4th cycle, in which Cvi-TA entire activity could not be recovered, lower yield would be expectable. Therefore, it may be considered if Cvi-TA reuse justifies all the mentioned expenses, as well as PLP used to recover its activity between cycles.

Table 7.8 Comparison between overall process metrics in 3-APB synthesis obtained during initial reactions with free enzymes and during the reaction cycles with immobilized enzymes. In the case of Vfl-TA, also results obtained by adding 10 % glycerol into the medium were included.

Enzyme	Description	Reaction time (h)	Total 3-APB (mmol)	Overall yield (%)	STY ($mmol \cdot L^{-1} \cdot h^{-1}$)	BY ($mmol \cdot mg\ TA^{-1}$)
Cvi-TA	Free enzymes[a]	8	0.06 ± 0.01	64.22 ± 10.14	0.78 ± 0.12	5.01 ± 0.79
	Reaction cycles[b]	48	0.12 ± 0.01	19.12 ± 0.99	0.04 ± 0.00	9.45 ± 0.50
Vfl-TA	Free enzymes[c]	8	0.06 ± 0.01	60.77 ± 6.58	0.74 ± 0.08	8.61 ± 0.93
	10 % glicerol[d]	30	0.10 ± 0.00	68.16 ± 0.07	0.34 ± 0.01	14.83 ± 0.30
	Reaction cycles[e]	32	0.06 ± 0.00	14.59 ± 0.17	0.05 ± 0.00	8.51 ± 0.06

[a] 4-PB 10 mM; Cvi-TA in CFE form 1.52 $mg \cdot mL^{-1}$; PDC in CFE form 30 $U \cdot mL^{-1}$

[b] 4-PB 10 mM; immobilized Cvi-TA 1.52 $mg \cdot mL^{-1}$; immobilized PDC 20 $U \cdot mL^{-1}$

[c] 4-PB 10 mM; Vfl-TA in CFE form 1.16 $mg \cdot mL^{-1}$; PDC in CFE form 30 $U \cdot mL^{-1}$

[d] 4-PB 15 mM; Vfl-TA in CFE form 1.16 $mg \cdot mL^{-1}$; PDC in CFE form 30 $U \cdot mL^{-1}$

[e] 4-PB 10 mM; immobilized Vfl-TA 1.16 $mg \cdot mL^{-1}$; immobilized PDC 28 $U \cdot mL^{-1}$

Regarding Vfl-TA, in addition to comparing its cycles with reaction in aqueous medium, also results obtained when a 10 % glycerol was added into the soluble-enzymes reaction medium were considered in Table 7.8, because they represent the best 3-APB synthesis results obtained during chapter 5. As in the case of Cvi-TA, PDC activity reduction when reaction was performed with immobilized enzymes must be also taken into account, even though the major drawback identified in this case was Vfl-TA immobilization (see section 7.3.3.1). First of all, it must be mentioned that, due to the yield reduction when Vfl-TA is immobilized (see section 7.3.1.1), the same total 3-APB amount was obtained in the soluble reaction and in the reaction cycles. In consequence, STY was deeply reduced in cycles and BY remained the same, thus more advantage was not taken of Vfl-TA by immobilizing it. Moreover, the low efficiency of the activity recovery phases observed supposed another reason to discard the use of this immobilized derivative. In contrast, the cosolvent approach supposed a 67 % increase on the obtained product amount. It is true that reaction time was enlarged, which supposes a lower STY, but reaction yield was slightly higher than without the cosolvent, thus the higher 4-PB expense

(when 10% glycerol is used, 4-PB is increased from 10 mM to 15 mM) may be considered worthy. Altogether leads to the best obtained BY in 3-APB synthesis. Therefore, the strategy in which more advantage of TA is taken is when glycerol is added into the medium.

The same comparison between reaction process strategies was performed with 1-PEA synthesis case (

Table ***7.9***). As in the case of 3-APB synthesis with Vfl-TA, the decrease on reaction yield observed when this enzyme is immobilized had a major repercussion, leading to lower 1-PEA total amount when reaction cycles are performed than when soluble enzymes are used, which also supposed a lower BY. It is true that during the cycles overall reaction time was not highly enlarged in relation with the soluble reaction. However, in the last cycles, low 1-PEA amounts were obtained for the larger volume, which made STY deeply decrease. Again, the use of Vfl-TA in immobilized form should be discarded. As it happened with 3-APB synthesis, adding 10 % glycerol into the medium may be considered the best strategy, even though the overall lower yield reflects a higher AP expense (in this case, AP is increased from 10 mM to 30 mM). This strategy, led to the highest 1-PEA amount, STY and BY.

Table 7.9 Comparison between overall process metrics in 1-PEA synthesis obtained during initial reactions with free enzymes and during the reaction cycles with immobilized enzymes. Also results obtained by adding 10 % glycerol into the medium were included.

Description	Reaction time (h)	Total 3-APB (mmol)	Overall yield (%)	STY (mmol/L/h)	BY (mmol/ mg TA)
Free enzymes[a]	24	0.05 ± 0.00	48.51 ± 0.06	0.21 ± 0.00	7.47 ± 0.01
10 % glicerol[b]	24	0.09 ± 0.01	28.08 ± 0.26	0.37 ± 0.02	13.04 ± 0.06
Reaction cycles[c]	32	0.04 ± 0.00	10.10 ± 0.19	0.03 ± 0.00	5.75 ± 0.12

[a] AP 10 mM; Vfl-TA in CFE form 1.16 mg·mL^{-1}; PDC in CFE form 30 U·mL^{-1}

[b] AP 30 mM; Vfl-TA in CFE form 1.16 mg·mL^{-1}; PDC in CFE form 30 U·mL^{-1}

[c] AP 10 mM; immobilized Vfl-TA 1.16 mg·mL^{-1}; immobilized PDC 28 U·mL^{-1}

7.4. Conclusions

Synthesis of 3-APB was carried out with the two transaminases immobilized both in MANA-agarose and epoxy-agarose and using PDC in soluble form. In the case of Cvi-TA the same reaction profile as in reactions with free enzymes was obtained in all cases. However, also

activity profiles during reaction were similar, which means that immobilization was not able to improve operational stability. In the case of Vfl-TA, immobilization reduced reaction rates, enlarged reaction time and supposed a 25-30% decrease on yield. Also 1-PEA reaction rate was lower when Vfl-TA immobilized was used and, this time, reaction yield was 50 % lower in respect to reaction with soluble TA. Moreover, immobilizing had a negative repercussion on operational stability during 1-PEA synthesis, especially in epoxy-agarose. Regarding that similar results were obtained for MANA-agarose and epoxy-agarose derivatives, MANA-agarose was selected to perform the next studies since, with this immobilization method, TA load was higher, thus less derivative amount was needed. After that, also the combined effect of immobilization and cosolvent addition was tested, but any improve was detected.

Hypothesizing that the activity loss observed in immobilized TAs was mainly due to PLP dissociation, further studies were carried out in regards to the cofactor. It was observed that performing 1 mM PLP addition increased the final 3-APB concentration 1.2-fold, both in the case of immobilized Cvi-TA and Vfl-TA. However, starting the reaction directly with higher PLP concentration did not enhance reactions catalyzed by Cvi-TA and had a slight negative repercussion in the case of using Vfl-TA. As a previous step for studying the possibility of reusing the biocatalysts, enzymes were incubated at different PLP concentrations after its deactivation in reaction. It was concluded that a two hours incubation with a fresh buffer solution containing 5 mM PLP enables the entire transaminase activity recovery.

Finally, regarding that TA activity could be recovered after reaction, a reaction process strategy based on several reaction cycles was planned alternating enzyme recovery phases. For this new strategy, also PDC immobilized in MANA-agarose was used, which in some cases could have led to lower yields. In the case of Cvi-TA, 6 reaction cycles could be performed. A deep yield decrease was observed in the second cycle, which was related to a significant PDC activity loss. Also in the case of reactions with Vfl-TA, both for 3-APB and 1-PEA synthesis, the highest difference on yield took place between cycle 1 and 2; and only 4 cycles were reached. However, in this case, yield loss could not be only attributed to the decrease on PDC activity since only part of TA activity could be recovered between the two mentioned cycles. Finally, comparing the cycles strategy with reactions with soluble enzymes, it was concluded that 3-APB concentration could be doubled performing Cvi-TA cycles, which means that more advantage of this enzyme can be taken by immobilizing it. However, performing cycles with Vfl-TA did not improve the process in comparison with soluble enzymes, neither in the case of 3-APB nor 1-PEA. In contrast, it was concluded that the best strategy is the free-enzymes reactions with 10 % glycerol into the medium.

7.5. References

[1] F. Guo and P. Berglund, "Transaminase biocatalysis: optimization and application," *Green Chem.*, vol. 19, no. 2, pp. 333–360, Jan. 2017.

[2] B.-Y. Hwang and B.-G. Kim, "High-throughput screening method for the identification of active and enantioselective ω-transaminases," *Enzyme Microb. Technol.*, vol. 34, no. 5, pp. 429–436, Apr. 2004.

[3] M. S. Malik, E.-S. Park, and J.-S. Shin, "Features and technical applications of ω-transaminases," *Appl. Microbiol. Biotechnol.*, vol. 94, no. 5, pp. 1163–1171, Jun. 2012.

[4] I. Slabu, J. L. Galman, R. C. Lloyd, and N. J. Turner, "Discovery, Engineering, and Synthetic Application of Transaminase Biocatalysts," *ACS Catal.*, vol. 7, no. 12, pp. 8263–8284, 2017.

[5] S. A. Kelly *et al.*, "Application of ω-Transaminases in the Pharmaceutical Industry," *Chem. Rev.*, vol. 118, pp. 349–367, 2017.

[6] D. Ghislieri and N. J. Turner, "Biocatalytic Approaches to the Synthesis of Enantiomerically Pure Chiral Amines," *Top. Catal.*, vol. 57, no. 5, pp. 284–300, Mar. 2014.

[7] S. E. Lowe' and J. G. Zeikus', "Purification and characterization of pyruvate decarboxylase from Sarcina ventriculi," *J. Gen. Microbiol.*, vol. 138, pp. 803–807, 1992.

[8] S. König, M. Spinka, and S. Kutter, "Allosteric activation of pyruvate decarboxylases. A never-ending story?," *J. Mol. Catal. B Enzym.*, vol. 61, no. 1–2, pp. 100–110, 2009.

[9] D. Gocke *et al.*, "Comparative characterisation of thiamin diphosphate-dependent decarboxylases," *J. Mol. Catal. B Enzym.*, vol. 61, pp. 30–35, 2009.

[10] K. Tittmann, A. Balakrishnan, Y. Gao, P. Moorjani, N. S. Nemeria, and F. Jordan, "Bifunctionality of the thiamin diphosphate cofactor: Assignment of tautomeric/ionization states of the 4'-aminopyrimidine ring when various intermediates occupy the active sites during the catalysis of yeast pyruvate decarboxylase," *J. Am. Chem. Soc.*, vol. 134, no. 8, pp. 3873–3885, 2012.

[11] L. J. Van Zyl, W.-D. Schubert, M. I. Tuffin, and D. A. Cowan, "Structure and functional characterization of pyruvate decarboxylase from Gluconacetobacter diazotrophicus," *BMC Struct. Biol.*, vol. 14, no. 21, pp. 1–13, 2014.

[12] L. Buddrus, E. S. V. Andrews, D. J. Leak, M. J. Danson, V. L. Arcus, and S. J. Crennell, "Crystal structure of an inferred ancestral bacterial pyruvate decarboxylase," *Acta Crystallogr. Sect. F Struct. Biol. Commun.*, vol. 74, no. 3, pp. 179–186, Mar. 2018.

[13] M. A. Lie, L. Celik, K. A. Jørgensen, and B. Schiøtt, "Cofactor activation and substrate binding in pyruvate decarboxylase. Insights into the reaction mechanism from molecular dynamics simulations," *Biochemistry*, vol. 44, no. 45, pp. 14792–14806, 2005.

[14] O. P. Ward and A. Singh, "Enzymatic asymmetric synthesis by decarboxylases," *Curr. Opin. Biotechnol.*, vol. 11, pp. 520–526, 2000.

[15] A. Shrestha, S. Dhamwichukorn, and E. Jenwitheesuk, "Bioinformation Modeling of pyruvate decarboxylases from ethanol producing bacteria Bioinformation," *Bioinformation*, vol. 4, no. 8, pp. 378–384, 2010.

[16] T. Börner *et al.*, "Explaining Operational Instability of Amine Transaminases: Substrate-Induced Inactivation Mechanism and Influence of Quaternary Structure on Enzyme−Cofactor Intermediate Stability," *ACS Catal.*, vol. 7, pp. 1259–1269, 2016.

[17] S. Chen, J. C. Campillo-Brocal, P. Berglund, and M. S. Humble, "Characterization of the stability of Vibrio fluvialis JS17 amine transaminase," *J. Biotechnol.*, vol. 282, pp. 10–17, Sep. 2018.

[18] R. Fernandez-Lafuente, "Stabilization of multimeric enzymes: Strategies to prevent subunit dissociation," *Enzyme Microb. Technol.*, vol. 45, no. 6–7, pp. 405–418, Dec. 2009.

[19] C. Mateo, J. M. Palomo, G. Fernandez-Lorente, J. M. Guisan, and R. Fernandez-Lafuente, "Improvement of enzyme activity, stability and selectivity via immobilization techniques," *Enzyme Microb. Technol.*, vol. 40, no. 6, pp. 1451–1463, May 2007.

[20] W. Hartmeier, "Immobilized biocatalysts - From simple to complex systems," *Trends Biotechnol.*, vol. 3, no. 6, pp. 149–153, 1985.

[21] H. Mallin, U. Menyes, T. Vorhaben, M. Höhne, and U. T. Bornscheuer, "Immobilization of two (R)-Amine Transaminases on an Optimized Chitosan Support for the Enzymatic Synthesis of Optically Pure Amines," *ChemCatChem*, vol. 5, no. 2, pp. 588–593, 2013.

[22] W. Böhmer *et al.*, "Highly efficient production of chiral amines in batch and continuous flow by immobilized ω-transaminases on controlled porosity glass metal-ion affinity carrier," *J. Biotechnol.*, vol. 291, pp. 52–60, Feb. 2019.

[23] E. Abaházi *et al.*, “Covalently immobilized Trp60Cys mutant of ω-transaminase from Chromobacterium violaceum for kinetic resolution of racemic amines in batch and continuous-flow modes,” *Biochem. Eng. J.*, vol. 132, pp. 270–278, Apr. 2018.

[24] C. Mateo, V. Grazu, J. M. Palomo, F. Lopez-Gallego, R. Fernandez-Lafuente, and J. M. Guisan, “Immobilization of enzymes on heterofunctional epoxy supports,” *Nat. Protoc.*, vol. 2, no. 5, pp. 1022–1033, May 2007.

[25] A. I. Denesyuk, K. A. Denessiouk, T. Korpela, and M. S. Johnson, “Functional Attributes of the Phosphate Group Binding Cup of Pyridoxal Phosphate-dependent Enzymes.”

[26] U. Schell, R. Wohlgemuth, and J. M. Ward, “Synthesis of pyridoxamine 5’-phosphate using an MBA:pyruvate transaminase as biocatalyst,” *J. Mol. Catal. B Enzym.*, vol. 59, no. 4, pp. 279–285, Aug. 2009.

[27] S. Mathew and H. Yun, “ω-Transaminases for the Production of Optically Pure Amines and Unnatural Amino Acids,” *ACS Catal.*, vol. 2, pp. 993–1001, 2012.

[28] D. Koszelewski, K. Tauber, K. Faber, and W. Kroutil, “ω-Transaminases for the synthesis of non-racemic α-chiral primary amines,” *Trends in Biotechnology*, vol. 28, no. 6. pp. 324–332, Jun-2010.

[29] P. Christen and P. K. Mehta, “From cofactor to enzymes. The molecular evolution of pyridoxal-s’-pliosphate-dependent enzymes,” *Chem. Rec.*, vol. 1, no. 6, pp. 436–447, 2001.

[30] M. D. Patil, G. Grogan, A. Bommarius, and H. Yun, “Recent advances in ω-transaminase-mediated biocatalysis for the enantioselective synthesis of chiral amines,” *Catalysts*, vol. 8, no. 7. 2018.

[31] C. Sayer, M. N. Isupov, A. Westlake, and J. A. Littlechild, “Structural studies of Pseudomonas and Chromobacterium ω- aminotransferases provide insights into their differing substrate specificity,” *Acta Crystallogr. Sect. D Biol. Crystallogr.*, vol. 69, no. 4, pp. 564–576, 2013.

[32] B. A. Kikani, S. Pandey, and S. P. Singh, “Immobilization of the a-amylase of Bacillus amyloliquifaciens TSWK1-1 for the improved biocatalytic properties and solvent tolerance,” *Bioprocess Biosyst Eng*, vol. 36, pp. 567–577, 2013.

[33] E. Katchalski-Katzir, “Immobilized enzymes - learning from past successes and failures,” *Trends Biotechnol.*, vol. 11, no. 11, pp. 471–478, 1993.

[34] M. Höhne and U. T. Bornscheuer, “Biocatalytic routes to optically active amines,” *ChemCatChem*, vol. 1, no. 1, pp. 42–51, 2009.

[35] C. López, S. D. Ríos, J. López-Santín, G. Caminal, and G. Álvaro, “Immobilization of PLP-dependent enzymes with cofactor retention and enhanced stability,” *Biochem. Eng. J.*, vol. 49, pp. 414–421, 2010.

[36] P. Zucca, R. Fernandez-Lafuente, and E. Sanjust, “Agarose and Its Derivatives as Supports for Enzyme Immobilization,” *Molecules*, vol. 21, pp. 1577–1599, 2016.

8. General conclusions

In the present thesis, different tools and approaches were applied for the development and optimization of chiral amine synthesis. The feasibility of the enzymatic cascade reaction of TA and PDC was explored through the synthesis of two target amines: 3-APB and 1-PEA.

To overcome the commercial limitations of PDC, a novel PDC-producing *E. coli* strain was obtained by cloning the *Z. palmae* PDC gene. After that, a production process was developed in bench-top bioreactor applying a substrate-limited fed-batch. This strategy led to a volumetric productivity of 6942 $U \cdot L^{-1} \cdot h^{-1}$ and a final PDC specific activity of 3677 $U \cdot gDCW^{-1}$.

Both the obtained PDC and several transaminases proceeding from different microorganisms were characterized. Optimum pH conditions studies showed that TAs are more affected by pH changes than PDC, reason why the compromise conditions were defined by TA needs. Stability studies revealed that all enzymes have a high long-time stability not only in the established pH compromise conditions but also in a wide pH range. Also the influence of pH and cofactors presence to PDC activity was studied, concluding that TPP and Mg^{2+} addition is critical for ZpPDC activity maintenance, especially in high pH conditions, in which enzyme dissociation takes place. However, this dissociation has shown to be reversible in the pH range from 8 to 9. Taking into account the characterization results, a preliminary transaminase screening was performed and Cvi-TA and Vfl-TA were selected for 3-APB synthesis and, for 1-PEA synthesis, Vfl-TA was selected.

Cascade reactions were constructed by coupling the selected TAs and PDC, and it was demonstrated that the pyruvate removing by decarboxylation was critical for chiral amine synthesis. In 3-APB synthesis, yields higher than 60 % were reached with both Cvi-TA and Vfl-TA in 8 hours reaction, even though low operational TA stabilities were observed. Using a medium engineering approach, final 3-APB concentration could be increased to the maximum reported for the TA/PDC system (10.20 mM final 3-APB concentration) when Vfl-TA was used and 10 % glycerol into the medium was added. Regarding 1-PEA synthesis, around 50% yield was obtained after 24 h by coupling Vfl-TA with PDC. Improvements were also achieved when 10% glycerol was added into the medium (8.96 mM final 1-PEA concentration). In all cases products with high enantiopurity were obtained for enantiomer S (around 90% ee in all 3-APB synthesis reactions; >99% in 1-PEA synthesis reactions).

Aiming to increase their operational stability, immobilization of the two transaminases was carried out in MANA-agarose and in epoxy-agarose. Immobilized derivatives of Cvi-TA and Vfl-TA in MANA-agarose were obtained with a maximum transaminase load of around 20 mg of each TA per mL support, while epoxy-agarose derivatives showed lower maximum loading capacity. Also PDC immobilization was performed with the same methods, even though epoxy-agarose support was discarded because of the low PDC stability in the required immobilization conditions. A novel simultaneous purification and immobilization procedure was developed in MANA-agarose, with which a maximum enzymatic load of 3000 U per mL of MANA-agarose could be loaded. However, an activity loss was detected during covalent bound formation phase, which led to PDC immobilized derivatives of around 700 U per mL of MANA-agarose.

The obtained immobilized enzymes were applied in reaction. While TA immobilization did not suppose any effect on reaction in the case of Cvi-TA, reaction rates and final yields decreased when Vfl-TA was immobilized, both in the synthesis of 3-APB and 1-PEA. Since the same results were obtained both with MANA-agarose and epoxy-agarose, the first immobilization method was selected for further studies, since it contained higher TA load. In studies focusing on PLP effect, it was observed that, even though immobilized derivatives lost their activities during reaction, they could be recovered with a two-hours incubation with a fresh buffer solution containing 5 mM PLP. Therefore, reaction process strategy based on several reaction cycles with both TA and PDC immobilized was planned alternating enzyme recovery phases. In the case of Cvi-TA, 6 reaction cycles could be performed, while in reactions with Vfl-TA cycles number was reduced to 4. Comparing the cycles strategy with reactions with soluble enzymes, it was concluded that 3-APB concentration could be doubled performing Cvi-TA cycles, which means that more advantage of this enzyme can be taken by immobilizing it. However, performing cycles with Vfl-TA did not improve the process in comparison with soluble enzymes, neither in the case of 3-APB nor 1-PEA. In contrast, it was concluded that the best strategy is the free-enzymes reactions with 10 % glycerol into the medium.

Scientific contributions

N. Alcover, A. Carceller, G. Álvaro, and M. Guillén, “Zymobacter palmae pyruvate decarboxylase production process development: Cloning in Escherichia coli, fed-batch culture and purification,” *Eng. Life Sci.*, vol. 19, no. 7, pp. 502–512, 2019.

N. Alcover, G. Álvaro and M. Guillén, "Chiral synthesis of 3-amino-1-phenylbutane by a multi-enzymatic cascade system", *submited to Microbial Biotechnology.*